

VOL. 686 NO. 2 2 DECEMBER 1994

THIS ISSUE COMPLETES VOL. 686

JOURNAL OF

# CHROMATOGRAPHY A

INCLUDING ELECTROPHORESIS AND OTHER SEPARATION METHODS

## EDITORS

U.A.Th. Brinkman (Amsterdam)  
R.W. Giese (Boston, MA)  
J.K. Haken (Kensington, N.S.W.)  
L.R. Snyder (Orinda, CA)  
S. Terabe (Hyogo)

EDITORS, SYMPOSIUM VOLUMES,  
E. Heftmann (Orinda, CA), Z. Deyl (Prague)

## EDITORIAL BOARD

D.W. Armstrong (Rolla, MO)  
W.A. Aue (Halifax)  
P. Boček (Brno)  
A.A. Boulton (Saskatoon)  
P.W. Carr (Minneapolis, MN)  
N.H.C. Cooke (San Ramon, CA)  
V.A. Davankov (Moscow)  
G.J. de Jong (Weesp)  
Z. Deyl (Prague)  
S. Dilli (Kensington, N.S.W.)  
Z. El Rassi (Stillwater, OK)  
H. Engelhardt (Saarbrücken)  
F. Erni (Basle)  
M.B. Evans (Hatfield)  
J.L. Glajch (N. Billerica, MA)  
G.A. Guiochon (Knoxville, TN)  
P.R. Haddad (Hobart, Tasmania)  
I.M. Hais (Hradec Králové)  
W.S. Hancock (Palo Alto, CA)  
S. Hjertén (Uppsala)  
S. Honda (Higashi-Osaka)  
Cs. Horváth (New Haven, CT)  
J.F.K. Huber (Vienna)  
K.-P. Hupe (Waldbronn)  
J. Janák (Brno)  
P. Jandera (Pardubice)  
B.L. Karger (Boston, MA)  
J.J. Kirkland (Newport, DE)  
E. sz. Kováts (Lausanne)  
K. Macek (Prague)  
A.J.P. Martin (Cambridge)  
L.W. McLaughlin (Chestnut Hill, MA)  
E.D. Morgan (Keele)  
J.D. Pearson (Kalamazoo, MI)  
H. Poppe (Amsterdam)  
F.E. Regnier (West Lafayette, IN)  
P.G. Righetti (Milan)  
P. Schoenmakers (Amsterdam)  
R. Schwarzenbach (Dübendorf)  
R.E. Shoup (West Lafayette, IN)  
R.P. Singhal (Wichita, KS)  
A.M. Siouffi (Marseille)  
D.J. Strydom (Boston, MA)  
N. Tanaka (Kyoto)  
K.K. Unger (Mainz)  
R. Verpoorte (Leiden)  
Gy. Vigh (College Station, TX)  
J.T. Watson (East Lansing, MI)  
B.D. Westerlund (Uppsala)

## EDITORS, BIBLIOGRAPHY SECTION

Z. Deyl (Prague), J. Janák (Brno), V. Schwarz (Prague)

ELSEVIER

# JOURNAL OF CHROMATOGRAPHY A

INCLUDING ELECTROPHORESIS AND OTHER SEPARATION METHODS

**Scope.** The *Journal of Chromatography A* publishes papers on all aspects of **chromatography, electrophoresis** and related methods. Contributions consist mainly of research papers dealing with chromatographic theory, instrumental developments and their applications. In the *Symposium volumes*, which are under separate editorship, proceedings of symposia on chromatography, electrophoresis and related methods are published. *Journal of Chromatography B: Biomedical Applications*—This journal, which is under separate editorship, deals with the following aspects: developments in and applications of chromatographic and electrophoretic techniques related to clinical diagnosis or alterations during medical treatment; screening and profiling of body fluids or tissues related to the analysis of active substances and to metabolic disorders; drug level monitoring and pharmacokinetic studies; clinical toxicology; forensic medicine; veterinary medicine; occupational medicine; results from basic medical research with direct consequences in clinical practice.

**Submission of Papers.** The preferred medium of submission is on disk with accompanying manuscript (see *Electronic manuscripts* in the Instructions to Authors, which can be obtained from the publisher, Elsevier Science B.V., P.O. Box 330, 1000 AH Amsterdam, Netherlands). Manuscripts (in English; *four* copies are required) should be submitted to: Editorial Office of *Journal of Chromatography A*, P.O. Box 681, 1000 AR Amsterdam, Netherlands, Telefax (+31-20) 485 2304, or to: The Editor of *Journal of Chromatography B: Biomedical Applications*, P.O. Box 681, 1000 AR Amsterdam, Netherlands. Review articles are invited or proposed in writing to the Editors who welcome suggestions for subjects. An outline of the proposed review should first be forwarded to the Editors for preliminary discussion prior to preparation. Submission of an article is understood to imply that the article is original and unpublished and is not being considered for publication elsewhere. For copyright regulations, see below.

**Publication information.** *Journal of Chromatography A* (ISSN 0021-9673): for 1995 Vols. 683–714 are scheduled for publication. *Journal of Chromatography B: Biomedical Applications* (ISSN 0378-4347): for 1995 Vols. 663–674 are scheduled for publication. Subscription prices for *Journal of Chromatography A*, *Journal of Chromatography B: Biomedical Applications* or a combined subscription are available upon request from the publisher. Subscriptions are accepted on a prepaid basis only and are entered on a calendar year basis. Issues are sent by surface mail except to the following countries where air delivery via SAL is ensured: Argentina, Australia, Brazil, Canada, China, Hong Kong, India, Israel, Japan, Malaysia, Mexico, New Zealand, Pakistan, Singapore, South Africa, South Korea, Taiwan, Thailand, USA. For all other countries airmail rates are available upon request. Claims for missing issues must be made within six months of our publication (mailing) date. Please address all your requests regarding orders and subscription queries to: Elsevier Science B.V., Journal Department, P.O. Box 211, 1000 AE Amsterdam, Netherlands. Tel.: (+31-20) 485 3642; Fax: (+31-20) 485 3598. Customers in the USA and Canada wishing information on this and other Elsevier journals, please contact Journal Information Center, Elsevier Science Inc., 655 Avenue of the Americas, New York, NY 10010, USA, Tel. (+1-212) 633 3750, Telefax (+1-212) 633 3764.

**Abstracts/Contents Lists** published in Analytical Abstracts, Biochemical Abstracts, Biological Abstracts, Chemical Abstracts, Chemical Titles, Chromatography Abstracts, Current Awareness in Biological Sciences (CABS), Current Contents/Life Sciences, Current Contents/Physical, Chemical & Earth Sciences, Deep-Sea Research/Part B: Oceanographic Literature Review, Excerpta Medica, Index Medicus, Mass Spectrometry Bulletin, PASCAL-CNRS, Referativnyi Zhurnal, Research Alert and Science Citation Index.

**US Mailing Notice.** *Journal of Chromatography A* (ISSN 0021-9673) is published weekly (total 52 issues) by Elsevier Science B.V., (Sara Burgerhartstraat 25, P.O. Box 211, 1000 AE Amsterdam, Netherlands). Annual subscription price in the USA US\$ 5389.00 (US\$ price valid in North, Central and South America only) including air speed delivery. Second class postage paid at Jamaica, NY 11431. **USA POSTMASTERS:** Send address changes to *Journal of Chromatography A*, Publications Expediting, Inc., 200 Meacham Avenue, Elmont, NY 11003. Airfreight and mailing in the USA by Publications Expediting.

**See inside back cover** for Publication Schedule, Information for Authors and information on Advertisements.

© 1994 ELSEVIER SCIENCE B.V. All rights reserved.

0021-9673/94/\$07.00

No part of this publication may be reproduced, stored in a retrieval system or transmitted in any form or by any means, electronic, mechanical, photocopying, recording or otherwise, without the prior written permission of the publisher, Elsevier Science B.V., Copyright and Permissions Department, P.O. Box 521, 1000 AM Amsterdam, Netherlands.

Upon acceptance of an article by the journal, the author(s) will be asked to transfer copyright of the article to the publisher. The transfer will ensure the widest possible dissemination of information.

*Special regulations for readers in the USA*—This journal has been registered with the Copyright Clearance Center, Inc. Consent is given for copying of articles for personal or internal use, or for the personal use of specific clients. This consent is given on the condition that the copier pays through the Center the per-copy fee stated in the code on the first page of each article for copying beyond that permitted by Sections 107 or 108 of the US Copyright Law. The appropriate fee should be forwarded with a copy of the first page of the article to the Copyright Clearance Center, Inc., 222 Rosewood Drive, Danvers, MA 01923, USA. If no code appears in an article, the author has not given broad consent to copy and permission to copy must be obtained directly from the author. The fee indicated on the first page of an article in this issue will apply retroactively to all articles published in the journal, regardless of the year of publication. This consent does not extend to other kinds of copying, such as for general distribution, resale, advertising and promotion purposes, or for creating new collective works. Special written permission must be obtained from the publisher for such copying.

No responsibility is assumed by the Publisher for any injury and/or damage to persons or property as a matter of products liability, negligence or otherwise, or from any use or operation of any methods, products, instructions or ideas contained in the materials herein. Because of rapid advances in the medical sciences, the Publisher recommends that independent verification of diagnoses and drug dosages should be made.

Although all advertising material is expected to conform to ethical (medical) standards, inclusion in this publication does not constitute a guarantee or endorsement of the quality or value of such product or of the claims made of it by its manufacturer.

Ⓢ The paper used in this publication meets the requirements of ANSI/NISO Z39.48-1992 (Permanence of Paper).

## CONTENTS

(Abstracts/Contents Lists published in *Analytical Abstracts*, *Biochemical Abstracts*, *Biological Abstracts*, *Chemical Abstracts*, *Chemical Titles*, *Chromatography Abstracts*, *Current Awareness in Biological Sciences (CABS)*, *Current Contents/Life Sciences*, *Current Contents/Physical, Chemical & Earth Sciences*, *Deep-Sea Research/Part B: Oceanographic Literature Review*, *Excerpta Medica*, *Index Medicus*, *Mass Spectrometry Bulletin*, *PASCAL-CNRS*, *Referativnyi Zhurnal*, *Research Alert* and *Science Citation Index*)

## REGULAR PAPERS

*Column Liquid Chromatography*

- Effect of bed compression on high-performance liquid chromatography columns with gigaporous polymeric packings  
by R. Freitag, D. Frey and C. Horváth (New Haven, CT, USA) (Received 25 July 1994) . . . . . 165
- Sorption kinetics and breakthrough curves for pepsin and chymosin using pepstatin A affinity membranes  
by S.-Y. Suen and M.R. Etzel (Madison, WI, USA) (Received 26 July 1994) . . . . . 179
- Experimental studies in metal affinity displacement chromatography of proteins  
by Y.J. Kim (Albany, NY, USA) and S.M. Cramer (Troy, NY, USA) (Received 19 July 1994) . . . . . 193
- Pharmaceutical application of liquid chromatography-mass spectrometry. II. Ion chromatography-ion spray mass spectrometric characterization of alendronate  
by X.-Z. Qin and E.W. Tsai (West Point, PA, USA), T. Sakuma (Toronto, Canada) and D.P. Ip (West Point, PA, USA) (Received 18 August 1994) . . . . . 205
- Determination of clavam-2-carboxylate in clavulanate potassium and tablet material by liquid chromatography-tandem mass spectrometry  
by C. Eckers and K.A. Hutton (Welwyn, UK), V. de Biasi (Harlow, UK), P.B. East and N.J. Haskins (Welwyn, UK) and V.W. Jacewicz (Tonbridge, UK) (Received 15 August 1994) . . . . . 213
- Reversed-phase high-performance liquid chromatographic separation of 1-naphthyl isocyanate derivatives of linear alcohol polyethoxylates  
by K. Lemr, M. Zanette and A. Marcomini (Venice, Italy) (Received 1 July 1994) . . . . . 219

*Gas Chromatography*

- Statistical treatment of large digital chromatographic data sets  
by D.C. Freeman and D.W. Byrd (Detroit, MI, USA) (Received 8 June 1994) . . . . . 225
- Automated static headspace sampler for gas chromatography  
by D.W. Byrd and D.C. Freeman (Detroit, MI, USA) (Received 8 December 1993) . . . . . 235
- Retention of halocarbons on a hexafluoropropylene epoxide-modified graphitized carbon black. III. Ethene-based compounds  
by T.J. Bruno and M. Caciari (Boulder, CO, USA) (Received 5 August 1994) . . . . . 245
- Identification of halogenated compounds produced by chlorination of humic acid in the presence of bromide  
by R.J.B. Peters and E.W.B. de Leer (Delft, Netherlands) and J.F.M. Versteegh (Bilthoven, Netherlands) (Received 1 August 1994) . . . . . 253
- Gas chromatographic determination of organochlorine and pyrethroid pesticides of horticultural concern  
by A.R. Fernandez-Alba, A. Valverde, A. Agüera and M. Contreras (Almería, Spain) (Received 13 June 1994) . . . . . 263
- Determination of nonylphenols as pentafluorobenzyl derivatives by capillary gas chromatography with electron-capture and mass spectrometric detection in environmental matrices  
by N. Chalaux, J.M. Bayona and J. Albaigés (Barcelona, Spain) (Received 11 August 1994) . . . . . 275

*Electrophoresis*

- Zone sharpening of neutral solutes in micellar electrokinetic chromatography with electrokinetic injection  
by K.R. Nielsen and J.P. Foley (Villanova, PA, USA) (Received 6 August 1994) . . . . . 283
- Enantiomeric differentiation of a wide range of pharmacologically active substances by capillary electrophoresis using modified  $\beta$ -cyclodextrins  
by A. Aumatell and R.J. Wells (Pymble, Australia) and D.K.Y. Wong (Sydney, Australia) (Received 4 July 1994) . . . . . 293

(Continued overleaf)

*Contents (continued)*

Preparative capillary zone electrophoresis of synthetic peptides. Conversion of an autosampler into a fraction collector  
by H.G. Lee and D.M. Desiderio (Memphis, TN, USA) (Received 29 August 1994) . . . . . 309

Separation of imidazole and its derivatives by capillary electrophoresis  
by C.P. Ong, C.L. Ng, H.K. Lee and S.F.Y. Li (Singapore, Singapore) (Received 1 August 1994) . . . . . 319

Speciation of heavy metals by capillary electrophoresis  
by C. Vogt and G. Werner (Leipzig, Germany) (Received 1 August 1994) . . . . . 325

**SHORT COMMUNICATIONS**

*Column Liquid Chromatography*

Synthesis and characterization of biospecific adsorbents containing glucose, usable to retain concanavalin A  
by C. Alvarez, H. Bertorello and M. Strumia (Córdoba, Argentina) and E.I. Sanchez (Chubut, Argentina) (Received  
2 August 1994) . . . . . 333

Combined pH gradient and anion-exchange high-performance liquid chromatographic separation of oligodeoxyribonu-  
cleotides  
by T. Lu and H.B. Gray, Jr. (Houston, TX, USA) (Received 14 July 1994) . . . . . 339

Ion-pair reversed-phase liquid chromatographic determination of dihydralazine  
by C. Laugel, P. Chaminade, A. Baillet and D. Ferrier (Châtenay-Malabry, France) (Received 30 August 1994). . . 344

*Column Liquid Chromatography and Gas Chromatography*

Determination of atropine and obidoxime in automatic injection devices used as antidotes against nerve agent intoxication  
by J. Pohjola and M. Harpf (Helsinki, Finland) (Received 17 August 1994) . . . . . 350

**AUTHOR INDEX** . . . . . 355

**NEWS SECTION** . . . . . 357

# Effect of bed compression on high-performance liquid chromatography columns with gigaporous polymeric packings<sup>☆</sup>

Ruth Freitag<sup>1</sup>, Douglas Frey<sup>2</sup>, Csaba Horváth\*

*Department of Chemical Engineering, Yale University, New Haven, CT 06520-8286, USA*

First received 29 March 1994; revised manuscript received 25 July 1994

## Abstract

The behavior of chromatographic columns packed with gigaporous, highly cross-linked styrenic particles was investigated for use in protein separation by reversed-phase chromatography at high flow velocities. Stainless-steel columns which were 3.5 or 7.5 cm long and had an inner diameter of 0.46 mm were slurry packed with 8 or 20 mm diameter spherical particles of 4000 Å mean pore size by using methanol as the packing fluid. It was found that the conditions employed during the packing process have a dramatic effect on the properties of such columns and that this can be attributed in part to the deformability of the particles. An increase in the packing pressure to approximately 6000 p.s.i. (41 MPa) resulted in a higher mass-transfer efficiency for the column with a concomitant decrease in permeability. This is ascribed to a decrease in the interstitial porosity with increasing packing pressure since the experimentally measured plate heights for these columns were found to agree quantitatively with theoretical predictions that relate changes in the interstitial porosity to intraparticle mass transfer. However, the theoretically derived relationship between porosity, permeability, and efficiency does not hold for columns packed at pressures higher than 6000 p.s.i., in which case the total column porosity was found to be high while the permeability and column efficiency were low. This behavior is explained by the formation of a low-porosity layer of highly compressed particles at the downstream end of the column during high pressure packing so that the assumption of axially uniform column properties used in the theoretical approach leads to very large errors.

## 1. Introduction

There is a growing need for rapid chromatographic separation of biopolymers such as proteins, nucleic acids and complex carbohydrates.

In conventional packed columns, the intrinsically low diffusivity of large molecules has limited the speed of separation due to the low rate of intraparticle mass transfer [1]. In order to circumvent this obstacle, pellicular stationary phases consisting of a fluid-impervious spherical support with a thin retentive layer have been introduced [2,3]. Because of the relatively low surface area available for adsorption with pellicular stationary phases, however, the use of such packings is restricted primarily to high-speed separations in analytical chromatography.

Recently, bidisperse gigaporous particles with

\* Corresponding author.

<sup>☆</sup> Presented in part at the 14th International Symposium on Column Liquid Chromatography, Boston, 1990.

<sup>1</sup> Present address: Institut für Technische Chemie der Universität, Hannover, Germany.

<sup>2</sup> Present address: Department of Chemical and Biochemical Engineering, University of Maryland Baltimore County, Baltimore, MD 21228, USA.

pore diameters on the order of 1000 Å have been introduced for protein chromatography [4,5]. It has been suggested that under appropriate conditions, intraparticle mass transfer is augmented by convective transport within the gigapores [6], so that even though mass transfer to the adsorptive surface in the smaller pores still occurs solely by molecular diffusion, the speed of protein separation is considerably enhanced [7,8]. The theoretical aspects of convective mass transfer within gigaporous stationary phases have been investigated [9–14] with particular regard to the enhancement of column efficiency at high flow velocities where intraparticle convection is expected to yield higher column efficiencies than those obtained with columns packed with conventional porous particles.

Highly cross-linked, polymeric stationary phases having large pores are emerging as an alternative to siliceous and polysaccharide-based stationary phases in liquid chromatography. They are stable in aqueous salt solutions over a wide pH range, which is a considerable advantage in protein chromatography where columns are frequently cleaned with strongly basic solutions. In contact with organic and hydro-organic solvents, however, polymeric stationary phases are less stable mechanically than silica-based sorbents. Solvation of the polymer leads to some swelling and thus softening of the support so that columns packed with porous polymeric particles cannot withstand the entire pressure range attainable with current HPLC equipment [15,16]. In particular, at sufficiently high pressures, bed compression occurs with a concomitant decrease in column permeability. This compression process consists of particles moving, becoming deformed, breaking, or being forced into the frit at the column outlet [17].

At moderate packing pressures, several investigators have observed bed compression, i.e., a reduction in the interstitial porosity, which has favorably affected column efficiency. For example, Hjertén and co-workers [18–22] found that a reduction in the interstitial void volume in columns packed with highly cross-linked agarose beads had a beneficial effect on column efficiency. The results were interpreted using an

equation introduced by Janson and Hedman [23] which relates the resolution to the ratio of the intraparticle and interstitial void volumes. Others have found that the efficiency of columns packed with styrenic particles increases in contact with mobile phases which cause particle swelling and have attributed this effect to a reduction in the amount of accessible micropores [24,25]. Meyer and Hartwick [26] investigated the relationship between column efficiency and packing pressure for narrow-bore columns packed with siliceous stationary phase particles and found evidence for the existence of an optimum column packing pressure. However, the authors made no attempt to explain this observation and presented no data concerning the interstitial porosities of the columns obtained at different packing pressures.

To date, we have not found data in the literature on the effect of bed compression in columns packed with polymeric gigaporous particles. This is rather surprising in view of the need to understand the relationship between the conditions for column packing and the magnitude of bed compression, as well as the effect of bed compression on column efficiency, in order to fully exploit the potential of gigaporous adsorbents in macromolecular chromatography.

## 2. Theory

### 2.1. Column efficiency

An efficient HPLC column is characterized by a small theoretical plate height,  $H$ . In order to facilitate the comparison of different packing materials, dimensionless values for the plate height and flow velocity are often used. The reduced plate height,  $h$ , is given by  $H/d_p$ , and the reduced velocity,  $\nu$ , also termed the Peclet number, is defined as  $ud_p/D_m$  where  $d_p$  is the particle diameter,  $u$  is the interstitial fluid velocity and  $D_m$  is the diffusion coefficient of the elute in the mobile phase. In the absence of kinetic resistances at the chromatographic surface, the total reduced plate height is the sum of three major independent contributions as follows [27–31]

$$h = h_{\text{disp}} + h_{\text{ext}} + h_{\text{int}} \quad (1)$$

In Eq. 1,  $h_{\text{disp}}$  expresses the combined effect of axial dispersion, longitudinal diffusion, flow maldistribution and extra column band-broadening and, in its simplest form, can be written as

$$h_{\text{disp}} = A + \frac{B}{\nu} \quad (2)$$

where  $A$  and  $B$  are constants.

For an unretained eluite, the plate height increment representing external mass-transfer resistances,  $h_{\text{ext}}$ , can be expressed using standard mass-transfer correlations as [14]

$$h_{\text{ext}} = \frac{(1 - \alpha)\epsilon^2\alpha^{5/3}}{3.27[\alpha + (1 - \alpha)\epsilon]^2} \cdot \nu^{2/3} \quad (3)$$

where  $\epsilon$  and  $\alpha$  are the intraparticle and interstitial porosities, respectively.

For an unretained eluite, the plate height increment arising from internal mass-transfer resistances in conventional porous particles is given as [29–31]

$$h_{\text{int}} = \frac{\theta\alpha(1 - \alpha)\epsilon}{30[\alpha + (1 - \alpha)\epsilon]^2} \cdot \nu \quad (4)$$

where  $\theta$  is the diffusional tortuosity in the pores of the particles.

Recently, Eq. 4 has been extended to account for convective mass transfer inside a gipaporous particle by defining an apparent diffusivity,  $D_{\text{app}}$ , which accounts for the effects of both diffusion and convection. Eq. 4 can therefore be modified to yield the following result [6,13,14,32]:

$$h_{\text{int}} = \frac{\theta'\alpha(1 - \alpha)\epsilon'D'_e}{30[\alpha + (1 - \alpha)\epsilon']^2 D_{\text{app}}} \cdot \nu \quad (5)$$

where  $D'_e$  is the effective diffusivity within the gigapores. Note that the symbols and nomenclature used in this study are identical to those used in Frey et al. [14]. Accordingly, a single prime in Eq. 5 denotes properties associated with the gigapores, e.g.,  $\epsilon'$  denotes the volume fraction of gigapores in the particle. On the other hand, in the equations below, a double prime denotes properties associated with the domains between the gigapores. These domains, which contain the

micropores, will be termed here the “subsidiary particles”.

As shown by Frey et al. [14], for small mass-transfer rates, a linear driving force approximation applies not only to intraparticle mass transfer by diffusion, but also to intraparticle mass transfer by convection. If these two approximations are compared, the following relation results for the apparent diffusion coefficient

$$\frac{D_{\text{app}}}{D'_e} = \left(1 + \frac{2\nu'}{45}\right) \cdot f \quad (6)$$

where  $\nu' = u'd'_p/D'_e$  and where the parameter  $f$ , which accounts for the diffusional resistance in the subsidiary particles, can be estimated as described in Ref. [33]. Under the restriction that linear driving forces apply for intraparticle mass transfer by both diffusion and convection, Eq. 6 is exact in the limit  $\nu' \rightarrow \infty$  and also accurately represent mass-transfer behavior for finite  $\nu'$  [14].

If it is assumed that the Carman–Kozeny equation (see Eq. 12) applies to both the flow inside the particle and in the region between particles, then the convective velocity in the gigapores,  $u'$ , can be related to the interstitial flow velocity,  $u$ , as [14]

$$\sqrt{\frac{u'}{u}} = \frac{d''_p}{d'_p} \cdot \frac{\epsilon'(1 - \alpha)}{\alpha(1 - \epsilon')} \quad (7)$$

where  $d'_p$  is the particle diameter, and  $d''_p$  is the diameter of the subsidiary particles, which is generally taken to be twice the diameter of the gigapore.

## 2.2. Packing of the column as a filtration process

Slurry packing of chromatographic columns is closely related to the process of filtration — a classical solid–liquid separation method that involves phenomena related to interfacial science, transport in porous media, rheology, fine particle technology and filtration theory [34–36]. The following treatment of the column packing process at constant pressure is based on widely used theories of filtration and assumes one-di-

dimensional geometry where only axial gradients in interstitial porosity exist.

The first step in the column packing procedure is the preparation of a stable suspension of the stationary phase in a suitable liquid. The solid content of such a slurry typically ranges from 5 to 20% (w/w). After the empty column tube is connected to the packing apparatus, a reservoir is filled with the packing liquid. The frit at the bottom of the tube serves as a “filter” which is permeable to the liquid, but impermeable to the stationary phase particles. The column tubing and the reservoir are filled with the slurry while the packing liquid is pumped through the column at constant pressure. As the packing process proceeds, the particles form a growing filter cake on the frit as the particles are deposited at the top of the packing and the liquid is forced through the interstices of the bed.

The drag force generated by the liquid flow on each particle is transmitted to the adjacent particles downstream. For simplicity, it is assumed here that the particles are in point contact, the liquid completely fills the voids between the particles and only axial pressure gradients exist. In this case, at any particular point in the bed, the total drag force on all the particles upstream from that point is exactly balanced by a compressive force at the point transmitted through the particles. Furthermore, the net force resulting from the pressure difference between any two column cross-sections equals the total drag force on the particles located between those cross-sections. This implies that

$$F(x) = [P - P_1(x)]A_c \quad (8)$$

where  $F(x)$  is the drag force on all the particles upstream from a point a distance  $x$  from the inlet,  $P_1(x)$  is the liquid pressure at  $x$ ,  $P$  is the applied packing pressure and  $A_c$  is the column cross-sectional area.

If the compressive force on the particles at a particular point is divided by the column cross-sectional area to yield an apparent pressure,  $P_s$ , it follows that

$$P_s(x) + P_1(x) = P \quad (9)$$

According to Eq. 9, the sum of the pressures on the solid particles and on the packing liquid is at every point in the column equal to the momentary gauge pressure,  $P$ , of the packing apparatus. In going towards the column outlet,  $P_1$  decreases while  $P_s$  increases.

Due to the pressure gradients developed during the packing process, the interstitial porosity and the linear flow velocity of the mobile phase will vary along the column axis. A logarithmic change in the interstitial porosity with bed height is often found in filter cakes formed at low pressures. However, due to the high pressures used in the packing of HPLC columns, the change in porosity is most likely represented by an exponential relationship of the form [37]

$$\alpha = \alpha_0 e^{-cP_s} = \alpha_0 e^{-c(P-P_1)} \quad (10)$$

where  $\alpha_0$  is the interstitial porosity in the absence of a drag pressure, and  $c$  is a constant. Differentiation of Eq. 10, assuming  $P$  is constant, yields

$$\frac{d\alpha}{dP_1} = -\alpha_0 c e^{-c(P-P_1)} \quad (11)$$

For spherical particles, the change in  $P_1$  with column length ( $L$ ) is given by the Carman-Kozeny equation [38] as follows

$$\frac{dP_1}{dL} = \eta u_s \cdot \frac{180(1-\alpha)^2}{\alpha^3 (d_p')^2} \quad (12)$$

where  $\eta$  is the viscosity of the packing fluid and  $u_s$  is the superficial flow velocity of the fluid.

In some cases, no simple relation is known for the dependence of the local interstitial porosity and the local pressure. For example, with highly compressible latex particles,  $\alpha$  changes little over the major part of the bed, but decreases rapidly adjacent to the filter [37]. Although an axially non-uniform bed structure of this type has a high average interstitial porosity, it exhibits a high flow resistance due to the formation of a very dense layer over the bottom frit. The preceding equations are unlikely to apply under these conditions. However, provided that these types of severe axial non-uniformities do not exist,



Eqs. 11 and 12 can be combined and integrated along the column length to yield an expression for the porosity as a function of distance from the column inlet.

### 3. Experimental

#### 3.1. Instrumentation

The liquid chromatograph consisted of a Model 100A precision metering pump (Beckman, San Ramon, CA, USA), a Model LC-85 B variable-wavelength detector (Perkin-Elmer, Norwalk, CT, USA) with a 1.4- $\mu$ l flow cell, a Model 7125 sampling valve (Rheodyne, Cotati, CA, USA) with a 5- $\mu$ l loop, and a Model B 41 stripchart recorder (Kipp & Zonen, Delft, Netherlands). The extracolumn dead volume was kept to a minimum by using a 0.12 mm I.D. capillary tube to connect the column to the injector and the flow cell of the detector.

#### 3.2. Columns and stationary phases

The columns were prepared by slurry packing 30, 50 and 75 mm long No. 316 stainless-steel tubes of 4.6 mm I.D. and 1/4 in. O.D. (1 in. = 2.54 cm). Highly cross-linked, gigaporous, spherical particles of 8 and 20  $\mu$ m diameter (PLRP-S), made by co-polymerization of styrene and divinylbenzene, were kindly donated by Polymer Labs. (Shropshire, UK). The average pore size of the particles used in this study was 4000 Å according to the manufacturer.

#### 3.3. Chemicals

Urea was obtained from Mallinckrodt (St. Louis, MO, USA), nitromethane from Fisher (Fair Lawn, NJ, USA). HPLC-quality acetonitrile, methanol and trifluoroacetic acid (TFA) were purchased from J.T. Baker (Phillipsburg, NJ, USA). Carbonic anhydrase from bovine erythrocytes and the tripeptide Phe-Gly-Gly were supplied by Sigma (St. Louis, MO, USA). Water was purified by a Barnsted Nanopure unit

(Boston, MA, USA). All eluents were filtered and degassed by sonification before use.

#### 3.4. Column packing procedure

The particles were dispersed by sonification in 5 ml methanol for the packing of 3- and 5-cm columns and in 10 ml methanol for that of the 7.5-cm columns. The solid content of the slurry was 10% (w/v). The column tubing with a 0.5- $\mu$ m frit at the bottom end was connected to the reservoir of the packing apparatus. The latter was assembled from a No. DSHF-302 air-driven fluid pump (Haskel, Burbank, CA, USA), a Craftsman 4 HP-20 air compressor, and a laboratory-made 50-ml packing reservoir from stainless steel No. 316 and rated to 25 000 p.s.i. (1 p.s.i. =  $6.8 \cdot 10^3$  Pa). The column tubing and the bottom part of the reservoir were filled with slurry, while the rest of the reservoir was filled with methanol. Methanol was pumped into the device from a fluid supply reservoir at a fixed pressure in the range from 1000 to 9000 p.s.i. The applied pressure was regulated within  $\pm 50$  p.s.i. In some cases the column was conditioned at the end of the packing procedure by pumping water through the bed for an additional 20 min at the packing pressure. At the end of the packing procedure, the column inlet and outlet pressures were allowed to equalize, and subsequently the column was disconnected from the apparatus. Finally, a stainless-steel frit was placed at the inlet end of the column.

#### 3.5. Chromatography

Experiments were performed by isocratic elution at room temperature with acetonitrile containing 30% (v/v) water and 0.1% (v/v) TFA as the mobile phase at room temperature. Under these conditions the eluents did not interact with the chromatographic surface and therefore traversed the column without retention. Samples were prepared by dissolving the eluite in the mobile phase to obtain concentrations between 1 and 3 mg/ml. The detection wavelength was 215 nm. The column inlet pressure during the chromatographic experiments was kept below the

packing pressure. Both the linear flow velocity and the volumetric flow-rate were monitored throughout the experiments. For the evaluation of plate heights, urea, nitromethane, L-phenylalanyl-L-glycyl-L-glycine and carbonic anhydrase were employed as non-retained elutes.

### 3.6. Measurement of permeability, porosity and packing density

The chromatographic flow velocity,  $u_c$ , was determined from the residence time,  $t_0$ , of an unretained elute [32]. Under the conditions employed in the study, urea and nitromethane were found to be suitable probes for this purpose. The packing density, i.e., the mass of stationary phase per unit column volume, was determined by carefully removing the packing material from the column and weighing it after drying. The average total porosity of the columns,  $\epsilon_T$ , was calculated from the relationship

$$\epsilon_T = \frac{t_0 F}{V_0} \quad (13)$$

where  $F$  is the volumetric flow-rate and  $V_0$  is the empty column volume. The specific column permeability,  $B^0$ , was evaluated as

$$B^0 = \frac{u_s \eta L}{\Delta P} \quad (14)$$

where  $\Delta P$  is the pressure drop across the column. Plate heights were determined from the peak widths measured at the peak half height. The diffusion coefficients for these calculations were either taken from the literature [39] or calculated using the Wilke–Chang equation [40].

## 4. Results and discussion

### 4.1. Properties of columns prepared at different packing pressures

According to Eq. 12, the flow-rate should increase linearly with the applied column inlet pressure as long as the permeability of the bed, i.e., the structure of the packing, remains con-

stant. Fig. 1 illustrates the volumetric flow-rate as a function of the column inlet pressure for 5-cm long columns packed with 20- $\mu\text{m}$  particles using a methanol slurry at various packing pressures. It is seen that the relationship between the flow-rate and inlet pressure is non-linear, indicating that the column permeability decreased significantly at high inlet pressures even though the operating inlet pressure never exceeded the packing pressure. In fact, the relationship between the flow-rate and inlet pressure is non-linear even at pressures well below the typical upper limit specified by manufacturers of columns containing polymeric particles. The change in permeability was, however, reversible, i.e., the column permeability at low flow-rates was the same, before and after exposure to high inlet pressures.

The behavior described above is likely due to the swelling of the polymeric particles in contact with the methanol used as the suspending and

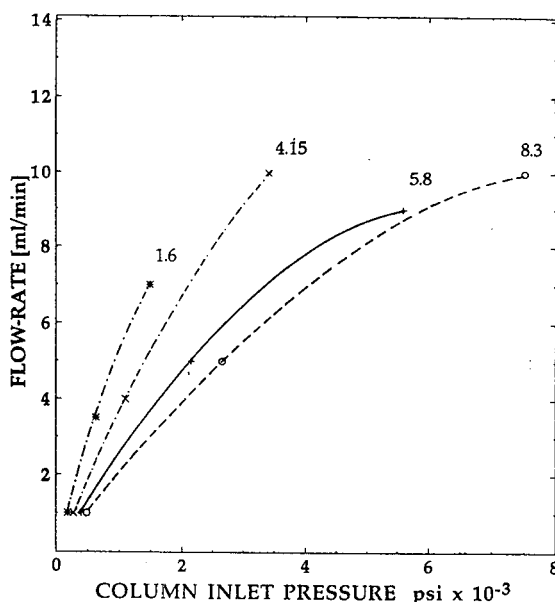


Fig. 1. The volumetric flow-rate as a function of the inlet pressure for columns packed at different pressures. The mobile phase was acetonitrile containing 30% (v/v) water and 0.1% trifluoroacetic acid. The 50 × 4.6 mm columns were slurry packed with 20- $\mu\text{m}$  gigaporous, styrenic particles at the packing pressures indicated. Methanol served as both slurry and packing fluid.

packing fluid [41]. The substitution of water for methanol would have circumvented this swelling problem; however, this substitution was not possible because the particles were poorly wetted by neat water, which precluded the preparation of a suitable slurry. A compromise method was attempted, however, in which the column was packed according to the protocol given above, and afterwards rinsed for 20 min with water at the packing pressure so that most of the methanol was removed and some shrinking of the particles occurred. In subsequent contact with the hydro-organic mobile phase, however, the particles took up the organic modifier and consequently the relationship between the inlet pressure and the flow-rate of aqueous acetonitrile for the columns conditioned with water was essentially the same as that depicted in Fig. 1.

The permeability and total porosity of the columns packed at different pressures with and without water conditioning were determined from the residence time,  $t_0$ , of urea at a flow-rate of 1 ml/min as described in the Experimental section. Typical data obtained with 5-cm long columns packed with 20- $\mu\text{m}$  particles and without water conditioning are illustrated in Fig. 2. The dependence of the density of the column packing on the packing pressure is also depicted in Fig. 2. The results show that while the column permeability decreases monotonically with the packing pressure, the total column porosity and the packing density go through a minimum and maximum, respectively. According to additional experiments (not shown here), the observed trends in the changing column properties with increasing packing pressure were independent of the column length or packing procedure.

Comparison of the results obtained with columns packed with or without water conditioning shows that water-conditioned columns have generally higher packing densities, and consequently lower total column porosities, than columns that were not subjected to water conditioning. In contradistinction, the permeability of water-conditioned columns tends to be higher than that of columns packed from methanol only. These trends are likely due to the swelling of the polymer particles in methanol. Presumably, the

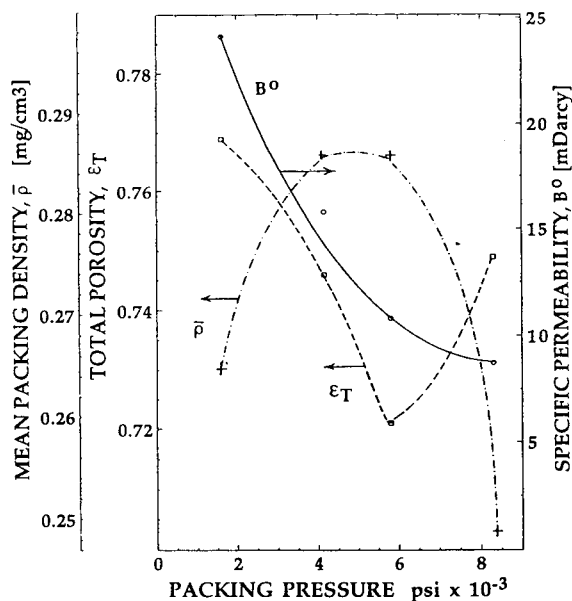


Fig. 2. The packing density,  $\rho$ , total column porosity,  $\epsilon_T$ , and specific permeability,  $B^0$ , as a function of the packing pressure for 50  $\times$  4.6 mm columns packed with 20- $\mu\text{m}$ , gigaporous, styrenic particles. Methanol was used as both the slurry and packing fluid. Urea was the unretained tracer and acetonitrile containing 30% (v/v) water and 0.1% TFA the mobile phase.

resulting deformation of these swollen particles accounts for the comparatively high flow resistance of unconditioned columns.

It is seen in Fig. 2, that up to a packing pressure of 6000 p.s.i. the dependence of column porosity and permeability on the packing pressure reflects the behavior predicted by Eqs. 12 and 14 in that both the porosity and permeability decrease with increasing packing pressure. However, for columns packed at pressures higher than 6500 p.s.i., the permeability of the column decreases, albeit at a lower rate, with increasing packing pressure, whereas the porosity of the column increases. This finding suggests that packing pressures higher than 6500 p.s.i. yield columns having a bed structure different from that of columns packed at lower pressures. This difference is not due to particle breakage during the packing procedure since an examination of the particles by scanning electron microscope gave no evidence of particle fragmentation.

Instead, the situation appears to be similar to the filtration behavior of certain compressible latex particles described earlier where the interstitial porosity changes little over the larger part of the bed, but decreases dramatically in the proximity of the filter proper [42]. As a result, the filter cake manifested not only a high average interstitial porosity, but also a high flow resistance. By analogy, the relatively low permeability of the column in our case also originates from a densely packed layer of particles at the top of the frit. Otherwise, most of the column contains a loose and highly porous packing, which would account for the observed behavior of the columns packed at the highest pressures.

For the column packings considered here, the total porosity is the only type of porosity directly measurable by chromatographic methods since we did not have access to an inert tracer with sufficiently large molecular dimensions to ensure its complete exclusion from all gigapores. However, the interstitial porosity can be estimated for a given column by measuring the pressure drop and flow-rate, and substituting those values into Eq. 12. The results are given in Table 1 for

Table 1  
Interstitial porosities of columns packed with gigaporous 20- $\mu\text{m}$  styrenic particles at different pressures using methanol as the slurry and packing fluid

| Column length<br>(cm) | Packing pressure<br>(p.s.i.) | Interstitial porosity |      |
|-----------------------|------------------------------|-----------------------|------|
|                       |                              | A                     | B    |
| 3                     | 1000                         | 0.18                  | –    |
| 3                     | 2000                         | –                     | 0.17 |
| 3                     | 2500                         | 0.16                  | –    |
| 3                     | 3500                         | 0.14                  | –    |
| 3                     | 5000                         | 0.13                  | 0.14 |
| 5                     | 1600                         | 0.19                  | –    |
| 5                     | 2000                         | –                     | 0.19 |
| 5                     | 4150                         | 0.17                  | –    |
| 5                     | 5800                         | 0.15                  | 0.17 |
| 7.5                   | 2000                         | –                     | 0.22 |
| 7.5                   | 2450                         | 0.20                  | –    |
| 7.5                   | 5000                         | –                     | 0.18 |
| 7.5                   | 5800                         | 0.17                  | –    |

A = Standard packing procedure; B = column conditioned with water after packing procedure.

packing pressures lower than 6000 p.s.i., where axial gradients in porosity appear to be relatively small, and Eq. 12 can be assumed to apply with reasonable accuracy.

In most cases, the apparent interstitial column porosities calculated by the above procedure are lower than 0.2, which is significantly less than the value of 0.35–0.40 normally observed for random packings of rigid spherical particles. It is known that the Carman–Kozeny equation does not apply accurately to a compressible bed, since it tends to underestimate the interstitial porosity in such cases [34]. The total porosities of the water-conditioned columns are lower than those of the corresponding unconditioned columns, whereas according to our calculations the reverse is true for the apparent interstitial column porosities. This would appear to indicate that the particles in the water-conditioned packing are less deformed than in the unconditioned bed.

As mentioned previously, the measurement of the average column porosity does not give information on the variation of the local interstitial porosity,  $\alpha$ , within the packed bed. In order to illustrate the type of porosity profiles expected in the bed, Eq. 12 was employed assuming a value of  $\alpha_0 = 0.2$  at the top of the column, and also assuming an exponential decrease in  $\alpha$  in terms of  $P_s$  over the length of the column according to Eq. 11. The change in local interstitial porosity with distance in a 5-cm column packed with 20- $\mu\text{m}$  particles was calculated by using a value for the constant  $c$  that gave interstitial porosity values closest to the pertinent experimental data. The results are presented in Fig. 3 to illustrate the effect of axial non-uniformity on the increase of the local porosity with the packing pressure for a given stationary phase.

#### 4.2. Column efficiency

In order to investigate the influence of the packing pressure on column efficiency, plate heights were measured at different flow velocities with carbonic anhydrase as the unretained tracer. Our main interest was in examining the plate height dependence on the flow velocity at high flow-rates where intraparticle mass trans-

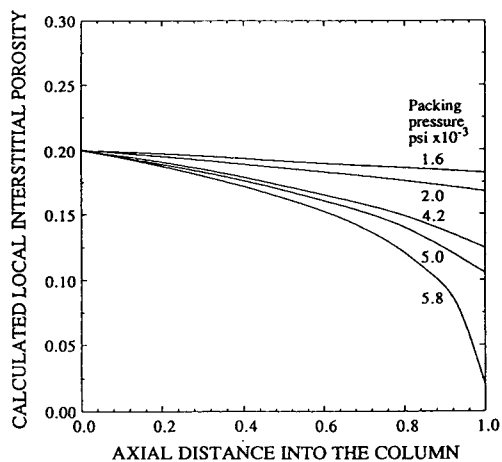


Fig. 3. Calculated local interstitial porosity as a function of axial distance in  $50 \times 4.6$  mm columns packed with  $20\text{-}\mu\text{m}$ , gigaporous, styrenic particles at different pressures as indicated. The axial profile of interstitial porosity was calculated using Eqs. 11 and 12 with  $\alpha_0 = 0.2$ .

fer dominates. The results obtained by using 5-cm long columns packed with  $20\text{-}\mu\text{m}$  particles in methanol at different packing pressures are depicted in Fig. 4 with the data points connected by solid lines. For several columns, the otherwise identical packing procedure was followed by the water-conditioning step. The plate heights obtained by these columns are also illustrated in Fig. 4 with the data points connected by broken lines. Similar behavior was observed with 7.5-cm columns packed in the same manner (data not shown). Inspection of the results presented in Fig. 4 suggests that, in general, the column efficiency increases with packing pressure up to about 6000 p.s.i., while a further increase in packing pressure results in lower efficiency. Furthermore, water-conditioned columns exhibit higher plate heights, i.e., lower efficiency in the flow-rate range studied, than those without this conditioning. This trend agrees with the calculations of the interstitial porosities from the Carman–Kozeny equation discussed earlier and again indicates that the water-conditioned packing is less deformed than the unconditioned packing.

Plate heights for 3-cm long columns packed with 8- or  $20\text{-}\mu\text{m}$  particles were also measured

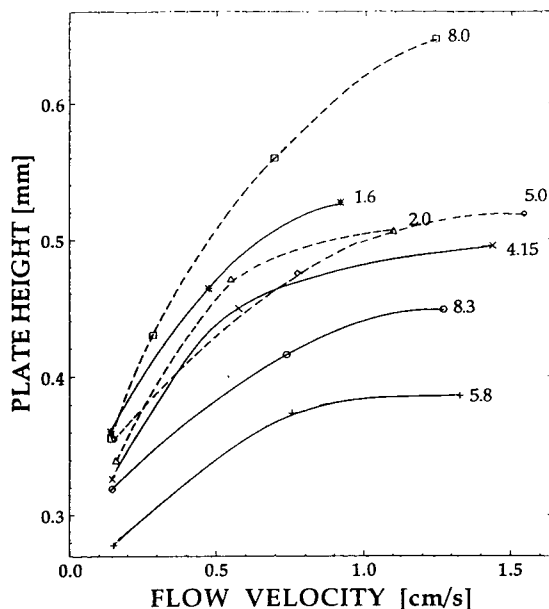


Fig. 4. The plate height as a function of the flow velocity measured with  $50 \times 4.6$  mm columns packed at different pressures. Carbonic anhydrase was used as an unretained tracer, and acetonitrile containing 30% (v/v) water and 0.1% trifluoroacetic acid as the mobile phase. Columns were packed with  $20\text{-}\mu\text{m}$ , gigaporous, styrenic particles from a methanol slurry at the pressures indicated in  $\text{p.s.i.} \times 10^{-3}$ . Methanol served as the sole packing fluid for the cases represented by solid lines. A subsequent, water-conditioning step was used in the cases represented by the broken lines.

with carbonic anhydrase under conditions of no retention in order to investigate the effect of particle size. The packing pressures were 3500 and 5000 p.s.i. for the  $8\text{-}\mu\text{m}$  particles and 2000 and 5000 p.s.i. for the  $20\text{-}\mu\text{m}$  particles, and all columns were conditioned with water at the end of the packing procedure. Fig. 5 illustrates the relation between the reduced plate height and the reduced velocity thus obtained. It can be seen that the column efficiency increases with the packing pressure for columns containing either particle size, and that columns packed with  $20\text{-}\mu\text{m}$  particles are more efficient in the terms of the reduced plate height in the Peclet number range considered than those packed with  $8\text{-}\mu\text{m}$  particles. This is likely due to the fact that the larger particles are less rigid than the smaller particles and therefore deform to a greater

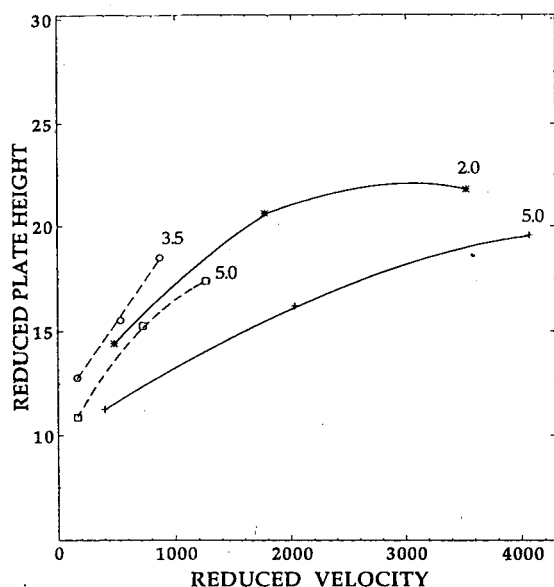


Fig. 5. The reduced plate height as a function of the reduced flow velocity measured with columns packed at different pressures. Columns were  $30 \times 4.6$  mm and packed with either 8- (broken line) or  $20\text{-}\mu\text{m}$  (solid line), gigaporous styrenic particles, from a methanol slurry and with methanol as the packing fluid at the pressures indicated in p.s.i.  $\times 10^{-3}$ . Mobile phase and inert tracer as in Fig. 4.

degree at a given packing pressure. Note that the permeability of columns packed with  $20\text{-}\mu\text{m}$  particles is higher than that of those packed with  $8\text{-}\mu\text{m}$  particles such that the former type of column can be operated at a higher flow-rate than the latter at a given column inlet pressure.

#### 4.3. Comparison of experimental data and theoretical calculations

According to Eqs. 3 and 5, the interstitial porosity of the column influences both  $h_{\text{ext}}$  and  $h_{\text{int}}$  in Eq. 1. In particular, provided that all other parameters are held constant, a decrease in interstitial porosity will reduce the magnitudes of both of these plate height contributions. More importantly, however, in the case of gigaporous particles there is an additional effect; namely, a decrease in the interstitial porosity may result in an increase in the amount of intraparticle fluid flow, and thereby in an enhancement of mass transfer inside the particles.

In order to assess the importance of this effect, as well as to see whether an expression for the plate height employing an average interstitial porosity for the bed can describe the overall column efficiency, Eqs. 5–7 were employed together with the apparent interstitial porosities from Table 1 to calculate the reduced plate height as a function of the flow-rate. In the application of Eqs. 5–7, the volume fraction of the particles occupied by the gigapores,  $\epsilon'$ , was assumed to be 0.4, and for the pore size the value of  $4000 \text{ \AA}$  reported by the particle supplier was used. As discussed above, interstitial porosities could not be calculated from Eq. 12 for columns packed at pressures greater than 6500 p.s.i. since those columns appeared to contain a dense layer of low permeability adjacent to the bottom frit. Thus, plate height calculations are not shown for those columns.

Figs. 6 and 7 illustrate both the experimentally measured and theoretically calculated reduced plate heights as a function of the reduced velocity for 5-cm long columns packed with  $20\text{-}\mu\text{m}$  particles with and without subsequent water conditioning. The calculations were performed as described above. In both figures, the reduced plate height calculated for unretained carbonic anhydrase are shown by solid lines, whereas the experimentally determined plate heights are represented by data points. As seen, the calculated values agree well with the experimental results for columns packed at pressures below 6000 p.s.i. This suggests that essentially all the improvement in the column efficiency with increasing packing pressure up to the optimal value is accounted for quantitatively by the effect of changes in interstitial porosity on the magnitude of interparticle convection. Furthermore, the degree to which the theoretical and experimental results agree in Figs. 6 and 7 lends further support to the assumptions underlying Eqs. 5–7, i.e., that intraparticle flow exists under the experimental conditions employed, that the fluid velocity in the particle can be described by an equation analogous to Eq. 12, and that the resulting effect on mass transfer can be described by Eq. 6. The treatment outlined here should also be applicable to other chromatographic

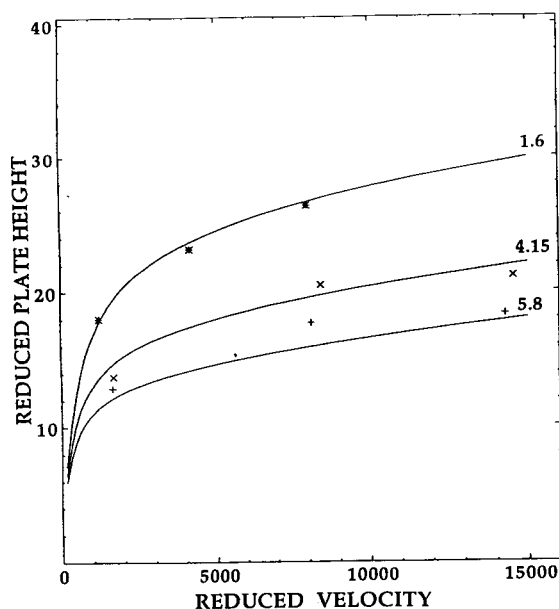


Fig. 6. The reduced plate height as a function of the reduced velocity for  $50 \times 4.6$  mm columns packed at different pressures as indicated in p.s.i.  $\times 10^{-3}$ , with methanol serving as both the slurry and the packing fluid. The mobile phase was acetonitrile containing 30% (v/v) water and 0.1% trifluoroacetic acid. Carbonic anhydrase was used as the inert tracer. The interstitial column porosities were evaluated from experimentally measured permeability data and used together with the parameters  $\epsilon' = 0.4$  and  $d_p'' = 8000 \text{ \AA}$  to calculate the solid lines using Eqs. 5-7. Experimental data are shown by the data points.

systems involving columns packed with deformable particles, such as those described by Hjertén and co-workers [18–22] who investigated the use of agarose particles in compressed beds.

## 5. Conclusions

In the practice of modern liquid chromatography, a wide variety of column packing materials are employed, including stationary phases based on organic polymer, silica or polysaccharide supports. These materials vary considerably in their physical properties so that the study described here does not represent all of the considerations that influence the effect of the

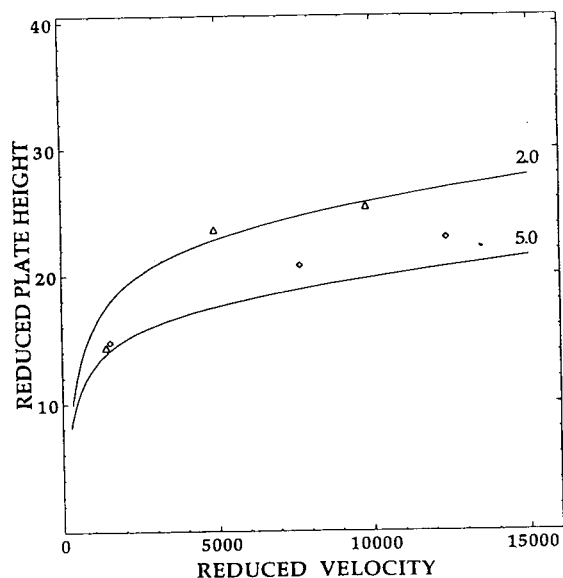


Fig. 7. The reduced plate height as a function of the reduced velocity for  $50 \times 4.6$  mm columns packed at different packing pressures as indicated in p.s.i.  $\times 10^{-3}$ , using methanol for the slurry and as the packing fluid. The packing process was followed by a water-conditioning step. The calculation of the lines and the measurement of the data points shown were carried out as in Fig. 6.

packing process on column efficiency. For a given type of packing material, the solvent used in the packing process should be chosen so that it wets the solid surface and has a density close to that of the solid in order to form a stable suspension. As shown in this study, however, another solvent property should also be considered; namely, the ability of the solvent to swell and therefore soften the support particles. In most cases, this type of softening is not desired since it complicates the packing processes. In contrast to this general rule, our results indicate that it may be possible to exploit this type of softening to produce a column which has a high mass-transfer efficiency at the expense of a greater pressure drop.

Although the various phenomena which underlie the effect of the packing conditions on the column efficiency can be difficult to quantify for a given system, we have shown that a relatively simple theoretical approach can be used to explain the effect of the packing pressure on

column efficiency for the particular case of gigaporous styrenic particles where intraparticle convection may facilitate the rate of mass transfer. In particular, we have shown that at moderate packing pressures an increase in the packing pressure leads to a reduction in the interstitial column porosity, which in turn leads to an increase in the magnitude of intraparticle fluid flow relative to the flow-rate. This enhancement of intraparticle convection then brings about a decrease in the plate height. However, as the packing pressure is increased above a certain optimal value, the column porosity becomes highly non-uniform due to the formation of a very dense layer of particles with a low porosity on the bottom frit of the column during the initial stages of the packing process, whereas the remainder of the column has a relatively high porosity. Such a column has a low overall permeability as well as a high average porosity so that its fluid mechanical and mass-transfer behavior cannot be described by a single average interstitial porosity.

### Acknowledgements

R.F. is grateful for the support by the Deutsche Forschungsgemeinschaft. The authors are indebted to F.P. Warren of Polymer Laboratories Ltd. for providing the bulk materials of the stationary phases and to A.S. Pooley of Yale University for providing the scanning electron microscopy data. This work was supported by grants No. GM 20993 from the National Institutes of Health US Public Health Service and No. BCS-9014119 from the National Science Foundation, and from the National Foundation of Cancer Research.

### References

- [1] Cs. Horváth and H.-J. Lin, *J. Chromatogr.*, 149 (1978) 43.
- [2] Cs. Horváth and S.R. Lipsky, *J. Chromatogr. Sci.*, 7 (1969) 109.
- [3] K. Kalghatgi and Cs. Horváth, *J. Chromatogr.*, 398 (1987) 335.
- [4] J.V. Dawkins, L.L. Lloyd and F.P. Warner, *J. Chromatogr.*, 352 (1986) 157.
- [5] L.L. Lloyd and F.P. Warner, *J. Chromatogr.*, 512 (1990) 365.
- [6] N.B. Afeyan, N.F. Gordon, I. Mazsaroff, L. Varady, S.P. Fulton, Y.B. Yang and F.E. Regnier, *J. Chromatogr.*, 519 (1990) 1.
- [7] N. Afeyan, S.P. Fulton, N.F. Gordon, I. Mazsaroff, L. Varady and F.E. Regnier, *Bio/Technology*, 8 (1990) 203.
- [8] S.P. Fulton, N. Afeyan, N.F. Gordon and F.E. Regnier, *J. Chromatogr.*, 547 (1991) 452.
- [9] A.E. Rodrigues, Z.P. Lu and J.M. Loureiro, *Chem. Eng. Sci.*, 46 (1991) 2765.
- [10] A.E. Rodrigues, J.M. Loureiro and R.M.Q. Ferreira, *Chem. Eng. Commun.*, 107 (1991) 21.
- [11] G. Carta, M. Gregory, D. Kirwan and H. Massaldi, *Sep. Technol.*, 2 (1992) 62.
- [12] A.I. Liapis and M.A. McCoy, *J. Chromatogr.*, 599 (1992) 87.
- [13] A.E. Rodrigues, *LC·GC*, 9 (1993) 273.
- [14] D. Frey, E. Schweinheim and Cs. Horváth, *Biotech. Prog.*, 9 (1993) 273.
- [15] K.A. Tweeten and T.N. Tweeten, *J. Chromatogr.*, 395 (1986) 111.
- [16] N. Tanaka, K. Hashizume and M. Araki, *J. Chromatogr.*, 400 (1987) 38.
- [17] F.B. Hutton, Jr., *Chem. Eng. Progr.*, 53 (1957) 328.
- [18] S. Hjertén, Z.-Q. Liu and D. Yang, *J. Chromatogr.*, 296 (1984) 115.
- [19] S. Hjertén, B.-L. Wu and J.-L. Liao, *J. Chromatogr.*, 396 (1987) 101.
- [20] S. Hjertén and J.-L. Liao, *J. Chromatogr.*, 457 (1988) 165.
- [21] S. Hjertén, J.-P. Li and J.-L. Liao, *J. Chromatogr.*, 475 (1989) 177.
- [22] S. Hjertén and D. Yang, *J. Chromatogr.*, 316 (1984) 301.
- [23] J.-Ch. Janson and P. Hedman, in A. Fichter (Editor), *Advances in Biochemical Engineering*, Vol. 25, Springer, Berlin, 1982, pp. 43–99.
- [24] M. Stuurman, J. Köhler, O. Jansson and A. Litzen, *Chromatographia*, 23 (1986) 341.
- [25] D.C. Shelly and Th.J. Edkins, *J. Chromatogr.*, 411 (1987) 185.
- [26] R.F. Meyer and R.A. Hartwick, *Anal. Chem.*, 56 (1984) 2211.
- [27] J.C. Giddings, *J. Chromatogr.*, 5 (1961) 61.
- [28] E. Grushka, L.R. Snyder and J.H. Knox, *J. Chromatogr. Sci.*, 13 (1975) 25.
- [29] Cs. Horváth and H.-J. Lin, *J. Chromatogr.*, 126 (1976) 401.
- [30] E. Kucera, *J. Chromatogr.*, 19 (1965) 237.
- [31] P. Schneider and J.M. Smith, *AIChE J.*, 14 (1968) 763.
- [32] A. Rodrigues, J. Lopes, Z.P. Lu, J. Loureiro and M. Dias, *J. Chromatogr.*, 590 (1992) 93.



- [33] H.W. Haynes and P.N. Sarma, *AIChE J.*, 19 (1973) 1043.
- [34] F.M. Tiller, *Filtr. Sep.*, 4 (1975) 386.
- [35] D.C. Shelly, V.L. Antonucci, Th.J. Edkins and T.J. Dalton, *J. Chromatogr.*, 458 (1989) 267.
- [36] D.C. Shelly and Th.J. Edkins, *J. Chromatogr.*, 411 (1987) 185.
- [37] R.S. Spencer, G.D. Gilmore, R.M. Wiley, *J. Appl. Phys.*, 21 (1950) 527.
- [38] P.C. Carman, *Trans. Inst. Chem. Eng.*, 16 (1938) 168.
- [39] H.A. Sober (Editor), *CRC Handbook of Biochemistry*, CRC Press, Cleveland, OH, 2nd ed., 1970, p. C-10.
- [40] C.R. Wilke and P. Chang, *AIChE J.*, 1 (1955) 264.
- [41] Y.-F. Maa and Cs. Horváth, *J. Chromatogr.*, 445 (1988) 71.
- [42] F.M. Tiller and T.C. Green, *AIChE J.*, 19 (1973) 1266.





ELSEVIER

Journal of Chromatography A, 686 (1994) 179–192

JOURNAL OF  
CHROMATOGRAPHY A

# Sorption kinetics and breakthrough curves for pepsin and chymosin using pepstatin A affinity membranes

Shing-Yi Suen<sup>a,1</sup>, Mark R. Etzel<sup>b,\*</sup>

<sup>a</sup>*Department of Chemical Engineering, 1415 Johnson Drive, University of Wisconsin, Madison, WI 53706-1619, USA*

<sup>b</sup>*Department of Food Science, 1605 Linden Drive, University of Wisconsin, Madison, WI 53706-1519, USA*

First received 24 May 1994; revised manuscript received 26 July 1994

## Abstract

Isotherms and kinetic parameters for pepsin and chymosin sorption to immobilized pepstatin A were measured in batch experiments. The measured single-solute parameters were used in an affinity-membrane model which included competitive sorption kinetics, axial diffusion and dead volume mixing. The predictions made using the affinity-membrane model matched the experimental breakthrough curves, whereas predictions made using local-equilibrium theory were a distinct mismatch. The performance of affinity-membrane separations was dominated by slow sorption kinetics.

## 1. Introduction

Among the bioseparation techniques available today, affinity separations are popular due to their simplicity and high degree of specificity. Conventionally, affinity separations are carried out in columns packed with porous beads to which the ligand is immobilized. The desired biomolecule adsorbs to the ligand via a specific binding recognition, and is separated from the solution. In general, the adsorption rate in columns is limited by either slow intraparticle diffusion for large beads, or low axial velocities and high pressure drops for small beads [1,2]. These limitations result in long cycle times or low throughputs, both of which are economically

unattractive. To overcome these limitations, affinity membranes, which utilize convection through the fine pores of the membrane, were recently introduced [2,3]. The advantages of adsorptive-membrane separations have been shown in previous experimental studies [3–7].

In our previous work [8,9], single-solute and multi-solute mathematical models were established to describe the performance of affinity membranes. The effects of axial diffusion, flow velocity and sorption kinetics on separation performance were discussed. It was found that axial diffusion, which is insignificant in affinity column separations, may dominate over convection at low flow-rates or for thin membranes. On the other hand, at high flow velocities, some solutes may pass directly through the membrane without binding due to slow sorption kinetics. Sorption kinetics were shown to dominate affinity-membrane performance. Slow sorption

\* Corresponding author.

<sup>1</sup> Present address: Department of Chemical Engineering, National Chung Hsing University, Taichung, Taiwan.

kinetics may explain the elution peak broadness for increased flow-rate reported by Briefs and Kula [3], and the reduction in ligand capture efficiency at high flow-rates presented by Nachman et al. [10]. Considering the extremes defined by the effects of axial diffusion and sorption kinetics, there should exist a suitable flow-rate range for optimal performance in affinity-membrane separations. Such an optimal flow-rate was found experimentally by Josić et al. [5], and supports these model predictions.

Our theoretical model was used to determine that a small variation in either thickness or porosity may cause a significant degradation in separation performance. As a result, the use of stacked membranes was proposed to avoid these problems. Josić et al. [5] and Liu and Fried [11] studied the influence of membrane thickness experimentally and verified this proposal. Kim et al. [12] indicated that the dispersion in their experimental breakthrough curves may be due to the effect of residence time distribution resulting from pore size distributions.

In 1994, Liu and Fried [11] adapted our theoretical model to analyze their experimental breakthrough curves using Cibacron Blue 3GA-cellulose affinity-membrane separations. However, they did not directly compare their experimental results with predictions from our theoretical model. Also in 1994, Serafica et al. [13] adapted our model to analyze their experimental breakthrough curves using metal chelate affinity membranes with a hollow-fiber geometry. The experimental and modeling results were in good agreement at low effluent concentrations, but showed a discrepancy at high concentrations. It should be noted that the above studies primarily concerned single-solute performance.

The binary-solute affinity-membrane model in our previous work [9] described competition and interference effects between solutes due to differences in either sorption kinetics or isotherms. The purpose of this study was to validate the affinity-membrane model using experimental results. The system of pepsin and chymosin was chosen for study. The sorption kinetic and equilibrium parameters of pepsin and chymosin to affinity membranes containing immobilized

pepstatin A were measured in batch adsorption experiments. These parameters were used in our affinity-membrane model to provide an independent and quantitative validation of the model by comparison to experimental breakthrough curves.

## 2. Affinity-membrane model

The equation of continuity for solute  $i$  was [8,9]:

$$\frac{\partial C_i}{\partial \tau} + \frac{\partial C_i}{\partial \zeta} + m_i \cdot \frac{\partial C_{s,i}}{\partial \tau} - \frac{1}{Pe_i} \cdot \frac{\partial^2 C_i}{\partial \zeta^2} = 0 \quad (1)$$

where axial diffusion was characterized by the axial Peclet number,  $Pe_i$ . Eq. 1 quantified changes in solute concentration with time due to solute convection, sorption and diffusion. For adsorption in the loading stage, the multi-solute Langmuir sorption model was used to describe the binding kinetics between solute  $i$  and the ligand:

$$m_i \cdot \frac{\partial C_{s,i}}{\partial \tau} = n_i \left[ C_i \left( 1 - \sum_j C_{s,j} \right) - \frac{C_{s,i}}{r_i - 1} \right] \quad 0 < \tau \leq \tau_w \quad (2)$$

where  $\tau_w$  is the time at which washing starts.

Two models were developed for the washing stage in affinity-membrane separations. First, association and dissociation were assumed to occur during washing. In this work, loading buffer was used as washing buffer. This presented the same environment for protein sorption during the washing stage as existed during the loading process. Therefore, the adsorption equation for loading was used for washing,

$$m_i \cdot \frac{\partial C_{s,i}}{\partial \tau} = n_i \left[ C_i \left( 1 - \sum_j C_{s,j} \right) - \frac{C_{s,i}}{r_i - 1} \right] \quad \tau > \tau_w \quad (3)$$

In the second model, no adsorption and desorption was assumed in the washing stage,

$$m_i \cdot \frac{\partial C_{s,i}}{\partial \tau} = 0 \quad \tau > \tau_w \quad (4)$$

The initial conditions were set such that there was no solute in the membrane:

$$C_i = 0 \text{ at } \zeta \geq 0, \tau = 0 \quad (5)$$

$$C_{s,i} = 0 \text{ at } \zeta \geq 0, \tau = 0 \quad (6)$$

In order to include axial diffusion at the front surface of the membrane, and instantaneous mixing at the exit of the membrane, Danckwerts' boundary conditions [14] for frontal chromatography were used:

$$C_i - \frac{1}{Pe_i} \cdot \frac{\partial C_i}{\partial \zeta} = 1 \text{ at } \zeta = 0, 0 < \tau \leq \tau_w$$

$$= 0 \text{ at } \zeta = 0, \tau > \tau_w \quad (7)$$

$$\frac{\partial C_i}{\partial \zeta} = 0 \text{ at } \zeta = 1, \tau > 0. \quad (8)$$

During the washing step, the second form of Eq. 7 was used wherein no protein was fed into the system. The PDASAC software package [15] was used to solve Eqs. 1–8.

### 3. Experimental

#### 3.1. Materials

Immobilon AV (IAV) affinity membranes were purchased from Millipore (Bedford, MA, USA). The average membrane pore size was  $0.65 \mu\text{m}$  [16]. The IAV membranes were cut into discs of 47 mm diameter. A membrane holder (Product No. 11101) was obtained from Amicon (Beverly, MA, USA). Porcine pepsin (P6887), pepstatin A (P4265), 1,6-hexanediamine (H2381) and dichlorotriazinylaminofluorescein (DTAF, D0531) were purchased from Sigma (St. Louis, MO,

USA). Recombinant chymosin (CHY-MAX) was a gift from Pfizer (Milwaukee, WI, USA). The buffer for loading and washing was  $0.01 M$  imidazole with  $1 M$  NaCl, pH 6 [17–19]. The elution buffer was  $0.01 M$  sodium phosphate, pH 12. Chymosin was dialyzed with 12 000 MWCO cellulose tubing (Sigma) against loading buffer to remove unwanted salts. Dialyzed chymosin was used directly without further concentration. All buffers and liquid solutions contained the preservative sodium azide 0.005% and were vacuum-filtered with  $0.2\text{-}\mu\text{m}$  filters (Supor 200; Gelman Sciences, Ann Arbor, MI, USA). Protein solutions were made with the loading buffer and filtered with  $0.45\text{-}\mu\text{m}$  filters (F9888, Sigma). All solutions were vacuum degassed prior to use.

#### 3.2. Properties of pepsin and chymosin solutions

The system studied in this work was soluble pepsin (EC 3.4.4.1) and chymosin (EC 3.4.4.15) bound to immobilized pepstatin A. Reasons for using this system were: (1) the biophysical properties of chymosin and pepsin are well-known [18,20–22] (see Table 1), (2) the equilibrium and kinetic properties of this system have been studied using gel beads [17–19], (3) binding to the ligand is monovalent [17–19] and (4) competitive and interactive sorption was exhibited for this system in our previous theoretical study of binary-solute affinity-membrane separations [9].

Pure and mixed solutions of chymosin and pepsin were held at pH 6 in order to prevent proteolysis and yet maintain affinity binding. Both pepsin and chymosin are acid proteases which are active only in acidic environment

Table 1  
Properties of pepsin and chymosin solutions

|  | Pepsin                      | Chymosin                     | Ref.   |
|--|-----------------------------|------------------------------|--------|
| $M_r$                                  | 34 500                      | 33 500                       | 18     |
| $E_{1 \text{ mg/ml}}^{280 \text{ nm}}$ | 1.44 (pH 6)                 | 1.16 (pH 6)                  | 18     |
| pI                                     | < 1.0                       | 4.5                          | 20     |
| $D_{20,w}$ ( $\text{cm}^2/\text{s}$ )  | $8.71 \cdot 10^{-7}$ (pH 6) | $8.5 \cdot 10^{-7}$ (pH 5.8) | 21, 22 |

[20,21]. Mixtures of pepsin and chymosin are stable between pH 5 and 6 [20]. Denaturation occurs rapidly at higher pH.

The stability of pure and mixed solutions of pepsin and chymosin at pH 6 was confirmed by HPLC analysis (data not shown). The HPLC system consisted of a pump (Model 2350; ISCO, Lincoln, NE, USA), a detector (Model V<sup>4</sup>, ISCO) and a size-exclusion column (300 mm × 7.8 mm Bio-Sil SEC-125 with 80 mm × 7.8 mm Bio-Sil SEC Guard; Bio-Rad, Hercules, CA, USA). Neither degradation nor aggregation was observed for pure pepsin, pure chymosin or the mixture, even after storage for several weeks at 4°C. In subsequent experiments, protein solutions were discarded after one month of storage at 4°C.

### 3.3. Immobilization of pepstatin A

The IAV membrane surface contains an imidazole moiety which is displaced by amino nucleophiles during immobilization to form a stable amide bond [16,23]. Using the diffusional immobilization method recommended by the manufacturer [24], 1,6-hexanediamine was coupled to the membrane. Pepstatin A was attached to the free amine group of 1,6-hexanediamine using the carbodiimide method of Fu [18], except that for membrane compatibility *n*-butanol was used as the solvent for pepstatin A. After being washed sequentially with *n*-butanol, ethanol, water and loading buffer, IAV membrane discs with immobilized pepstatin A were ready for use.

### 3.4. Batch adsorption experiments

Sorption kinetics and adsorption isotherms of pepsin and chymosin were measured in a batch system. All the experiments were conducted in clean 150-ml glass beakers at room temperature.

#### Adsorption isotherm

Fifteen IAV membranes with immobilized pepstatin A were incubated with 15 ml of protein solution having different concentrations. The incubation time was over 4 h for chymosin, and

over 6 h for pepsin. Final protein concentrations were determined from the measured absorbance at 280 nm using a spectrophotometer (Cary 1 UV-Vis; Varian Instrument Group, Sugarland, TX, USA) and the extinction coefficients are listed in Table 1.

#### Association rate constant determination

The association rate constant was determined at room temperature using 30 ml of protein solution at concentrations of 0.28 and 0.16 mg/ml for pepsin, and at 0.53 and 0.36 mg/ml for chymosin. The protein solution and 15 dry IAV membranes were added to a 150-ml beaker, then the beaker was covered with Parafilm and shaken by hand. Aliquots of 1 ml were removed at selected time intervals and analyzed for protein concentration, and then returned to the beaker.

#### Dissociation rate constant determination

Proteins were labeled with the fluorescent reagent DTAF using labeling procedures from Fu [18]. The labeled protein was separated from the unreacted fluorescent reagent using a gel-filtration column (XK 26/40; Pharmacia, Piscataway, NJ, USA) packed with Sephacryl beads (S-200-HR, Sigma). The column was connected to an absorbance detector set at 280 nm (UA-5, ISCO), a fluorescence detector with a 490-nm filter for excitation and a 510–650-nm filter for emission (FL-2, ISCO), and a pump consisting of a speed-controlled motor (Model 7520-25; Cole-Parmer, Chicago, IL, USA) driving a positive-displacement pump head (Model RH0CKC; Fluid Metering, Oyster Bay, NY, USA). The purified labeled protein solutions were filtered with 0.45- $\mu$ m filters prior to use.

The 15 dry IAV membranes were incubated with 15 ml of fluorescently labeled protein solution in a beaker overnight. The equilibrium concentration of the incubated labeled protein solution was determined using the spectrophotometer, and the membranes were then washed with washing buffer to remove unbound protein. Washing was conducted using the flow system which will be described in the next section. When the effluent absorbance from the flow system

reached a stable value, washing was stopped. An aliquot of 20 ml of unlabeled protein solution at a concentration 10 times the equilibrium concentration was added to a clean 150-ml beaker by pipette. The washed and wet membranes were then immersed into the beaker containing unlabeled protein solution. The contents of the beaker were mixed by manual shaking. A 2-ml sample was taken for fluorescence analysis at each time increment and then returned to the beaker. The protein solution was analyzed using a fluorometer (Deltascan Model 4000; Photon Technology International, South Brunswick, NJ, USA) and excitation and emission wavelengths of 492 and 513 nm, respectively.

### 3.5. Flow experiments

The equipment for the flow experiments included the positive-displacement pump described above, the Amicon membrane holder, an absorbance detector with a built-in chart recorder (UA-5, ISCO) and a datalogger (Model 50; Electronic Controls Design, Milwaukie, OR, USA). A fraction collector (Retriever II, ISCO) was used to collect effluent samples for the binary-solute separations. All experiments were conducted at room temperature.

The membrane holder was assembled from the bottom up in the order [25]: bottom part of the holder, screen, 4 regenerated cellulose (RC) membranes, 15 IAV membranes, 4 RC membranes, O-ring and finally the top part of the holder. The RC membranes (SM11607; Sartorius, Bohemia, NY, USA) served as flow distributors, and had a pore size of 0.2  $\mu\text{m}$  and a thickness of 80  $\mu\text{m}$ . The top part of the holder was screwed very tightly into the bottom part to compress the O-ring, which prevented fluid from leaking laterally towards the wall of the housing. Prior to experiments, air bubbles trapped in the holder were eliminated using the built-in vent in the top part of the holder while pumping buffer through the holder.

To determine the flow-rate, the effluent solution was collected through the loading stage in the single-solute experiment. The mass of the collected solution was measured and was con-

verted to volume. The density of protein solution was 1.03 g/ml. The calculated loading volume divided by the loading time (collecting time) was equal to the flow-rate. The same procedure was repeated several times to assure the accuracy of the measured flow-rate. In the binary-solute experiments, the same pump settings as in the single-solute experiments were used to achieve the desired flow-rate.

### *Non-adsorption breakthrough curve measurement*

The effect of dead volume mixing in the flow system was determined by measuring the breakthrough curve for a feed solution in which the protein did not adsorb to the membranes. The 15 IAV membranes were inserted as a stack into the membrane holder, sandwiched between the 8 RC membranes. The non-adsorbing solution for this experiment was 0.4 mg/ml pepsin in 0.1 M sodium phosphate pH 9.7 buffer. Pepsin was denatured at this pH and did not bind to the immobilized ligand. The volume loaded was 42 ml at a flow-rate of 1 ml/min. The washing buffer was 0.1 M sodium phosphate pH 9.7.

### *Breakthrough curve measurement*

The membrane discs (4 RC/15 IAV/4 RC) were placed in the holder and equilibrated with loading buffer. In the single-solute experiments, 97 ml of protein solution were pumped through the membrane holder at flow-rate of 1 ml/min. The feed solutions were 0.4 mg/ml pepsin or 0.4 mg/ml chymosin. The protein absorbance was detected at 280 nm, and recorded by the datalogger. After loading, about 20 ml of washing buffer were pumped through the discs until the absorbance returned to baseline. Elution buffer (0.01 M sodium phosphate, pH 12) was used to elute the bound protein from the membranes. A higher flow-rate (4 ml/min) was used for elution because the elution buffer had a higher pH than the recommended pH range (4–10) for IAV membranes [24]. Elution was stopped when the absorbance returned to baseline. Because it was difficult to elute chymosin from membranes using only elution buffer, membranes containing bound chymosin were rinsed with more than 40

ml of 10 mg/ml pepsin in 0.5 M glycine buffer pH 3 until the breakthrough curve reached a stable value. At this pH, pepsin binds to pepstatin A very strongly and displaces all the bound chymosin from the membranes. Then, elution buffer was used to completely remove pepsin from the membranes. Lastly, loading buffer was used to rinse the membranes after elution. The membranes were stored in the holder for a short time period when experiments were conducted, and were stored in a clean 150-ml beaker with the loading buffer for longer time periods.

In the binary-solute experiments, two feed solution concentrations were used: either 0.1 mg/ml pepsin and 0.4 mg/ml chymosin, or 0.4 mg/ml pepsin and 0.1 mg/ml chymosin. Flow-rates of 1 ml/min were used with the same experimental setup as that in the single-solute experiments. In the loading stage, 97 ml of the protein mixture were pumped through the membrane cartridge. In the washing stage, 20 ml washing buffer were loaded. The fraction collector was employed to collect 2-ml fractions of effluent solution. The effluent fractions and the feed solution were analyzed by HPLC. The HPLC system, described above, was calibrated at 280 nm using samples of pure protein solutions at selected concentrations. The volume of the HPLC injection loop was 50  $\mu$ l. The mobile phase was 0.002 M  $\text{Na}_2\text{HPO}_4$ , 0.005 M  $\text{Na}_2\text{SO}_4$ , 0.1 M KCl with 0.005%  $\text{NaN}_3$ , pH 6.2 [26]. The mobile-phase flow-rate was 1 ml/min. The elution procedure for the mixture of pepsin and chymosin is the same as that for chymosin. First, membranes in the flow system were loaded with 10 mg/ml pepsin in 0.5 M glycine buffer pH 3 until the breakthrough curve reached a stable value. Then, 0.01 M sodium phosphate pH 12 elution buffer was used to completely remove pepsin from membranes. Lastly, loading buffer was used to rinse and store the membranes.

## 4. Results

### 4.1. Batch performance

#### Single-solute adsorption isotherm

The experimental adsorption isotherms for

pure pepsin and chymosin are plotted in Fig. 1. The bound protein concentration based on solid membrane volume ( $c_s$ ) was plotted against the free protein concentration in solution ( $c$ ) at equilibrium. To determine the dissociation equilibrium constant ( $K_d$ ) and maximum binding capacity ( $c_1$ ), these data were fitted to the single-solute Langmuir isotherm equation

$$c_s = \frac{cc_1}{K_d + c} \quad (9)$$

The fitted values were:  $K_d = 9(2) \cdot 10^{-6}$  M and  $c_1 = 2.3(0.1) \cdot 10^{-4}$  M for pepsin;  $K_d = 4(1) \cdot 10^{-6}$  M and  $c_1 = 2.9(0.2) \cdot 10^{-4}$  M for chymosin, where values in parentheses indicate the standard error.

#### Single-solute association

The association rate data are presented in Fig. 2. To determine the association rate constant

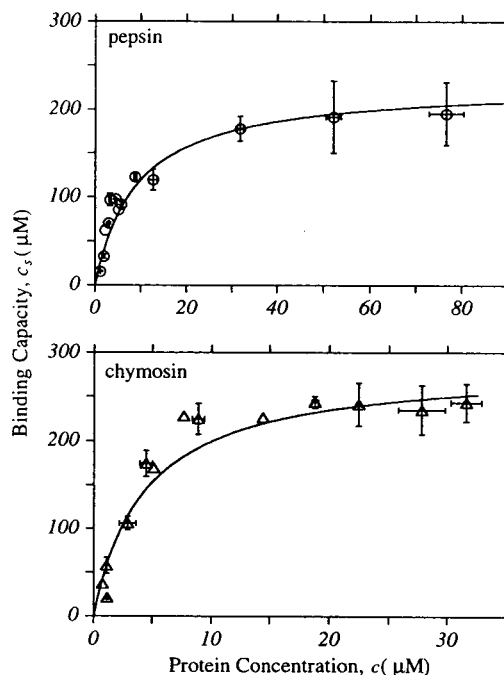


Fig. 1. Single-solute adsorption isotherms for pepsin (O) and chymosin ( $\Delta$ ) using 15 IAV membranes. The loading buffer was 0.01 M imidazole with 1 M NaCl at pH 6. The data were fitted by least-squares to Eq. 9 and plotted as solid lines. Error bars span 2 S.D., and points without error bars were measured in only one trial.



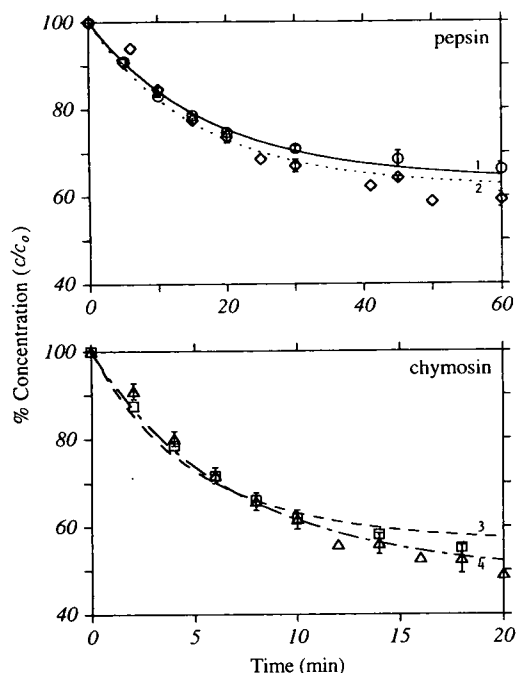


Fig. 2. Single-solute association curves using 15 IAV membranes. For pepsin, the feed solution concentrations were 0.28 mg/ml ( $\circ$ ) and 0.16 mg/ml ( $\diamond$ ). For chymosin, the feed solution concentrations were 0.53 mg/ml ( $\square$ ) and 0.36 mg/ml ( $\triangle$ ). The data were fitted by least-squares to Eq. 10:  $c_0 = 0.28$  mg/ml pepsin (curve 1),  $c_0 = 0.16$  mg/ml pepsin (curve 2),  $c_0 = 0.53$  mg/ml chymosin (curve 3) and  $c_0 = 0.36$  mg/ml chymosin (curve 4).

( $k_a$ ), the data were fitted to the Langmuir kinetic equation [27]

$$\frac{c}{c_0} = 1 - \frac{2c_1 \sinh\left(\frac{\hat{V}G}{2} \cdot k_a t\right)}{G \cosh\left(\frac{\hat{V}G}{2} \cdot k_a t\right) + B \sinh\left(\frac{\hat{V}G}{2} \cdot k_a t\right)} \quad (10)$$

where

$$B = \frac{c_0}{\hat{V}} + c_1 + \frac{K_d}{\hat{V}} \quad (11)$$

$$G = \left(B^2 - \frac{4c_0c_1}{\hat{V}}\right)^{1/2} \quad (12)$$

$$\hat{V} = \frac{(1 - \epsilon)(\text{total membrane volume})}{(\text{experimental solution volume})} \quad (13)$$

The fitted values were: for pepsin,  $k_a = 43(4) M^{-1} s^{-1}$  when  $c_0 = 0.28$  mg/ml, and  $k_a = 49(8) M^{-1} s^{-1}$  when  $c_0 = 0.16$  mg/ml; and for chymosin,  $k_a = 150(30) M^{-1} s^{-1}$  when  $c_0 = 0.53$  mg/ml, and  $k_a = 127(8) M^{-1} s^{-1}$  when  $c_0 = 0.36$  mg/ml. Four equilibrium points were obtained from these association experiments, and plotted in the corresponding adsorption isotherms of Fig. 1.

The time scales for protein diffusion to and association with the ligand were calculated and compared. The time scale for protein diffusion was  $l^2/D$  [28]. The diffusion path length ( $l$ ) was  $70 \mu\text{m}$ , one half the thickness of an individual membrane. Thus, the time scale for protein diffusion was 0.9 min for both pepsin and chymosin. The average time scale for protein association with the ligand ( $1/k_a c_0$ ) was 70 min for pepsin, and 10 min for chymosin. The time scale for protein diffusion was negligible in comparison to the time scale for protein association with the ligand.

#### Single-solute dissociation

The dissociation rate data were fitted to a first-order kinetic equation [1,27]

$$F = F_{\max}(1 - e^{-k_d t}) \quad (14)$$

where  $F$  was the measured fluorescence in the solution over time, and  $F_{\max}$  was the maximum fluorescence attained at long time. To normalize each experimental data set in terms of  $F/F_{\max}$  (%), the data were fitted to Eq. 14 to determine  $F_{\max}$ . Then  $F/F_{\max}$  was plotted in Fig. 3, and the data were fitted to Eq. 14 to determine  $k_d$ . The fitted values were:  $k_d = 4.5(0.7) \cdot 10^{-4} s^{-1}$  for pepsin and  $k_d = 6.1(0.8) \cdot 10^{-4} s^{-1}$  for chymosin. These values of  $k_d$  along with the experimentally determined dissociation equilibrium constant were used to calculate values for  $k_a$  ( $= k_d/K_d$ ) of  $50 M^{-1} s^{-1}$  for pepsin and  $150 M^{-1} s^{-1}$  for chymosin. The calculated values of  $k_a$  were within one standard error of the values determined from the data of Fig. 2.

The time scale for protein diffusion (0.9 min)

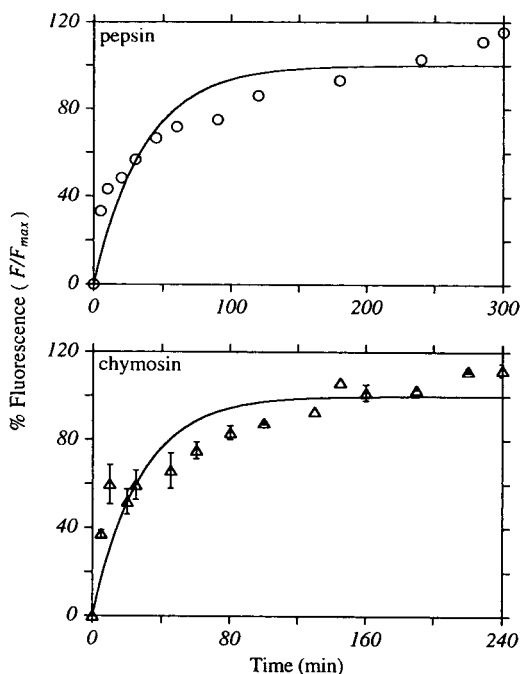


Fig. 3. Single-solute dissociation curves using 15 IAV membranes. The membranes were equilibrated with the fluorescently labeled protein solution first, and then excess unlabeled protein was used to displace the bound labeled protein. Eq. 14 was used to determine the  $F_{\max}$  and  $k_d$  values, and the fitted curves are presented as solid lines for pepsin (○) and chymosin (△).

was negligible compared to the average time scale for protein dissociation ( $1/k_d$ ) of 30 min.

#### 4.2. Breakthrough curves

##### Non-adsorption experiments

The breakthrough curve for a non-adsorbing feed solution at a flow-rate of 1 ml/min is presented in Fig. 4. There were delay volume and dead volume mixing effects evident in the breakthrough curves. To simplify the model for this behavior, a model of one plug-flow reactor (PFR) plus one continuous stirred-tank reactor (CSTR) was used as described in the work of Raths [29] on dead volume mixing in an ion-exchange membrane cartridge. The CSTR model was

$$V \cdot \frac{dc_{\text{out}}}{dt} = Q(c_{\text{in}} - c_{\text{out}}) \quad (15)$$

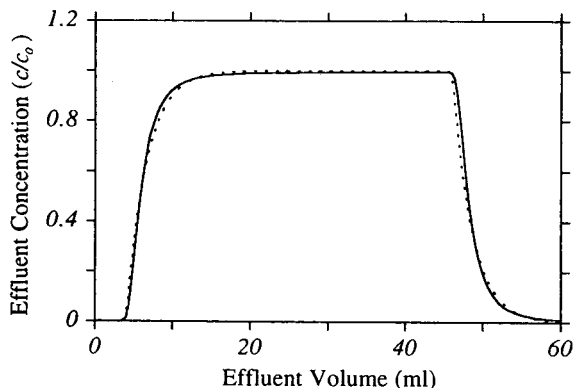


Fig. 4. Non-adsorption breakthrough curves at 1 ml/min for 4 RC/15 IAV/4 RC membranes. Solid line = experimental data; dotted line = model prediction. The model included a plug-flow volume of 2.55 ml for the affinity membranes, a CSTR mixing volume of 2.6 ml, and a plug-flow volume of 1.45 ml for the remainder of the system.

where  $V$  is the CSTR volume,  $Q$  is the flow-rate through the CSTR,  $c_{\text{in}}$  is the inlet concentration, and  $c_{\text{out}}$  is the outlet concentration. The plug-flow model accounted for a delay time ( $t_{\text{delay}}$ ) such that at  $t < t_{\text{delay}}$  the effluent concentration from the system was zero, and at  $t \geq t_{\text{delay}}$  the effluent concentration was equal to  $c_{\text{out}}$  at the time  $t - t_{\text{delay}}$ .

The first temporal moment method was used to determine  $V$  and  $t_{\text{delay}}$  [30]. The mean time the fluid spent in the experimental system was

$$t_{\text{1st moment}} = \frac{M_1 - \mu_1}{M_0} \quad (16)$$

where  $M$  is the moment of effluent concentration and  $\mu$  is the moment of inlet concentration.

The mean residence volume ( $Qt_{\text{1st moment}}$ ) consists of all the postulated dead volumes in the membrane system. From Fig. 4, the calculated mean residence volume was 6.6 ml, and the delay volume was 4 ml. Therefore, by difference the CSTR volume was 2.6 ml. The void volume of 15 IAV membranes was 2.55 ml, leaving 1.45 ml as the remaining PFR volume of the system. Accordingly, the dead volume mixing model consisted of 2.55 ml PFR volume for the affinity membranes, 1.45 ml PFR volume for the remainder of the flow system, and 2.6 ml CSTR

volume. The result of the dead volume mixing model was plotted in Fig. 4. The model predictions were nearly identical to the experimental results.

#### *Parameter values used in the affinity-membrane model*

The values for the membrane parameters were taken from the manufacturer [16,24]. The porosity,  $\epsilon$ , was 0.7, and the individual IAV membrane thickness,  $L$ , was 140  $\mu\text{m}$ . In this work, 15 membranes were stacked together, resulting in a total thickness of 0.21 cm. The flow-rate used in this work was 1 ml/min. Consequently, using the membrane diameter of 47 mm, the interstitial flow velocity passing through the membrane pores,  $\nu$ , was  $1.37 \cdot 10^{-3}$  cm/s. The single-solute isotherm parameters were:  $K_d = 9 \cdot 10^{-6}$  M and  $c_1 = 2 \cdot 10^{-4}$  M for pepsin;  $K_d = 4 \cdot 10^{-6}$  M and  $c_1 = 3 \cdot 10^{-4}$  M for chymosin, as determined experimentally (Fig. 1). The association rate constants were:  $k_a = 50 \text{ M}^{-1} \text{ s}^{-1}$  for pepsin and  $k_a = 150 \text{ M}^{-1} \text{ s}^{-1}$  for chymosin, based on experimental results (Fig. 2). The dimensionless number of transfer units ( $n$ ) was calculated from these values:  $n = 0.66$  for pepsin and  $n = 2.95$  for chymosin. The dissociation rate constant was calculated from  $k_d = k_a K_d$ .

The dimensionless separation factor ( $r$ ) was: 1.3 for 0.1 mg/ml pepsin, 2.3 for 0.4 mg/ml pepsin, 1.7 for 0.1 mg/ml chymosin and 4.0 for 0.4 mg/ml chymosin. The four initial concentrations used experimentally yield dimensionless saturation capacities ( $m$ ) of 30 (0.1 mg/ml pepsin), 7 (0.4 mg/ml pepsin), 43 (0.1 mg/ml chymosin) and 11 (0.4 mg/ml chymosin), respectively, using the values of  $\epsilon$  and  $c_1$  described above.

The axial Peclet numbers ( $Pe$ ) were calculated from the diffusion coefficients (Table 1) and the above values of the parameters  $\nu$  and  $L$ , and were: 330 for pepsin and 340 for chymosin.

The model calculations were performed in sequence. First, the affinity-membrane model, Eqs. 1–8, was solved using the PDASAC software package. This yielded the breakthrough curves which included only the effects of slow

and competitive sorption kinetics, and axial diffusion. The effluent concentrations were then used as the inlet concentrations for the CSTR mixing model, Eq. 15, which was solved using a finite-difference method. This included the effects of dead volume mixing into the breakthrough curves from the affinity-membrane model. Lastly, the PFR model was used to shift the results to longer times. This accounted for the delay time which resulted from plug flow through the dead volume in the flow system. The final result of the calculations was breakthrough curves which included the effects of slow and competitive sorption kinetics, axial diffusion, and CSTR mixing and plug flow in the dead volume of the flow system.

#### *Single-solute breakthrough curves including adsorption*

Experimental single-solute breakthrough curves at a flow-rate of 1 ml/min are shown in Fig. 5. For pepsin, protein first appeared in the effluent at an effluent volume of 2.5 ml. The effluent concentration rose quickly to 80% of the feed solution concentration after 20 ml effluent volume, and then increased slowly towards the feed solution concentration. The breakthrough curve for chymosin had a front shoulder after emerging at an effluent volume of 4.5 ml. The effluent concentration increased to 30% of the feed solution concentration at 20 ml effluent volume, and then increased to 80% at 30 ml effluent volume.

In Fig. 5, the curves predicted from the model were in close agreement with the experimental curves early on, but the model curves fell somewhat below the experimental curves in the range of 20 to 40 ml effluent volume. After 80 ml effluent volume, both the model and experimental curves approached the feed solution concentration. However, the model curves reached the level of the feed solution concentration, and the experimental curves fell slightly short of this level. Generally, the differences between the predictions and the experimental data were small. The predictions of the model were sensitive to doubling and halving the values of the parameters used for the sorption isotherm and

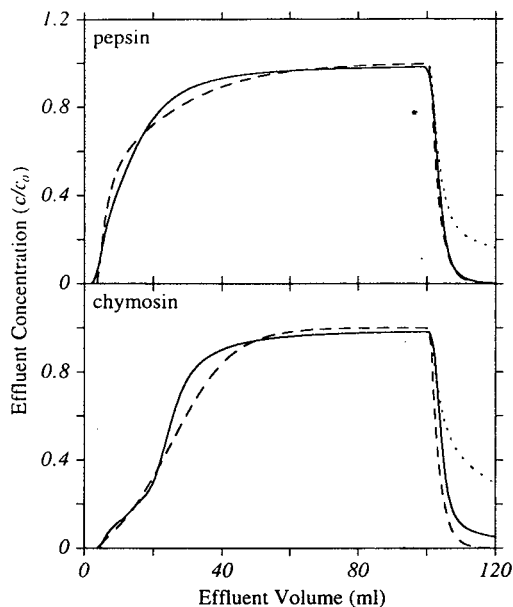


Fig. 5. Single-solute breakthrough curves for pepsin and chymosin at 1 ml/min. The measured curves (solid lines) were plotted along with predictions from the model (broken lines). Two washing models were used: without sorption during washing (broken lines) and with sorption during washing (dotted lines).

kinetics (results not shown). Values different than the experimentally determined values produced inaccurate model predictions.

In Fig. 5, the washing curves predicted using the model with sorption (Eq. 3) contained a long tail due to protein dissociation. The curves predicted using the model without sorption (Eq. 4) predicted fast washing, which more closely resembled the experimental curves. The washing process in affinity-membrane separations was best described by neglecting protein sorption kinetics.

#### *Binary-solute breakthrough curves including adsorption*

Experimental binary-solute breakthrough curves are presented in Figs. 6d and 7d. In both experiments, pepsin appeared first in the effluent. After an additional 5 ml of effluent volume, chymosin appeared in the effluent. Chymosin had a sharper breakthrough curve

when its concentration was elevated compared to pepsin as shown in Fig. 6d.

The breakthrough curves were compared with the predictions of the model. The equilibrium and kinetic parameters used in the model were the same as those used for the single-solute breakthrough curves (Fig. 5). For both feed solution compositions, the predicted curves fitted the experimental data well.

#### *Affinity-membrane model and local-equilibrium theory*

In Figs. 6 and 7, model predictions using (a) local-equilibrium theory, (b) local-equilibrium theory with CSTR mixing, (c) affinity-membrane model and (d) affinity-membrane model with CSTR mixing were plotted along with the experimental data. Local-equilibrium theory was compared to the experimental data in order to distinctly isolate the effects of dead volume mixing, slow sorption kinetics, and interactive competition due to differences in either affinity strength or sorption kinetics. Local-equilibrium theory is based on thermodynamics, and does not include any mass-transfer effects. Local-equilibrium separations occur when the sorption kinetics are fast enough to allow equilibrium to exist between protein and ligand at all binding sites [9].

The predictions from local-equilibrium theory contained two square-wave plateaus as shown in Figs. 6a and 7a. The first plateau contained only pepsin, the lower-binding-strength protein. In the beginning of loading, both pepsin and chymosin completely bound to the ligand and no protein emerged in the effluent. As the binding sites were saturated with protein, the stronger-binding chymosin started to displace bound pepsin off the membrane surface. This displacement resulted in an effluent concentration of pepsin higher than the feed solution concentration of pepsin. Displacement was more rapid and noticeable for ideal local-equilibrium behavior when the concentration of strong-binding chymosin was elevated. When the membrane reached equilibrium, chymosin emerged in the effluent and pepsin displacement stopped. After this point the effluent concentration of both

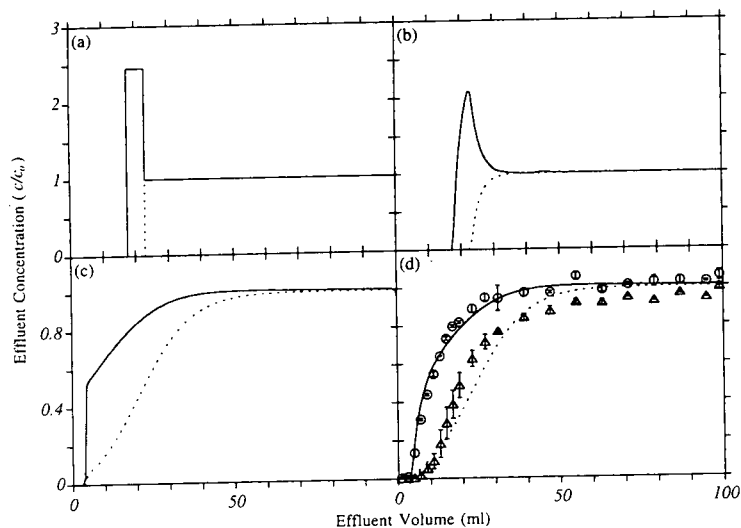


Fig. 6. Comparison of experimental breakthrough curves for a feed solution containing 0.1 mg/ml pepsin (O) and 0.4 mg/ml chymosin ( $\Delta$ ) at 1 ml/min to predictions (solid lines = pepsin; dotted lines = chymosin) made using (a) local-equilibrium theory, (b) local-equilibrium theory with CSTR mixing, (c) affinity-membrane model and (d) affinity-membrane model with CSTR mixing.

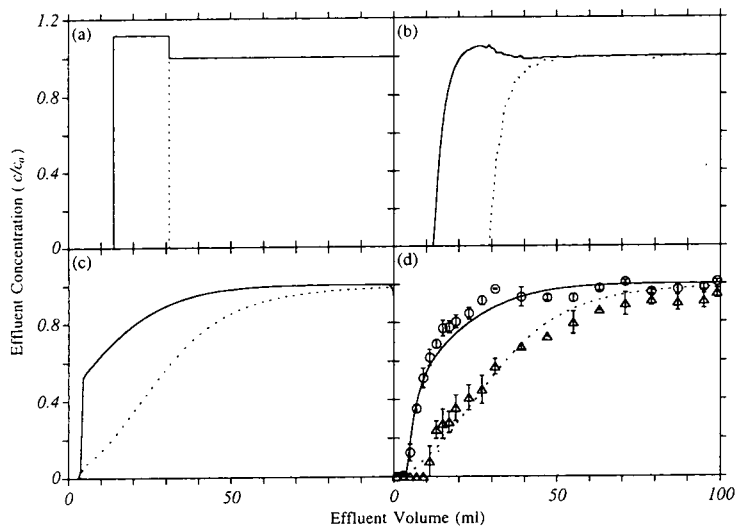


Fig. 7. Comparison of experimental breakthrough curves for a feed solution containing 0.4 mg/ml pepsin (O) and 0.1 mg/ml chymosin ( $\Delta$ ) at 1 ml/min to predictions (solid lines = pepsin; dotted lines = chymosin) made using (a) local-equilibrium theory, (b) local-equilibrium theory with CSTR mixing, (c) affinity-membrane model and (d) affinity-membrane model with CSTR mixing.

proteins was equal to the feed solution concentration.

As shown in Figs. 6b and 7b, when CSTR mixing in the flow system was added to the predictions from local-equilibrium theory, the mixing effect broadened the edges of square waves and decreased the effluent concentration during displacement. The mixing effect degraded the separation performance.

The experimental results using affinity membranes (Figs. 6d and 7d) bore no resemblance to either local-equilibrium theory (Figs. 6a and 7a) or this theory with CSTR mixing (Figs. 6b and 7b). Although including CSTR mixing in the affinity-membrane model gave the best predictions (Figs. 6d and 7d), predictions made without the CSTR mixing model were close to the experimental data (Figs. 6c and 7c). The dominant effect was the slowness of the interactive and competitive sorption kinetics.

The sharp or sudden increase in the calculated effluent concentration for pepsin in Figs. 6c and 7c was the result of slow sorption kinetics. The residence time of the fluid in the membrane was 2.55 min, which was too short for pepsin to bind to the membrane. Therefore, pepsin emerged in the effluent immediately after the delay volume of the system of 4 ml. However, chymosin, which had an association rate constant three-times greater than that of pepsin, did bind to the membrane in this residence time. Therefore, there was not a sharp increase in the calculated effluent concentration for chymosin.

## 5. Discussion

In this work, an affinity-membrane model of breakthrough curves was validated by extensive experimentation. Sorption equilibrium isotherm and kinetic parameters were measured in batch experiments. These measurements were completely independent of the affinity-membrane model. Breakthrough curves were then measured and compared to the predictions made using the model. For both single-solute and binary-solute separations, the predictions using

the model were in good agreement with the experimental breakthrough curves.

Predictions made using either local-equilibrium theory or the affinity-membrane model were compared to the experimental data. The predictions made using the binary-solute affinity-membrane model closely matched the experimental data, and predictions made using local-equilibrium theory were a distinct mismatch. This confirmed that slow sorption kinetics were the dominant cause of broad breakthrough curves in affinity-membrane separations.

In addition to slow sorption kinetics, it is possible that broad breakthrough curves may result from two mass-transfer effects analyzed in our previous work [8]: boundary-layer mass transfer (BLMT) and axial diffusion. Due to the small pore size of the membrane matrix used in this research, BLMT was fast and did not affect the shape of the breakthrough curves [10,31]. Axial diffusion dominates membrane performance at low flow velocity. When  $Pe$  is smaller than 40, axial diffusion causes broad breakthrough curves [8]. Because  $Pe$  was 330 for pepsin and 340 for chymosin, axial diffusion did not affect the shape of the breakthrough curves.

Lower flow-rates would be necessary to achieve sharper breakthrough curves. Operating conditions which produce sharp breakthrough curves from affinity membranes have been defined previously using the affinity-membrane model [8]. Based on the parameter values determined experimentally in this work, flow-rates of 0.013 ml/min for pepsin and 0.053 ml/min for chymosin would be required to achieve sharp breakthrough curves in the experiments of Fig. 5. At the 1 ml/min flow-rate used in these experiments, slow sorption kinetics would be expected to dominate affinity-membrane performance and produce broad breakthrough curves.

This work employed the Langmuir model to determine the sorption equilibrium and rate constants. Although the Langmuir model did not perfectly fit the batch experimental data, the affinity-membrane model using these fitted parameter values was a good predictor of experimental breakthrough curves from the mem-

brane. Perhaps because the flow system operated far from equilibrium, the Langmuir model needs only to accurately describe the association kinetics at short times in order to produce accurate predictions of the breakthrough behavior. The residence time of the fluid in the affinity membranes was 2.55 min. From Fig. 2, at this residence time, the system was not only far from equilibrium for both pepsin and chymosin, but also the Langmuir model was able to accurately describe the association kinetics at this short time. This made the use of Langmuir model valid for this affinity system.

For other adsorptive membrane systems which may operate closer to equilibrium there is a need for more accurate multi-solute sorption models in order to ensure the predictions of the affinity-membrane model are equally valid. Ion-exchange membranes are an example of such a system. In the work of Weinbrenner and Etzel [32],  $\alpha$ -lactalbumin and bovine serum albumin were separated using an ion-exchange membrane. The separation performance qualitatively matched the predictions from local-equilibrium theory together with the CSTR mixing model. Apparently, the ionic interaction between protein and ligand was fast enough to allow local-equilibrium behavior to occur, but small amounts of mixing in the flow system impaired attainment of exact local-equilibrium behavior in the breakthrough curve. Further theoretical and experimental research on the thermodynamics and kinetics of multi-solute sorption are crucial to developing a better understanding of adsorptive-membrane separations such as this one.

In practice, affinity membranes are frequently used to separate a desired biomolecule from a crude solution which may contain extracellular and intracellular components, salts, detergents and other undesired materials. These components may not bind with high affinity to the membrane, but may be present in much higher concentration than the desired component, and may have greater association rate constants for the ligand. Consequently, contaminating low-affinity components may compete with the desired high-affinity component for binding sites.

This work demonstrated that under carefully

chosen and controlled conditions, the performance of affinity-membrane systems can be predicted well using the affinity-membrane model. Thus, the fundamental factors governing affinity-membrane performance were identified as slow and competitive sorption kinetics, axial diffusion and dead volume mixing. However, realistic modelling of affinity-membrane separations using crude solutions will have to await experimentally validated mathematical models of the fundamental sorption behavior occurring in these complicated solutions.

### Symbols

|       |  |
|-------|--|
| $B$   | parameter defined in Eq. 11  |
| $c$   | solute concentration in the mobile phase, $M$  |
| $c_1$ | ligand capacity in the stationary phase based on the solid volume, $M$                       |
| $c_0$ | feed solute concentration in the mobile phase, $M$   |
| $c_s$ | concentration of solute–ligand complex in the stationary phase, $M$                          |
| $C$   | dimensionless solute concentration in the mobile phase ( $= c/c_0$ )                         |
| $C_s$ | dimensionless concentration of solute–ligand complex in the stationary phase ( $= c_s/c_1$ ) |
| $D$   | axial diffusion coefficient, $\text{cm}^2/\text{s}$  |
| $E$   | extinction coefficient   |
| $F$   | fluorescence in the solution   |
| $G$   | parameter defined in Eq. 12  |
| $k_a$ | association rate constant, $M^{-1} \text{s}^{-1}$  |
| $k_d$ | dissociation rate constant, $\text{s}^{-1}$  |
| $K_d$ | dissociation equilibrium constant, $M$ ( $= k_d/k_a$ )                                       |
| $l$   | diffusion path, $\text{cm}$  |
| $L$   | membrane thickness, $\text{cm}$  |
| $m$   | dimensionless saturation capacity [ $= (1 - \epsilon)c_1/\epsilon c_0$ ]                     |
| $M_n$ | $n$ th moment of the effluent concentration  |
| $M_r$ | molecular mass   |
| $n$   | dimensionless number of transfer units [ $= (1 - \epsilon)c_1 k_a L/\epsilon v$ ]            |

|           |  |
|-----------|--|
| $Pe$      | axial Peclet number ( $= vL/D$ )                       |
| $pI$      | isoelectric point                                      |
| $Q$       | flow-rate, ml/s  |
| $r$       | dimensionless separation factor<br>( $= 1 + c_0/K_d$ ) |
| $t$       | time, s  |
| $v$       | interstitial flow velocity, cm/s                       |
| $V$       | CSTR volume, ml  |
| $\hat{V}$ | parameter defined in Eq. 13                            |
| $z$       | axial distance along the membrane, cm                  |

#### Greek letters

|            |   |
|------------|---|
| $\epsilon$ | porosity of membrane                          |
| $\zeta$    | dimensionless spatial variable<br>( $= z/L$ ) |
| $\mu_n$    | $n$ th moment of the inlet concentration      |
| $\tau$     | dimensionless time ( $= vt/L$ )               |

#### Subscripts

|            |                       |
|------------|-----------------------|
| 1st moment | first temporal moment |
| delay      | plug-flow delay       |
| $i, j$     | solute index          |
| in         | inlet                 |
| max        | maximum value         |
| out        | outlet                |
| w          | washing               |

#### Acknowledgements

Funding for this work was provided by Grant BCS-9109577 from the National Science Foundation and Hatch Grant 3318 from the United States Department of Agriculture. Paul Soltys supplied important technical advice while reviewing the manuscript.

#### References

- [1] F.H. Arnold, H.W. Blanch and C.R. Wilke, *Chem. Eng. J.*, 30 (1985) B9.
- [2] S. Brandt, R.A. Goffe, S.B. Kessler, J.L. O'Connor and S.E. Zale, *Bio/Technology*, 6 (1988) 779.
- [3] K.-G. Briefs and M.-R. Kula, *Chem. Eng. Sci.*, 47 (1992) 141.
- [4] M. Unarska, P.A. Davies, M.P. Esnouf and B.J. Bellhouse, *J. Chromatogr.*, 519 (1990) 53.
- [5] Dj. Josić, J. Reusch, K. Löster, O. Baum and W. Reutter, *J. Chromatogr.*, 590 (1992) 59.
- [6] J.A. Gerstner, R. Hamilton and S.M. Cramer, *J. Chromatogr.*, 596 (1992) 173.
- [7] T.B. Tennikova and F. Svec, *J. Chromatogr.*, 646 (1993) 279.
- [8] S.-Y. Suen and M.R. Etzel, *Chem. Eng. Sci.*, 47 (1992) 1355.
- [9] S.-Y. Suen, M. Caracotsios and M.R. Etzel, *Chem. Eng. Sci.*, 48 (1993) 1801.
- [10] M. Nachman, A.R.M. Azad and P. Bailon, *J. Chromatogr.*, 597 (1992) 155.
- [11] H.-C. Liu and J.R. Fried, *AIChE J.*, 40 (1994) 40.
- [12] M. Kim, K. Saito, S. Furusaki, T. Sato, T. Sugo and I. Ishigaki, *J. Chromatogr.*, 585 (1991) 45.
- [13] G.C. Serafica, J. Pimbley and G. Belfort, *Biotech. Bioeng.*, 43 (1994) 21.
- [14] P.V. Danckwerts, *Chem. Eng. Sci.*, 2 (1953) 1.
- [15] M. Caracotsios and W.E. Stewart, *Comput. Chem. Eng.*, (1994) in press.
- [16] L.A. Blankstein and L. Dohrman, *Am. Clin. Prod. Rev.*, 11 (1985) 33.
- [17] T.-J. Fu and A. Carlson, presented at the 24th ACS Mid-Atlantic Regional Meeting, Madison, NJ, 1990, paper 165.
- [18] T.-J. Fu, *M.S. Thesis*, Pennsylvania State University, University Park, PA, 1988.
- [19] T.-J. Fu, *Ph.D. Thesis*, Pennsylvania State University, University Park, PA, 1992.
- [20] C.A. Ernstrom and N.P. Wong, in B.H. Webb, A.H. Johnson and J.A. Alford (Editors), *Fundamentals of Dairy Chemistry*, AVI Publishing, Westport, 2nd ed., 1974, Ch. 12.
- [21] H. Edelhoich, *J. Am. Chem. Soc.*, 79 (1957) 6100.
- [22] R. Djurtoft, B. Foltmann and A. Johansen, *Compt. Rend. Trav. Lab. Carlsberg*, 34 (1964) 287.
- [23] A.J. Weiss, S.A. McElhinney and L.A. Blankstein, *BioTechniques*, 7 (1989) 1012.
- [24] Millipore, *Immobilon™ Tech Protocol*, Bedford, MA, 1987.
- [25] S.-Y. Suen, *Ph.D. Thesis*, University of Wisconsin, Madison, WI, 1994.
- [26] A. Carlson and R. Nagarajan, *Biotechnol. Prog.*, 8 (1992) 85.
- [27] W.C. Olson, T.M. Spitznagel and M.L. Yarmush, *Mol. Immunol.*, 26 (1989) 129.
- [28] R.B. Bird, W.E. Stewart and E.N. Lightfoot, *Transport Phenomena*, Wiley, New York, 1960.
- [29] K.-R. Raths, *M.S. Thesis*, University of Wisconsin, Madison, WI, 1992.
- [30] E.N. Lightfoot, A.M. Lenhoff and R.L. Rodriguez, *Chem. Eng. Sci.*, 37 (1982) 954.
- [31] D.D. Frey, R. van de Water and B. Zhang, *J. Chromatogr.*, 603 (1992) 43.
- [32] W.F. Weinbrenner and M.R. Etzel, *J. Chromatogr. A*, 662 (1994) 414.



# Experimental studies in metal affinity displacement chromatography of proteins

Young J. Kim<sup>a</sup>, Steven M. Cramer<sup>b,\*</sup>

<sup>a</sup>*Department of Research, Albany Medical College, Albany, NY 12208, USA*

<sup>b</sup>*Howard P. Isermann Department of Chemical Engineering, Rensselaer Polytechnic Institute, Troy, NY 12180-3590, USA*

First received 11 February 1994; revised manuscript received 19 July 1994

---

## Abstract

Metal affinity displacement chromatography was employed for the purification of proteins. The mobile phase modifier imidazole was shown to exhibit complex induced gradients in these displacement systems resulting in different imidazole microenvironments in each protein displacement zone. Furthermore, the induced imidazole gradient produced an elevated displacer concentration at the rear of the displacement train. While adsorption isotherms measured under the initial carrier conditions were unable to predict these displacements, isotherms measured under the induced imidazole conditions qualitatively predicted the effluent displacement profiles. It is believed that these induced imidazole gradients speed up the kinetics of the displacement process and are in part responsible for the sharp boundaries seen in these separations. This work demonstrates the ability of this bioseparation technique to effect efficient multicomponent separations and illustrates the importance of mobile phase modifier effects in metal affinity displacement chromatography.

---

## 1. Introduction

The concept of ligand-exchange chromatography using stationary phases with immobilized metal chelates was first introduced by Helfferich [1]. In 1975, Porath et al. [2] extended the technique to the separation of proteins and nucleic acids. In immobilized metal affinity chromatographic (IMAC) systems, the exposed electron-donating amino acid residues on the protein surface, such as the imidazole group of histidine, the thiol group of cysteine, and the indoyl group of tryptophan, contribute to the binding of proteins to immobilized metal ions [3]. These unique interactions enable IMAC systems to

selectively interact with classes of complementary biopolymers. Furthermore, the relatively inexpensive IMAC adsorbents have distinct economic advantages over biospecific affinity systems [4,5]. Several workers have attempted to elucidate the mechanism of adsorption in IMAC systems [6–16]. However, the physicochemical properties of protein retention in IMAC are not well understood at present. Porath et al.'s pioneering work has catalyzed considerable work on the purification of biomolecules using IMAC systems [17–28].

Displacement chromatography is rapidly emerging as a powerful bioseparation method due to the high throughput and product purity associated with the process [29–31]. The displacement process is based on the competition of

\* Corresponding author.

solutes for adsorption sites on the stationary phase according to their relative binding affinities and mobile phase concentrations. This technique offers distinct advantages in preparative chromatography as compared to the conventional elution mode. The displacement process takes advantages of the non-linearity of the isotherms such that a larger feed can be separated on a given column with the purified components recovered at significantly higher concentrations. Furthermore, the tailing observed in elution chromatography is greatly reduced in displacement chromatography due to self-sharpening boundaries formed in the process. Whereas in elution chromatography the feed components are diluted during the separation, the feed components are often concentrated during displacement chromatography. These advantages are particularly significant for the isolation of biopolymers from dilute solutions such as those encountered in biotechnology processes. Although traditional stationary phase materials such as reversed-phase and ion-exchange have been successfully employed in the displacement mode [29–38], research on displacement chromatography with more specific adsorbent materials is scarce at present [39–43].

Metal affinity displacement chromatography (MADC) is a bioseparation technique which combines the unique selectivity of IMAC systems with the high throughput and purity of displacement chromatography. We have previously demonstrated that MADC can be successfully carried out using ribonuclease A as the displacer [42]. Furthermore, tailing observed in these displacement separations was significantly improved by the appropriate use of imidazole as a mobile phase modifier. While imidazole and histidine have been employed as mobile phase modifiers in elution IMAC systems [3,9], their behavior is quite different from more traditional mobile phase modifiers (e.g. salt, methanol). In this paper, we present experimental results of MADC for multicomponent protein separations. In addition, an investigation of the effects of induced imidazole gradients in these MADC systems is presented.

## 2. Experimental

### 2.1. Materials

Bulk chelating Superose (10  $\mu\text{m}$ ) containing covalently bound iminodiacetic acid (IDA) and 110  $\times$  5 mm I.D. glass columns were donated by Pharmacia LKB Biotechnology (Uppsala, Sweden). Bulk Bioseries strong cation exchanger (SCX) material was obtained from Rockland Technologies (Newport, DE, USA). POROS R/H reversed-phase chromatographic columns (100  $\times$  4.6 mm I.D.) were purchased from PerSeptive Biosystems (Cambridge, MA, USA). The chelating Superose and SCX materials were slurry packed into 110  $\times$  5 mm and 250  $\times$  4.6 mm I.D. columns, respectively. Acetonitrile and sodium monophosphate were obtained from Fisher Scientific (Fairlawn, NJ, USA). Cytochrome *c* from horse heart, lactoferrin from bovine milk, myoglobin from horse heart, ribonuclease A from bovine pancreas, cupric sulfate, ethylenediaminetetraacetic acid (EDTA), imidazole, sodium chloride and urea were obtained from Sigma (St. Louis, MO, USA).

### 2.2. Apparatus

An fast protein liquid chromatography (FPLC) system (Pharmacia LKB) was employed for the displacement experiments and analysis of proteins. This system consisted of two Model P-500 pumps connected to the chromatographic column via a Model MV-7 valve. The column effluent was monitored by a Model UV-M detector and a Pharmacia strip-chart recorder. Fractions of the column effluent were collected with a Model Frac-100 fraction collector for further analysis. The system was controlled using a LCC-500-Plus controller.

An HPLC system was employed for the analysis of imidazole. This system consisted of a Model LC 2150 pump (LKB, Bromma, Sweden), a Model 7125 sampling valve with a 20- $\mu\text{l}$  sample loop (Rheodyne, Cotati, CA, USA), a spectroflow 757 UV-Vis detector (Applied Biosystems, Foster City, CA, USA) and a Model C-

R3A Chromatopac integrator (Shimadzu, Kyoto, Japan).

An MI-410 pH microelectrode was purchased from Microelectrodes (Londonderry, NH, USA).

### 2.3. Procedures

#### *Immobilization of Cu<sup>2+</sup>*

The IDA columns were loaded with Cu<sup>2+</sup> by sequential perfusion with ten column volumes of 0.3 M cupric sulfate aqueous solution, pH 3.9, six column volumes of deionized water, and ten column volumes of the carrier solutions described below.

#### *Adsorption isotherms of proteins and imidazole*

Adsorption isotherms were determined by frontal chromatography according to the technique of Jacobson et al. [44] by using a 36 × 2 mm I.D. microbore column packed with Cu<sup>2+</sup>-charged IMAC material. The column effluents were monitored at 280 nm for proteins and 230 nm for imidazole.

#### *Operation of displacement chromatograph*

In all displacement experiments, the columns were initially equilibrated with the carrier and then sequentially perfused with feed, displacer and regenerant solutions. Fractions of the column effluent were collected directly from the column outlet to avoid extra column dispersion of the purified components. Fractions collected throughout the displacement runs were assayed by analytical HPLC. The pH values of the fractions were measured by a microelectrode pH meter.

#### *MADC of proteins*

Displacement experiments were carried out using 110 × 5 mm I.D. columns packed with Cu<sup>2+</sup>-charged IMAC stationary phase materials. The feed mixture contained 3 mg cytochrome *c*, 12 mg lactoferrin, and 30 mg ribonuclease A in 3 ml of a 25 mM phosphate buffer carrier, pH 5.0, containing 1.0 M sodium chloride and 5 mM imidazole. Displacer was 15 mg/ml myoglobin in

a 25 mM phosphate buffer carrier, pH 8.0, containing 1.0 M sodium chloride and 5 mM imidazole. The regenerant was 15 column volumes of 25 mM phosphate buffer, pH 12.0, containing 2.0 M sodium chloride. After each displacement run, Cu<sup>2+</sup> of the column was removed completely using 0.1 M EDTA solution (pH 7.0) and recharged with 0.3 M cupric sulfate solution. In all displacements the feed was loaded at a flow-rate of 0.2 ml/min and the displacement was performed at 0.1 ml/min at 22°C. Sodium chloride was added to all carrier solutions in order to quench non-specific ionic adsorption. Imidazole was included in all carrier solutions in order to enhance the displacement kinetics.

#### *Imidazole frontal chromatography with a pH step change*

Frontal chromatography was carried out using pH step change from 5.0 to 8.0 in the presence of 5 mM imidazole and 1.0 M sodium chloride in 25 mM phosphate buffer. Flow-rate was 0.2 ml/min.

#### *FPLC analysis of proteins*

Fractions collected during the displacement experiments were analyzed by gradient elution reversed-phase chromatography. The analyses were carried out using a 100 × 4.6 mm I.D. POROS reversed-phase column on the FPLC system. A 4-min linear gradient of 10–70% acetonitrile in 50 mM phosphate buffer, pH 2.2 was employed. Displacement fractions were diluted 20–100-fold with the first eluent buffer and 25- $\mu$ l samples were injected. The flow-rate was 1.0 ml/min. The column effluents were monitored at 280 nm and column temperature was maintained at 22°C. Quantitative analyses were carried out and the data was used to construct displacement chromatograms.

#### *HPLC analysis of imidazole*

Imidazole analysis was carried out with an HPLC system. A 250 × 4.6 mm SCX column was employed for the separation of imidazole. The carrier consisted of 15 mM phosphate, pH 5.0.

Displacement fractions were diluted 20-fold with the carrier buffer and 20- $\mu$ l samples were injected. Flow-rate was 1.2 ml/min. The column effluents were monitored at 230 nm.

#### Copper analysis

Copper was analyzed using a Perkin-Elmer Model 3030 atomic absorption spectrophotometer. Effluent fractions were diluted and the atomic absorbance was monitored at 320.4 nm. The copper ion concentration was then calculated using an appropriate calibration plot.

### 3. Results and discussion

We have previously reported on the use of immobilized metal ion chromatographic systems in the displacement mode for the purification of proteins using ribonuclease A as the displacer [42]. The appropriate use of imidazole as a mobile phase modifier significantly improved tailing observed with certain proteins in MADC.

In this manuscript, we present experimental results of MADC for the efficient separation of a multicomponent protein mixture. In addition, an investigation of the effects of induced imidazole gradients in these MADC systems is presented.

#### 3.1. MADC of proteins using imidazole as a mobile phase modifier

A displacement experiment using myoglobin as the displacer was carried out using a model feed mixture of cytochrome *c*, lactoferrin and ribonuclease A. In this separation, imidazole was used as a mobile phase modifier to increase the displacement kinetics [42]. Furthermore, a pH step change was employed between the feed (pH 5.0) and displacer solutions (pH 8.0) in order to concentrate the feed proteins at the front of the column during the loading process. In the presence of imidazole, relatively higher affinity of proteins at lower pH was observed due to the lack of effective imidazole adsorption [45]. As

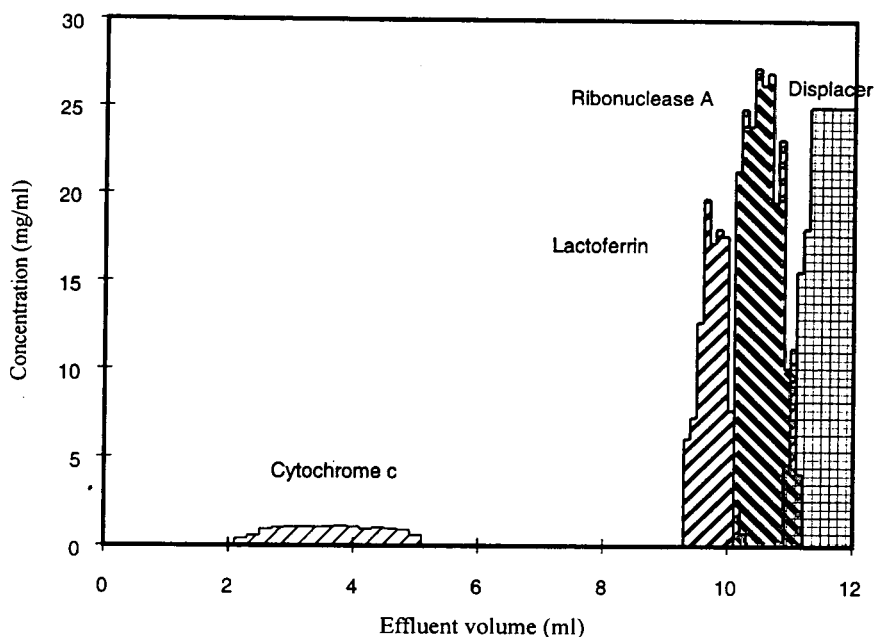


Fig. 1. Displacement chromatogram of a three-protein mixture. Column, 110  $\times$  5 mm I.D.  $\text{Cu}^{2+}$ -charged metal chelate Superose (10  $\mu$ m); carrier, 1.0 M sodium chloride and 5.0 mM imidazole in 25 mM phosphate buffer, pH 8.0; displacer, 15 mg/ml myoglobin in carrier; flow-rate 0.1 ml/min; temperature 22°C; feed, 3 mg cytochrome *c*, 12 mg lactoferrin and 30 mg ribonuclease A in 3 ml carrier (pH 5.0); fraction volume, 100  $\mu$ l.

seen in Fig. 1, cytochrome *c* eluted ahead of the displacement train while lactoferrin and ribonuclease A were well displaced by the myoglobin. This separation resulted in the concentration of lactoferrin and ribonuclease A and produced extremely sharp boundaries between the displacement zones. In fact, this is the first multi-component displacement separation with sharp boundaries in IMAC systems reported in the literature.

A solute movement analysis of this displacement system was carried out using experimentally determined adsorption isotherms of the feed proteins and myoglobin displacer under the displacement conditions (i.e. 5 mM imidazole and pH 8.0). As seen in Fig. 2, the isotherms of lactoferrin and ribonuclease A remained in the linear adsorption region while the myoglobin demonstrated non-linear behavior. Since the operating line lies above the feed protein isotherms, one would expect elution of the feed proteins. However, as shown earlier in Fig. 1, both ribonuclease A and lactoferrin are in fact displaced by the myoglobin front. Clearly, the

isotherms under the carrier conditions fail to predict the displacement behavior.

In order to examine this displacement system in the absence of pH effects, the experiment was repeated at constant pH 8.0. In addition, imidazole content and pH was measured from the fractions of the column effluent using HPLC analysis and microelectrode pH probe, respectively. As expected from the solute movement analysis, shown in Fig. 2, this experiment resulted in the elution of the feed proteins ahead of the displacement train (Fig. 3). Furthermore, the desorption of the bound imidazole by the proteins resulted in the elevated imidazole concentrations between each protein zone while pH was maintained at 8.0 throughout the displacement experiment.

### 3.2. pH and imidazole profiles in MADC

Our laboratory has recently demonstrated that induced mobile phase modifier effects can have a profound effect on the behavior of ion-exchange displacement systems [34,35,38]. In order to

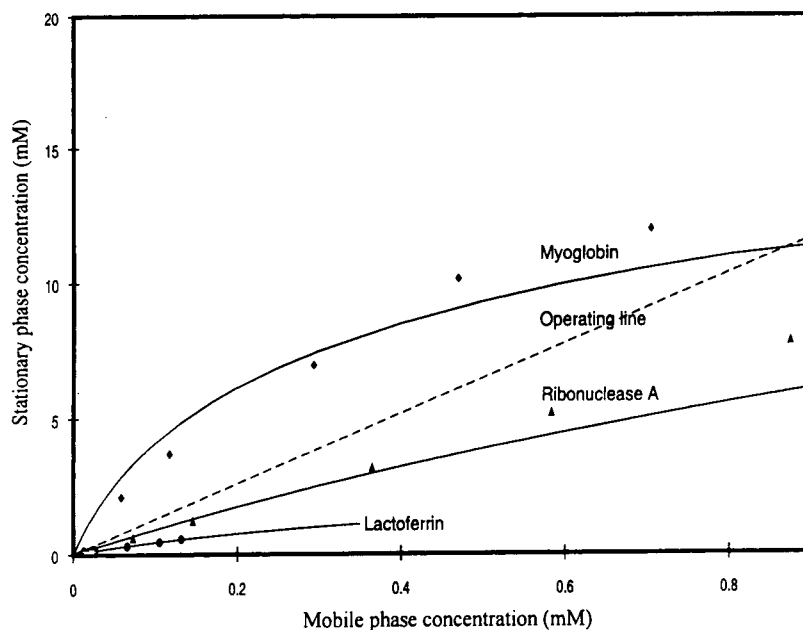


Fig. 2. Adsorption isotherms of proteins at 5 mM imidazole concentration and operating line. Column, 36 × 2 mm I.D. Cu<sup>2+</sup>-charged metal chelate Superose; carrier, 1.0 M sodium chloride and 5 mM imidazole in 25 mM phosphate buffer, pH 8.0.

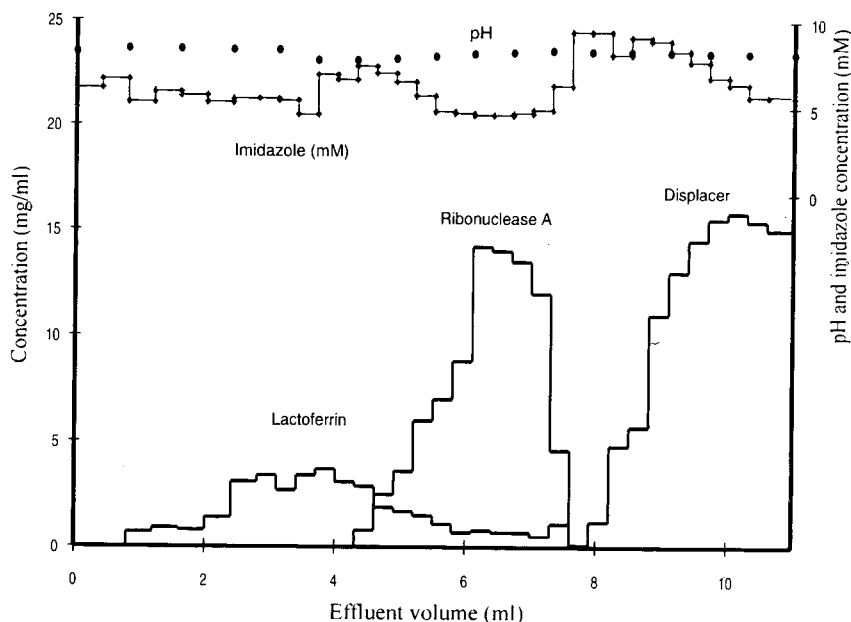


Fig. 3. Displacement chromatogram of a two-protein mixture at constant pH. Chromatographic conditions as in Fig. 1 with the exception of: feed, 12 mg lactoferrin, and 30 mg ribonuclease A in 3 ml carrier (pH 8.0). pH and imidazole concentration were measured.

better understand these metal affinity displacement separations, a detailed study of the effects of induced imidazole gradients in these systems was carried out. The displacement separation presented in Fig. 1 was repeated and the collected fractions were evaluated for their pH and imidazole content as well as their protein compositions. Again, the same pH step change was employed between the feed (pH 5.0) and displacer solutions (pH 8.0). The resulting pH and imidazole profile is shown in the displacement chromatogram presented in Fig. 4. In this separation, the feed volume was 3 ml and the column dead volume (i.e. the total void volume of the system) was 2.2 ml. While the pH change propagated through the column at the void volume of the system, the imidazole concentration profile was quite unusual. During the loading of the feed (0–3.0 ml), the imidazole concentration increased immediately after the column void volume. This initial increase in imidazole concentration can be attributed to the desorption of bound imidazole by the adsorbing feed proteins. At approximately 5.2 ml (corresponding to the

pH breakthrough), the imidazole concentration abruptly decreased down to approximately 0.07 mM. The concentration of imidazole then increased in each successive protein displacement zone. Local imidazole concentrations of 0.3, 0.8, 1.2 and 5.0 mM were observed in the lactoferrin, ribonuclease A, initial myoglobin and final myoglobin displacer zones, respectively. As seen in the figure, the myoglobin concentration profile exhibited two distinct concentrations. The initial myoglobin zone was concentrated to 22 mg/ml while the final displacer emerged at the inlet concentration of 15 mg/ml. The successive step changes in imidazole concentration play an important role in the unique characteristics of this displacement separation and can be expected to increase the kinetics of the displacement process.

### 3.3. $\text{Cu}^{2+}$ leakage during the displacement experiments

In order to determine the extent of  $\text{Cu}^{2+}$  leakage during the displacement experiment, the  $\text{Cu}^{2+}$  ion contents of collected fractions were

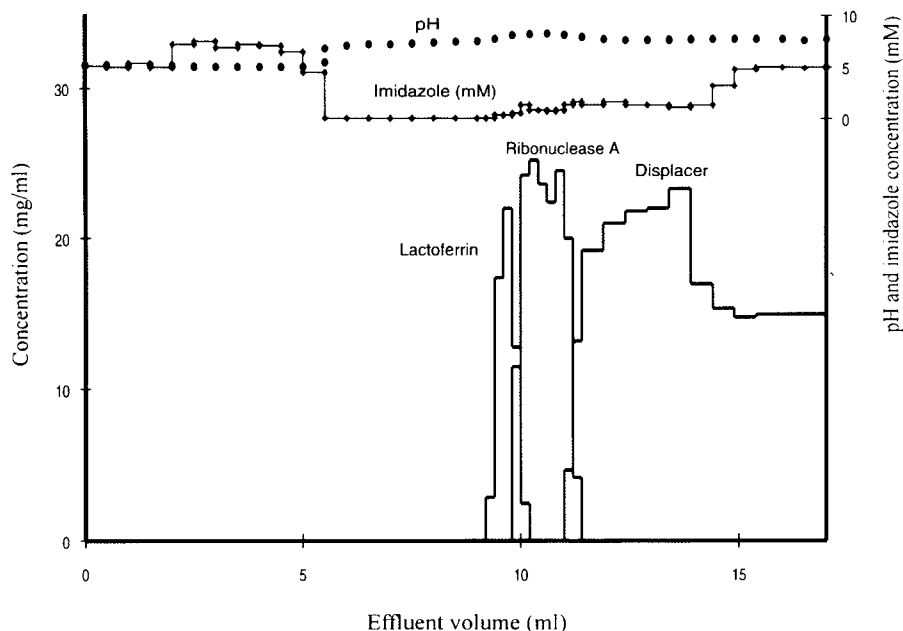


Fig. 4. Displacement chromatogram of a two-protein mixture. Chromatographic conditions as in Fig. 1 with the exception of: feed, 12 mg lactoferrin, and 30 mg ribonuclease A in 3 ml carrier (pH 5.0). pH and imidazole concentration were measured.

analyzed using atomic absorption. The amount of the  $\text{Cu}^{2+}$  ions leaching during the initial equilibration of the column was less than 0.1 ppm. During the displacement experiment a continuous leaching of 0.5 ppm was detected. The total amount of  $\text{Cu}^{2+}$  ions co-eluting in the product zones (lactoferrin and ribonuclease A) was 0.001 mg  $\text{Cu}^{2+}$  as compared to 42 mg of protein. This relatively low level of  $\text{Cu}^{2+}$  leaching had no observable effect on the reproducibility of the displacement experiments. However, in order to assure reproducibility, the  $\text{Cu}^{2+}$  ions were removed from the stationary phase after the displacement experiment and the column was reloaded with  $\text{Cu}^{2+}$  ions prior to the next experiment. Future work with alternative stationary phase ligands (e.g. nitrilotriacetic acid or trimethylethylenediamine) which bind  $\text{Cu}^{2+}$  more strongly will attempt to minimize  $\text{Cu}^{2+}$  leakage in displacement systems.

### 3.4. Adsorption isotherms and frontal chromatography of imidazole

In order to gain insight into the effect of pH

on imidazole adsorption behavior, several experiments were carried out. The imidazole adsorption isotherms were measured at pH 5, 6 and 8. As seen in Fig. 5, the imidazole isotherm moved upwards with steeper initial slopes as the pH increased. Thus, the sudden step change from pH 5.0 to 8.0, carried out during the displacement experiment, resulted in a shift of the equilibrium, causing the immediate uptake of imidazole by the stationary phase material. This explains the dramatic reduction in imidazole concentration observed following the pH breakthrough in Fig. 4.

A control experiment was carried out to examine the imidazole response to a pH step change. Frontal chromatography was carried out using a pH step change from 5.0 to 8.0 in the presence of 5 mM imidazole in carrier. As seen in Fig. 6, the imidazole concentration profile was quite similar to that observed during the displacement experiment (Fig. 4). Again, the pH change produced a dramatic reduction of imidazole concentration (0.07 mM) at 5.2 ml of effluent volume and a reappearance of the imidazole front at approximately 15 ml. In fact, it is

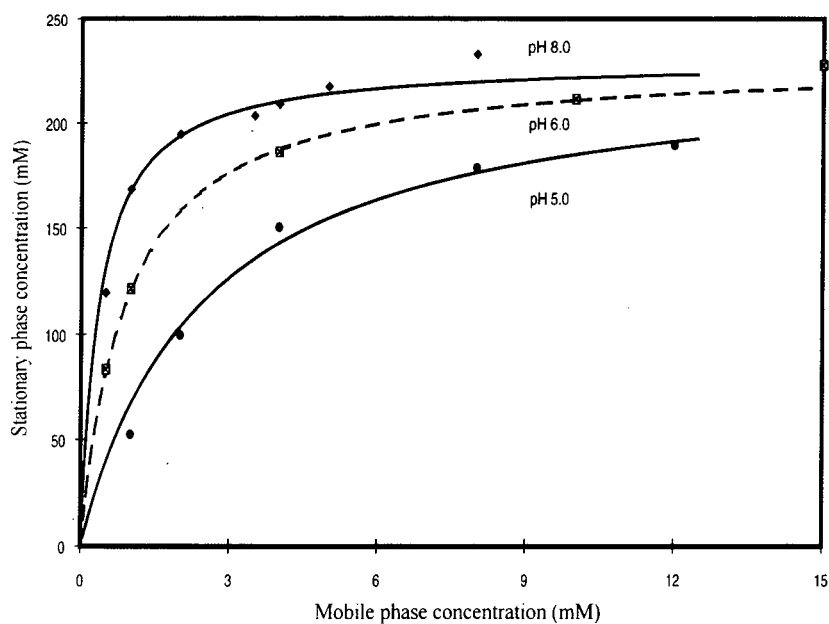


Fig. 5. Adsorption isotherms of imidazole at various pH. Column,  $36 \times 2$  mm I.D.  $\text{Cu}^{2+}$ -charged metal chelate Superose; carrier, 1.0 M sodium chloride in 25 mM phosphate buffer, pH 5.0, 6.0 and 8.0.

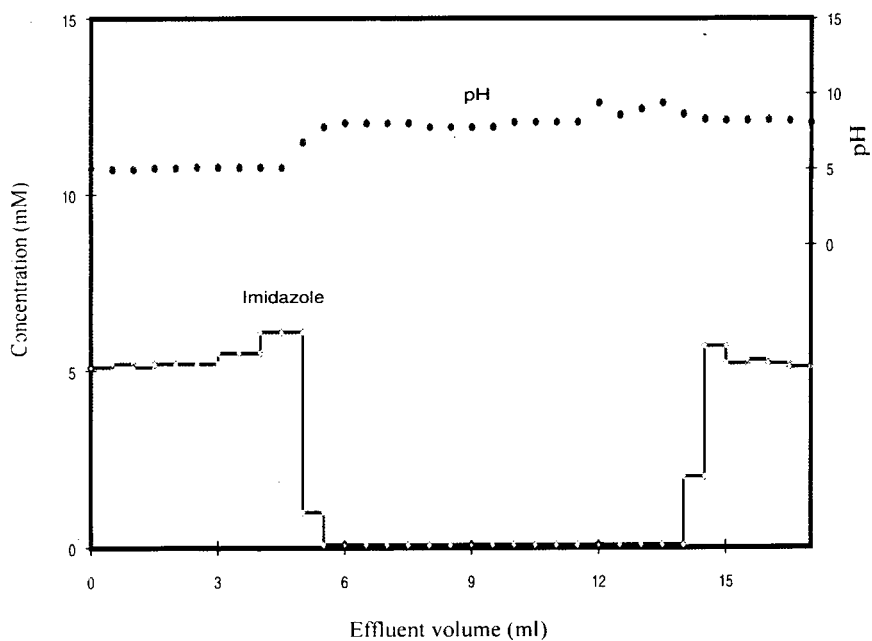


Fig. 6. Imidazole frontal chromatogram with a pH step change. Column,  $110 \times 5$  mm I.D.  $\text{Cu}^{2+}$ -charged metal chelate Superose ( $10 \mu\text{m}$ ); carrier, 1.0 M sodium chloride and 5.0 mM imidazole in 25 mM phosphate buffer, pH 5.0; temperature  $22^\circ\text{C}$ ; feed, carrier with pH adjusted to pH 8.0; fraction volume,  $500 \mu\text{l}$ .



likely that the breakthrough of imidazole at 15 ml is responsible for the initial elevated concentration of myoglobin in the displacement zone. Due to the absence of proteins, the step increase in imidazole concentrations seen in Fig. 4 were not observed in this control experiment shown in Fig. 6.

It is important to note that these complex imidazole profiles can be readily obtained in the absence of pH step change. By equilibrating the column with a large volume (250 column volumes) of 0.07 mM imidazole, pH 8.0, and by adding 5 mM imidazole to the displacer solution, very similar profiles can be obtained. Clearly, incorporating the pH step change, results in a dramatic reduction in the equilibration time and concomitant increases in product throughput.

### 3.5. Adsorption isotherms of proteins under induced imidazole concentrations

Fig. 7 shows the adsorption isotherms measured under the induced imidazole gradient

conditions of 0.3, 0.8 and 1.2 mM for lactoferrin, ribonuclease A and myoglobin, respectively. In contrast to the solute movement analysis presented in Fig. 2, the operating line in this analysis was seen to intersect the effective isotherms of lactoferrin and ribonuclease A. (Note: the operating line was constructed using the effective myoglobin concentration at the front of the displacement zone, 22 mg/ml). Furthermore, the intersection of the operating line with these isotherms qualitatively predicted the concentrations and breakthrough volumes observed in the displacement experiment of Fig. 4. Thus, once the local imidazole concentrations in the displacement zones are known, a solute movement analysis can then be carried out using the appropriate adsorption isotherms. Clearly, a quantitative understanding of mobile phase modifier effects would facilitate the design and optimization of efficient MADC separations. We are currently developing a detailed model of the non-linear adsorption of proteins in immobilized metal affinity systems [46].

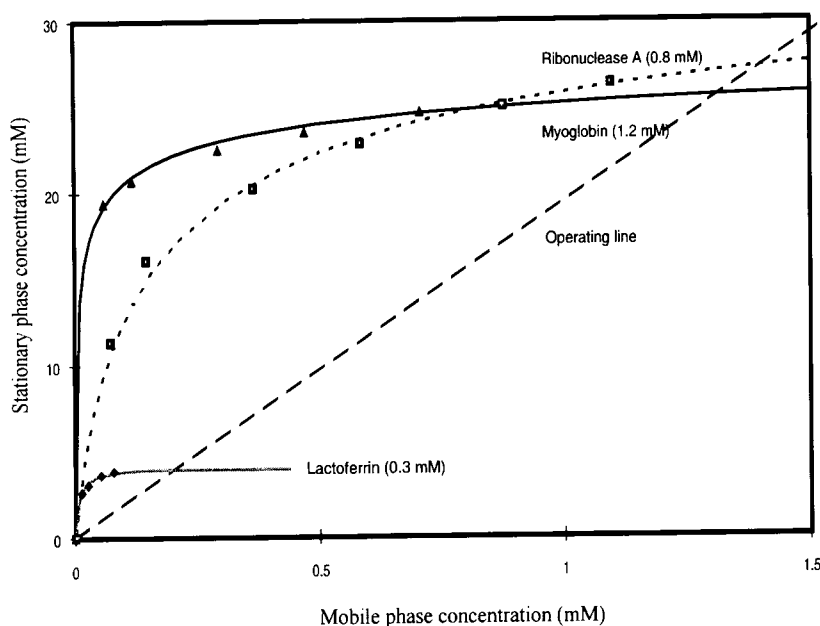


Fig. 7. Adsorption isotherms of proteins under induced imidazole concentrations and operating line. Column, 36 × 2 mm I.D. Cu<sup>2+</sup>-charged metal chelate Superose; carrier, 1.0 M sodium chloride in 25 mM phosphate buffer, pH 8.0, containing 0.3, 0.8 and 1.2 mM imidazole for lactoferrin, ribonuclease A and myoglobin, respectively.

#### 4. Conclusions

We have demonstrated that MADC resulted in multicomponent separations with very sharp boundaries between the zones. The mobile phase modifier imidazole was shown to exhibit complex induced gradients in these displacement systems resulting in different imidazole concentrations in each protein displacement zone. Furthermore, the induced imidazole gradient produced an elevated displacer concentration at the front of the displacer breakthrough. While adsorption isotherms measured under the initial carrier conditions were unable to predict these displacements, isotherms measured under the induced imidazole conditions qualitatively predicted the effluent displacement profiles. This work demonstrates the ability of this bioseparation technique to effect efficient multicomponent separations and illustrates the importance of mobile phase modifier effects in MADC. Work is currently underway in our laboratory to develop a theoretical framework to explain these complex IMAC displacement systems [46].

#### Acknowledgements

This research was supported by the Eastman Kodak Company and grant No. CTS-8900566 from the National Science Foundation. The gift of stationary phase materials from Pharmacia LKB Biotechnology (Uppsala, Sweden) is gratefully acknowledged.

#### References

- [1] F. Helfferich, *Nature*, 189 (1961) 1001.
- [2] J. Porath, J. Carlsson, I. Olsson and G. Belfrage, *Nature*, 258 (1975) 598.
- [3] E. Sulkowski, *Trends Biotechnol.*, 3 (1985) 1.
- [4] J. Porath, *Trends Anal. Chem.*, 7 (1988) 254.
- [5] M.A. Vijayalakshmi, *Trends Biotechnol.*, 7 (1989) 71.
- [6] E.S. Hemdan and J. Porath, *J. Chromatogr.*, 323 (1985) 255.
- [7] E.S. Hemdan and J. Porath, *J. Chromatogr.*, 323 (1985) 265.
- [8] J. Porath, *Biotechnol. Prog.*, 3 (1987) 14.
- [9] M. Belew and J. Porath, *J. Chromatogr.*, 516 (1990) 333.
- [10] T.W. Hutchens and T.-T. Yip, *J. Chromatogr.*, 500 (1990) 531.
- [11] T.W. Hutchens and T.-T. Yip, *J. Chromatogr.*, 604 (1992) 133.
- [12] S.-S. Suh and F.H. Arnold, *Biotechnol. Bioeng.*, 35 (1990) 682.
- [13] R.J. Todd, R.D. Johnson and F.H. Arnold, *J. Chromatogr. A*, 662 (1994) 13.
- [14] G. Dobrowolka, G. Muszynska and J. Porath, *J. Chromatogr.*, 541 (1991) 333.
- [15] H. Goubran-Botros, E. Nanak, J.A. Nour, G. Birkenmeir and M.A. Vijayalakshmi, *J. Chromatogr.*, 597 (1992) 357.
- [16] M. Zachariou and M.T.W. Hearn, *J. Chromatogr.*, 599 (1992) 171.
- [17] B. Lonnerdal, J. Carlsson and J. Porath, *FEBS Lett.*, 75 (1977) 89.
- [18] J.P. Salier, J.P. Martin, P. Lambin, H. McPhee and K. Hochstrasser, *Anal. Biochem.*, 109 (1980) 273.
- [19] J. Porath, B. Olin and B. Granstrand, *Arch. Biochem. Biophys.*, 225 (1983) 543.
- [20] Z. El Rassi and Cs. Horváth, *J. Chromatogr.*, 359 (1986) 241.
- [21] M. Belew, T.-T. Yip, L. Andersson and R. Ehrnstrom, *J. Biochem.*, 164 (1987) 457.
- [22] E. Sulkowski, in R. Burgess (Editor), *Protein Purification: Micro to Macro (UCLA Symposium on Molecular and Cellular Biology, New Series, Vol. 68)*, Alan R. Liss, New York, 1987, p. 149.
- [23] J. Porath, *J. Chromatogr.*, 443 (1988) 3.
- [24] Z. El Rassi and Cs. Horváth, in K.M. Gooding and F.E. Regnier (Editors), *HPLC of Biological Macromolecules (Methods and Applications)*, Marcel Dekker, New York, 1990, p. 179.
- [25] E. Li-Chan, L. Kwan and S. Nakai, *J. Dairy Sci.*, 73 (1990) 2075.
- [26] P. Hansen, G. Lindeberg and L. Andersson, *J. Chromatogr.*, 627 (1992) 125.
- [27] S. Ritter, J. Komenda, E. Setlikova, I. Setlik and W. Welte, *J. Chromatogr.*, 625 (1992) 21.
- [28] R.R. Beitle and M.M. Ataii, *Biotechnol. Prog.*, 9 (1993) 64.
- [29] Cs. Horváth, in F. Bruner (Editor), *The Science of Chromatography*, Elsevier, Amsterdam, 1985, p. 179.
- [30] J. Frenz and Cs. Horváth, in Cs. Horváth (Editor), *High Performance Liquid Chromatography—Advances and Perspectives*, Vol. 8, Academic Press, Orlando, FL, 1988, p. 211.
- [31] S.M. Cramer and G. Subramanian, *Sep. Purif. Methods*, 19 (1990) 31.
- [32] S.M. Cramer and Cs. Horváth, *Prep. Chromatogr.*, 1 (1988) 29.
- [33] G. Subramanian, M.W. Phillips and S.M. Cramer, *J. Chromatogr.*, 439 (1988) 341.
- [34] C.A. Brooks and S.M. Cramer, *AIChE J.*, 38 (1992) 1969.

- [35] J.A. Gerstener and S.M. Cramer, *Biotechnol. Prog.*, 8 (1992) 540.
- [36] K. Kalghatgi, I. Fellegvari and Cs. Horváth, *J. Chromatogr.*, 604 (1992) 47.
- [37] A.R. Torres and E.A. Peterson, *J. Chromatogr.*, 604 (1992) 39.
- [38] G. Jayaraman, S.A. Gadam and S.M. Cramer, *J. Chromatogr.*, 630 (1993) 53.
- [39] G. Vigh, G. Quintero and G. Farkas, *J. Chromatogr.*, 484 (1989) 237.
- [40] G. Vigh, G. Farkas and G. Quintero, *J. Chromatogr.*, 484 (1989) 251.
- [41] H. Caruel, L. Rigal and A. Gaset, *J. Chromatogr.*, 558 (1991) 89.
- [42] Y.J. Kim and S.M. Cramer, *J. Chromatogr.*, 549 (1991) 89.
- [43] M. Stefansson and D. Westerlund, *Chromatographia*, 35 (1993) 199.
- [44] J. Jacobson, J. Frenz and Cs. Horváth, *J. Chromatogr.*, 316 (1984) 53.
- [45] S. Vunnum, S.R. Gallant and S.M. Cramer, *Biotechnol. Bioeng.*, submitted.
- [46] S. Vunnum, S.R. Gallant, Y.J. Kim and J.M. Cramer, *Chem. Eng. Sci.*, submitted.



# Pharmaceutical application of liquid chromatography–mass spectrometry

## II<sup>☆</sup>. Ion chromatography–ion spray mass spectrometric characterization of alendronate

Xue-Zhi Qin<sup>a,\*</sup>, Eric W. Tsai<sup>a</sup>, Takeo Sakuma<sup>b</sup>, Dominic P. Ip<sup>a</sup>

<sup>a</sup>Pharmaceutical Research and Development, Merck Research Laboratories, West Point, PA 19486, USA

<sup>b</sup>PE SCIEX, Toronto, Ontario, Canada

First received 6 May 1994; revised manuscript received 18 August 1994

### Abstract

The trihydrate of alendronate sodium (MK-0217) is an important bisphosphonate drug for the treatment of a variety of bone diseases. Determination and characterization of this compound in dosage formulations is challenging since it has no chromophore, and as a highly polar and thermally labile compound, it is not amenable to electron impact mass spectrometry. Ion chromatography coupled with an ion spray mass detector (IC–ISP–MS) in the negative ionization mode was developed and applied to the characterization of this compound. Under these conditions alendronate ( $m/z$  248,  $[M - H]^-$ ,  $M$  = parent alendronic acid) was readily observed. The anion can form cluster anions with acid molecules including that of the alendronic acid in the gas phase, which is a distinguishing feature of the IC–ISP–MS spectrum. IC–ISP–MS–MS study of the anion shows that cleavage of the C–P bond(s) is the dominant fragmentation pathway(s) of the anion, characteristic of its structure.

### 1. Introduction

The monosodium salt trihydrate of 4-amino-1-hydroxybutane-1,1-bisphosphonic acid, or trihydrate of alendronate sodium (MK-0217, **1**, Fig. 1) is an important bisphosphonate drug, which possesses therapeutic indications in the treatment of many bone diseases such as hypercalcemia of malignancy, osteoporosis and Paget's disease [2,3]. The compound has been characterized by various techniques such as the infrared transmittance spectrum (IR), magnetic reso-

nance spectrum (NMR) and X-ray powder diffraction (XRPD) methods [4]. But, as a highly polar and thermally labile compound, it is not amenable to electron impact (EI) mass spectrometry [4]. In this paper, we report characterization of **1** by ion chromatography–ion spray (pneumatically assisted electrospray [5]) mass spectrometry (IC–ISP–MS) in the negative ionization mode.

Determination and characterization of **1** in dosage formulations is challenging since it has no chromophore for UV or fluorescence detection. The determination of **1** and other bisphosphonate drugs has mainly been accomplished by reversed-phase HPLC–UV methods by intro-

\* Corresponding author.

\* For Part I, see Ref. [1].

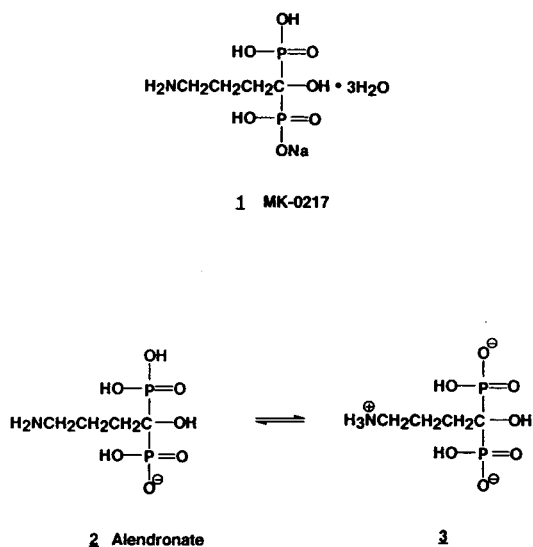


Fig. 1. Structures of MK-0217 and alendronate.

ducing a chromophore into their molecules using either pre- or post-column derivatization. Recently, analytical methods for determining bisphosphonate drugs without derivatization have attracted considerable attention. Examples include the development of an ion-exchange method with on-line flame photometric detection for dichloromethylene diphosphonate [6], an inductively coupled plasma (ICP) detector for specific phosphorus detection for etidronate disodium [7], an IC method with conductivity detection for alendronate [8] and an IC-indirect UV method for the direct quantitation of some bisphosphonate drugs in dosage formulations [9,10]. Mass detectors can detect compounds without a chromophore, and have been coupled with gas chromatography (GC) for the analysis of dichloromethylene bisphosphonate in urine [11], which required time-consuming extraction and derivatization. IC coupled with an ion spray mass detector, reported here, provides a convenient and specific method for the direct detection of **1** in the dosage formulations. The IC-ISP-MS method may also be useful for the study of other bisphosphonate compounds as the IC-indirect UV method [9,10].

The development of the IC-ISP-MS method should be of interest in the field of IC-MS

interfaces. Especially, the IC-ISP-MS method avoided the use of post-micromembrane suppressors commonly used in the IC-thermal spray (TSP) MS [12] and in an IC-ISP-MS study of organic ammonium and sulfate compounds [13].

## 2. Experimental

### 2.1. Chemicals

Trihydrate of alendronate sodium (**1**, MK-0217,  $C_4H_{12}NO_7P_2Na \cdot 3H_2O$ ,  $M_r$  325.1) was manufactured by Merck Research Labs. (Rahway, NJ, USA). Acetonitrile (Optima grade) and nitric acid (Optima grade) were purchased from Fisher Scientific (Philadelphia, PA, USA). Formic acid (certified ACS grade) was purchased from Aldrich (Milwaukee, WI, USA). They were used as received, without further purification. Deionized water with at least 18 M $\Omega$  purified by a Milli-Q (Bedford, MA, USA) system was used for mobile phase and sample preparations.

### 2.2. Sample preparation

Standard was prepared by dissolving 32.6 mg (equivalent to 25 mg free acid) of MK-0217 reference standard in 500 ml of water to yield a concentration of 0.05 mg/ml. Samples of both initial and stressed tablets [stressed at 40°C and 75% relative humidity (RH) in an open container for 2 months], at a concentration of 0.05 mg/ml, were prepared by dissolving one 5 mg MK-0217 tablet in 100 ml of deionized water.

### 2.3. IC-indirect UV conditions

IC-indirect UV was performed using a Dionex 4500i Bio-LC. The conditions were: a Waters IC-Pak HR anion-exchange column (75  $\times$  4.6 mm, 6  $\mu$ m particle size), ambient (about 26°C) column temperature, 1.6 mM HNO<sub>3</sub> aqueous mobile phase, flow-rate of 0.5 ml/min, injection volume of 25  $\mu$ l and UV detection at 235 nm with "inverse polarity" and 0.1 AUFS (0.1 V output).

#### 2.4. IC–ISP–MS and IC–ISP–MS–MS analysis

IC–ISP–MS and IC–ISP–MS–MS were performed on a PE Sciex (Thornhill, Canada) Model API III triple-quadrupole mass spectrometer, fitted with an articulated, pneumatically assisted nebulization probe and an atmospheric pressure ionization source, which was connected to an LC system consisting of a Perkin-Elmer ISS-100 autoinjector equipped with a 200- $\mu$ l loop.

The IC conditions used in IC–ISP–MS were modified from the IC–indirect UV method, which were: an Applied Biosystems AX-300 anion-exchange column (30  $\times$  2 mm I.D., 5  $\mu$ m particle size), ambient (about 26°C) column temperature, 95% water (containing 0.1% HCOOH) and 5% acetonitrile mobile phase, flow-rate of 200  $\mu$ l/min, and injection volume of 10  $\mu$ l.

The settings of the interface and the MS conditions were: the ion spray voltage was operated at –3.35 kV with 35–40 p.s.i. (1 p.s.i. = 6894.76 Pa) “zero” grade compressed air nebulization gas flow at 0.8 l/min. A curtain of nitrogen gas (99.999%), at a flow-rate of 1.2 l/min, was used to keep atmospheric gases out of the analyzer. The orifice potential was –60 V. Normal mass spectra were acquired by scanning Q1 after negative (deprotonated) ions (alendronate, 2) were emitted into the quadrupole mass analyzer through a 0.0045-in. (1 in. = 2.54 cm) pinhole aperture. Product-ion spectra were taken by colliding the Q1-selected alendronate at “ $m/z = 248$ ” with collision gas (argon, 50 eV, 400  $\cdot 10^{12}$  atoms/cm) in Q2 and scan Q3 to analyze the fragment ions. The dwell time was 1.00 ms. Q1 was scanned from  $m/z$  200 to 1000 at a step size of 0.2 u. Q3 was scanned from  $m/z$  14 to 249. The mass spectrometer was tuned and calibrated across the  $m/z$  range 10 to 2400.

### 3. Results and discussion

#### 3.1. IC–ISP–MS conditions

The IC conditions used in IC–ISP–MS were modified from the IC–indirect UV method,

which was developed in this laboratory for the determination of bisphosphonate drugs. The indirect UV detection monitors the decrease in UV absorbance of the nitric acid eluent (maximum absorption near 220 nm) due to the replacement of nitrate by bisphosphonate molecules. Both initial and stressed MK-0217 tablets were studied by the IC–indirect UV method. Inset a of Fig. 2 shows an IC chromatogram of a 5-mg MK-0217 initial tablet, obtained under the optimized IC–indirect UV conditions described in the Experimental section. Alendronate was eluted at a retention time of ca. 10 min. There was an additional peak observed at ca. 6.4 min, which is attributed to the solvent. The assignments were confirmed by studying the MK-0217 standard. Inset b of Fig. 2 shows an IC chromatogram of a 5-mg MK-0217 stressed tablet. In addition to the solvent and the alendronate peaks, a small peak was observed, eluting at ca. 8.8 min. This peak was identified as a degradate—an alendronate/excipient adduct from a detailed study, which will be reported in a separate paper. It should be pointed out that the stressed tablets were used to demonstrate the method specificity. The tablets were made by a non-commercialized manufacturing process and the alendronate/excipient adduct was formed under the stress conditions only from these tablets. Tablets made by the final commercial formulation and process are very stable and the adduct under the stress conditions was not observed.

Although the IC–indirect UV method could separate alendronate and its potential degradate, it did not provide structural information. In order to characterize their structures, the IC was interfaced with ISP–MS. Rapid on-line MS characterization of the degradate is preferred to isolation because isolation of the very low level degradate in dosage formulations was difficult and time-consuming.

Since the ionization efficiency of the ISP interface is promoted by weak solvation by a volatile solvent, the mobile phase of the IC–indirect UV method was modified. First, it was found that when a very strong mineral acid, nitric acid, was used in the mobile phase, the ion spray needle flew toward the sample injector under the applied high voltage. To have an ion

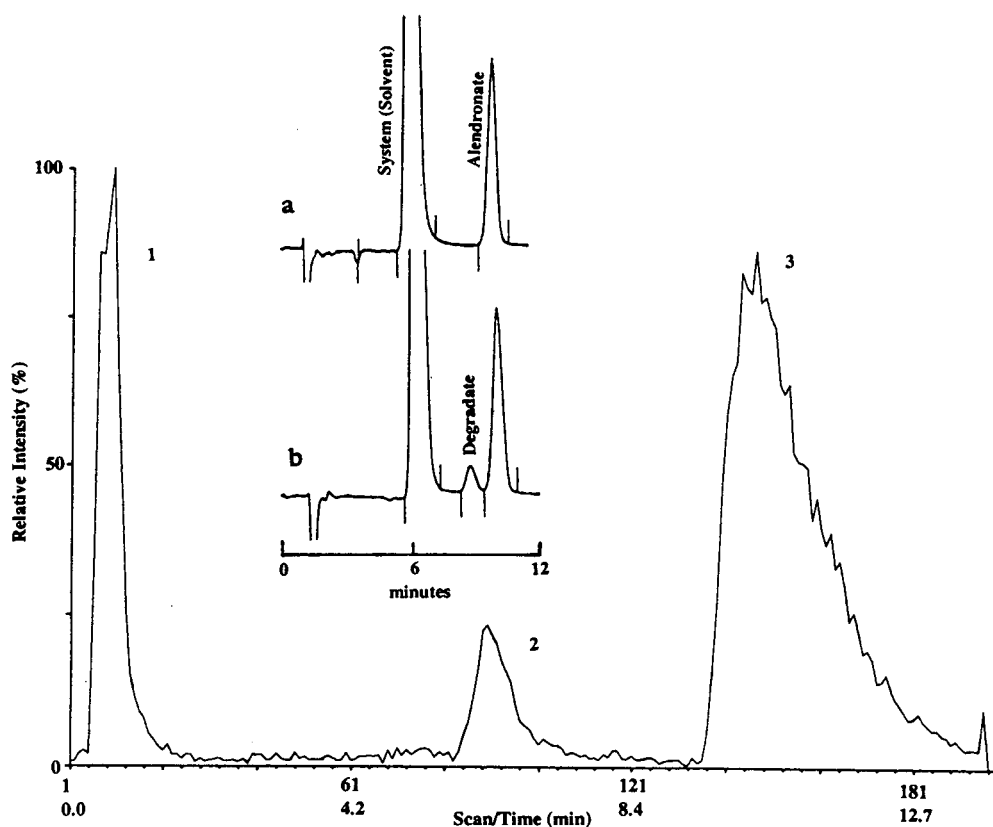


Fig. 2. Total ion current chromatogram (TIC) of a 5-mg MK-0217 stressed tablet; and IC-UV chromatogram of a 5-mg MK-0217 initial tablet (inset a) and stressed tablet (inset b).

current going towards the MS interface, the 1.6 mM nitric acid was replaced by 0.1% formic acid that is more volatile. Secondly, the 0.1% formic acid aqueous solvent was mixed with 5% acetonitrile, which is preferred over 100% aqueous mobile phase since a finer mist could be formed in the interface as the mixture had a lower surface tension than pure water. These modifications did not affect the IC separation of alendronate and the alendronate/excipient adduct. The desired pH of the mobile phase (pH 3) was readily achieved by using formic acid. The IC was coupled with ISP-MS in the negative ionization mode, which was chosen simply because alendronate and its excipient adduct were negatively charged in the mobile phase. Because no non-volatile salts were used in the mobile phase, a micromembrane suppressor

[12,13] was deemed unnecessary between the IC column outlet and the ISP-MS inlet, and not used.

Fig. 2 shows a total ion current (TIC) chromatogram of a 5-mg MK-0217 stressed tablet, obtained under the IC-ISP-MS conditions. The first peak (ca. 1 min) is an excipient peak, which is not observed as a positive peak in the IC-indirect UV chromatogram (inset b). It is probable that the excipient peak was included in the negative peak of the indirect UV chromatogram (ca. 1.5 min). The second peak (ca. 6 min) is the alendronate/excipient adduct peak, which was observed at ca. 8.8 min with indirect UV detection. The third peak observed at ca. 10 min is clearly assigned to the alendronate, which was also observed at ca. 10 min with indirect UV detection. The peak was broad, but it is typical



in IC. In a separate experiment, alendronate was isolated and examined by fast atom bombardment (FAB) MS, which showed that no other species co-eluted with alendronate. The IC–ISP–MS method is stability-indicating since it well separated alendronate from excipients and one potential degradate. Only three peaks were observed in TIC. The solvent (water) peak observed with indirect UV detection was not seen in TIC, indicating that water anions were successfully declustered by nitrogen curtain gas and free jet expansion at the orifice in the ISP interface.

### 3.2. IC–ISP–MS of alendronate

According to the observed molecular mass by IC–ISP–MS and fragmentation pattern by IC–ISP–MS–MS, alendronate and the alendronate/excipient adduct shown in TIC were both characterized. As mentioned above, this paper focuses on alendronate.

Fig. 3 shows the IC–ISP–MS spectrum of the alendronate peak in TIC. Alendronic free acid has bifunctional groups, namely, the acidic OH and the basic  $\text{NH}_2$  groups. The  $\text{p}K_{\text{a}}$  values for the parent bisphosphonic acid, obtained by potentiometric titration in water with 0.1 M sodium hydroxide, are  $\text{p}K_{\text{a}1} < 2$ ;  $\text{p}K_{\text{a}2} < 2$ ,  $\text{p}K_{\text{a}3} = 6.2$ ,  $\text{p}K_{\text{a}4} = 9.9$  and  $\text{p}K_{\text{a}5} = 10.2$  [4]. The basic primary-amine group has a  $\text{p}K_{\text{b}}$  value less than 4 (for example,  $\text{CH}_3\text{NH}_2$  has a  $\text{p}K_{\text{b}}$  value of 3.38 at 25°C). Thus, in the mobile phase used in IC–ISP–MS, which had a pH about 3, the zwitterionic alendronate mono-anion **3** was formed. In the ISP interface in the negative ionization mode, the mono-anions **3** were transported from the IC effluent (liquid phase) into the mass analyzer (gas phase). The most intense peak in the IC–ISP–MS spectrum shown in Fig. 3 has  $m/z$  248, which is clearly attributed to the alendronate mono-anion. Whether the mono-anion in the gas phase is still a zwitterionic anion is an interesting question, which cannot be

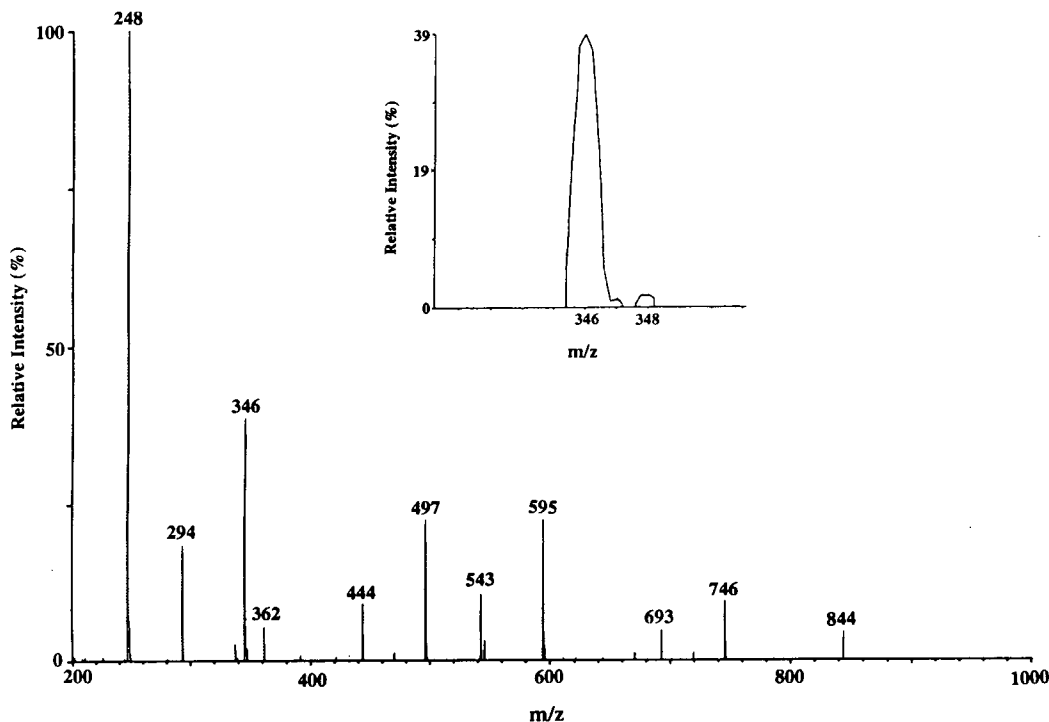


Fig. 3. IC–ISP–MS spectrum of alendronate.

answered on the basis of the  $m/z$  value since both the zwitterionic anion **3** and the non-zwitterionic anion **2** have the same  $m/z$  value. In the IC–ISP–MS–MS study discussed below, the fragmentation pattern(s) of the anion was interpreted in terms of the non-zwitterionic anion **2** although this did not prove it since rapid proton transfer could occur during the fragmentation process.

A distinguishing feature of the IC–ISP–MS spectrum shown in Fig. 3 is that in addition to the strongest peak of the alendronate mono-anion, there are additional weaker peaks, which all have  $m/z$  values greater than 248 of alendronate. These peaks except for the peak of the  $m/z$  ratio of 362 are attributable to the non-covalent cluster ions formed by hydrogen bonding of alendronate with acid molecules in the gas phase [14–16]. The peak of  $m/z$  362 is not identified, but it is a very weak, insignificant peak.

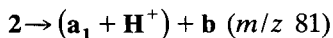
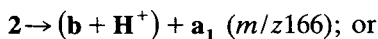
The identifications of the cluster ions are summarized in Table 1. All the cluster ions can be accounted for by a series  $m/z$  [ $248 + (46n) + (249m) + (98p)$ ]. The acid molecules having mass 46 and 249 are attributed to formic acid used in the mobile phase, and the parent alendronic acid, respectively. The acid molecule having mass 98 is attributed to sulfuric acid, which was a contaminant from the column according to the manufacturer's information. The observation of  $M + 2$  isotope ions, as exemplified by the ion of  $m/z$  346 (see the inset in Fig. 3), confirms this assignment. Phosphoric acid, which also has the mass 98, was excluded.

It is well documented that there are two

competing processes in the negative ionization mode: deprotonation to form molecular anion and anion attachment to form cluster ions via the formation of hydrogen bonding. The latter process can be thermodynamically favorable [17]. Nevertheless, under the IC–ISP–MS conditions alendronate was the predominant anion, which facilitates the characterization and quantitation of the anion. The cluster ions formation might depend on factors such as the concentration of alendronate and injection volume. However, in this study, the relatively higher concentration of alendronate and injection volume were necessary to the MS and MS–MS detection of the low-level alendronate/excipient adduct.

### 3.3. IC–ISP–MS–MS of alendronate

The product ion spectrum of the alendronate mono-anion of  $m/z$  248, obtained by the use of the IC–ISP–MS–MS conditions described in the Experimental section, is shown in Fig. 4. The spectrum shows five main fragment ions with  $m/z$  166, 148, 81, 79 and 63, respectively. The ion with  $m/z$  166 was the most intense fragment ion. As shown in Fig. 5, the C–P bond(s) breaking in alendronate (**2**) initially leads to two fragment anions **a**<sub>1</sub> ( $m/z$  166) and **b** ( $m/z$  81), depending where the negative charge was contained during the fragmentation:



The fragmentation was suggested to occur in a concerted process involving either of the five-membered ring transition states illustrated in Fig. 5. In the process, the pentavalent phosphorus was changed to trivalent phosphorus.

The anions **a**<sub>1</sub> and **b** underwent further fragmentation as indicated by the more fragment ions observed in the product ion spectrum. The ion with  $m/z$  148 is suggested to be the six-membered ring **c**<sub>1</sub> formed by the loss of a water from **a**<sub>1</sub>. The anion **c**<sub>1</sub> possessed a P–N bond. P–N bonds are stable and occur widely in phosphorus-containing compounds [18]. The ion with

Table 1  
Cluster ions of alendronate with acid molecules

| $m/z$ | Cluster ions                                      |
|-------|---|
| 294   | Alendronate + formic acid                         |
| 346   | Alendronate + sulfuric acid                       |
| 444   | Alendronate + two sulfuric acid                   |
| 497   | Alendronate + alendronic acid                     |
| 543   | Alendronate + alendronic acid + formic acid       |
| 595   | Alendronate + alendronic acid + sulfuric acid     |
| 693   | Alendronate + alendronic acid + two sulfuric acid |
| 746   | Alendronate + two alendronic acid                 |
| 844   | Alendronate + two alendronic acid + sulfuric acid |

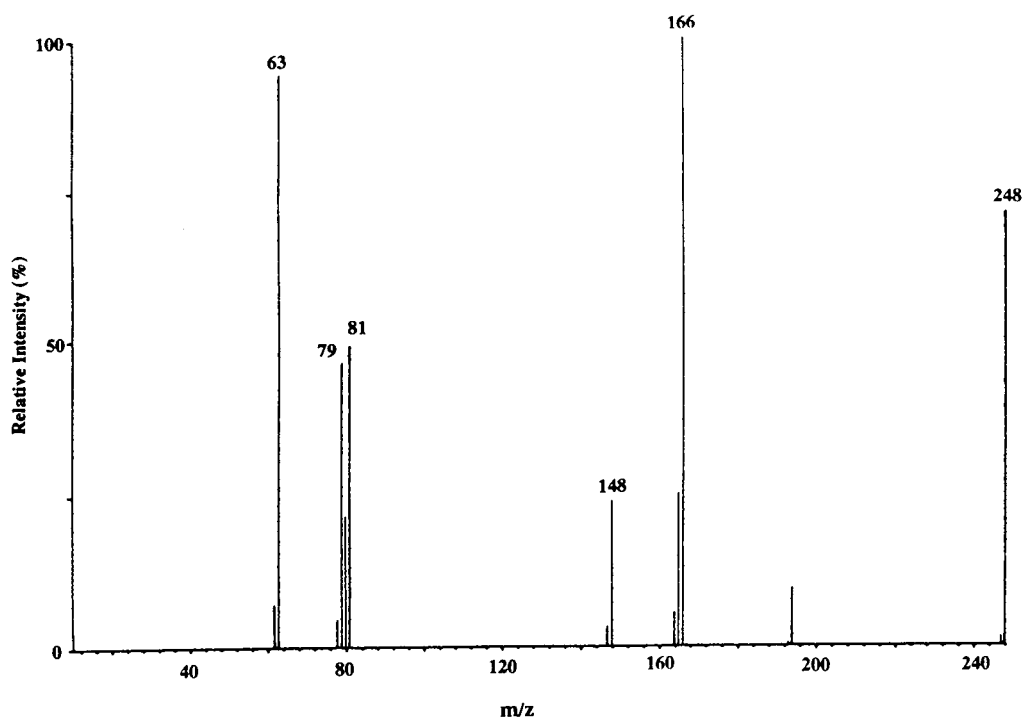


Fig. 4. Product ion spectrum of alendronate.

$m/z$  79 is suggested to be **d** formed by the transfer of two H from **b** to other molecules. It could also be formed by the loss of  $H_2$  from **b**. But, the loss of  $H_2$  from a secondary fragment ion is generally thermodynamically unfavorable. It is worth indicating that **d**, metaphosphate anion, is an important intermediate in the phosphate chemistry [19]. It is highly reactive in aqueous solution [20], but relatively stable and unreactive in gas phase [21]. The ion with  $m/z$  63 is suggested to be **e** formed by the loss of a water from **b**. The characteristic fragmentation patterns provide structural identification of alendronate.

It should be pointed out that **a**<sub>1</sub> could undergo cyclization to form **a**<sub>2</sub>, which also has  $m/z$  166, and then **a**<sub>2</sub> could lose a water to form **c**<sub>2</sub> which has  $m/z$  148. Although these species cannot be absolutely excluded, they are considered energetically less favorable than **a**<sub>1</sub> and **c**<sub>1</sub> because of the ring strain of their five-membered ring structures.

#### 4. Conclusions

Alendronate, an important bisphosphonate drug (in the form of trihydrate of alendronate sodium **1**), has been successfully detected and characterized by IC–ISP–MS in the negative ionization mode. To the best of the authors' knowledge, there is no MS report of alendronate and other bisphosphonate drugs in the literature. The present study has demonstrated the advantage of the soft ionization of the ISP technique in this application to pharmaceutical research and development.

#### Acknowledgement

The authors thank Dr. M.A. Brooks for critical review and helpful discussion of the paper before its publication. The authors also thank reviewers in the Merck Research Laboratories and referees for critical comments.

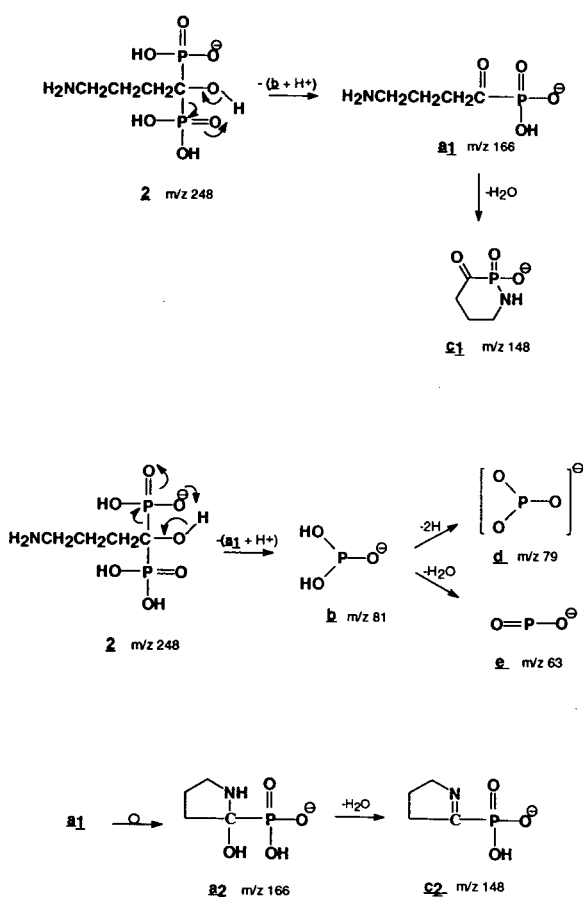


Fig. 5. Fragmentation pathways of alendronate.

## References

- [1] X.-Z. Qin, D.P. Ip, K. H.-C. Chang, P.M. Dradransky, M.A. Brooks and T. Sakuma, *J. Pharm. Biomed. Anal.*, 12 (1994) 221–234.
- [2] G. Heynen, P. Delwaide, O.L.M. Bijvoet and P. Franchimont, *Eur. J. Clin. Invest.*, 11 (1982) 29–35.
- [3] H.P. Sleeboom, O.L.M. Bijvoet, A.T. van Oosterom, J.H. Gleed and J.L.H. O’Riordan, *Lancet*, ii (1983) 239–243.
- [4] Merck Research Laboratories, unpublished results.
- [5] A.P. Bruins, T.R. Covey and J.D. Henion, *Anal. Chem.*, 59 (1987) 2642–2646.
- [6] T.L. Chester, E.C. Lewis, J.J. Benedict, R.J. Sunberg and W.C. Tettenhorst, *J. Chromatogr.*, 225 (1981) 17–25.
- [7] K.A. Forbes, J. Vecchiarelli, P.C. Uden and R.M. Barnes, in P. Jandik and R.M. Cassidy (Editors), *Advance in Ion Chromatography*, Century International, Franklin, MA, 1989, pp. 487–502.
- [8] E.W. Tsai, D.P. Ip and M.A. Brooks, *J. Chromatogr.*, 596 (1992) 217–224.
- [9] E.W. Tsai, S.D. Chamberlin, R.J. Forsyth, C. Bell, D.P. Ip and M.A. Brooks, *J. Pharm. Biomed. Anal.*, 11 (1993) 513–516.
- [10] E.W. Tsai, D.P. Ip and M.A. Brooks, *J. Pharm. Biomed. Anal.*, 12 (1994) 983–991.
- [11] S. Auriola, R. Kostiainen, M. Ylinen, J. Monkkonen and P. Ylitalo, *J. Pharm. Biomed. Anal.*, 7 (1989) 1623–1629.
- [12] W.M.A. Niessen, R.A.M. van der Hoeven, J. van der Greef, H.A. Schols, G. Lucas-Lokhorst, A.G.J. Vorage and C. Bruggink, *Rapid Commun. Mass Spectrom.*, 6 (1992) 474–478.
- [13] J.J. Conboy, J.D. Henion, M.W. Martin and J.A. Zweigenbaum, *Anal. Chem.*, 62 (1990) 800–807.
- [14] J.B. Fenn, M.C. Mann, K. Meng, S.F. Wong and C.M. Whitehouse, *Science*, 246 (1989) 64–71.
- [15] T.R. Covey, R.F. Bonner, B.I. Shushan and J.D. Henion, *Rapid Commun. Mass Spectrom.*, 2 (1988) 249–256.
- [16] D. Suckau, Y. Shi, S.C. Beu, M.W. Senko, J.P. Quinn, F.M. Wampler, III and F.W. McLafferty, *Proc. Natl. Acad. Sci. U.S.A.*, 90 (1993) 790–793.
- [17] C.E. Parker, R.W. Smith, S.J. Gaskell and M.M. Bursery, *Anal. Chem.*, 58 (1986) 1661.
- [18] H. R. Allcock, *Chem. Rev.*, 72 (1972) 315.
- [19] B. Ma, Y. Xie, M. Shen, P.v.R. Schleyer and H.F. Schaefer, III, *J. Am. Chem. Soc.* 115 (1993) 11169–11179.
- [20] D. Herschlag and W.P. Jencks, *J. Am. Chem. Soc.* 111 (1989) 7579.
- [21] R.G. Keesee and A.W. Castleman, Jr., *J. Am. Chem. Soc.* 111 (1993) 9015.

## Determination of clavam-2-carboxylate in clavulanate potassium and tablet material by liquid chromatography–tandem mass spectrometry

Christine Eckers<sup>a,\*</sup>, Kathryn A. Hutton<sup>a</sup>, V. de Biasi<sup>b</sup>, P.B. East<sup>c</sup>, N.J. Haskins<sup>a</sup>, V.W. Jacewicz<sup>d</sup>

<sup>a</sup>Analytical Sciences Department, SmithKline Beecham Pharmaceuticals, The Frythe, Welwyn, Herts. AL6 9AR, UK

<sup>b</sup>Separation Sciences Department, SmithKline Beecham Pharmaceuticals, Coldharbour Road, The Pinnacles, Harlow, Essex CM19 5AD, UK

<sup>c</sup>Drug Metabolism and Pharmacokinetics, SmithKline Beecham Pharmaceuticals, The Frythe, Welwyn, Herts. AL6 9AR, UK

<sup>d</sup>Chemical Development, SmithKline Beecham Pharmaceuticals, Old Powder Mills, Near Leigh, Tonbridge, Kent TN11 9AN, UK

First received 9 June 1994; revised manuscript received 15 August 1994

### Abstract

A liquid chromatography–thermospray tandem mass spectrometric (LC–MS–MS) method was developed to determine the presence of clavam-2-carboxylate in clavulanate potassium at below the 0.01% level stated in the US Pharmacopeia (USP). The USP method is for bulk chemical but it was hoped to extend the determination to formulated products. The method described here involves selected reaction monitoring of  $m/z$  156 giving rise to  $m/z$  114, using negative ion thermospray ionisation. The selected reaction monitoring method was highly specific for clavam-2-carboxylate and was capable of detecting clavam-2-carboxylate in clavulanate potassium at levels of 0.001% (w/w), an order of magnitude better than the sensitivity required by the USP.

### 1. Introduction

Clavulanic acid (Fig. 1, left) is an inhibitor of  $\beta$ -lactamase [1] and, as such, it is used in conjunction with penicillins sensitive to the enzyme to render them effective against  $\beta$ -lactamase producing bacteria.

Clavam-2-carboxylate (Fig. 1, right) may be found in clavulanic acid.

The US Pharmacopeia (USP) [2] states that clavam-2-carboxylate must not be present in clavulanate potassium at levels in excess of

0.01%. The USP method for clavam-2-carboxylate determination in clavulanate potassium chemical uses HPLC alone. The purpose of this work is to investigate the possibility of the determination of clavam-2-carboxylate in clavulanate potassium by liquid chromatog-

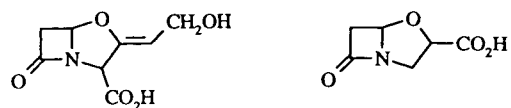


Fig. 1. Structures of clavulanic acid (left) and clavam-2-carboxylate (right).

\* Corresponding author.

raphy–tandem mass spectrometry (LC–MS–MS) with a view to increasing the sensitivity and specificity of the USP HPLC method, and to then modify the method to make it suitable for the screening of formulated tablet samples, which contain other active ingredients such as amoxicillin. The tablet excipients and other active ingredients could affect the specificity of an HPLC assay with UV detection alone, and increased sensitivity is required as clavulanate potassium is only one part of the formulated product.

## 2. Experimental

### 2.1. Chemicals

HPLC-grade methanol and glacial acetic acid (Romil, Loughborough, UK) were used. Ammonium acetate was supplied by Fisons (Loughborough, UK). The deionised water used was from a Milli-Q water system (Millipore, Bedford, MA, USA).

### 2.2. Preparation of solutions

#### *Clavam-2-carboxylate solutions*

Clavam-2-carboxylate (10 mg) was dissolved in deionised water (100 ml) to give a 0.1 mg/ml solution that was diluted as appropriate.

#### *Clavulanate potassium solutions*

Clavulanate potassium (50 mg) was dissolved in deionised water (0.5 ml).

#### *Spiked clavulanate potassium solutions*

Clavulanate potassium (50 mg) was dissolved in a clavam-2-carboxylate solution (0.5 ml) of appropriate concentration.

#### *Tablet material solutions*

The mass of the whole tablet was recorded and the tablet was then ground to a fine powder. An amount equivalent to 20 mg clavulanate potassium was taken. A 400- $\mu$ l volume of water was added. The mixture was then shaken for 1 min and centrifuged for 2 min at 11 600 g. The

supernatant was removed and re-centrifuged for 2 min at the same rpm. The resulting supernatant was transferred to a vial for injection.

#### *Spiked tablet solutions*

These were prepared in the same way as the tablet solutions using 400  $\mu$ l clavam-2-carboxylate solution of appropriate concentration to dissolve the tablet material.

### 2.3. Equipment

#### *Chromatography*

HPLC was carried out on a Hewlett-Packard (Palo Alto, CA, USA) 1090L liquid chromatograph. The separations were carried out using two 150  $\times$  3.9 mm Waters NovaPak C<sub>18</sub> (4  $\mu$ m particle size) columns arranged in series. A flow-rate of 1 ml/min was used. The column was eluted with 95% 0.1 M ammonium acetate (pH adjusted to 4.0 with glacial acetic acid) and 5% methanol for 5 min. The clavam-2-carboxylate elutes from the column during this time. The column was then washed with 100% methanol for a further 5 min to remove any other components from the column.

A make up flow of 0.8 ml/min 0.1 M ammonium acetate in water–methanol (80:20) was added post column to provide a total flow of 1.8 ml/min into the MS system, which was found to be the optimum flow for this instrument. An Applied Biosystems (Warrington, UK) 400 solvent-delivery system was used for this purpose.

#### *Mass spectrometry*

A Finnigan MAT triple-stage quadrupole mass spectrometer TSQ 46 (Finnigan Instruments, San Jose, CA, USA) fitted with a modified Finnigan thermospray (TSP) ion source [3] was used to acquire data in the negative ion mode. The TSP jet temperature was 280°C and the vaporiser temperature was 115°C. The electron multiplier was operated at 2000 V for LC–MS and 3000 V for LC–MS–MS and the repeller was set to 120 V. Argon at a pressure of 1.5 mTorr (1 Torr = 133.322 Pa) and a collision energy of 12 eV was used as the collision gas for LC–MS–MS. Select-

ed reaction monitoring (SRM) was carried out on  $m/z$  156 going to  $m/z$  114.

#### Other equipment

A Micro Centaur micro centrifuge (Fisons) was used in the preparation of samples.

#### Modifications for the screening of tablet samples

The two NovaPak columns were replaced by a Rosil C<sub>18</sub> high-load 250 × 4.6 mm column (Capital HPLC, Bathgate, UK). The elution scheme was also altered. The column was eluted with 100% 0.1 M ammonium acetate (pH 4.5 glacial acetic acid) for 7 min followed by washing with 100% methanol for a further 8 min.

### 3. Results

#### 3.1. Determination of sensitivity

The USP states that clavam-2-carboxylate must not be present in clavulanate potassium at levels in excess of 0.01% (w/w). A 100-mg amount of clavulanate potassium is readily soluble in 1 ml water so a method capable of detecting clavam-2-carboxylate at levels of 0.001 mg/ml [equivalent to 0.001% (w/w) clavam-2-carboxylate in clavulanate potassium] was developed.

Clavulanate potassium and clavam-2-carboxylate have very similar structures and, as a result, very similar retention times. In order to achieve sufficient separation of these compounds, a number of HPLC column systems were examined. Of these, the two NovaPak C<sub>18</sub> columns linked in series initially proved to be the most efficient. These were replaced by the Rosil column in the screening of the tablet samples to further improve the separation of clavam-2-carboxylate and clavulanate potassium.

Fig. 2 shows the total ion chromatogram (RIC) and spectrum for the LC-MS run after injecting an aliquot (50  $\mu$ l) of standard clavam-2-carboxylate 0.1 mg/ml. The spectrum shows a base peak at  $m/z$  156 ( $M - H$ )<sup>-</sup>. An MS-MS experiment to determine the product ions of  $m/z$  156 for standard clavam-2-carboxylate 0.01 mg/

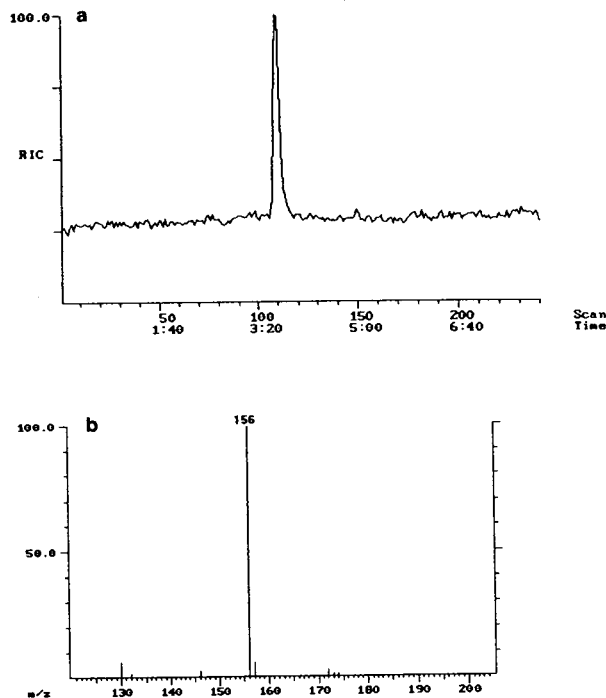
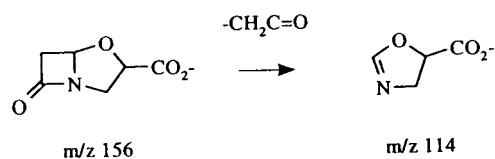


Fig. 2. (a) LC-MS chromatogram for standard clavam-2-carboxylate 0.1 mg/ml; time in min:s. (b) Spectrum for standard clavam-2-carboxylate 0.1 mg/ml.

ml, was carried out. Fig. 3 shows the TIC and product ion spectrum for this experiment. One major product ion is seen at  $m/z$  114 and another at  $m/z$  70, probably formed by loss of ketene from the parent anion, followed by a loss of 44 mass units (i.e., loss of CO<sub>2</sub>) from 114. However, when this method was applied to spiked clavulanate potassium samples too much interference from the clavulanate potassium was found to enable sensitivity of better than 0.01% (w/w) clavam-2-carboxylate in clavulanate potassium to be obtained. An SRM experiment, monitoring only  $m/z$  114 ions arising from  $m/z$  156, was used to improve the specificity of the assay.



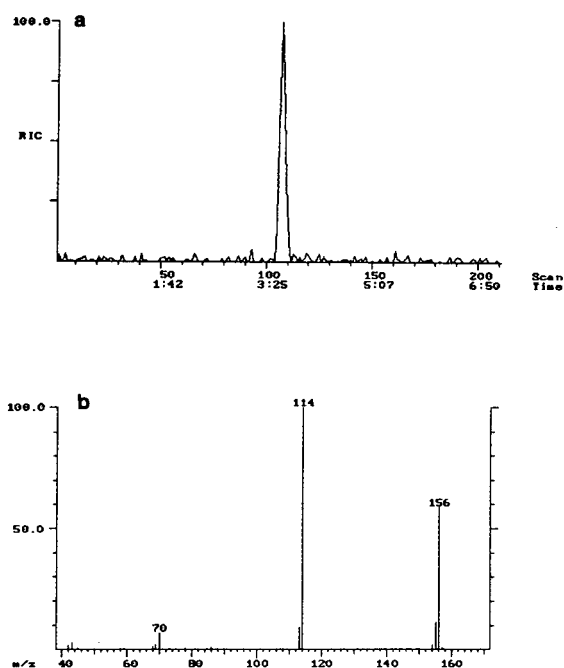


Fig. 3. (a) LC-MS-MS chromatogram for standard clavam-2-carboxylate 0.01 mg/ml; time in min:s. (b) Product ion spectrum for LC-MS-MS of standard clavam-2-carboxylate 0.01 mg/ml.

Fig. 4 shows the chromatogram obtained for an approximately 0.001% spike of clavam-2-carboxylate in clavulanate potassium. A peak for clavam-2-carboxylate can clearly be seen maximising at around scan 150. The sensitivity ob-

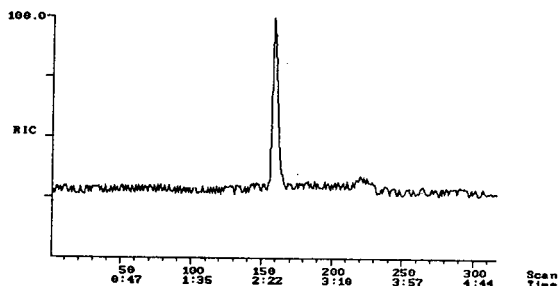


Fig. 4. SRM LC-MS-MS chromatogram for 0.001% spike of clavam-2-carboxylate in clavulanate potassium. (The apparent retention time for the clavam-2-carboxylate peak differs between Figs. 3 and 4 because of the different scan parameters.) Time in min:s.

tained is an order of magnitude better than that required by the USP limit.

When this method was applied to tablet material, the clavulanate potassium and various other components of the tablet were found to rapidly contaminate the source of the instrument. Accordingly, the HPLC procedure was modified to increase the separation of clavam-2-carboxylate and clavulanate potassium in order to facilitate the diversion of the eluent containing clavulanate potassium and other components away from the mass spectrometer. Fig. 5 shows the SRM LC-MS-MS chromatogram obtained for an approximately 0.0025% spike of clavam-2-carboxylate in a tablet sample.

### 3.2. Calibration lines

Calibration lines were prepared for clavam-2-carboxylate in clavulanate potassium (Fig. 6) and in tablet samples (Fig. 7), prepared by obtaining the SRM LC-MS-MS traces for solutions spiked with varying quantities of clavam-2-carboxylate and calculating the area of the peak produced. (The peak areas were calculated using the SuperIncos data system attached to the instrument.) Linear regression was used to calculate the equation of the straight line.

The calibration lines show that the relationship between the amount of clavam-2-carboxylate added to the sample and the instrument response is linear. The equation of the straight line for the

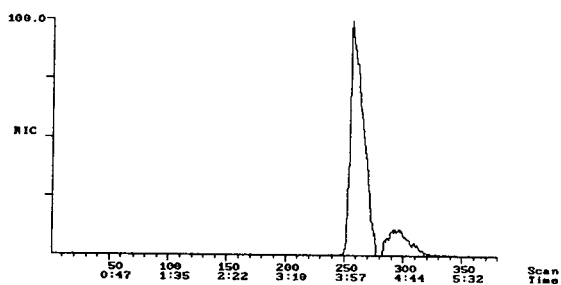


Fig. 5. SRM LC-MS-MS chromatogram for 0.0025% spike of clavam-2-carboxylate in a tablet sample. (The retention time for clavam-2-carboxylate in Figs. 4 and 5 differs as the column and elution scheme were altered for the screening of tablet samples.) Time in min:s.



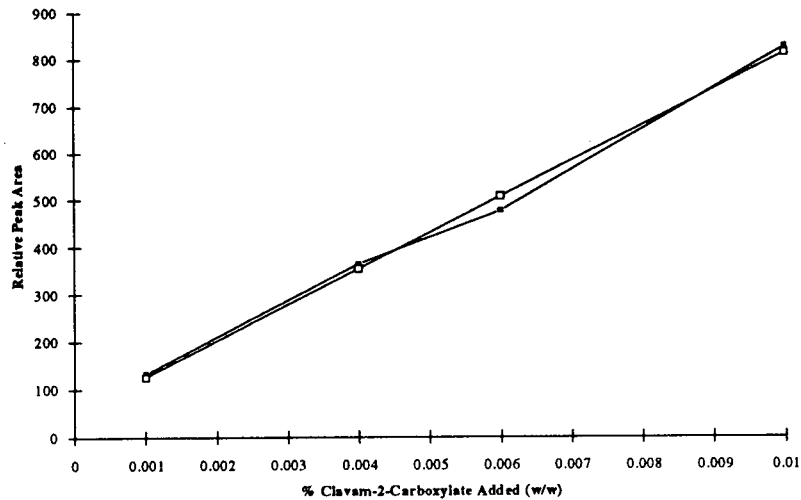


Fig. 6. Calibration line for clavam-2-carboxylate in clavulanate potassium. ■ = Experimental; □ = calculated.

calibration line for the clavulanate potassium sample can be extrapolated in order to determine the clavam-2-carboxylate content of the clavulanate potassium sample used. In this case the sample could be estimated to contain 0.0005% clavam-2-carboxylate.

The calibration line for the tablet sample crosses the y axis at a point below the origin. As

a result of this, the amount of clavam-2-carboxylate in the tablet sample used in the spiked solutions cannot be estimated. The fact that the calibration line has a negative intercept may be due to a compound co-eluting with the clavam-2-carboxylate which is suppressing its ionisation. The amount of suppression is independent of the amount of clavam-2-carboxylate present.

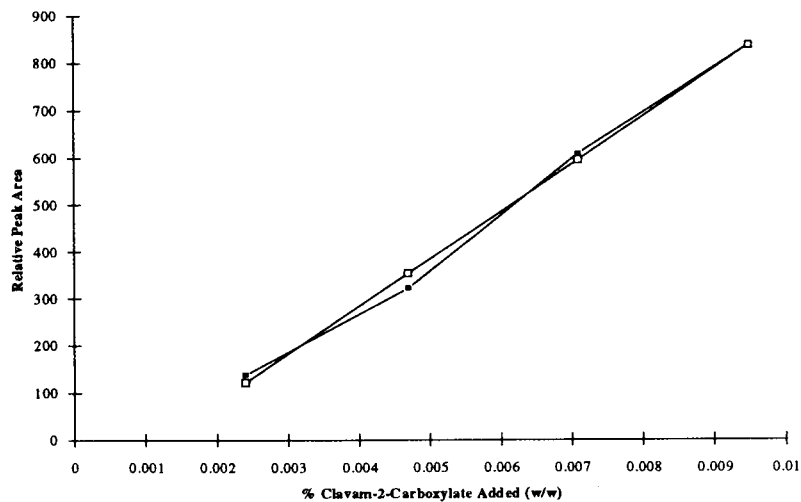


Fig. 7. Calibration line for clavam-2-carboxylate in tablet samples. (The straight lines seen in Figs. 6 and 7 are calculated using linear regression.) ■ = Experimental; □ = calculated.

#### 4. Discussion

This method is capable of detecting clavam-2-carboxylate in clavulanate potassium and formulated tablets at levels lower than that specified in the USP. However, this method is very labour intensive in terms of instrument maintenance. Clavam-2-carboxylate and clavulanate potassium have very close retention times, and it is not possible to divert all the clavulanate potassium away from the mass spectrometer. This means that only about five sample solutions may be run before the source of the instrument becomes contaminated, due to the clavulanate potassium, resulting in a drop in sensitivity. It was for this reason that only four solutions were used in the preparation of the calibration lines and, as a result of this, the calibration lines will only suffice to show that the relationship between clavam-2-carboxylate concentration and instrument response (peak area) is linear.

The Rosil column improved the separation of clavam-2-carboxylate and clavulanate potassium and facilitated the diversion of the acid away from the mass spectrometer thus reducing the amount of instrument maintenance. However, clavulanate potassium is not the major component of the tablet samples and in order to achieve the required concentration, a large amount of tablet material must be dissolved in a small amount of water (approximately 200 mg/400  $\mu$ l). This results in a highly concentrated solution being injected into the system which, despite efforts to divert all but the eluent containing clavam-2-carboxylate away from the mass spectrometer, quickly contaminates the source

and reduces the sensitivity. Clavam-2-carboxylate and clavulanate potassium are both very soluble in water, therefore the extraction efficiency should be very high, however, this has not been investigated.

In order to use LC-MS for accurate quantification of clavam-2-carboxylate concentration in clavulanate potassium, an internal standard would have to be chosen and incorporated into the sample material, to overcome any effects on the linearity of response as the instrument becomes contaminated.

#### 5. Conclusions

This method has been shown to meet the specificity and sensitivity requirements for the determination of the presence of clavam-2-carboxylate in clavulanate potassium and tablet samples at levels below that of the USP limit. The method is very labour intensive and is not recommended to replace the USP method; however, it does give the added specificity allowing clavam-2-carboxylate to be determined in formulated products.

#### References

- [1] A.E. Bird, J.M. Bellis and B.C. Gasson, *Analyst*, 107 (1982) 1241.
- [2] *US Pharmacopeia*, XXII, The US Pharmacopeial Convention, Rockville, MD, 1990, p. 316.
- [3] P.B. East, C. Eckers, N.J. Haskins, J.F. Hare and J. James, *Rapid Commun. Mass Spectrom.*, 6 (1992) 179.

# Reversed-phase high-performance liquid chromatographic separation of 1-naphthyl isocyanate derivatives of linear alcohol polyethoxylates

Karel Lemr<sup>1</sup>, Mauro Zanette, Antonio Marcomini\*

*Department of Environmental Sciences, University of Venice, Calle Larga S. Marta 2137, I-30123 Venice, Italy*

First received 31 March 1994; revised manuscript received 1 July 1994

## Abstract

The optimization procedure for the reversed-phase HPLC separation of 1-naphthyl isocyanate derivatives of linear alcohol polyethoxylates (LAEs) is reported. Using a C<sub>18</sub>-bonded silica stationary phase and acetonitrile–water mixtures as mobile phase, different trends in the chromatographic separation of selected 1-tetradecanol polyethyleneglycol ether ethoxymers were observed. In the investigated range of acetonitrile–mobile phase volume ratio ( $\varphi$ ), the elution order of the ethoxymers was inverted by increasing the organic solvent content of the mobile phase, and the mobile phase composition was found which provides the co-elution of the tested compounds. On the basis of the trends of capacity factor logarithm ( $\log k'$ ) versus the number of ethoxy units ( $n$ ) at different  $\varphi$ , an increased retention by increasing  $\varphi$  was also predicted for higher ethoxymers. The separation under the same chromatographic conditions of a C<sub>12</sub>–C<sub>18</sub> LAE mixture with an average number of 10 ethoxy units, confirmed the strong variability of LAE chromatographic behaviour in the investigated  $\varphi$  range. The isoeluting conditions found for the C<sub>14</sub> LAE ethoxymers were also applied successfully to the homologue-by-homologue separation of the C<sub>12</sub>–C<sub>18</sub> LAE mixture.

## 1. Introduction

The non-ionic surfactants of the linear alcohol polyethoxylate (LAE) type are widely used in both domestic and industrial detergent formulations. During the early 1990s they accounted for more than 50% of the total annual production of non-ionics (500 · 10<sup>6</sup> kg in 1991 [1]). The hydrophobic part of LAEs is represented by linear,

primary alkyl chains with 10 to 18 carbon atoms including both even and odd homologues for oxo-LAEs and only even homologues for oil-derived LAEs. Industrially produced oxoalcohol polyethoxylates contain also slightly branched primary alcohols in variable proportion (10–50%), depending on the synthesis conditions. Each homologue itself consists of a mixture of oligomers differing by the number of monomeric units in the polyethoxy chain. LAEs used for detergency purposes typically present an average ethoxylation grade of 5–10.

The determination of LAEs by reversed-phase high-performance liquid chromatography (RP-

\* Corresponding author.

<sup>1</sup> On leave from the Department of Analytical and Organic Chemistry, Palacky University, Svobody 8, 77146 Olomouc, Czech Republic.

HPLC) [2–12] in biodegradation test liquors, as well as environmental samples, requires adequate derivatization. The proposed derivatizing agents were so far the UV-absorbing phenyl isocyanate [2–7] and 3,5-dinitrobenzoyl chloride [8], and the fluorescent 1-anthrolylnitrile [10], 1-naphthyl isocyanate [11] and the naphthoyle chlorides [12]. Derivatization by fluorescent agents is preferable for environmental analysis particularly because of the increased selectivity. Modification of LAE molecule through derivatization can change remarkably the partitioning between mobile and stationary phases of each ethoxymer with the same alkyl chain. For determining LAEs in environmental samples, where the concentration is typically very low and matrix interferences are present, the achievement of high sensitivity and the easy peak identification in the resulting RP-HPLC chromatogram is a quite important goal which can be attained by the so called “homologue-by-homologue” separation, i.e. by co-eluting all the oligomers of each homologue. In this work we focus on the optimization procedure for the homologue-by-homologue separation of the 1-naphthyl isocyanate (NIC) derivatives of LAEs.

Once defined the chromatographic retention in terms of capacity factor  $k'$  (Eq. 1):

$$k' = (V_R - V_m) / V_m \quad (1)$$

where  $V_R$  is the retention volume of a given compound and  $V_m$  is the dead volume of the column, the relationship between  $\log k'$  and the mobile phase composition can be expressed in RP-HPLC by linear or quadratic relationships [13,14] such as:

$$\log k' = a - m\varphi \quad (2)$$

$$\log k' = a - m\varphi + d\varphi^2 \quad (3)$$

where  $\varphi$  is the organic solvent fraction (v/v) in the mobile phase and  $a$ ,  $m$  and  $d$  are constants. For homologue or oligomer series, relationships were reported [15,16] between  $\log k'$  and a number of repeating structural units,  $n$ , of the type:

$$\log k' = \log \beta + n \log \alpha \quad (4)$$

$$\log k' = \log \beta + n \log \alpha + n^2 \log \gamma \quad (5)$$

The knowledge of the constants in the Eqs. 2–5 allows the prediction of the capacity factors of different members of homologue or oligomer series under different compositions of mobile phase. We determined experimentally the constants of Eq. 2 measuring the capacity factors of the NIC derivatives of the  $n$ -tetradecanol and a series of individual ethoxymers of the  $C_{14}$  LAE homologue at different  $\varphi$ . Eq. 2 was then used for the calculation of the mobile phase composition allowing the optimal ethoxymer co-elution. The same mobile phase was finally applied to the homologue-by-homologue separation of a  $C_{12}$ – $C_{18}$  LAE mixture after derivatization with NIC.

## 2. Experimental

The chromatographic work was carried out by a 1050 series liquid chromatograph (Hewlett-Packard) equipped with a variable-wavelength UV-visible absorption detector (flow cell volume: 8  $\mu$ l). A Model 1046 fluorescence detector (Hewlett-Packard) was alternatively used for the analysis of the LAE commercial mixture. UV-absorption chromatograms were recorded at 291 nm. Excitation and emission wavelengths of 229 and 358 nm were used for the fluorescence detection. A Chemstation HP 3365 Series II data system (Hewlett-Packard) was used for chromatogram acquisition and handling. The samples were injected by a 100- $\mu$ l syringe (Hamilton) in a manual 7125 injector (Rheodyne) equipped with a 20- $\mu$ l loop (Rheodyne). The flow-rate was 1.25 ml/min, at controlled room temperature ( $22 \pm 0.5^\circ\text{C}$ ).

The separations were carried out using a 125  $\times$  4 mm I.D. LiChrospher 100 RP-18 end-capped 5- $\mu$ m LiChrocart column (Merck).

The tested mobile phases were prepared by mixing accurately weighed aliquots of HPLC-grade acetonitrile (Baker) and Milli-Q (Millipore) purified water. Both solvents were thermostated at  $20^\circ\text{C}$  before being weighed.

The capacity factors were measured at seven different  $\varphi$  values, namely 0.860, 0.880, 0.900, 0.920, 0.940, 0.960 and 0.980. Dead volumes were estimated by injecting 10  $\mu\text{l}$  of Milli-Q water under each mobile phase composition. Mean values of triplicate determinations were used for calculation of the capacity factors.

Normal tetradecanol ( $\text{C}_{14}\text{OH}$ ) (Aldrich), and the diethyleneglycol ( $\text{C}_{14}\text{E2}$ ), tetraethyleneglycol ( $\text{C}_{14}\text{E4}$ ), hexaethyleneglycol ( $\text{C}_{14}\text{E6}$ ) and octaethyleneglycol ( $\text{C}_{14}\text{E8}$ ) monotetradecyl ethers (Fluka) were used as standards of individual oligomers. Marlipal 28/100 (Hüls), a mixture of even linear primary fatty alcohol ( $\text{C}_{12}\text{--C}_{18}$ ) polyethoxylates with an average number of 10.2 ethoxy units was used as standard of LAE homologues. Stock solutions of these compounds (concentration  $\approx 300 \mu\text{g/ml}$ ) were prepared in acetone.

The derivatization reaction was carried out according to the following conditions: 0.5–1-ml aliquots of LAE stock solution were transferred into a screw-capped glass vial and evaporated to dryness under gentle stream of nitrogen. A 10- $\mu\text{l}$  volume of NIC (Aldrich) were then added to the residue. The vial was heated in an oven at 35°C for 30 min. The resulting reaction mixture was finally dissolved in 1 ml acetonitrile [12].

### 3. Results and discussion

The capacity factors of  $\text{C}_{14}\text{OH}$  and individual  $\text{C}_{14}$  ethoxymer (i.e.  $\text{C}_{14}\text{E2}$ ,  $\text{C}_{14}\text{E4}$ ,  $\text{C}_{14}\text{E6}$  and  $\text{C}_{14}\text{E8}$ ) NIC derivatives, experimentally determined in the  $\varphi = 0.860\text{--}0.980$  range, were used to evaluate the constants  $a$  and  $m$  in Eq. 2 by performing a linear regression calculation. In Fig. 1 the experimental points (i.e. capacity factor logarithms versus mobile phase composition) and the resulting linear regression curves are shown. The correlation coefficients were 0.9965 for  $\text{C}_{14}\text{E8}$ , representing the worst case, 0.9995 for  $\text{C}_{14}\text{E6}$  and  $>0.9995$  for all other compounds. A quadratic relationship like Eq. 3 could provide a better fitting of the experimental points and a more accurate prediction of the capacity factors. Nevertheless we did not use this equation because of the high uncertainty in the determination of its coefficients. The results reported below confirmed that a valuable optimization of mobile phase composition for ethoxymer co-elution can be reached using the linear Eq. 2.

Fig. 1 shows that the difference among capacity factors of the tested compounds gradually decreases by increasing  $\varphi$ . Capacity factor logarithms get increasingly closer in the  $\varphi$  range

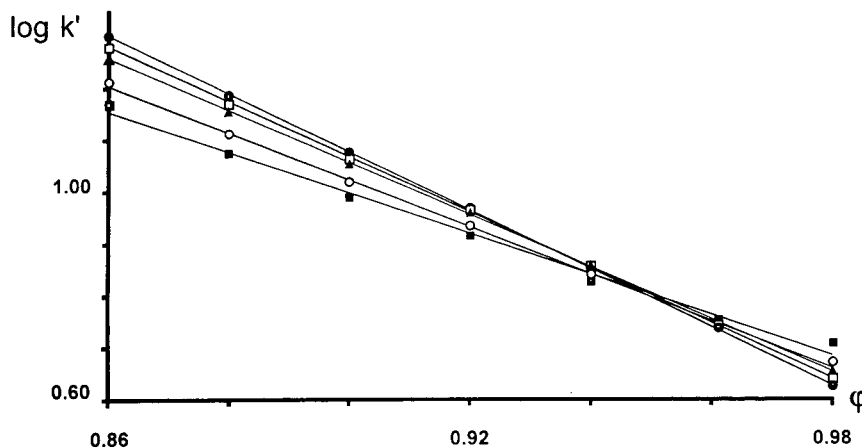


Fig. 1. Capacity factor logarithm versus the fraction of acetonitrile in the mobile phase for NIC derivatives of  $\text{C}_{14}\text{OH}$  ( $\bullet$ ),  $\text{C}_{14}\text{E2}$  ( $\square$ ),  $\text{C}_{14}\text{E4}$  ( $\blacktriangle$ ),  $\text{C}_{14}\text{E6}$  ( $\circ$ ) and  $\text{C}_{14}\text{E8}$  ( $\blacksquare$ ) in the range  $\varphi = 0.86\text{--}0.98$ . Stationary phase: LiChrospher 100 RP-18 end-capped. Column: LiChrocart 125  $\times$  4 mm I.D. Mobile phase: acetonitrile–water (flow-rate: 1.25 ml/min). Detection: UV absorption at 291 nm.

0.940–0.960, where an inversion of elution order does occur, and then begin again to increase gradually for  $\varphi > 0.960$ . It follows that it is possible to find the mobile phase composition corresponding to the very near values of the capacity factors. Kudoh [9] carried out a similar chromatographic screening on underivatized LAEs. He found out that LAE ethoxymers co-elution was possible only by using a well determined acetone–water mixture, regardless the length of the LAE hydrophobic chain. Jandera [16] provided a theoretical description for this chromatographic behaviour.

According to the definition [17] of the separation factor ( $S$ ) as:

$$S = \frac{k'_{\max} - k'_{\min}}{k'_{\max} + k'_{\min} + 2} \quad (6)$$

where  $k'_{\max}$  and  $k'_{\min}$  represent the capacity factors of the most and least retained compounds among the tested  $C_{14}$  LAE ethoxymers, respectively, and known the values of  $a$  and  $m$  in Eq. 2 for each of them, it is possible to find the value of  $\varphi$  providing the minimum  $S$  value. A numerical method was used for this estimation. Based on Eq. 2, the capacity factors at increasing values of  $\varphi$  (implementing step: 0.001) were calculated in the  $\varphi$  range 0.940–0.960. Maximum and minimum values of each  $k'$  set were extracted and the corresponding value of  $S$  was calculated. Finally the minimum value of  $S$ , corresponding to  $\varphi = 0.948$ , was identified. The results of the optimization are visualized in Figs. 2 and 3. Fig. 2 shows the chromatograms obtained when the derivatized  $C_{14}$ OH, -E2, -E4, -E6 and -E8 mixture was eluted under optimal and close-to-optimal mobile phase conditions. It emphasizes the change of elution order with increasing the fraction of acetonitrile in the mobile phase. In particular, the shift of the  $C_{14}$ OH peak from the back towards the front of the ethoxymer peaks is evident for  $\varphi$  increasing from 0.940 to 0.960. The RP-HPLC inverse retention order of polyethoxylic oligomers was already reported [18,19] and explained in terms of conformational changes of the polyethoxy chains.

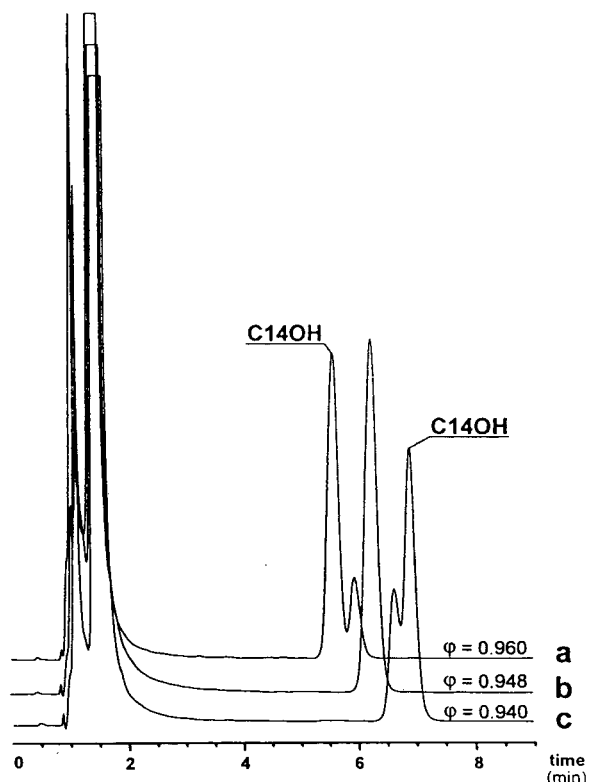


Fig. 2. RP-HPLC chromatograms of NIC derivatives of  $C_{14}$ OH,  $C_{14}$ E2,  $C_{14}$ E4,  $C_{14}$ E6 and  $C_{14}$ E8 mixture eluting under  $\varphi = 0.960$  (a), 0.948 (b) and 0.940 (c) mobile phase conditions. Conditions as in Fig. 1.

The NIC derivatives of a commercial  $C_{12}$ – $C_{18}$  LAE mixture, characterized by an average polyethoxy chain length of 10.2 E units, underwent chromatographic separation under the same conditions reported in Fig. 2 for the NIC derivatives of the  $C_{14}$ E0–E8 mixture. The corresponding chromatograms are reported in Fig. 3. As is clear from Fig. 3b, the calculated (and experimentally validated) mobile phase composition ( $\varphi = 0.948$ ) yielding optimal co-elution of the NIC derivatives of the  $C_{14}$ E0–E8 mixture (Fig. 2a), allowed the effective co-elution, among others, of the  $C_{14}$  LAE ethoxymer derivatives whose ethoxylation degree ranged from 0 to over 20 E units. Furthermore, the comparison of Fig. 3b with Fig. 3a and c shows that the optimum value

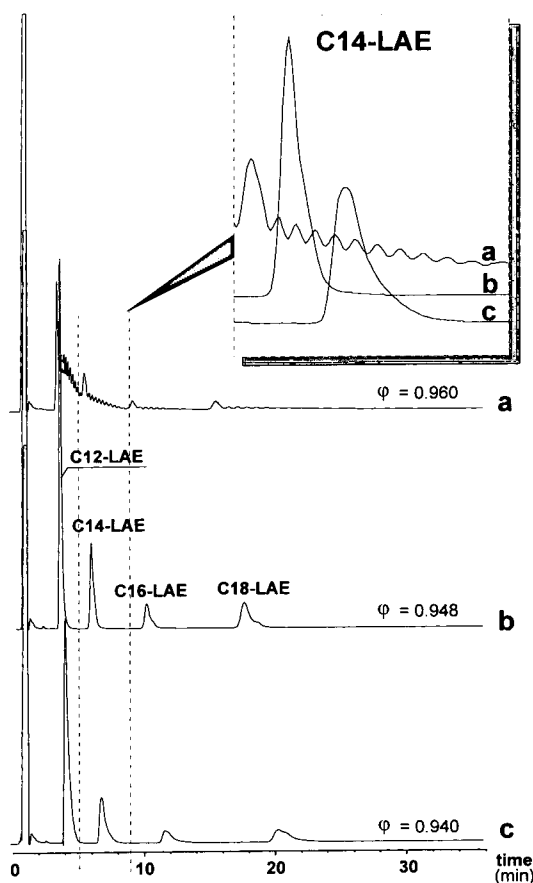


Fig. 3. RP-HPLC chromatograms of the NIC derivatives of Marlipal 28/100 (commercial  $C_{12}$ – $C_{18}$  LAEs even homologues mixture; average ethoxylation grade: 10.2) eluting under  $\varphi = 0.960$  (a), 0.948 (b) and 0.940 (c). Detection: fluorescence,  $\lambda_{ex} = 228$  nm,  $\lambda_{em} = 368$  nm. Other conditions as in Fig. 1.

of  $\varphi$  for the co-elution of the  $C_{14}E_0$ – $E_8$  ethoxymers led also to the most satisfying homologue-by-homologue separation of the derivatized commercial  $C_{12}$ – $C_{18}$  LAE mixture. A shift of  $\pm 1\%$  in the mobile phase content of the organic solvent causes significantly worse separations. A partial splitting of the homologue peaks into the corresponding ethoxymers (whose capacity factor increases with the increasing ethoxylation degree) and a partial overlapping of different homologues leading to serious identification and

quantitation problems were observed for  $\varphi > 0.948$  (Fig. 3a). A progressive tailing of the homologue peaks and a corresponding decrease of peak heights (i.e. poorer detection and quantitation limits) were obtained after minor increase of the water content (Fig. 3b).

By comparing Fig. 3b with Fig. 3a, a further interesting comment can be drawn. Some higher ethoxymers of each homologue (see magnified details for the  $C_{14}$  LAE in Fig. 3) exhibit increased retention by increasing the content of acetonitrile in the mobile phase. This behaviour, responsible for the worsening of the homologue-by-homologue separation for  $\varphi > 0.948$ , leads to conclude that the retention prediction model based on the linear Eq. 2 is no longer valid for highly ethoxylated LAEs. For these compounds, a model based on the quadratic Eq. 3 is likely to be more suited for the prediction of retention behaviour. In more detail, the higher increase of the quadratic term  $+d\varphi^2$  (Eq. 3), compared with that of the linear term  $-m\varphi$  (Eq. 2) by increasing  $\varphi$  is claimed to be responsible for the observed increase of retention at the upper limit of the studied  $\varphi$  range.

Fig. 4 visualizes the dependence of  $\log k'$  of the studied  $C_{14}$  LAE ethoxymers on the number of ethoxy units at different fractions of acetonitrile in the mobile phase. The resulting curves suggest that one (or more) curve intersections may occur in correspondence to polyethoxy chain lengths greater than the studied ones. Therefore, the observed increase of retention times of higher ethoxymers of  $C_{12}$ – $C_{18}$  LAE homologues by increasing  $\varphi$  (Fig. 3b and a) can be qualitatively foreseen on the basis of the plots reported in Fig. 4. Since these plots are clearly curved, we could use Eq. 5 for the description of the dependence of  $\log k'$  on  $n$ . Unfortunately, an estimation of the constants in Eqs. 3 and 5 based only on the achieved experimental retention data is affected by high uncertainty and practically not feasible. The validation of a retention prediction model based on such equations requires pure standards of highly ethoxylated  $C_{14}$  ethoxymers, which are not actually commercially available and difficult to isolate from commercial or laboratory-synthesized LAE mixtures.

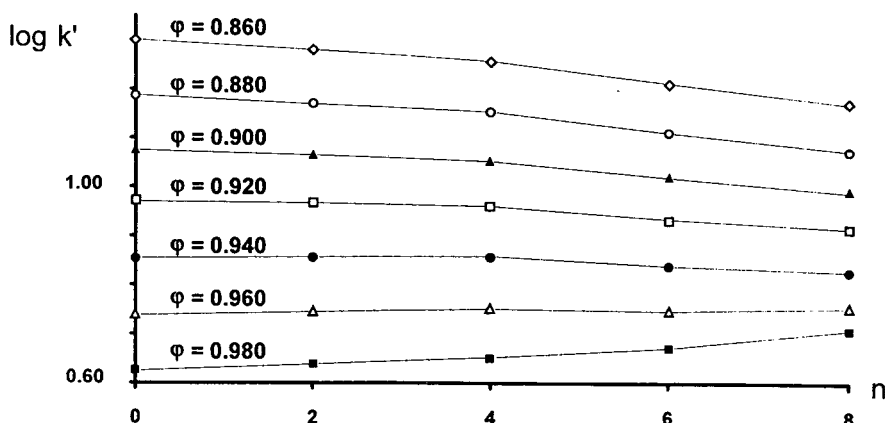


Fig. 4. Capacity factor logarithm versus the number of ethoxy units at different mobile phase composition for NIC derivatives of  $C_{14}OH$ ,  $C_{14}E_2$ ,  $C_{14}E_4$ ,  $C_{14}E_6$  and  $C_{14}E_8$ .

#### 4. Conclusions

The feasibility of the homologue-by-homologue separation of NIC derivatives of higher alcohol polyethoxylates was demonstrated. The two most important chromatographic features of the studied system were (a) the change of the retention order in the investigated interval of mobile phase composition and (b) the increasing of the retention of highly ethoxylated LAE molecules with the increasing of the organic solvent amount in the binary mobile phase.

It must be emphasized that the correct preparation of the mobile phase by accurately thermostating, weighing and mixing together the eluent solvents is an essential requisite to obtain the necessary chromatographic reproducibility. The actual most largely certified values of accuracy and precision in solvent proportioning of the commercial multi-channel chromatographic pump systems do not provide an acceptable reproducibility when critical  $\phi$  values (i.e. those near the isoeluting point) are required, since a slight change of the mobile phase composition leads to a remarkable decrease of both the resolution and the detection sensitivity.

#### References

- [1] B. Fell, *Tenside Deterg.*, 28 (1991) 385.
- [2] L. Nitschke and I. Huber, *Fresenius' J. Anal. Chem.*, 345 (1993) 585.
- [3] L. Cavalli, A. Gellera, G. Cassani, M. Lazzarin, C. Maraschin and G. Nucci, *Riv. Ital. Sost. Grasse*, 70 (1993) 447.
- [4] E. Mattheijs and E.C. Hennes, *Tenside Deterg.*, 28 (1991) 22.
- [5] T. Okada, *J. Chromatogr.*, 609 (1992) 213.
- [6] T.M. Schmitt, M.C. Allen, D.K. Brain, K.F. Guin, D.E. Lemmel and Q.W. Osburn, *J. Am. Oil Chem. Soc.*, 67 (1990) 103.
- [7] M.C. Allen and D.E. Linder, *J. Am. Oil Chem. Soc.*, 58 (1981) 950.
- [8] P.L. Desbène, B. Desmazières, J.J. Basselier and A. Desbène-Monvernay, *J. Chromatogr.*, 461 (1989) 305.
- [9] M. Kudoh, *J. Chromatogr.*, 291 (1984) 327.
- [10] M. Kudoh, H. Ozawa, S. Fudano and K. Tsuji, *J. Chromatogr.*, 287 (1984) 337.
- [11] G. Kloster, presented at the *AIS-CESIO Workshop on Method Development for Alcohol Ethoxylates*, Strombeek-Bever, 15 October, 1992.
- [12] A. Marcomini and M. Zanette, *Riv. Italiana Sost. Grasse*, 71 (1994) 203.
- [13] P.J. Schoemakers, H.A.H. Billiet and L. de Galan, *J. Chromatogr.*, 185 (1979) 179.
- [14] P. Jandera, H.L. Colin and G. Guiochon, *Anal. Chem.*, 54 (1982) 435.
- [15] P. Jandera, *J. Chromatogr.*, 314 (1984) 13.
- [16] P. Jandera, *J. Chromatogr.*, 449 (1988) 361.
- [17] P.J. Schoenmakers, *Optimization of Chromatographic Selectivity — A Guide to Method Development*, Elsevier, Amsterdam, 1986, p. 126.
- [18] W.R. Melander, A. Nahum and Cs. Horváth, *J. Chromatogr.*, 185 (1979) 129.
- [19] T. Okada, *Anal. Chim. Acta*, 281 (1993) 85.



# Statistical treatment of large digital chromatographic data sets

D.C. Freeman\*, D.W. Byrd

*Department of Biological Sciences, Wayne State University, Detroit, MI 48202, USA*

First received 8 December 1993; revised manuscript received 8 June 1994

---

## Abstract

Capturing vast amounts of digital chromatographic data is now routine, but it brings with it the onerous problems of data reduction, unification and analysis. The methods reported here provide a rapid means of storing, sorting, tabulating and analyzing large sets of chromatographic data.

---

## 1. Introduction

Static headspace gas chromatography (GC) is a sensitive method for analyzing the volatile and semivolatile hydrocarbons [1–4]. The method lends itself to automation, potentially allowing for the acquisition of large data sets with minimal labor. While headspace GC is a potent analytical tool, it has not been used extensively in large population studies. The correlation of retention time data across multiple samples is a significant problem that limits the ease whereby large data sets are accumulated and analyzed. Variability in retention time data among samples stems from human error in the manipulation of the samples as well as system related errors. Manual input of chromatographic data for statistical analysis is also a source of error. The automated static headspace sampling system and digital data storage system described in Byrd and Freeman [5] minimize both of these errors.

Here, we illustrate the assembly and analysis of large chromatographic data sets using the volatile and semivolatile terpene compounds

produced by two subspecies of big sagebrush (*Artemisia tridentata* ssp. *tridentata*, i.e. basin big sagebrush, and *A. tridentata* ssp. *vaseyana*, i.e. mountain big sagebrush) and various hybrids between these two taxa [6]. Like most chromatographic studies we are interested in comparing mean concentrations of one or more compounds among various treatments, but in addition we are also interested in comparing the ability of these sagebrush taxa to regulate the production of volatile compounds among leaves of the same plant. The process of hybridization disrupts long established intergene coordination (co-adapted genes complexes), and thus the ability of a plant to regulate its body. We have investigated this disruption by comparing within plant similarity indices among plant populations.

The majority of volatile and semivolatile compounds produced by sagebrush are monoterpenes [7–14], i.e. stable volatile or semivolatile non-saponifiable lipids, linked to essential metabolic processes. We also examined the distributions and concentrations of sesquiterpenes, coumarins and auxins that, like terpenes, are derived from isoprene [11]. Terpenes and related compounds are believed to function as pollinator

---

\* Corresponding author.

attractants, pesticides, phytotoxins, bacteriostats, predator defense compounds or insect larval abortives [7,8,10]. Several studies suggest that monoterpenes are taxa specific [6,8,10,12–15].

## 2. Methods

We examined a narrow hybrid zone in Salt Creek Canyon, UT, USA. There, basin big sagebrush occurs below 1740 m, while mountain big sagebrush occurs above 1860 m, with the hybrid zone found in between. Plants were collected from five sites, one from each of the two parental regions, and one from each of the three hybrid zones [6]. Twelve plants were sampled from each of the parental sites and from four plants in each of the hybrid sites. The plants were permanently marked and the same individuals were sampled in both the Spring and Fall (1991). For each season we collected two leaves per branch from two branches per plant. We also sampled two leaves from one flowering stalk (inflorescence) per branch in the Fall. The data set was derived from more than 400 samples. Since the concentrations of more than 100 compounds were determined using the protocols in Byrd and Freeman [5], the entire data set exceeded 40 000 data points. Manipulation of these data provided additional information (total hydrocarbons, percent area of a given component, mass of all components, mass of individual components and percent of area or mass of a component) and expanded the total data set to over 200 000 data points.

We used PeakSimple I software [16] to capture the chromatographic analog signals and converted them to an ASCII digital format. The digital storage consisted of a voltage file and a summary report file that included retention time, percent area, peak height, peak area and internal standard information. These summary files were imported directly to a spreadsheet (Lotus 2.1 [17]). These data were transposed for statistical procedures so that each sample represented a row of the matrix rather than a column, with retention time windows shown in columns. This step was repeated for each sample. Further

reduction of data was made on this data set by selecting specific time windows from the data set.

## 3. Statistical analyses

Below, we use a subset of our data to illustrate several parametric and non-parametric statistical procedures that may be used to analyze chromatographic data, comment on the limitations of various tests and report results for the whole data set (for details see [18–25]. Parametric tests utilize the variance in testing for differences among the means of treatments. Two assumptions must be met: (1) the data must be normally distributed and (2) the variances must be the same for each treatment. If both these assumptions are valid, then these statistically powerful parametric procedures can be utilized. If these assumptions are not met and the data cannot be transformed so that the assumptions hold, then one should use the less powerful non-parametric procedures.

### 3.1. Comparing means among treatments

#### *Parametric procedures*

To illustrate the use of parametric procedures, we have compared the concentration of a compound with a retention time of 7.92 min among the sagebrush taxa using a simple oneway analysis of variance (Table 1) and a multiple range test (Table 2). The former test determines if there is a significant difference among the means, but does not determine which means are different from one another. A oneway analysis of variance (also known as a fixed effect or Model 1 analysis of variance) using all the data for peak 7.92 showed that the concentration differed significantly among the sites ( $F_{4,125} = 13.86$ ,  $P < 0.0001$ ). The a posteriori Student–Newman–Keuls multiple range test does determine which means differ significantly from each other. The Student–Newman–Keuls multiple range test (Table 2) showed that the concentrations at site 1 ( $\bar{X} = 0.238 \pm 0.2053$ ) differed significantly from the concentrations at all other sites. However, sites 2, 3, 4 and 5 did not differ

Table 1

Data from one leaf per plant for four plants from each of the five sites used to illustrate the procedures of a oneway analysis of variance

| <i>Terpene concentration from sagebrush plants growing at five different sites, data are from the Fall of 1991</i> |        |        |        |  |        |
|--|--------|--------|--------|--|--------|
| Site   | 1.000  | 2.000  | 3.000  | 4.000                                    | 5.000  |
| Data   | 0.764  | 0.021  | 0.114  | 0.000                                    | 0.138  |
|  | 0.790  | 0.032  | 0.148  | 0.000                                    | 0.119  |
|  | 0.812  | 0.030  | 0.130  | 0.000                                    | 0.113  |
|  | 0.692  | 0.029  | 0.127  | 0.090                                    | 0.112  |
| <i>Oneway analysis of variance</i>   |        |        |        |  |        |
| Total  | Site 1 | Site 2 | Site 3 | Site 4                                   | Site 5 |
| Mean $\bar{X}$   | 0.764  | 0.028  | 0.130  | 0.023                                    | 0.120  |
| Sum  | 3.058  | 0.112  | 0.519  | 0.090                                    | 0.482  |
| $(\sum X)^2/N$   | 2.338  | 0.003  | 0.067  | 0.002                                    | 0.058  |
| $\sum(X^2)/N$  | 0.586  | 0.001  | 0.017  | 0.002                                    | 0.015  |
| Total $\sum_i \sum_j X_{i,j}$  | 4.261  |        |        |  |        |
| Total sum of squares   | 2.346  | 0.003  | 0.068  | 0.008                                    | 0.058  |
| $\sum_i \sum_j X^2 - C$  |        |        |        |  |        |
| $C[(\sum_i \sum_j X_{i,j})^2]/N$   | 0.908  |        |        |  |        |
| Total sum of squares = $T = \sum_i \sum_j X_{i,j}^2 - C$   |        |        | 1.576  |  |        |
| Group sum of squares = $G = \sum_i [(\sum_j X_{i,j})^2]/N_i - c$   |        |        | 1.560  | Error MS = $E/DF = 0.015/15 = 0.001$     |        |
| Error sum of squares = $E = T - G$   |        |        | 0.015  | Group MS = $G/DF = 1.560/4 = 0.390$      |        |
|  |        |        |        | $F = \text{group MS/error MS} = 390.000$ |        |

The  $F$  value is compared against tabulated using the degrees of freedom among groups (one less than the number of groups) and the error degrees of freedom. In this case there are 20 data points. One degree of freedom is assigned to the mean, four to the groups and so there are 15 degrees of freedom for error.

significantly from one another. The means for these sites were  $0.0472 \pm 0.0535$ ,  $0.0266 \pm 0.0531$ ,  $0.0106 \pm 0.0299$  and  $0.0794 \pm 0.1266$ , respectively. Despite the appealing result from the oneway analysis of variance its use is not appropriate for this data set. These chromatographic data have unequal variances among sites (as determined by Bartlett's test  $F = 20.622$ ; see Table 3), and the data are not normally distributed (as determined by the Kolmogorov–Smirnov goodness of fit test; see [18]). Therefore one should not use the parametric procedure but

should instead use a non-parametric Kruskal–Wallis procedure (Table 4).

#### *Non-parametric procedures*

The non-parametric Kruskal–Wallis test does not have the stringent assumptions of normality or homogeneity of variance. We have illustrated its use in Table 4 where we compare multiple means among treatments. Again, the results show a significant difference among the sites when all the data for the compound corresponding to peak 7.92 were used ( $\chi^2 = 41.90$ ).

Table 2  
Student-Newman-Keuls multiple range test

$SE = \sqrt{(S^2/2)(1/n_a - 1/n_b)}$ ;  $q = (\bar{X}_b - \bar{X}_a)/SE$ ;  $S^2$  is the error mean square from Table 1

| Comparison | Difference<br>$E\bar{X}_b - \bar{X}_a$ | SE     | $q$    | Critical<br>value<br>of $q$ | Conclusion |
|------------|--|--------|--------|-----------------------------|------------|
| 1 vs. 3    | 0.634                                  | 0.0158 | 40.126 | 4.367                       | $P < 0.05$ |
| 1 vs. 5    | 0.644                                  | 0.0158 | 40.759 | 4.367                       | $P < 0.05$ |
| 1 vs. 2    | 0.736                                  | 0.0158 | 46.582 | 4.367                       | $P < 0.05$ |
| 1 vs. 4    | 0.741                                  | 0.0158 | 46.898 | 4.367                       | $P < 0.05$ |
| 3 vs. 5    | 0.010                                  | 0.0158 | 0.633  | 4.367                       | $P > 0.05$ |
| 3 vs. 2    | 0.102                                  | 0.0158 | 6.456  | 4.367                       | $P < 0.05$ |
| 3 vs. 4    | 0.107                                  | 0.0158 | 6.772  | 4.367                       | $P < 0.05$ |
| 5 vs. 2    | 0.092                                  | 0.0158 | 5.822  | 4.367                       | $P < 0.05$ |
| 5 vs. 4    | 0.097                                  | 0.0158 | 6.139  | 4.367                       | $P < 0.05$ |
| 2 vs. 4    | 0.005                                  | 0.0158 | 0.316  | 4.367                       | $P > 0.05$ |

This test is used after an analysis of variance to determine which means differ from one another. See Table 1 for the analysis of variance. In performing this procedure the means must be ranked first. Critical values of  $q$  are obtained from the statistical tables.

#### Multivariate procedures

If the samples being analyzed contain more than one compound of interest, then the concentration of compound A in each sample is not independent of the concentration of compound

B, and one must use a multivariate analysis of variance (MANOVA) as the parametric procedure. The MANOVA test carries with it all the assumptions of analysis of variance and the same tests are used to determine if the assumptions

Table 3  
Bartlett's test, used to determine if the variances are homogenous among the various treatment groups

| Sites                            | 1.000  | 2.000    | 3.000        | 4.000       | 5.000    |
|----------------------------------|--|----------|--------------|-------------|----------|
| Data                             | 0.764  | 0.021    | 0.114        | 0.000       | 0.138    |
|                                  | 0.790  | 0.032    | 0.148        | 0.000       | 0.119    |
|                                  | 0.812  | 0.030    | 0.130        | 0.000       | 0.113    |
|                                  | 0.692  | 0.029    | 0.127        | 0.090       | 0.112    |
| Mean                             | 0.764  | 0.028    | 0.130        | 0.023       | 0.120    |
| $SS = \sum (\bar{X}_i - X_i)^2$  | 0.0082   | 0.000    | 0.0006       | 0.0061      | 0.0004   |
| $\nu_i$                          | The degree of freedom, i.e., $n_i - 1$                     |          |              |             |          |
| $\nu_i^2$                        | 3.000  | 3.000    | 3.000        | 3.000       | 3.000    |
| $s_i^2 = ss_i/\nu_i$             | 0.0027   | 0.0000   | 0.00012      | 0.002       | 0.0001   |
| $\log s_i^2$                     | -2.5686  | -4.6320  | -3.6990      | -2.6990     | -4.0000  |
| $\nu_i \log s_i^2$               | -7.7059  | -13.8961 | -11.0969     | -8.0969     | -12.0000 |
| $s_p^2 = \sum SS_i / \sum \nu_i$ | 0.0008   |          | $\log s_p^2$ | -3.1144     |          |
| $B$                              | $B = \ln(s_p^2) \cdot (\sum \nu_i) - \sum \nu_i \ln s_i^2$ |          |              |             |          |
| $B$                              | -17.9505   |          |              |             |          |
| $C$                              | $C = 1 + [1/3(k-1)] [(\sum 1/\nu_i) - 1/\sum \nu_i]$       |          |              |             |          |
| $C$                              | 1.1333   |          |              |             |          |
| $B_c = B/C$                      | -15.8387   |          |              | $P < 0.005$ |          |

Data are the same as used in Table 1.  $B_c$  is compared to a  $\chi^2$  distribution. In this case the variances are not homogenous and one should use a non-parametric test as illustrated in Table 4.

Table 4  
The Kruskal–Wallis test, a non-parametric procedure for comparing three or more means; it uses ranked data

| Sites   | 1.000                                | 2.000  | 3.000                                | 4.000                            | 5.000                               |
|---|--------------------------------------|--|--------------------------------------|----------------------------------|-------------------------------------|
| Ranks ( $R_i$ )   | 18.000<br>19.000<br>20.000<br>17.000 | 4.000<br>7.000<br>6.000<br>5.000   | 11.000<br>16.000<br>14.000<br>13.000 | 2.000<br>2.000<br>2.000<br>8.000 | 15.000<br>12.000<br>10.000<br>9.000 |
| $n_i$   | 4.000                                | 4.000  | 4.000                                | 4.000                            | 4.000                               |
| $\sum \text{rank } (R_i)$   | 74.000                               | 22.000   | 54.000                               | 14.000                           | 46.000                              |
| $R_i^2/n_i$   | 1369.000                             | 121.000  | 729.000                              | 49.000                           | 529.000                             |
| $\sum T = \sum (t_i^3 - t_i)$   | $(3^3 - 3)$                          | $t_i$ refers to the number of ties. In this case three numbers were tied |                                      |                                  |                                     |
| $C = 1 - \left[ \left( \sum T \right) / (N^3 - N) \right]$                      | 0.9970                               |  |                                      |                                  |                                     |
| $H = 12/[N(N+1)] \cdot \frac{\sum R_i^2/n_i - 3(N+1)}{\sum R_i^2/n_i - 3(N+1)}$ | 16.914                               |  |                                      |                                  |                                     |
| $H_c = H/C$   | 16.9650                              | $P < 0.005$  |                                      |                                  |                                     |

The analysis is performed on the ranks and not the data itself. The data are given in Table 1. The distribution of  $H_c$  is approximated by that of a  $\chi^2$  with one degree of freedom less than the number of groups being compared.

are met. Some authors mistakenly use multiple “ $t$ ” test (or other tests such as correlations — $\chi^2$ , etc.) for such comparisons, but this causes a build up of type 1 errors, i.e. the probability of rejecting a true hypothesis. The null hypothesis in most cases is that there is no difference among the treatments. So the use of multiple tests leads to the reporting of significant differences where none may exist. If one chooses to use multiple “ $t$ ” tests one can correct for the build up of type 1 error by using the sequential Bonferroni test (see [19]).

To distinguish sources of variation in the data set, we recommend principal component analysis. The method can be used to obtain a visual display of multivariate data. Principal component analysis requires the determination of new axes in the multivariate space formed by the original variables. These new axes are usually generated using least squares regression techniques [20,23,26,27]. The first component (new axis) is that line which accounts for the greatest variation. The second axis is that line which is perpendicular to the first axis and accounts for the greatest amount of the remaining variation among all the possible lines that could be drawn perpendicular to the first line. The third component must be perpendicular to both the first

and second components and similarly accounts for the greatest amount of the remaining variation (i.e. it is also chosen from among all the lines that are mutually perpendicular to the first and second components). The procedure can be carried on until all the variation is accounted for. Because each principal component is in fact a linear combination of the various chemical concentrations, one can compute the principle component score of each sample. These scores can then be plotted against each other to determine if the samples came from one, or more than one, population. We have done this for our terpene data. In Fig. 1 we have plotted the first versus the second principal component for terpenes sampled in the Fall for the two parental taxa. The results clearly show that the terpene profile of basin big sagebrush differs from that of mountain big sagebrush. Hybrids form intermediate distributions when compared to the parentals. While a number of pretreatments of the data are possible and influence the data, for this analysis we did not pretreat the data. Principal component analysis assumes linearity; if this assumption does not hold, there are non-linear ordinations that can be used, e.g. detrended principal components [20] or non-metric multi-dimensional scaling [21].

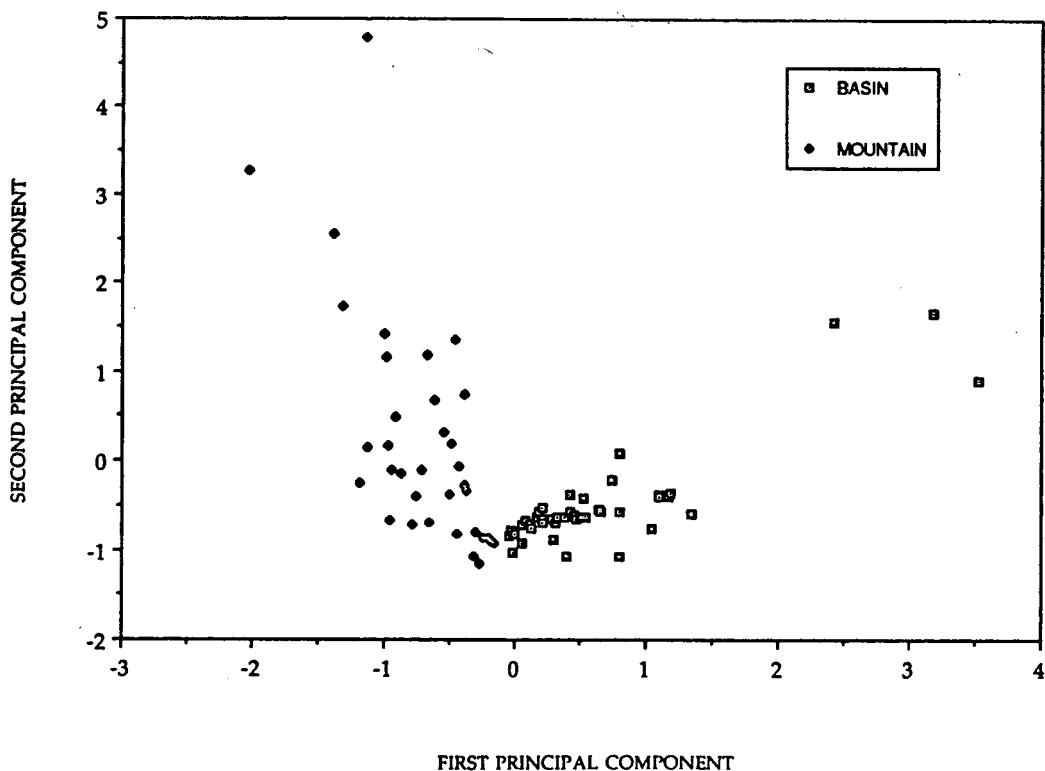


Fig. 1. Fall principal component analysis. First versus second component.

### 3.2. Within individual variation as a measure of developmental control, i.e. stress

Chromatographic data may also be used to determine if organisms are under stress. The premise for this is rather simple. Organisms that are not stressed tightly regulate the development of their own bodies, while stress interferes with this regulation. By examining this within individual variation in concentration or proportions of compounds, one can assess the degree of stress organisms are under [22,24].

One can use either a parametric approach, i.e. analysis of variance, or a non-parametric approach for this analysis. In our case, the parametric approach involves computing a within plant variance for the concentration or proportion of one or more compounds, and determining if the within plant variance differs among the taxa of sagebrush. Our full data set fails to meet the assumptions for the analysis of variance. We

have opted instead to use various non-parametric Euclidean distance measures.

#### Distance measures

To compute the Euclidean distance, let  $A_1$  be the concentration of one compound and  $B_1$  be the concentration of a second compound taken from sample 1. Similarly,  $A_2$  and  $B_2$  are the concentrations found in sample 2 from the same individual (i.e. in our case multiple leaves on the same plant). Now, we simply plot the concentrations in Euclidean space where compound A represents the  $x$  axis and compound B represents the  $y$  axis. The formula for the Euclidean distance (ED) is given in Eq. 1.

$$ED_{jk} = \sqrt{(X_{ij} - X_{ik})^2} \quad (1)$$

Each sample represents a point in this Euclidean space, and the distance between two points from the same individual represents a measure of

the dissimilarity, thus is an indicator of the degree of stress individuals are under [22–24]. These distances can then be analyzed using either analysis of variance or Kruskal–Wallis tests.

The results of our study show that mountain big sagebrush is less able to regulate the production of terpenes than either basin big sagebrush or the hybrids (Tables 5 and 6). The Euclidian distance described above will increase

Table 5  
Measure of within-plant similarity using resemblance functions computed with data from the Spring

|  | Basin             | Hybrid            | Mountain          |
|--|-------------------|-------------------|-------------------|
| Euclidean distance   | 0.39              | 0.27              | 0.41              |
| between leaves from the same branch                          | 0.26              | 0.29              | 0.37              |
| Euclidean distance among leaves from different branches      | 0.38              | 0.30              | 0.43              |
| among leaves from different branches                         | 0.22              | 0.27              | 0.36              |
| Chord distances between leaves from the same branch          | 1.30              | 1.26              | 1.22              |
| between leaves from the same branch                          | 0.15              | 0.11              | 0.19              |
| Chord distances among leaves from different branches         | 1.29              | 1.27              | 1.22              |
| among leaves from different branches                         | 0.15              | 0.10              | 0.18              |
| Mean absolute distance between leaves from the same branch*  | 0.90              | 0.58              | 0.82              |
| distance between leaves from the same branch*                | 0.59              | 0.52              | 0.68              |
| Mean absolute distance among leaves from different branches* | 0.91              | 0.66              | 0.83              |
| distance among leaves from different branches*               | 0.54              | 0.50              | 0.64              |
| Jaccard index for leaves from the same branch                | 0.77              | 0.58              | 0.51              |
| leaves from the same branch                                  | 1.48              | 0.26              | 0.25              |
| Jaccard index for leaves from different branches             | 0.49              | 0.55              | 0.48              |
| leaves from different branches                               | 0.26              | 0.26              | 0.22              |
| Diversity index for leaves from the same branch              | 1.86 <sub>a</sub> | 1.92 <sub>a</sub> | 1.54 <sub>b</sub> |
| leaves from the same branch                                  | 0.48              | 0.45              | 0.34              |
| Diversity index for leaves from different branches           | 1.96 <sub>a</sub> | 1.97 <sub>a</sub> | 1.48 <sub>b</sub> |
| leaves from different branches                               | 0.51              | 0.46              | 0.40              |

\* Taxa differ significantly from one another at  $P < 0.05$ .

<sup>a,b</sup> Means subscripted by the same letter do not differ significantly; means subscripted by different letters differ significantly at  $P < 0.05$ .

Table 6  
Measure of within plant similarity using resemblance functions computed with data from the fall

|  | Basin               | Hybrid            | Mountain          |
|--|---------------------|-------------------|-------------------|
| Euclidean distance   | 0.11 <sub>a</sub>   | 0.26 <sub>b</sub> | 0.41 <sub>c</sub> |
| between leaves from the same branch                          | 0.07                | 0.20              | 0.29              |
| Euclidean distance among leaves from different branches      | 0.23 <sub>a</sub>   | 0.36 <sub>b</sub> | 0.62 <sub>c</sub> |
| among leaves from different branches                         | 0.10                | 0.22              | 0.20              |
| Chord distances between leaves from the same branch          | 1.21 <sub>a</sub>   | 1.29 <sub>b</sub> | 1.30 <sub>b</sub> |
| between leaves from the same branch                          | 0.13                | 0.08              | 0.09              |
| Chord distances among leaves from different branches         | 1.23 <sub>a</sub>   | 1.31 <sub>b</sub> | 1.36 <sub>b</sub> |
| among leaves from different branches                         | 0.13                | 0.07              | 0.12              |
| Mean absolute distance between leaves from the same branch*  | 0.24 <sub>a</sub>   | 0.59 <sub>b</sub> | 0.91 <sub>c</sub> |
| distance between leaves from the same branch*                | 0.15                | 0.43              | 0.64              |
| Mean absolute distance among leaves from different branches* | 0.53 <sub>a</sub>   | 0.84 <sub>b</sub> | 1.47 <sub>c</sub> |
| distance among leaves from different branches*               | 0.25                | 0.49              | 0.46              |
| Jaccard index for leaves from the same branch                | 0.79 <sub>a</sub>   | 0.68 <sub>b</sub> | 0.56 <sub>b</sub> |
| leaves from the same branch                                  | 0.14                | 0.13              | 0.22              |
| Jaccard index for leaves from different branches             | 0.70 <sub>a</sub>   | 0.53 <sub>b</sub> | 0.53 <sub>b</sub> |
| leaves from different branches                               | 0.16                | 0.22              | 0.16              |
| Diversity index for leaves from the same branch              | 1.85 <sub>a,b</sub> | 2.06 <sub>b</sub> | 1.74 <sub>a</sub> |
| leaves from the same branch                                  | 0.40                | 0.39              | 0.36              |
| Diversity index for leaves from different branches           | 1.70 <sub>a</sub>   | 2.02 <sub>b</sub> | 1.70 <sub>a</sub> |
| leaves from different branches                               | 0.40                | 0.37              | 0.34              |

Footnotes as in Table 5.

as the number of compounds is increased. Ludwig and Reynolds [23] have reviewed a large number of resemblance functions and advocated dividing the total Euclidian distance by the number of compounds. They refer to this as the mean absolute Euclidean distance (MAD, Eq. 2).

$$MAD_{jk} = \sum |X_{ij} - X_{ik}| / S \quad (2)$$

In our case the taxa also differ significantly for this distance measure as well (Tables 5 and 6).

Distance measures can also be used to compare the proportions of compounds among sam-

ples from the same individual. To do this one projects the data on to a unit circle. The length of the chord separating the data points (chord distance, CHD; Eq. 3) is the measure of dissimilarity [23,25].

$$\text{CHD}_{jk} = \sqrt{2(1 - \text{ccos}_{jk})} \quad (3a)$$

$$\text{ccos}_{jk} = \sum(X_{ij}X_{ik}) / \sqrt{\sum X_{ij}^2 \cdot \sum X_{ik}^2} \quad (3b)$$

Our data again showed that the mountain big sagebrush was less able to regulate the proportions of volatile and semivolatile compounds than the other two taxa (Table 5 or 6).

Much can be learned by examining the presence or absence of a compound. Jaccard's index (JI, see [23]) is based upon such data and simply examines the percent of compounds that are common to all samples. We have computed the percent of compounds in common among two leaves from the same branch.

$$\text{JI} = a / (a + b + c) \quad (4)$$

where  $a$  = number of compounds made by both leaves,  $b$  = number of compounds made by leaf 1 that are not produced by leaf 2,  $c$  = number of compounds produced by leaf 2 that are not produced by leaf 1.

Surprisingly, not all leaves make all the compounds the plant is capable of making. Once again, mountain big sagebrush was less able to regulate its physiology than either of the other taxa (Tables 5 and 6).

Using the Shannon–Weaver information index (entropy  $H'$ , Eq. 5) we can also examine the information (entropy) content of a given sample.  $H'$  increases as the number of compounds increase and as the concentrations of the compounds become more uniform.

$$-H' = -\sum p_i \ln p_i \quad (5)$$

where  $p$  is the frequency of the component measured.

This information provides an idea of the complexity of the chemical environment that must be dealt with by both predators and

pathogens. Our results show that the information content varied significantly among the groups.

### 3.3. Sample size

The sample size required varies with the test being used. In general the greater the number of samples taken, the greater the confidence in the mean. For parametric procedures one can use the procedure given in Ref. [23] where  $n = (s^2 t_{\alpha(2), n-1}^2 F_{\beta(1), (n-1), \nu}) / d^2$ , where  $s^2$  is the sample variance from a pilot study, where  $t_{\alpha(2), n-1}^2$  refers to the tabulated value of a two-tailed  $t$  distribution with  $n-1$  degrees of freedom,  $F_{\beta(1), (n-1), \nu}$  is the tabulated value of an  $F$  distribution with  $n-1$  and  $\nu$  degrees of freedom,  $\nu$  is the degrees of freedom from the pilot study and  $d$  is the half width of the desired confidence interval. The  $n$  in the above equation is the desired sample size and the equation must be solved by iteration. In our work, we have found greater variability among plants than within plants. Thus, one needs to sample many more plants per treatment than leaves within a plant. We have found that 10 plants per treatment and four leaves per plant (total of 40 samples per treatment) is adequate to discriminate among the sagebrush taxa.

## 4. Conclusions

We have provided a conceptual approach and background for statistical interpretations of large amounts of digitally stored chromatographic data in a routine and efficient manner. Examples have been provided to demonstrate the transformation of GC data into a format compatible for direct importation into statistics software programs and guidance on the proper use of statistical tools. We have demonstrated that the coupling of automated GC procedures and digital storage of data provide a viable method for the accumulation of large sets of data that can be subjected to statistical analysis. The approach used in this study is applicable to other chromatographic analytical techniques which provide for the digital storage of retention data.



## References

- [1] E. Droz, *Anal. Chem.*, 16 (1973) 1132.
- [2] R.G.S. Bidwell, *Plant Physiology*, MacMillan, New York, 1974.
- [3] J.D. Cedarleaf, B.L. Welch and J.D. Brotherson, *J. Range Manage.*, 36 (1983) 492.
- [4] J.A. Corkill, *J. High Resolut. Chromatogr. Chromatogr. Commun.*, 11 (1988) 211.
- [5] D.W. Byrd and D.C. Freeman, *J. Chromatogr.*, 686 (1994) 235.
- [6] D.C. Freeman, W.A. Turner, E.D. McArthur and J.H. Graham, *Am. J. Botany*, 78 (1991) 805.
- [7] R. Croteau, *Chem. Rev.*, 67 (1987) 829.
- [8] S.O. Duke, R.N. Paul, Jr. and S.M. Lee, *Biologically Active Natural Products*, (ACS Symposium Series, No. 380), American Chemical Society, Washington, DC, 1988, p. 318.
- [9] W.W. Epstein and L.A. Gaudioso, *Phytochemistry*, 23 (1984) 2257.
- [10] R.G. Kelsey, *Symposium on the Biology of Artemisia and Chrysothamus; General Technical Report INT-200*, Department of Agriculture, Forest Service, Intermountain Research Station, Ogden, UT, 1984, pp. 375–388.
- [11] A.T. Lihninger, *Biochemistry*, Worth Publishers, New York, 1979.
- [12] R.G. Kelsey, J.R. Stephens and F. Sharizadeh, *J. Range Manage.*, 35 (1982) 617.
- [13] E.D. McArthur, B.L. Welch and S.C. Sanderson, *J. Heredity*, 79 (1988) 268.
- [14] B.L. Welch and E.D. McArthur, *J. Range Manage.*, 34 (1981) 380.
- [15] E.D. McArthur, in K.L. Johnson (Editor), *Utah Shrub Ecology Workshop I*, Utah State Univ., Logan, UT, 1983, p. 3.
- [16] *PeakSimple I*, SRI Co., Torrance, CA, 1988.
- [17] *Lotus 123*, Lotus Development Corp., Cambridge, MA, 1985.
- [18] J.H. Zar, *Biostatistical Analysis*, Prentice-Hall, Englewood Cliffs, NJ, 1984.
- [19] W.R. Rice, *Evolution*, 43 (1989) 223.
- [20] H.G. Gauch, *Multivariate Analysis in Community Ecology*, Cambridge University Press, New York, 1982.
- [21] M.J.R. Fasham, *Ecology*, 58 (1977) 551.
- [22] D.W. Byrd, *Master's Thesis*, Department of Biology, Wayne State University, Detroit, MI, 1992.
- [23] J.A. Ludwig and J.F. Reynolds, *Statistical Ecology*, Wiley, New York, 1988.
- [24] D.C. Freeman, J.M. Emlen and J.H. Graham, *Genetica*, 89 (1993) 97.
- [25] E.C. Pielou, *The Interpretation of Ecological Data*, Wiley, New York, 1984.
- [26] M.H. Kaspar and W.H. Ray, *AIChE J.*, 38 (1992) 1593.
- [27] S.T. Balke, *Quantitative Column Liquid Chromatography: A Survey of Chemometric Methods*, Elsevier, Amsterdam, 1984.



# Automated static headspace sampler for gas chromatography

D.W. Byrd\*, D.C. Freeman

*Department of Biological Sciences, Wayne State University, Detroit, MI 48202, USA*

First received 8 December 1993

## Abstract

A new automated static headspace thermal desorption system is described. This system allows for total control of the autosampler–gas chromatographic system, analog to digital conversion and data storage, prepurge functions to eliminate cross sample contamination and multiple modes of sample delivery. The system's ease of gas flow valve control and timing allows for optimal manipulation of carrier and headspace improving resolution. Larger-scale data acquisition and digital-to-analog control of the autosampler functions are discussed. System performance is illustrated using biological and environmental samples. The system's qualitative and quantitative performance was examined using statistical measures of retention time data and standard error for analyte responses.

## 1. Introduction

Static headspace (SHS) or equilibrium headspace gas chromatography (GC) methods are based upon the distribution of volatile and semivolatile sample constituents into the volume surrounding the containerized sample [1,2]. This method provides a simple means of sample preparation that separates the volatile and semivolatile constituents from the solid or liquid sample matrix. Typically the sample is weighed or measured into a sealed container with a septum and then heated to liberate volatile and semivolatile sample constituents. If the container volume and temperature are held constant an equilibrium develops between the vapor and condensed state of the analytes [3,4]. Quantitative measures are possible when the temperature of the vial is greater than the ambient temperature, the pressure of the vial is equal to or

greater than the column inlet pressure, and the pressure of the vial is equal to or greater than the ambient pressure [2,4]. Under these conditions the headspace is sampled and the area produced by the analyte(s) in the headspace subsample is proportional to the concentration in the headspace [2].

The distribution of the analyte between the sample and the headspace vapor phase of the vial is described by the distribution coefficient,  $K$ .  $K$  represents the ratio of analyte in the sample (S) divided by the analyte which is in the gas (G) or vapor phase.

$$K = c_S/c_G$$

where  $c_S$  and  $c_G$  are the equilibrium concentrations of the analyte in the sample and the headspace of the vial, respectively.  $K$  is constant under the equilibrium conditions and proportional to the peak area and the concentration of the analyte in the sample [2].

The qualitative use of this technique has a

\* Corresponding author.

general acceptance for the facile separation and identification of volatile and semivolatile hydrocarbons in liquid and solid matrices. The use of headspace GC methods by such agencies and uniform test method bodies as the US Environmental Protection Agency, American Society for Testing and Materials, International Standard Organization and Association of Official Analytical Chemists is evidence of the growing popularity of this technique. Although SHS–GC analysis is gaining acceptance as a qualitative tool, there has been debate on the suitability of SHS–GC as a quantitative methodology for solid matrices [5,6].

The interest in SHS–GC for solid and liquid matrices is evident by the plethora of recent technical papers demonstrating quantitative approaches. The use of quantitative SHS methods has replaced less specific photometric methods for the analysis of residual solvents in pharmaceutical products as a rapid and sensitive test [7]. Quantitative methods have been developed using internal and external standardization methods as well as the methods of standard additions [4]. Using first-order kinetics, Kolb and Etre [8] recently developed a theoretical basis to support empirically derived absolute quantitative analysis for the multiple headspace extraction (MHE) method. In practice MHE makes use of multiple injections of the same equilibrated sample and uses interpolation methods to derive absolute quantities of analyte(s). The technical control requirements for MHE as well as non-equilibrium methods [9] are possible with our system.

The device discussed here is characterized by a data system which integrates the control of an autosampler's mechanical functions, the capture of chromatographic data, valve-mediated injection methods including multiple headspace extractions, actuation of gas chromatograph transistor–transistor logic (TTL) start and ready states, and peripheral devices.

## 2. Methods

The static equilibrium autosampling–GC–data system is driven by an IBM-type personal com-

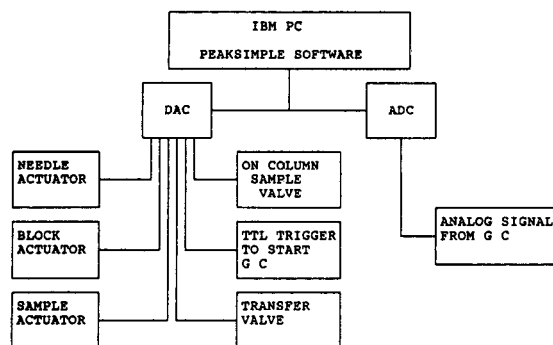


Fig. 1. Schematic overview of computer-mediated autosampler.

puter (PC). The system components consist of a sequence controller, analog-to-digital converter (ADC), and eight solenoids that are activated by digital-to-analog converters (DACs) (SRI, Torrence, CA, USA [10]) that control three mechanical–analytical subsystems. The solenoids used for this project are two- or three-way solenoid valves which are available in either normally on or normally off configurations. The strategic configuration of the solenoids allows for the simple control of the headspace system. SRI PeakSimple [10] software mediates all electrical and mechanical functions. An overview of the complete system is given in Fig. 1. One of the analytical subsystems controls the carrier gas and the sampling of the headspace (Fig. 2). This is accomplished by two three-way solenoid valves

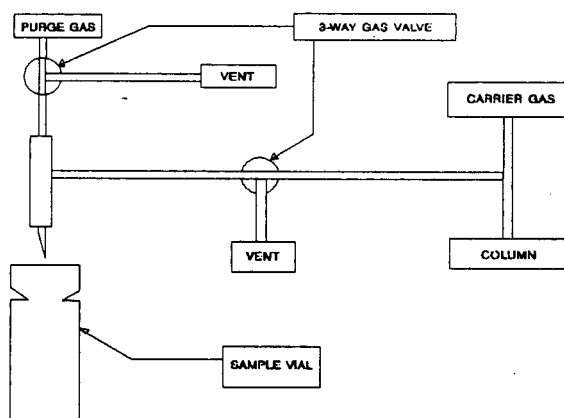


Fig. 2. Computer-mediated solenoid system for carrier and sampling gases.

and a proprietary sampling needle that are controlled by the DAC. The control of mechanical devices that manipulate the sampling needle and the sample vial positioning functions constitute a second subsystem. The manipulation of these mechanical devices is achieved with pneumatic actuators that are controlled by three-way solenoid gas valves. The actuation of the gas chromatograph TTL start function, file storage, control of run time autosampler functions, and integrator function comprise the third subsystem.

The autosampler consists of a pneumatically actuated aluminum sled that obtains the samples and places them in line with a pneumatically actuated sampling needle. The sled is thermostatically controlled and provides a dwell area for static equilibrium to take place. Sample degradation is minimized by the use of deactivated fused silica, PTFE and 313 stainless steel for all components that conduct the sample to the gas chromatograph.

The sequential control of the static equilibrium autosampler functions, data integrator, and the GC system is controlled by the data system and related interface hardware. The autosampler valve sequencing was initially configured to simulate a manual injection of a headspace sample onto the GC system with the carrier gas constantly flowing through the system. The electronic solenoid approach that is employed to load and control sample flow is a new method for sample delivery. Traditional techniques use mechanical methods to sample the headspace. We found that the use of stop carrier flow improved peak shape and chromatographic resolution. The actuation of the sample flow solenoid before actuating the on column solenoid to the gas chromatograph further improved resolution.

The sampling sequence is shown in Fig. 3. The sequence of operations of the autosampler consists of a period of sample equilibration in which the containerized sample is heated. During equilibration the sampling needle is not positioned over the sample septa (Fig. 3A). The equilibrated sample is then moved into position by the actuating pneumatic cylinder which lowers the vial into the sample holder of the heated block deletion. The sample vial is then

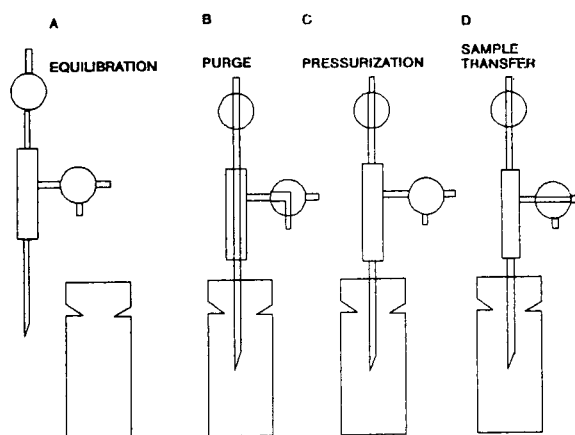


Fig. 3. Equilibration and injection sequence. For A–D, see text.

positioned for sampling (Fig. 3B). At this stage, activation of the sampling needle actuator inserts the transfer needle into the headspace of the sample vial. The autosampler system is now capable of a number of functions such as sample prepressurization (Fig. 3C), transfer line purge (Fig. 3B) or injection of the sample (Fig. 3D).

In this study, a portion of the headspace is purged through the transfer line to eliminate possible residues from prior samples. This is accomplished by the activation of the vent port of the injection valve and the activation of the sample transfer gas solenoid as depicted in Fig. 3B eliminating intersample contamination. The subsequent flow and valve states are tabulated in Table 1, showing the timed events comprising the various states the autosampler undergoes; these events are: standby flow path, purge, sampling and data acquisition. An optimized sequence timed events program is also included in Table 1.

The physical interface between the autosampler and the gas chromatograph consists of a three-way solenoid at the terminus of a deactivated fused-silica transfer line that is coupled directly to the analytical column. The autosampler operational conditions are given in Table 2.

The gas chromatograph is initiated by the computer interface card that has been modified to provide a TTL trigger to start the chromato-

Table 1  
Automated run parameters

| Timed event                                 | Time (min)  |
|---|-------------|
| Trap solenoid activated                     | 0.01        |
| Sample sled solenoid activated              | 0.03        |
| Sample sled solenoid deactivated            | 0.05        |
| Transfer needle solenoid activated          | 0.06        |
| Gas transfer solenoid purge activated       | 0.08        |
| Gas transfer solenoid purge deactivated     | 0.10        |
| Zero zero integrator baseline               | 0.80        |
| Gas transfer solenoid deactivated           | 1.22        |
| Column flow solenoid activated              | 1.24        |
| Column flow solenoid deactivated            | 1.32        |
| Gas transfer solenoid deactivated           | 1.34        |
| GC temperature cycle initiated              | 1.48        |
| Transfer needle solenoid deactivated        | 2.00        |
| Current sample is ejected                   | 2.20        |
| Data acquisition terminated                 | 15.00       |
| GC reequilibrates for next run              | 15.00–27.00 |
| Terminate current run and cycle to next run | 27.00       |

graph once the sample has been transferred to the analytical column. The integrator subsystem consists of pre/postdata acquisition as well as run time data acquisition; integration parameters are controlled through the data system. The data acquired from each run was stored in an ASCII format as a digital voltage output file and a report output file containing sample identification, program parameters, retention time, area, peak height and concentration data. The report output file was transferred to a Lotus 123 version 2.1 [11] spreadsheet program that extracts retention and area data and subsequently unifies the data for import into the statistical program [12].

The system reported here differs from the

Table 2  
Autosampler conditions

| Parameter                   | Value     |
|-----------------------------|-----------|
| Transfer line temperature   | 150°C     |
| Transfer line solenoid      | 180°C     |
| Sled and sample temperature | 100°C     |
| Sample equilibrium time     | 27 min    |
| Sample transfer flow-rate   | 30 ml/min |

conventional systems reported by Ettre and Kolb [2] in that: (1) the sample headspace may equilibrate along the entire conduit to the gas chromatograph, (2) multiple sequential injections are possible during the same run or separate runs, (3) either augmented or diverted carrier flows are possible, (4) integrated computer control of chromatographic, integrator and autosampler functions, (5) finer control of both sampling periods, volumes, sample introduction, and (6) a non-mechanical computer-mediated sampling method is used which allows for more flexible sampling methods.

The system was tested on terpenes and coumarin compounds stored in specialized leaf hairs called glandular trichomes of *Artemisia tridentata* ssp. *tridentata* and *Artemisia tridentata* ssp. *vaseyana* (basin and mountain sagebrush). The system was also evaluated using various petroleum products in soil matrices.

Analysis of terpenes using liquid extractions [13] and headspace analysis have been previously reported [14]. Analysis of coumarin type compounds using SHS derivatization is a new approach that utilizes the temperature and equilibration time to chemically derivatize non-volatile coumarins into their volatile methylated analogues. Separation of the terpenes and coumarin derivatives was accomplished using two capillary columns with differing phase polarity. The first column was an immobilized polyethylene glycol (30 m × 530 μm, film thickness  $d_f = 3 \mu\text{m}$ ). The second column contained immobilized dimethylsilicone (30 m × 530 μm,  $d_f = 5 \mu\text{m}$ ) and was connected to a low-dead-volume quartz union. Relative quantitative results were obtained for known and unknown terpene components by computing the ratio of mass and area of the internal standard (ethylbenzene) peak area to the unknown terpene component. This quantitation is based upon the assumption that hydrocarbons of the same mass will provide detector responses that are approximately the same when using the flame ionization detector [14]. Terpene standards were run in the same manner to determine retention times for peak identification. The GC conditions were optimized for high sample throughput (ca. 6

Table 3  
GC conditions

| Parameter                               | Value      |
|---|------------|
| Injector temperature                    | 200°C      |
| Detector temperature                    | 300°C      |
| Initial oven temperature                | 80°C       |
| Final oven temperature                  | 180°C      |
| Oven ramp                               | 8°C/min    |
| Carrier gas flow (hydrogen)             | 44 cm/s    |
| Make up gas flow (nitrogen)             | 30 ml/min  |
| Flame ionization detector<br>(hydrogen) | 40 ml/min  |
| Flame ionization detector<br>(air)      | 300 ml/min |
| Electrometer range                      | 1          |
| Electrometer attenuation                | 64         |

samples/h). The GC conditions are tabulated in Table 3.

### 3. Results

One advantage of the automated headspace–GC–data system is the reproducibility and precision of the integrated system. The 95% confidence intervals for the internal standard retention times variance is less than the sampling time window of the integrator, i.e. 1 s. In order to evaluate the reproducibility of the system, 200 ng of isopropylbenzene standards ( $n = 10$ ) were analyzed and the peak area measures used to determine the mean, standard deviation, variance and standard error (Table 4). These data indicate that the system reproducibility, accuracy and precision is on par with other ancillary automated GC devices and as such is suitable for quantitative studies.

One of the test materials consisted of leaves from a single plant that had three distinct leaf morphologies based upon lobes on the leaf.

Table 4  
Isopropyl benzene, 200 ng,  $n = 10$

| Test           | Result   |
|----------------|----------|
| Mean           | 198.8 ng |
| Standard error | 0.0186   |

Leaves that are not distinctly lobed are termed entire; leaves divided into two lobes or three lobes are termed bilobed and trilobed, respectively. An example of these features is seen in the chromatograms of various leaf morphs (i.e. entire, trilobed) that produce unique characteristic terpene chromatograms. An example of the selectivity of the system is shown in the analysis of two distinct leaf forms from the same plant as illustrated in Fig. 4. The upper chromatogram for the entire leaf came from the flowering stalk (inflorescence) and has a distinct chromatogram compared to the vegetative leaf from the same plant and branch. Fig. 5 illustrates the utility of the method to explore the time or seasonal expression of terpene and related volatile and semivolatile compounds. The system provides for rapid distinction of the two subspecies and the resulting hybrid (Fig. 6). The typical sample preparation time which consists of sample mass determination and addition of the internal standards can be manually executed in less than 2 min. With respect to sensitivity, the static headspace method reported here detected in excess of 110 components compared to 14 compounds reported in earlier studies [12,15–17].

We have demonstrated the feasibility of on-line SHS derivatization. In this approach many of the unwanted or partially derivatized reaction products are eliminated by sampling the non-volatile products that are successfully converted to volatile analogues. In this demonstration 1  $\mu$ l of a 80% bis(trimethylsilyl)trifluoroacetamide (BSTFA) and trimethylchlorosilane (TMCS) cocktail is added to the vial with the leaf. Coumarin-type compounds present on the leaf surface react with the vaporized cocktail. Fig. 7 illustrates the use of this technique. Fig. 7a is a reference chromatogram of the leaf prior to the addition of the derivatization agent. Fig. 7c illustrates headspace derivatization of coumarin, 9-hydroxycoumarin and 2,7-dihydroxycoumarin standards. Fig. 7b illustrates the derivatization of leaf surface coumarins. It is interesting to note that the terpenes are derivatized to a volatile product.

The system was used for the analysis of petroleum-derived hydrocarbons. In this analysis di-

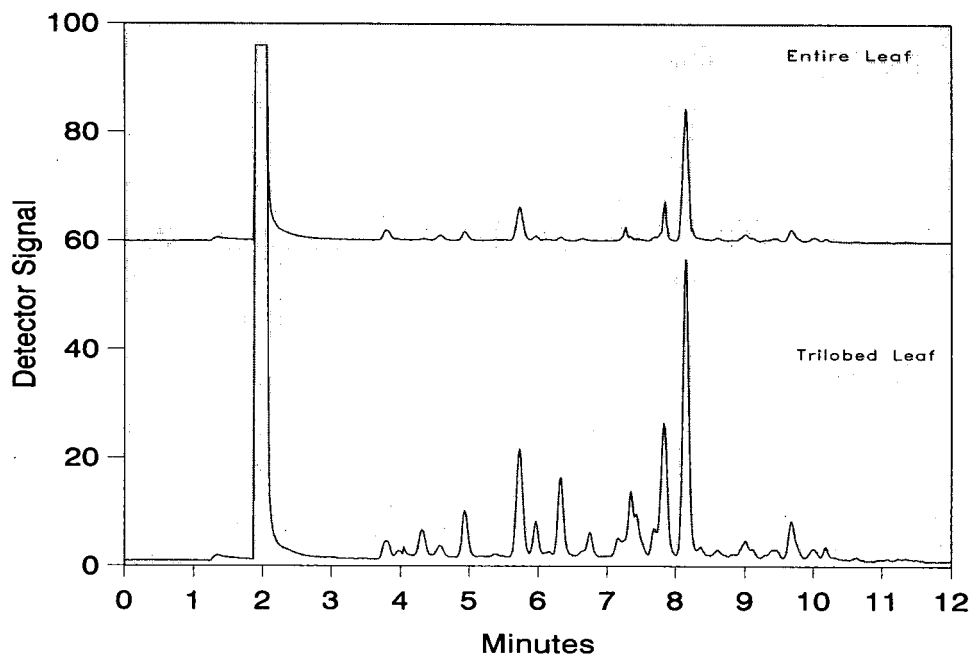


Fig. 4. Terpene chromatograms from trilobed and entire leaf morphs. Basin plant 79, branch 1.

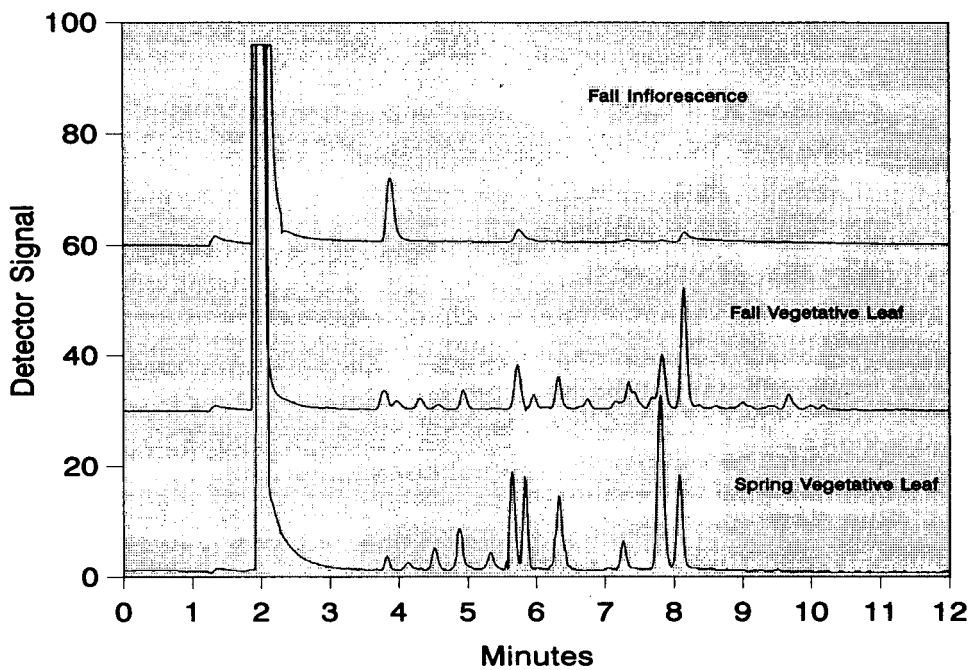


Fig. 5. Seasonal synthesis of terpenes. Hybrid plant 225, branch 1.



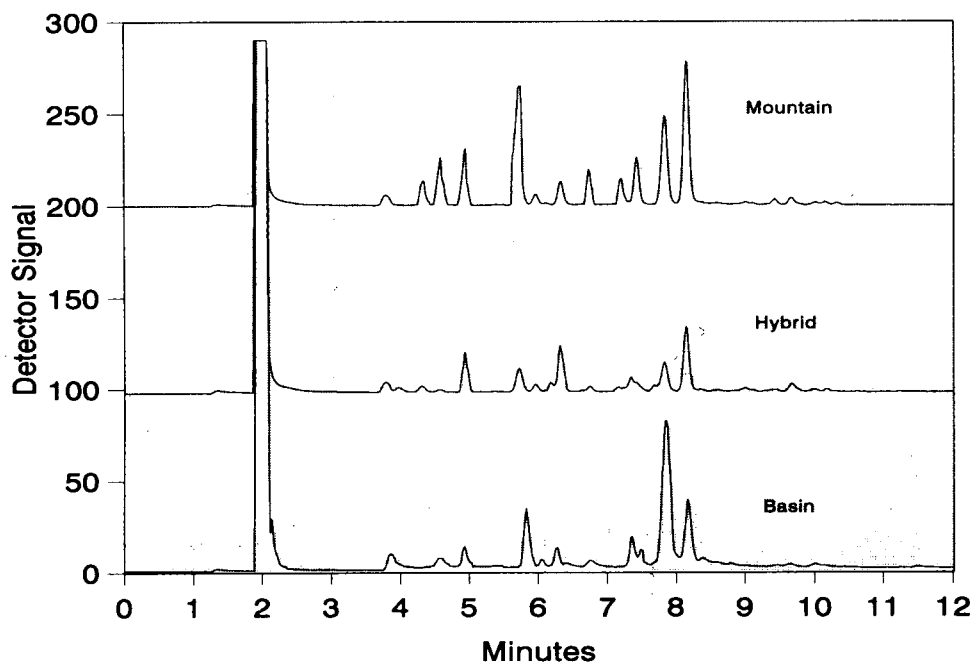


Fig. 6. Composite chromatograms illustrating the distinct terpene expressions of parental subspecies and the hybrid.

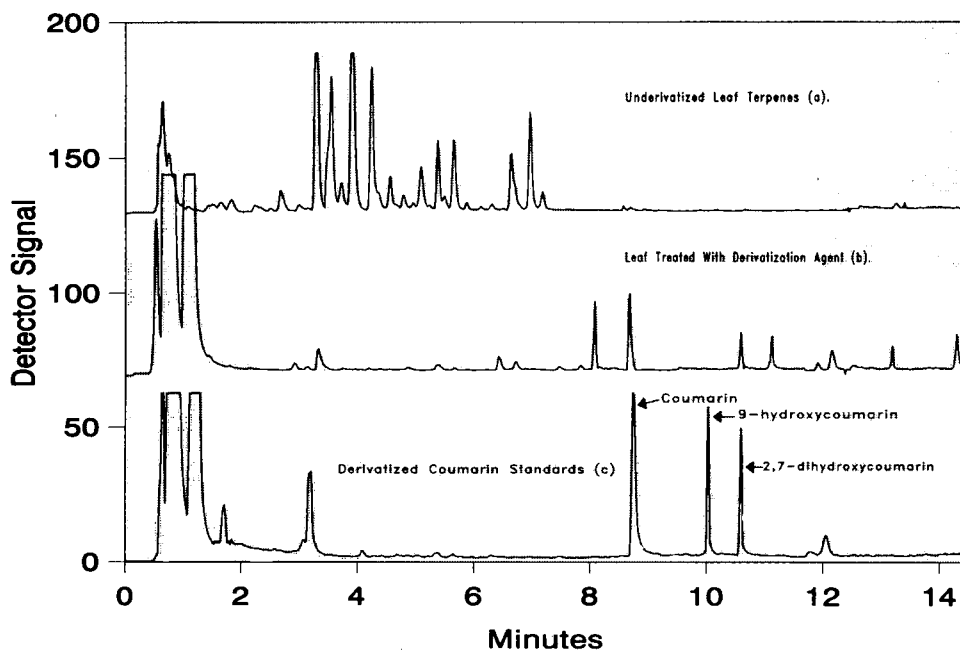


Fig. 7. Example of on-line derivatization of coumarin and related compounds.

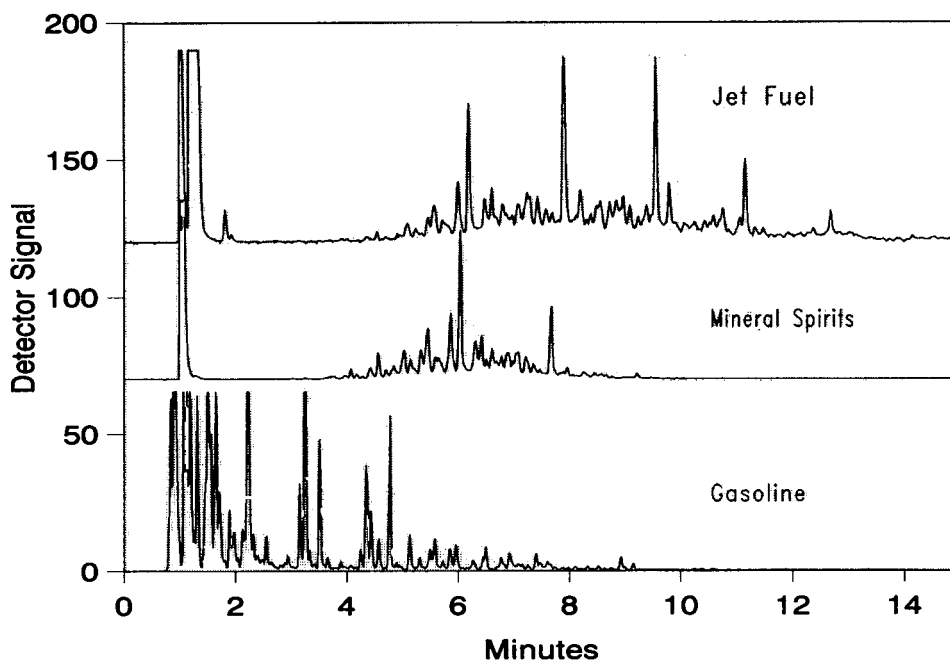


Fig. 8. Composite chromatograms of petroleum products.

lute fuel standards were either analyzed directly or in the presence of an environmental matrix (i.e. soil or debris). Fig. 8 illustrates a composite chromatogram of common fuels and their distinct chromatographic patterns.

#### 4. Discussion and conclusion

The method presented provides an automated analytical tool that is a reproducible, selective, sensitive and labor-saving approach for the quantitation of volatile, semivolatile and non-volatile hydrocarbons. The system has the advantage of high sensitivity and resolution coupled with simplicity in design and implementation. The use of an integrated headspace autosampling system allows for the precise control of several chromatographic and mechanical functions to be carried out in a routine and reproducible manner. The data indicates that precise qualitative and quantitative information can be obtained by this technique.

The system represents an extension of previ-

ous headspace sampling systems with the additional functions of flexible sampling protocols, MHE, carrier gas flow interruption and sample purge provisions.

We have shown the utility and functions of an integrated automated headspace-GC-data system that can differentiate terpenes of varying leaf morphs in close proximity. This implies a difference in biosynthetic pathways based upon leaf morphology. Similarly, we show differentiation of terpene chromatograms with respect to season, using leaves from the same plant and branch. We also demonstrate the feasibility of on-line derivatization of coumarin-type compounds using this system. An example of petrochemical differentiation (Fig. 8) illustrates the utility of this method for fuel identification and analyses.

#### References

- [1] B.A. Rudenko and G.I. Smirnova, *Zh. Anal. Khim.*, 32 (1977) 367.

- [2] L.S. Ettre and B. Kolb, *Chromatographia*, 32 (1991) 5.
- [3] J. Drodz and J. Novák, *J. Chromatogr.*, 165 (1979) 141.
- [4] K. Beyermann, *Organic Trace Analysis*, Ellis Horwood, Chichester, 1984.
- [5] A. Venema, *J. High Resolut. Chromatogr. Chromatogr. Commun.*, 11 (1988) 128.
- [6] A. Venema, *J. High Resolut. Chromatogr.*, 13 (1990) 537.
- [7] Z. Penton, *Determination of Solvents in Pharmaceuticals by Static Headspace Gas Chromatography; Technical Communication*, Varian Instrument Group, Walnut Creek, CA, 1991.
- [8] B. Kolb and L.S. Ettre, *Chromatographia*, 32 (1991) 505.
- [9] A. Shinohara, A. Sato, N. Ishii and N. Onada, *Chromatographia*, 32 (1991) 357.
- [10] *PeakSimple I*, SRI Co., Torrence, CA, 1988.
- [11] *Lotus 123*, Lotus Development Corp., Cambridge, MA, 1985.
- [12] M.J. Norusis, *SPSS/PC + V3.0. Update Manual*, SPSS Inc., Chicago, IL, 1988.
- [13] J.D. Cedarleaf, B.L. Welch and J.D. Brotherson, *J. Range Manage.*, 36 (1983) 492.
- [14] J.A. Corkill, *J. High Resolut. Chromatogr. Chromatogr. Commun.*, 11 (1988) 211.
- [15] E. Katz, *Quantitative Analysis using Chromatographic Techniques*, Wiley, Chichester, 1987.
- [16] E.D. McArthur, B.L. Welch and S.C. Sanderson, *J. Heredity*, 79 (1988) 268.
- [17] B.L. Welch and E.D. McArthur. *J. Range Manage.*, 34 (1981) 380.





ELSEVIER

Journal of Chromatography A, 686 (1994) 245–251

JOURNAL OF  
CHROMATOGRAPHY A

# Retention of halocarbons on a hexafluoropropylene epoxide-modified graphitized carbon black III. Ethene-based compounds<sup>☆</sup>

Thomas J. Bruno\*, Michael Caciari<sup>1</sup>*Thermophysics Division, National Institute of Standards and Technology, Boulder, CO 80303, USA*

First received 4 May 1994; revised manuscript received 5 August 1994

## Abstract

The retention characteristics of 11 ethene-based chlorofluorocarbon, bromochlorofluorocarbon and fluorocarbon fluids have been studied as a function of temperature on a stationary phase consisting of a 5% (m/m) coating of a low-molecular-mass polymer of hexafluoropropylene epoxide on a graphitized carbon black adsorbent. Measurements were performed at  $-20$ ,  $0$ ,  $20$  and  $40^{\circ}\text{C}$  for trifluoroethene (R-1123), 1,1-difluoroethene (R-1132a), and fluoroethene (vinyl fluoride, R-1141). Measurements were performed at  $40$ ,  $60$ ,  $80$  and  $100^{\circ}\text{C}$  for 1,1-dichloro-2,2-difluoroethene (R-1112a), chlorotrifluoroethene (R-1113), 2-chloro-1,1-difluoroethene (R-1122), 1-chloro-1-fluoroethene (R-1121a), 2-bromo-1,1-difluoroethene (R-1122B1) and bromoethene (vinyl bromide, R-1140B1). Measurements were performed at  $60$ ,  $80$ ,  $100$  and  $120^{\circ}\text{C}$  for *trans*-1,2-dichloro-1,2-difluoroethene (R-1112t) and *cis*-1,2-dichloro-1,2-difluoroethene (R-1112c). Net retention volumes, corrected to a column temperature of  $0^{\circ}\text{C}$ , were calculated from retention time measurements, the logarithms of which were fitted against reciprocal thermodynamic temperature. The relative retentions, also as a function of temperature, were calculated with respect to the retentions of tetrafluoromethane (R-14) and hexafluoroethane (R-116). Qualitative features of the data are examined, and trends are identified. In addition, the data were fitted to linear models for the purpose of predicting retention behavior of these compounds to facilitate chromatographic analysis.

## 1. Introduction

Many laboratories are engaged in a comprehensive research program geared toward the development of new fluids to be used as refrigerants, blowing and foaming agents, and pro-

pellants. The research that composes this effort includes thermophysical properties measurements and correlation, materials compatibility testing, chemical stability measurement, and cycle suitability studies [1,2]. An important part of all of these research programs is the chemical analysis of new fluids that are tested [3–6]. Gas chromatography is one of the major quantitative and qualitative analysis methods that is applied to the study of alternative refrigerants for several important reasons, not the least of which are

\* Corresponding author.

<sup>☆</sup> Contribution of the United States Government.

<sup>1</sup> Permanent address: Fort Lupton High School, Fort Lupton, CO, USA.

simplicity and economics of operation [7–9]. A knowledge of the retention characteristics of important fluids on the more useful stationary phases is an important component in the design of effective qualitative and quantitative chromatographic analyses. Corrected retention parameters, such as the net retention volume,  $V_N^0$  (corrected to a column temperature of 0°C), and relative retentions,  $r_{a/b}$ , provide the simplest avenue to achieve the desired goals.

In earlier papers, we presented measurements for 8 methane-based and 18 ethane-based fluids [10,11]. In this paper, we present temperature-dependent measurements of the net retention volume, corrected to a column temperature of 0°C, of 11 ethene-based fluids that are commonly encountered in alternative refrigerant research and testing. The fluids we have studied are listed in the left hand column of Table 1, along with the accepted code numbers [10,12]. The measurements were made on the packed-column stationary phase that has proven to be very useful for refrigerant analysis: a 5% coating of a low-molecular-mass polymer of hexafluoropropylene epoxide on a graphitized carbon black. The relative retentions were then calculated with respect to tetrafluoromethane (for three of the fluids) and hexafluoroethane (for all fluids). In addition to the discussion of qualitative trends in the data, fits to linear models are presented of the logarithms of the net retention volumes and the relative retentions against thermodynamic temperature, thus providing a predictive capability.

## 2. Theory

A discussion of the basic definitions, theory and application of corrected retention parameters was presented earlier [10].

## 3. Experimental

The measurements presented here were performed on a commercial gas chromatograph that had been modified to provide high precision

retention data. All of the experimental details were described earlier [10,11], so only a very general description will be provided here. The chromatograph was modified to provide a highly stable column temperature which was measured with a quartz-crystal oscillator thermoprobe (calibrated against a NIST-standard platinum resistance thermometer) that was accurate to within  $\pm 0.01^\circ\text{C}$ . Injection was done with a six-port sampling valve containing a sample loop of 0.1 ml volume. The valve was pneumatically actuated with pilot valves using helium as the actuation gas to inject very rapidly and thereby minimize the magnitude of the injection pressure pulse. The injection valve and loop were maintained at 50°C for all measurements. The carrier gas line to the injection valve was modified to allow the column head pressure to be measured with a calibrated Bourdon tube gauge. This gauge was calibrated against a dead mass pressure balance traceable to a NIST standard. The column outlet pressure was measured with an electronic barometer that had a resolution of 1.3 Pa (approximately 0.01 Torr). This barometer was also calibrated against a dead mass pressure balance. The column carrier gas flow-rate was measured with an electronic soap-bubble flow meter (corrected for water vapor pressure). Retention times were measured by a commercial integrator. A Ranque–Hilsch vortex tube was used to provide cooling in the column oven for the subambient temperature measurements [13, and references therein]. Thermal conductivity detection (TCD) was used with a carrier gas of research grade helium. The TCD system was maintained at 50°C for all measurements.

The stationary phase was a commercially prepared packing material consisting of a 5% (m/m) coating of a low-molecular-mass polymer of hexafluoropropylene epoxide modifier on a 60–80-mesh (177–250  $\mu\text{m}$ ) graphitized carbon black [14]. Some representative properties of this modifier and the column preparation procedure were presented earlier [10].

For each retention time measurement, five fluid injections were performed at each column temperature. Each series of injections was preceded and followed by five measurements of the

Table 1  
The net retention volume,  $V_N^0$ , and their logarithms, of the fluids measured in this study

| Name  | $V_N^0$ (ml)        |                   |                    |                    |                    |                    |                     |                     |                     |                   |                    |                    |                    |                    |                     |                     |  |
|---|---------------------|-------------------|--------------------|--------------------|--------------------|--------------------|---------------------|---------------------|---------------------|-------------------|--------------------|--------------------|--------------------|--------------------|---------------------|---------------------|--|
|   | -20°C<br>(253.15 K) | 0°C<br>(273.15 K) | 20°C<br>(293.15 K) | 40°C<br>(313.15 K) | 60°C<br>(333.15 K) | 80°C<br>(353.15 K) | 100°C<br>(373.15 K) | 120°C<br>(393.15 K) | -20°C<br>(253.15 K) | 0°C<br>(273.15 K) | 20°C<br>(293.15 K) | 40°C<br>(313.15 K) | 60°C<br>(333.15 K) | 80°C<br>(353.15 K) | 100°C<br>(373.15 K) | 120°C<br>(393.15 K) |  |
| Trifluoroethene (R-1123)                                | 280.0 ± 3.70        | 127.0 ± 1.50      | 60.7 ± 0.4         | 33.3 ± 0.5         |                    |                    |                     |                     | 2.45                | 2.10              | 1.78               | 1.52               |                    |                    |                     |                     |  |
| 1,1-Difluoroethene (R-1132a)                            | 152.7 ± 1.3         | 73.1 ± 0.9        | 38.6 ± 0.4         | 21.8 ± 0.3         |                    |                    |                     |                     | 2.18                | 1.86              | 1.59               | 1.34               |                    |                    |                     |                     |  |
| Fluoroethene (R-1141)                                   | 146.8 ± 1.3         | 71.4 ± 0.6        | 38.8 ± 0.4         | 21.7 ± 0.3         |                    |                    |                     |                     | 2.17                | 1.85              | 1.59               | 1.34               |                    |                    |                     |                     |  |
| 1,1-Dichloro-2,2-difluoroethene (R-1112a)               |                     |                   |                    |                    | 1503.5 ± 8.9       | 636.9 ± 5.3        | 310.0 ± 2.8         | 159.8 ± 2.6         |                     |                   |                    |                    |                    |                    |                     |                     |  |
| Chlorotrifluoroethene (R-1113)                          |                     |                   |                    |                    | 0.6%               | 0.8%               | 0.7%                | 1.6%                |                     |                   |                    |                    |                    |                    |                     |                     |  |
| 2-Chloro-1,1-difluoroethene (R-1122)                    |                     |                   |                    |                    | 225.3 ± 1.6        | 117.5 ± 1.3        | 63.4 ± 0.8          | 37.6 ± 0.3          |                     |                   |                    |                    |                    |                    |                     |                     |  |
| 1-Chloro-1-fluoroethene (R-1131a)                       |                     |                   |                    |                    | 0.7%               | 1.1%               | 1.3%                | 0.9%                |                     |                   |                    |                    |                    |                    |                     |                     |  |
| 2-Bromo-1,1-difluoroethene (R-1122B1)                   |                     |                   |                    |                    | 220.0 ± 2.5        | 116.6 ± 1.5        | 64.3 ± 1.0          | 37.8 ± 0.21         |                     |                   |                    |                    |                    |                    |                     |                     |  |
| Bromoethene (R-1140B1)                                  |                     |                   |                    |                    | 1.1%               | 1.2%               | 1.5%                | 0.5%                |                     |                   |                    |                    |                    |                    |                     |                     |  |
| <i>trans</i> -1,2-Dichloro-1,2-difluoroethene (R-1112t) |                     |                   |                    |                    | 154.8 ± 1.1        | 82.7 ± 0.7         | 48.8 ± 0.7          | 29.3 ± 0.2          |                     |                   |                    |                    |                    |                    |                     |                     |  |
| <i>cis</i> -1,2-Dichloro-1,2-difluoroethene (R-1112c)   |                     |                   |                    |                    | 0.7%               | 0.8%               | 1.5%                | 0.5%                |                     |                   |                    |                    |                    |                    |                     |                     |  |
|   |                     |                   |                    |                    | 509.7 ± 5.1        | 246.1 ± 2.0        | 131.8 ± 1.1         | 74.3 ± 0.4          |                     |                   |                    |                    |                    |                    |                     |                     |  |
|   |                     |                   |                    |                    | 1.0%               | 0.8%               | 0.8%                | 0.5%                |                     |                   |                    |                    |                    |                    |                     |                     |  |
|   |                     |                   |                    |                    | 375.4 ± 5.3        | 191.0 ± 1.3        | 106.0 ± 0.4         | 63.6 ± 0.5          |                     |                   |                    |                    |                    |                    |                     |                     |  |
|   |                     |                   |                    |                    | 1.4%               | 0.7%               | 0.4%                | 0.8%                |                     |                   |                    |                    |                    |                    |                     |                     |  |
|   |                     |                   |                    |                    | 698.7 ± 6.3        | 339.8 ± 2.7        | 172.7 ± 2.9         | 97.5 ± 0.98         |                     |                   |                    |                    |                    |                    |                     |                     |  |
|   |                     |                   |                    |                    | 0.9%               | 0.8%               | 1.6%                | 1.0%                |                     |                   |                    |                    |                    |                    |                     |                     |  |
|   |                     |                   |                    |                    | 667.7 ± 6.0        | 324.8 ± 2.3        | 172.7 ± 2.9         | 97.5 ± 0.98         |                     |                   |                    |                    |                    |                    |                     |                     |  |
|   |                     |                   |                    |                    | 0.9%               | 0.7%               | 1.6%                | 1.0%                |                     |                   |                    |                    |                    |                    |                     |                     |  |

The uncertainties cited are propagated from replicate measurements of the experimental parameters.

carrier gas flow rate, and the injection of five aliquots of air. The air was injected separately, before and after the injection of fluid, to measure the void volume of the column without introducing air as an impurity into the fluid containers. The corrected retention time was simply obtained by subtracting the average air retention time. At the start of each of these fifteen injections (five air, five fluid, five air), the requisite temperatures (column, flowmeter, and barometer) and pressures (column head and column exit) were recorded. These replicate measurements furnished the uncertainties used for the error propagation that provided the overall experimental uncertainties that are reported (two standard deviations,  $2\sigma$ ). The column head pressure was maintained uniformly at  $137.9 \pm 0.3$  kPa (approximately 20 p.s.i.g.) for the measurements, although measurements were initially performed at several other pressures to verify consistency in the operation of the chromatograph. The carrier gas flow-rate at the column exit was maintained at  $45 \pm 0.3$  ml/min.

Measurements were performed at four temperatures for each fluid. One fluid, the *cis*- and *trans*-geometric isomer mixture of 1,2-dichloro-1,2-difluoroethene, R-1112c,t, was measured between 60 and 120°C. The samples were all obtained from commercial sources in the highest available purity, and were used without further purification.

#### 4. Results and discussion

The corrected net retention volumes,  $V_N^0$ , for each fluid are presented in Table 1. The reported expanded uncertainties (with a coverage factor  $k=2$ ) are the result of an error propagation performed with the standard deviations obtained from replicate measurements of each experimental parameter. The uncertainties were found to be uncorrelated (as determined by examination of Spearman's  $\rho$  and Kendall's  $\tau$ ; see [15]), and the deviations were found to fit a normal distribution and were therefore treated as being entirely random [15]. In addition to the uncertainty, the coefficient of variation in percent is

provided. The precision of the measurements is generally between 0.5 and 1.5%, with the average precision of all the measurements on these compounds being 0.96%. This figure compares very well with the precision of typical retention parameters (generally between 1 and 2%) obtained in other physicochemical gas chromatographic measurements [16]. A plot of  $\log V_N^0$  against  $1/T$  for each fluid is provided in Fig. 1. These temperature-dependent data were then fitted with the best linear model (simple linear, logarithmic, power or exponential). The results of these fits are provided in Table 2. Included with each fluid are the coefficients, the Pearson correlation coefficient of the fit, and the temperature range over which the fit was taken [15]. All of the measurements performed on the ethene-based fluids are represented very well (within experimental error) with the simple linear model:

$$\log V_N^0 = m/T + b$$

where  $m$  is the slope and  $b$  is the intercept.

The relative retentions,  $r_{a/b}$ , were calculated with tetrafluoromethane (R-14) as the reference compound for the three most volatile fluids, and with hexafluoroethane (R-116) for all fluids.

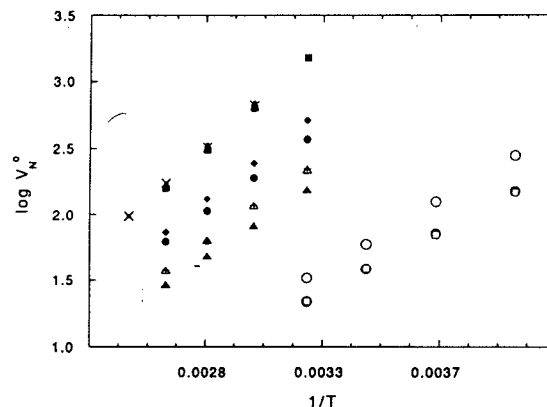


Fig. 1. A plot of the logarithm of the net retention volume,  $\log V_N^0$ , against  $1/T$ , for each fluid measured in this study.  $\circ$  = R-1123;  $\bullet$ (large) = R-1132a;  $\square$  = R-1141;  $\blacksquare$  = R-1112a;  $+$  = R-1113;  $\triangle$  = R-1122;  $\blacktriangle$  = R-1131a;  $\blacklozenge$ (large) = R-1122B1;  $\bullet$ (small) = R-1140B1;  $\blacklozenge$ (small) = R-1112t;  $\times$  = R-1112c.



Table 2  
Coefficients of the fits of  $\log V_N^0$  against  $1/T$ , with the respective correlation coefficients

| Compound | Model <sup>a</sup> | <i>m</i> | <i>b</i> | <i>r</i> | Temperature range (°C) |
|----------|--------------------|----------|----------|----------|------------------------|
| R-1123   | L                  | 1228.1   | −2.40    | 0.99988  | −20 to 40              |
| R-1132a  | L                  | 1111.5   | −2.21    | 0.99995  | −20 to 40              |
| R-1141   | L                  | 1082.6   | −2.11    | 0.99954  | −20 to 40              |
| R-1112a  | L                  | 1891.0   | −2.87    | 0.99994  | 40 to 100              |
| R-1113   | L                  | 1513.72  | −2.48    | 0.99989  | 40 to 100              |
| R-1122   | L                  | 1485.71  | −2.40    | 0.99991  | 40 to 100              |
| R-1131a  | L                  | 1402.21  | −2.29    | 0.99992  | 40 to 100              |
| R-1122B1 | L                  | 1626.52  | −2.49    | 0.99998  | 40 to 100              |
| R-1140B1 | L                  | 1507.70  | −2.24    | 0.99998  | 40 to 100              |
| R-1112t  | L                  | 1860.82  | −2.74    | 0.99996  | 60 to 120              |
| R-1112c  | L                  | 1808.57  | −2.61    | 0.99999  | 60 to 120              |

Note that in each case a simple linear model provided the best representation of the experimental measurements.

<sup>a</sup> L = Linear.

These values are provided in Table 3. Plots of  $\log r_{a/b}$  against  $1/T$  for each reference are provided in Figs. 2 and 3. The expected trend with temperature is observed, and the plots and fits can therefore be used for prediction of the retention behavior on other columns containing the same stationary phase.

It is clear from the retention behavior that some difficulty will be experienced with the separation of many of the ethene-based fluids on the stationary phase used in this study. Despite this packing's great utility in the separation the methane- and ethane-based fluids, and its outstanding chemical and thermal stability, many of the ethene fluids coelute at all temperatures. The coelution is especially pronounced for the following sets: R-1112c, R-1112t, R-1112a; R-1122, R-1113; and R-1141 and R-1132a.

As we have demonstrated in previous papers [10,11], it is possible to construct a kind of "periodic chart" or property diagram for low-molecular-mass halocarbons [2]. The chart has a triangular format that groups the fluids according to their molecular structures and properties. Such charts have been successful in systematizing, in a semiquantitative manner, properties such as normal boiling point, atmospheric lifetime, flammability and toxicity [2]. The retention parameters measured for the methane-

and ethane-based fluids were found to fit this scheme qualitatively, with expected minima in the fluorine-rich section, and expected maxima predicted to occur in the chlorine-rich section. We have found that the correlation with the ethene-based halocarbons that were examined in this study is much less satisfactory. We speculate that the potential of a specific interaction (such as a charge transfer interaction) resulting from the  $\pi$ -bond complicates the retention of the ethene-based halocarbons.

## 5. Conclusions

Measurements of the corrected net retention volumes and relative retentions of 11 ethene-based halocarbon fluids that are relevant to research on alternative refrigerants have been presented. The logarithms of these data were fitted against reciprocal thermodynamic temperature to several linear models. In all cases, a simple linear relationship accounts for all structure in the data. These derived equations can be used for the prediction of the retention behavior of these fluids on this important stationary phase, and therefore can be used for solute identification and also for the design of analytical and preparative-scale separations. In addition,

Table 3  
Relative retentions,  $r_{a/b}$ , and their logarithms, of the most volatile fluids measured in this study

| Compound  | $r_{a/b}$           |                   |                    |                    |                    |                    |                     |                     |                     |                   |                    |                    |                    |                    |                     |                     |
|---|---------------------|-------------------|--------------------|--------------------|--------------------|--------------------|---------------------|---------------------|---------------------|-------------------|--------------------|--------------------|--------------------|--------------------|---------------------|---------------------|
|   | -20°C<br>(253.15 K) | 0°C<br>(273.15 K) | 20°C<br>(293.15 K) | 40°C<br>(313.15 K) | 60°C<br>(333.15 K) | 80°C<br>(353.15 K) | 100°C<br>(373.15 K) | 120°C<br>(393.15 K) | -20°C<br>(253.15 K) | 0°C<br>(273.15 K) | 20°C<br>(293.15 K) | 40°C<br>(313.15 K) | 60°C<br>(333.15 K) | 80°C<br>(353.15 K) | 100°C<br>(373.15 K) | 120°C<br>(393.15 K) |
| <i>r<sub>a/b</sub> with respect to tetrafluoroethane (R-14)</i> |                     |                   |                    |                    |                    |                    |                     |                     |                     |                   |                    |                    |                    |                    |                     |                     |
| R-1123  | 15.22               | 12.83             | 9.34               | 8.33               |                    |                    |                     |                     | 1.18                | 1.11              | 0.97               | 0.92               |                    |                    |                     |                     |
| R-1132a   | 8.30                | 7.38              | 5.94               | 5.45               |                    |                    |                     |                     | 0.92                | 0.87              | 0.77               | 0.74               |                    |                    |                     |                     |
| R-1141  | 7.98                | 7.21              | 5.97               | 5.43               |                    |                    |                     |                     | 0.90                | 0.86              | 0.78               | 0.73               |                    |                    |                     |                     |
| <i>r<sub>a/b</sub> with respect to hexafluoroethane (R-116)</i> |                     |                   |                    |                    |                    |                    |                     |                     |                     |                   |                    |                    |                    |                    |                     |                     |
| R-1123  | 1.57                | 1.54              | 1.41               | 1.35               |                    |                    |                     |                     | 0.20                | 0.19              | 0.15               | 0.13               |                    |                    |                     |                     |
| R-1132a   | 0.85                | 0.89              | 0.89               | 0.89               |                    |                    |                     |                     | 0.07                | -0.05             | -0.05              | -0.05              |                    |                    |                     |                     |
| R-1141  | 0.82                | 0.87              | 0.90               | 0.88               |                    |                    |                     |                     | -0.09               | -0.06             | -0.05              | -0.05              |                    |                    |                     |                     |
| R-1112a   |                     |                   |                    | 61.12              |                    |                    |                     |                     |                     |                   |                    |                    |                    |                    |                     |                     |
| R-1113  |                     |                   |                    | 9.16               |                    |                    |                     |                     |                     |                   |                    |                    |                    |                    |                     |                     |
| R-1122  |                     |                   |                    | 7.99               | 43.33              |                    | 25.28               |                     |                     |                   |                    |                    |                    | 1.64               | 1.52                | 1.40                |
| R-1131a   |                     |                   |                    | 8.94               | 7.93               | 6.73               | 5.95                |                     |                     |                   |                    | 0.96               | 0.90               | 0.83               | 0.77                |                     |
| R-1122B1  |                     |                   |                    | 6.29               | 5.63               | 6.83               | 5.98                |                     |                     |                   |                    | 0.85               | 0.90               | 0.83               | 0.78                |                     |
| R-1140B1  |                     |                   |                    | 20.72              | 16.74              | 5.18               | 4.64                |                     |                     |                   |                    | 0.80               | 0.75               | 0.71               | 0.67                |                     |
| R-1112c   |                     |                   |                    | 15.26              | 12.99              | 13.99              | 11.76               |                     |                     |                   |                    | 1.32               | 1.22               | 1.15               | 1.07                |                     |
|   |                     |                   |                    |                    | 47.53              | 36.07              | 9.91                |                     |                     |                   |                    | 1.18               | 1.11               | 1.05               | 1.00                |                     |
|   |                     |                   |                    |                    | 45.52              | 34.38              | 27.33               | 22.06               |                     |                   |                    |                    | 1.68               | 1.56               | 1.44                | 1.34                |
|   |                     |                   |                    |                    |                    |                    | 27.33               | 22.06               |                     |                   |                    |                    | 1.66               | 1.54               | 1.44                | 1.34                |

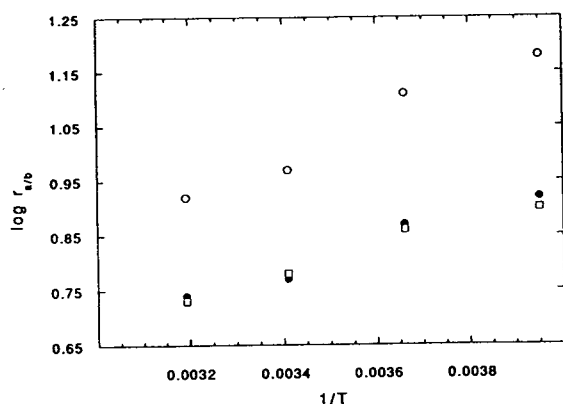


Fig. 2. A plot of the logarithm of the relative retention,  $\log r_{a/b}$ , with respect to tetrafluoromethane, against  $1/T$ , for the fluids measured between  $-20$  and  $40^\circ\text{C}$ .  $\circ$  = R-1123;  $\bullet$  = R-1132a;  $\square$  = R-1141.

we note that the retention parameters are not qualitatively correlated by the triangular diagram scheme that successfully describes the normal boiling point, flammability, atmospheric lifetime, and toxicity of low molecular mass halocarbons. We had found in previous work that the re-

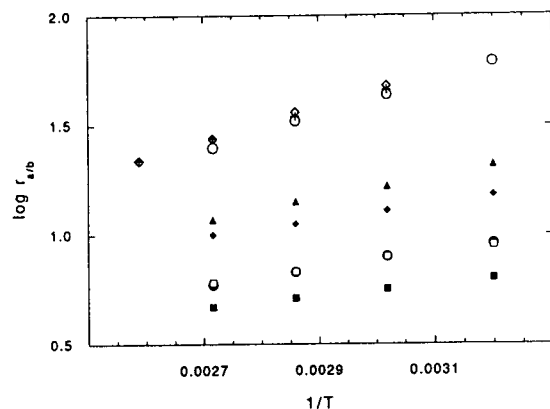


Fig. 3. A plot of the logarithm of the relative retention,  $\log r_{a/b}$ , with respect to hexafluoromethane, R-116, against  $1/T$ , for the fluids measured between  $40$  and  $120^\circ\text{C}$ .  $\circ$  = R-1112a;  $\bullet$  = R-1113;  $\square$  = R-1122;  $\blacksquare$  = R-1131a;  $\blacktriangle$  = R-1122B1;  $\blacklozenge$  = R-1140B1;  $\diamond$  = R-1112t;  $+$  = R-1112c.

tention parameters of methane- and ethane-based halocarbons were qualitatively predicted by this type of property diagram.

### Acknowledgements

The financial support of the Colorado Alliance for Science and the United States Environmental Protection Agency, Stratospheric Ozone Protection Branch, is gratefully acknowledged.

### References

- [1] E.J. Lizardos, *Maint. Tech.*, 6, No. 8 (1993) 17–19.
- [2] M.O. McLinden and D.A. Didion, *ASHRAE J.*, 29, No. 12 (1987) 32–42.
- [3] T.J. Bruno, *Spectroscopic Library for Alternative Refrigerant Analysis; Special Publication 794*, US National Institute of Standards and Technology (NIST), Washington, DC, 1990.
- [4] T.J. Bruno, *Strategy of Chemical Analysis of Alternative Refrigerants; Technical Note 1340*, US National Institute of Standards and Technology (NIST), 1990.
- [5] T.J. Bruno, *ASHRAE Trans.*, 98, No. 2 (1992) 204–208.
- [6] T.J. Bruno, *ASHRAE Trans.*, 98, No. 2 (1992) 210–215.
- [7] R.L. Grob (Editor), *Modern Practice of Gas Chromatography*, Wiley, New York, 2nd ed., 1985.
- [8] T.J. Bruno, *Chromatographic and Electrophoretic Methods*, Prentice-Hall, Englewood Cliffs, NJ, 1991.
- [9] J.E. Willett, *Gas Chromatography (Analytical Chemistry by Open Learning)*, Wiley, Chichester, 1987.
- [10] T.J. Bruno and M. Caciari, *J. Chromatogr. A*, 672 (1994) 149–158.
- [11] T.J. Bruno and M. Caciari, *J. Chromatogr. A*, 679 (1994) 123–132.
- [12] T.J. Bruno (Editor), *CRC Handbook for the Analysis and Identification of Alternative Refrigerants*, CRC Press, Boca Raton, FL, 1994.
- [13] T.J. Bruno, *Anal. Chem.*, 58 (1986) 1596.
- [14] J.L. Glajch and W.G. Schindel, *LC·GC*, 4 (1986) 574.
- [15] J.D. Gibbons and S. Chakraborti (Editors), *Non-parametric Statistical Inference*, Marcel Dekker, New York, 1992.
- [16] T.J. Bruno and D.E. Martire, *J. Phys. Chem.*, 87 (1986) 2430.





ELSEVIER

Journal of Chromatography A, 686 (1994) 253–261

JOURNAL OF  
CHROMATOGRAPHY A

# Identification of halogenated compounds produced by chlorination of humic acid in the presence of bromide

Ruud J.B. Peters<sup>a,\*</sup>, Ed W.B. de Leer<sup>a</sup>, Johanna F.M. Versteegh<sup>b</sup>

<sup>a</sup>*TNO Institute of Environmental Sciences, Department of Analytical Chemistry, Schoemakerstraat 97, 2600 JA Delft, Netherlands*

<sup>b</sup>*National Institute of Public Health and Environmental Protection, Antonie van Leeuwenhoeklaan 9, 3720 BA Bilthoven, Netherlands*

First received 5 April 1994; revised manuscript received 1 August 1994

## Abstract

The formation of halogenated compounds by chlorination of humic acid with and without bromide present was compared. The presence of bromide ion results in the production of many brominated and mixed bromo-chloro compounds. Trihalomethanes, halogenated aliphatic acids and diacids, and trihalomethane precursors are major products. The presence and identity of the halogenated compounds were also confirmed by the use of an atomic emission detector. The mutagenic activity was determined and shown to be 2–3 times higher when bromide is present during chlorination.

## 1. Introduction

Chlorine is often used for the disinfection of drinking water. Owing to its high reactivity, chlorine reacts very rapidly with many natural organic compounds, mainly humic materials, present in raw water. This results in the formation of numerous chlorination by-products and an increased mutagenic activity of chlorinated drinking water [1–3], indicating a potential risk for the consumer.

The type and relative amounts of the chlorination by-products varies not only with the organic content of the source water but also with the inorganic species present. If bromide is present then brominated compounds, such as bromoform

and the other bromochloro trihalomethanes (THMs), are also produced [4]. During chlorination, bromide is oxidized by chlorine to bromine and chlorination and bromination become competitive reactions. In a study of the concentrations of THMs and dihaloacetonitriles (DHANs) in drinking water by Peters et al. [5], it was shown that the major part of the THMs and DHANs found in Dutch drinking water were brominated. Further, many of the volatile mutagens identified in chlorinated drinking water are brominated or mixed chloro-bromo compounds [6].

However, the volatile halogenated compounds represent only a minor part of the total halogenated products, and these compounds account for only a small part (5–10%) of the total mutagenic activity [6,7]. The major part of the halogenated products is found in the non-volatile

\* Corresponding author.

polar fraction, which is also responsible for most of the mutagenic activity.

Until now, most studies of the non-volatile polar fraction have focused on chlorinated products and little is known about brominated and mixed chloro–bromo products. The aim of this paper is to report the results of the aqueous chlorination of humic acid with and without bromide present. The chlorination products were identified and the mutagenic activity of the extracts of the reaction mixtures was determined.

## 2. Experimental

### 2.1. Materials

Analytical-reagent grade chemicals were used and all solutions were prepared with water purified with a Milli-Q system (Millipore). Humic acid was obtained from Fluka. A raw water sample was collected at a treatment plant and stored at 5°C. The dissolved organic carbon (DOC) of the raw water was 1.7 mg/l and the bromide content was ca. 0.2 mg/l. Standards of a number of identified products were purchased from Aldrich and Fluka and some others were synthesized in our laboratory according to procedures described in the literature.

### 2.2. Chlorination/bromination of raw water

The raw water sample was filtered through glass-fibre filters and a volume of ca. 900 ml was collected in three different bottles. To two bottles NaBr solution was added to achieve bromide contents of 0.5 and 1.5 mg/l. Next, NaOCl solution was added to achieve a chlorine concentration of 0.2 mg/l. Finally, the volume was adjusted to 1000 ml with raw water and the bottles were stored in the dark for 16 h. The extraction and analyses of the trihalomethanes using GC with electron-capture detection were performed as described previously [5].

### 2.3. Chlorination/bromination of aqueous humic acid

A 400-mg amount of humic acid was dissolved in 500 ml of 0.02 M NaOH solution and stirred overnight. After neutralizing the mixture with hydrochloric acid, it was filtered through glass-fibre filters. The resulting humic solution was mixed with 200 ml of 1.0 M phosphate buffer (pH 7), 0.05 M NaBr solution was added to achieve bromide to chlorine molar ratios of 0, 0.05 and 0.10 and the total volume was adjusted to about 900 ml with deionized water. Then a calculated amount of chlorine, in the form of 0.5 M NaOCl solution, was added to establish Cl<sub>2</sub>/C molar ratios of 0.5 and 2.0, respectively. Finally, the volume was adjusted to 1000 ml with deionized water and the bottles were stored in the dark. After a reaction time of 16 h, any excess of chlorine was destroyed by the addition of solid sodium arsenite. The reaction mixture was saturated with sodium chloride and acidified to pH 0.5 with concentrated sulfuric acid. The mixture was extracted three times with 100 ml of glass-distilled diethyl ether. The combined ether extracts were stored overnight at –20°C to freeze out residual water and concentrated to 5 ml in a Kuderna–Danish apparatus. The extracts were then carefully purged with nitrogen until dryness. The residue was dissolved in 10.0 ml of ethyl acetate and divided into two portions to be used for the mutagenicity testing and GC–MS analysis. The samples were stored at –20°C.

### 2.4. Gas chromatographic analyses

Prior to analysis, the chlorinated humic acid extracts were methylated with diazomethane. To 2 ml of the extracts 2 ml of ethyl acetate and 0.2 ml of methanol were added to aid methylation. 1-Chlorododecane was added as an internal standard and the samples were methylated with diazomethane. Diazomethane gas was generated fresh from N-methyl-N-nitroso-*p*-toluenesulfonamide (Merck) and was stripped from the generation vessel into the sample vials with nitrogen gas.

The samples were analysed by GC–MS with an HP 5890 gas chromatograph interfaced with an HP 5970B mass-selective detector. The chromatograph was equipped with a 25 m × 0.2 mm I.D. HP-1 (film thickness 0.33 mm) fused-silica capillary column and helium was used as the carrier gas. The temperature settings were as follows; column oven, programmed from 50°C (5 min) to 300°C (10 min) at 8°C/min; and injector and transfer line, 280°C. For the identification of the chlorination products the mass spectrometer was operated in the scan mode ( $m/z = 40\text{--}400$ ). The samples were also analysed by GC–atomic emission spectrometry (AES) with an HP 5890 gas chromatograph interfaced with an HP 5921A atomic emission detector. The chromatograph was equipped with a 50 m × 0.2 mm I.D. HP-1 (film thickness 0.33 mm) fused-silica capillary column and helium was used as the carrier gas. The temperature settings were the same as in GC–MS. With AES, four elements, carbon, hydrogen, chlorine and bromine, were monitored simultaneously at 495.7, 486.1, 479.5 and 478.6 nm, respectively. The plasma power was 50 W and an additional make-up flow of 40 ml/min of helium.

### 2.5. Mutagenicity testing

Mutagenicity test were performed according to Ames et al. [8] using *Salmonella typhimurium* strain TA 100 with and without metabolic activation (S9 mix). The mutagenic response was calculated as the slope of the linear part of the dose–response curves.

## 3. Results and discussion

Bromide is often present in raw water, from either natural or anthropogenic sources. In Dutch waters bromide concentrations vary from 0.1 to 0.5 mg/l. During chlorination of the raw water, bromide ion is oxidized to bromine. Bromine seems to be more effective as a halogen-substituting agent [9] and if bromine

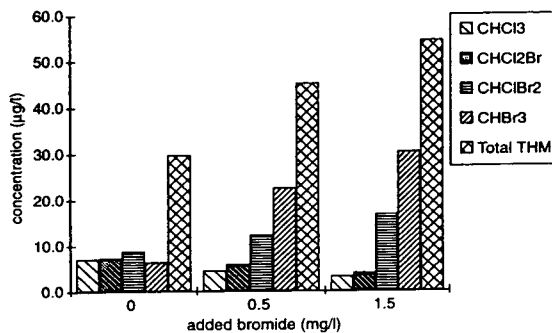


Fig. 1. Results of the chlorination (0.2 mg/l) of a raw water sample (DOC 1.8 mg/l) containing different amounts of bromide. The original raw water had a bromide content of approximately 0.2 mg/l.

acts as an oxidant it will be reduced to bromide ion, which may then be re-oxidized by chlorine. This results in a high bromine incorporation into the well known THMs, as is reflected by the results of the chlorination of raw water used to prepare drinking water (see Fig. 1). The bromide content of the raw water itself was not known exactly but was approximately 0.2 mg/l. Owing to this natural bromide background, chlorination of this raw water in the laboratory resulted in the production of all four THMs. However, if additional bromide was added to the samples the concentration of the higher brominated THMs increased, while that of chloroform and bromodichloromethane decreased. Finally, the total amount of THMs produced by chlorination also increased with high bromide concentrations. Ozone may be used as an alternative to chlorine but, like chlorine, ozone is also capable of oxidizing bromide to bromine, resulting in the production of brominated disinfection by-products [10].

In contrast to the THMs there is only very little information about the information of non-volatile brominated compounds, and there has been no systematic study of these products. Recently, we reported that the major part of the haloacetic acids (HAAs), typical representatives of the non-volatile polar fraction, found in Dutch drinking waters are brominated [11]. Aqueous

chlorination of phenol in the presence of bromide also resulted in the formation of brominated and chloro/bromoacetic acids [12]. These findings suggest that brominated compounds may form a substantial part of the chlorination products if bromide is present in the source water.

The chlorination/bromination of humic acid at pH 7 was performed with chlorine to carbon molar ratios of 0.5 and 2.0 and bromide to chlorine molar ratios of 0.00, 0.05 and 0.10, respectively. Chromatograms of two of the high-chlorine dose experiments are given in Fig. 2a (Br<sup>-</sup>/Cl<sub>2</sub> molar ratio = 0) and 2b (Br<sup>-</sup>/Cl<sub>2</sub> molar ratio = 0.10), and show that many prod-

ucts were formed. Dominant products identified after chlorination of humic acid without bromide were chlorinated aliphatic acids and diacids, especially dichloro- and trichloroacetic acid, chloro- and dichloromaleic acid and dichlorosuccinic acid. Several chloroform precursors, previously identified by De Leer et al. [3], were also found. These are structures with a di- or trihalomethane group which is easily hydrolysed to trihalomethanes, and are found predominantly in the low-chlorine-dose experiments. Non-chlorinated products include aliphatic diacids and aromatic acids, in addition to small amounts of methyl-substituted aromatic acids and aromatic

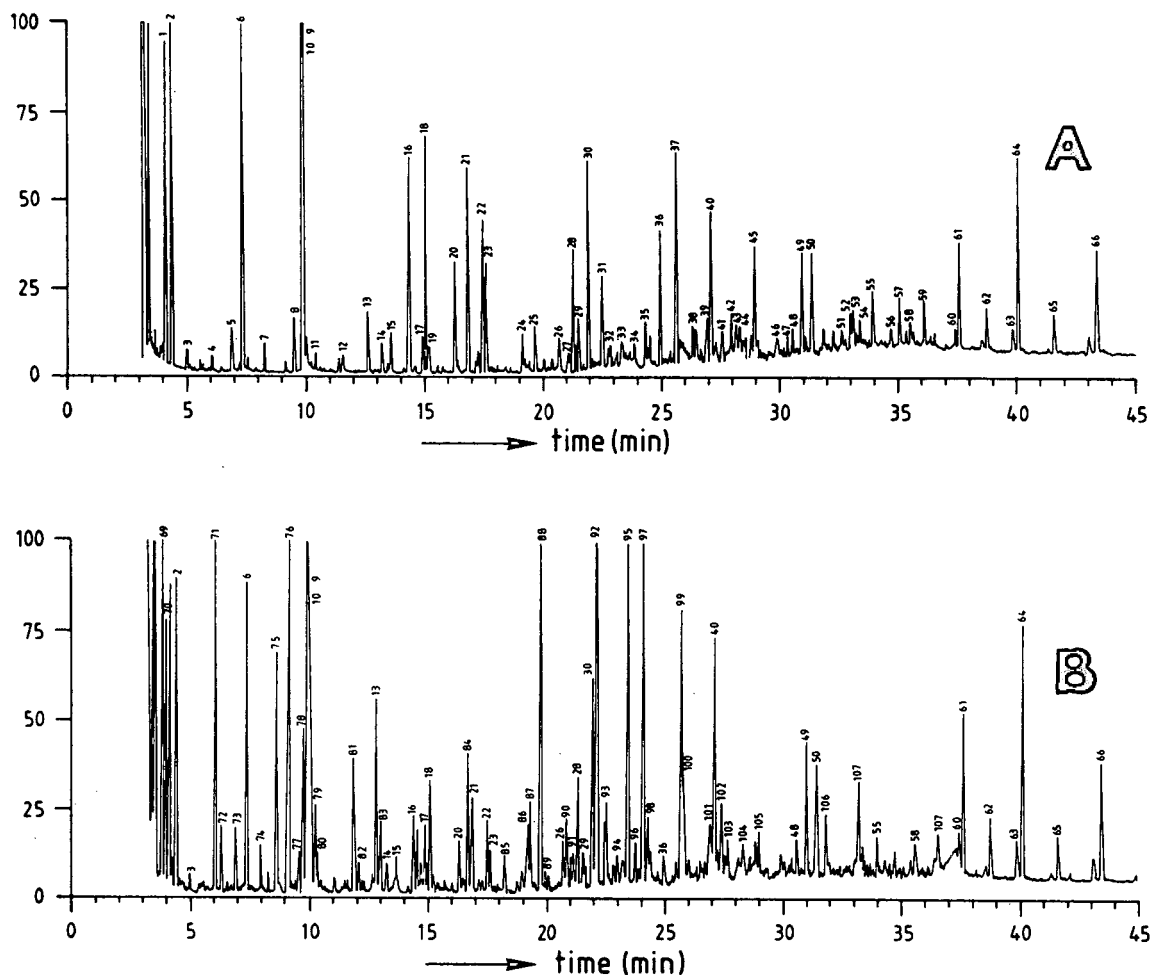


Fig. 2. Chromatograms of two of the high-chlorine-dose experiments (A) without, and (B) with bromide present during aqueous chlorination of humic acid. For peak identification, see Table 1.



glyoxylic acids. Generally, these results agree well with those of earlier studies [1–3].

If bromide was present during chlorination, the chlorinated products were present in smaller amounts, and in addition many brominated products with similar structures were identified. Although dichloro- and trichloroacetic acid are still major products, brominated and mixed bromo/chloroacetic acids are also important products. The same is true for the halogenated diacids. A noticeable difference is the presence of several halogenated alkanes. These include not only the THMs, but also dibromoethane and chlorobromo- and dibromopropane. The latter compounds have also been identified in mutagenic extracts of chlorinated drinking water and shown to be active mutagens [6]. Interesting also is the tentative identification of several THM precursors. The structures of these compounds are similar to the chloroform precursors that were identified by De Leer et al. [3], and they show major peaks in the chromatograms of the reaction mixtures. The non-chlorinated products that were identified were the same as in the chlorination experiment without bromide.

All products that were identified are given in Table 1. The compound numbers correspond with those in the chromatograms in Figs. 1 and 2. The identifications in Table 1 are differentiated into standard confirmed (SC), confident (C) and tentative (T) identifications. SC means that a standard of the identified compound was available, thus allowing confirmation on the same GC–MS system. C means that a reference mass spectrum of the identified compound was available. T means that no standard or reference mass spectrum was available and that the identity was determined from the mass spectrum. If a dash appears in the ID column the compound was not identified at all. However, it was possible to determine the number of chlorine/bromine atoms in the molecule from the isotopic clusters in the mass spectrum. In other instances the mass spectrum allowed the identification of part of the compound. In such an event, the known part of the structure is given in Table 1 and the unknown part is depicted by the letter X.

The reaction products were identified using GC–MS but additional information concerning the elemental composition of the chlorination products was obtained with the use of AES. AES is an element-specific detection method and hence is able to discriminate between chlorinated, brominated and mixed chloro/bromo compounds. In GC–AES, the GC effluent enters a high-temperature microwave-induced helium plasma. The organic compounds are decomposed into their elemental constituents, and the atoms are excited to a higher energy level. If a sufficient number of atoms are excited, the atomic emission signals can be recorded at element specific wavelengths. In this work the emissions of bromine, chlorine, carbon and hydrogen were recorded simultaneously. A multi-element chromatogram of the high-chlorine-dose experiment with bromide is given in Fig. 3. The peak heights of trichloro- and dibromoacetic acid and the internal standard *n*-chlorododecane were used to calculate the relative elemental response factors and thus the empirical formulae of the compounds. The results of the GC–AES analysis confirmed the MS interpretations.

The mutagenic activity of the samples was also determined to see if the addition of bromide resulted in an increased TA-100 activity. In general, the results in the Ames test without metabolic activation showed that the samples in the high-chlorine-dose experiments were twice as mutagenic as those in the low-chlorine-dose experiments. In both instances, however, the addition of bromide during chlorination led to a 2–3 times higher mutagenic activity of the samples. When the Ames test was performed with metabolic activation (S9 mix) the mutagenic activity was substantially lower. The bacterial mutagenicity assay, known as the Ames test, provides a rapid and relatively simple method for detecting mutagenic activity. *Salmonella typhimurium* strain TA-100, containing well characterized mutations in certain genes limiting the growth of colonies, is exposed to a part of the final ethyl acetate extract. If mutagenic compounds are present, reverse mutations will occur, and hence the number of colonies will increase. In order to simulate the metabolism in

Table 1

Compounds identified after chlorination/bromination of humic acid. Peak numbers refer to peak numbers in the chromatograms in Figs. 2 and 3

| Peak No. | Compound   | ID <sup>a</sup> | RRT <sup>b</sup> |
|----------|--|-----------------|------------------|
| 1        | Ethyl propionate   | SC              | 0.188            |
| 2        | 1-Butanol  | SC              | 0.200            |
| 3        | Chloroethanoic acid  | SC              | 0.227            |
| 4        | 2-Chloropropenoic acid                                       | C               | 0.277            |
| 5        | Propanedioic acid  | SC              | 0.314            |
| 6        | Dichloroethanoic acid  | SC <sup>c</sup> | 0.336            |
| 7        | Trichloroethanal   | SC <sup>c</sup> | 0.378            |
| 8        | 1,1,1-Trichloro-2,3-epoxypropane                             | C               | 0.434            |
| 9        | Trichloroethanoic acid                                       | SC <sup>c</sup> | 0.449            |
| 10       | Trimethyl phosphate  | SC              | 0.458            |
| 11       | 3,3-Dichloropropenoic acid                                   | C               | 0.476            |
| 12       | 2-Hydroxypropanoic acid                                      | C               | 0.529            |
| 13       | Butenedioic acid   | SC              | 0.576            |
| 14       | Chloropropanedioic acid                                      | SC              | 0.604            |
| 15       | 3,3,2-Trichloropropenoic acid                                | T <sup>c</sup>  | 0.614            |
| 16       | Chlorobutenedioic acid                                       | SC <sup>c</sup> | 0.656            |
| 17       | Chlorobutanedioic acid                                       | SC              | 0.682            |
| 18       | Dichloropropanedioic acid                                    | SC <sup>c</sup> | 0.688            |
| 19       | 3,3,3-Trichloro-2-hydroxypropanoic acid                      | T               | 0.693            |
| 20       | 2,3-Dichloro-4-oxopentenoic acid                             | T <sup>c</sup>  | 0.744            |
| 21       | 2,2-Dichlorobutanedioic acid                                 | SC <sup>c</sup> | 0.767            |
| 22       | 2,3-Dichlorobutenedioic acid                                 | SC <sup>c</sup> | 0.798            |
| 23       | Isomer of 22   | SC              | 0.803            |
| 24       | Dichlorinated compound                                       | –               | 0.874            |
| 25       | 2,2-Dichloropentanoic acid                                   | C               | 0.898            |
| 26       | Methylfurandicarboxylic acid                                 | C               | 0.944            |
| 27       | Benzenedicarboxylic acid                                     | SC              | 0.965            |
| 28       | 2,3-Dimethoxybutenedioic acid                                | T               | 0.971            |
| 29       | 2-Chloro-3-dichloromethylbutenedioic acid                    | SC              | 0.981            |
| 30       | 1-Chlorododecane   | SC <sup>c</sup> | 1.000            |
| 31       | Isomer of 27   | SC              | 1.027            |
| 32       | 2,3,4,4-Tetrachloro-2-pentenedioic acid                      | T               | 1.041            |
| 33       | 4-Oxoheptanoic acid  | T               | 1.068            |
| 34       | Trichlorinated compound                                      | –               | 1.089            |
| 35       | 2-Carboxy-3,5,5,5-tetrachloro-4-oxopentanoic acid            | T               | 1.100            |
| 36       | 2,3,3,5,5,5-Hexachloro-4-hydroxypentanoic acid               | T               | 1.137            |
| 37       | Isomer of 35   | T               | 1.169            |
| 38       | Trichlorinated compound                                      | –               | 1.207            |
| 39       | 2,3-Dicarboxybutenedioic acid                                | T               | 1.229            |
| 40       | Benzenetricarboxylic acid                                    | SC              | 1.235            |
| 41       | Phthalate  | T               | 1.257            |
| 42       | Isomer of 40   | –               | 1.275            |
| 43       | Trichlorinated compound                                      | –               | 1.284            |
| 44       | Methylbenzenetricarboxylic acid                              | C               | 1.291            |
| 45       | Trichlorinated compound                                      | –               | 1.321            |
| 46–53    | Benzenetetracarboxylic acid and glyoxylic acid isomers of 46 | C               |                  |
| 54–58    | Benzenepentacarboxylic acid and glyoxylic acid isomers of 54 | C               |                  |
| 59–68    | Fatty acids and alkanes                                      | C               |                  |
| 69       | Dibromometane  | SC <sup>c</sup> | 0.174            |
| 70       | Bromodichlorometane  | SC <sup>c</sup> | 0.179            |
| 71       | Chlorodibromomethane   | SC <sup>c</sup> | 0.274            |

Table 1 (continued)

| Peak No. | Compound                                     | ID <sup>a</sup> | RRT <sup>b</sup> |
|----------|--|-----------------|------------------|
| 72       | 1,2-Dibromoethane                            | SC <sup>c</sup> | 0.287            |
| 73       | Bromoethanoic acid                           | SC <sup>c</sup> | 0.314            |
| 74       | 1,3-Bromochloropropane                       | T <sup>c</sup>  | 0.363            |
| 75       | Tribromomethane                              | SC <sup>c</sup> | 0.393            |
| 76       | 2-Chlorobutenoic acid                        | T <sup>c</sup>  | 0.416            |
| 77       | Isomer of 76                                 | T <sup>c</sup>  | 0.437            |
| 78       | Bromochloroethanoic acid                     | SC <sup>c</sup> | 0.443            |
| 79       | Monochlorinated acid                         | –               | 0.468            |
| 80       | 1,2-Dibromopropane                           | T <sup>c</sup>  | 0.471            |
| 81       | Dibromoethanoic acid                         | SC <sup>c</sup> | 0.540            |
| 82       | 1,2-Bromochloropropanoic acid                | T               | 0.550            |
| 83       | Butanedioic acid                             | SC              | 0.588            |
| 84       | Tribromoethanoic acid                        | SC <sup>c</sup> | 0.759            |
| 85       | Dibromopropanedioic acid                     | T               | 0.831            |
| 86       | Bromochlorobutanedioic acid                  | T               | 0.876            |
| 87       | Isomer of 86                                 | T               | 0.879            |
| 88       | 2,4-Dichloro-2-bromo-3-oxobutanoic acid      | T <sup>c</sup>  | 0.899            |
| 89       | 2-Carboxy-3-bromobutanoic acid               | T               | 0.909            |
| 90       | Dibromobutanedioic acid                      | T               | 0.951            |
| 91       | 2-Chloro-3-bromobutanedioic acid             | T               | 0.965            |
| 92       | 2,5-Dichloro-4-bromo-3-oxopentanoic acid     | T <sup>c</sup>  | 1.008            |
| 93       | 2-Chloro-4-bromo-3-oxopentanedioic acid      | T               | 1.025            |
| 94       | Non-halogenated compound                     | –               | 1.028            |
| 95       | 4,5-Dibromo-2-chloro-3-oxopentanoic acid     | T <sup>c</sup>  | 1.067            |
| 96       | Non-halogenated acid                         | –               | 1.082            |
| 97       | 2,5-Dibromo-6-chloro-3-oxopentanoic acid     | T               | 1.097            |
| 98       | Halogenated acid                             | –               | 1.107            |
| 99       | X-COCHBrCH <sub>2</sub> COOH                 | –               | 1.171            |
| 100      | X-COCHClCOOH                                 | –               | 1.174            |
| 101      | X-COCHBrCH <sub>2</sub> COOH                 | –               | 1.226            |
| 102      | X-COCHBrCH <sub>2</sub> CH <sub>2</sub> COOH | –               | 1.249            |
| 103      | Dibrominated compound                        | –               | 1.262            |
| 104      | Phthalate                                    | T               | 1.313            |
| 105      | Halogenated acid                             | –               | 1.321            |
| 106      | X-COCHClCOOH                                 | –               | 1.449            |
| 107      | X-COCHClCOOH                                 | –               | 1.513            |

<sup>a</sup> SC = standard confirmed; C = confident; T = tentative.

<sup>b</sup> Retention time relative to the internal standard 1-chlorododecane.

<sup>c</sup> Elemental composition confirmed by GC–AES.

higher organisms, a rat liver homogenate (S9 mix) can be incorporated in the test. Compounds that are not mutagenic may be metabolically activated and vice versa.

The most important mutagen identified in chlorinated drinking water so far is 3-chloro-4-(dichloromethyl)-5-hydroxy-2(5H)-furanone, referred to as Mutant X or MX [13]. The identification of many brominated compounds in

finished drinking water and in model studies suggests that brominated MX analogues (BMX) may also be present in finished drinking waters. Although we have already confirmed the formation of BMX in model experiments their presence in drinking water is still unknown [14,15]. If BMX is present in drinking water this may explain the part of the mutagenicity not accounted for by MX.

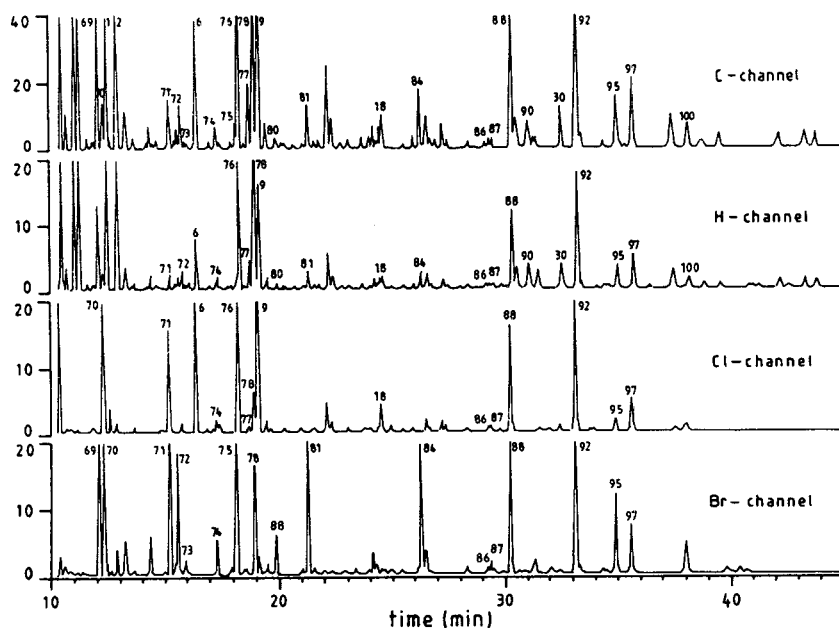


Fig. 3. Multi-element chromatogram of the GC-AES analysis of a sample of chlorinated/brominated humic acid. The emissions of carbon, hydrogen, chlorine and bromine were recorded simultaneously and are shown in that order. Compounds that were identified using GC-AES are indicated in Table 1.

#### 4. Conclusions

The chlorination of humic acid in the presence of bromide resulted in the production of many brominated and mixed bromo-chloro compounds. The type of compounds formed is similar to previously identified chlorinated products. Trihalomethanes, halogenated aliphatic acids and diacids and trihalomethane precursors were major chlorination products. The presence and elemental composition of several of the brominated compounds were also confirmed by the use of an atomic emission detector. If bromide was present during chlorination, the mutagenic activity increased significantly. The results of this study indicate that brominated organohalogen compounds are important disinfection by-products and that brominated MX analogues may explain that part of the mutagenic activity of chlorinated drinking water that is not accounted for to date.

#### References

- [1] J.D. Johnson, R.F. Christman, D.L. Norwood and D.S. Millington, *Environ. Health Perspect.*, 46 (1982) 63–71.
- [2] R.F. Christman, D.L. Norwood, D.S. Millington and J.D. Johnson, *Environ. Sci. Technol.*, 17 (1983) 625–628.
- [3] E.W.B. de Leer, J.S. Sinninghe Damste, C. Erkelens and L. de Galan, *Environ. Sci. Technol.*, 19 (1985) 512–522.
- [4] M.P. Italia and P.C. Uden, *J. Chromatogr.*, 605 (1992) 81–86.
- [5] R.J.B. Peters, E.W.B. de Leer and L. de Galan, *Water Res.*, 24 (1990) 797–800.
- [6] M. Fielding and H. Horth, *Water Supply*, 4 (1986) 103–126.
- [7] J.R. Meier, H.P. Ringhand, W.E. Coleman, J.W. Munch, R.P. Streicher, W.H. Kaylor and K.M. Schenk, *Mutat. Res.*, 157 (1985) 111–122.
- [8] B.N. Ames, J. McCann and E. Yamasaki, *Mutat. Res.*, 31 (1975) 346–364.
- [9] G.L. Amy, P.A. Chadik, Z.K. Chowdhury, P.H. King and W.J. Cooper, *Water Chlorination: Chemistry, Environmental Impact and Health Effects*, Vol. 5, Lewis, Chelsea, MI, 1985, pp. 907–922.

- [10] Y. Sayato, K. Nakamuro, M. Hayashi and H. Sano, *Chemosphere*, 20 (1990) 309–315.
- [11] R.J.B. Peters, E.W.B. de Leer and L. de Galan, *Water Res.*, 25 (1991) 473–477.
- [12] J.C. Ireland, L.A. Moore, H. Pourmoghaddas and A.A. Stevens, *Biomed. Environ. Mass Spectrom.*, 17 (1988) 483–486.
- [13] L. Kronberg and T. Vartiainen, *Mutat. Res.*, 206 (1988) 177–181.
- [14] H. Horth, *J. Fr. Hydrol.*, 38 (1990) 80–100.
- [15] R.J.B. Peters, C. Voogd, J.F.M. Versteegh, E.W.B. de Leer and L. de Galan, *Environ. Sci. Technol.*, (1994) in press.



# Gas chromatographic determination of organochlorine and pyrethroid pesticides of horticultural concern

Amadeo R. Fernandez-Alba<sup>a,\*</sup> Antonio Valverde<sup>b</sup> Ana Agüera<sup>c</sup>,  
Mariano Contreras<sup>c</sup>

<sup>a</sup>*Departamento de Química Analítica, Facultad de Ciencias de Almería, Universidad de Almería, 04071 Almería, Spain*  
<sup>b</sup>*Departamento de Química Inorgánica, Facultad de Ciencias de Almería, Universidad de Almería, 04071 Almería, Spain*  
<sup>c</sup>*Laboratorio de Análisis Agrícola de COEXPHAL, Cosecheros-Exportadores de Hortalizas de Almería, 04070 Almería, Spain*

Received 13 June 1994

## Abstract

An optimized gas chromatographic method is described for the determination of thirteen organochlorine and pyrethroid pesticides currently applied to vegetable and fruit crops. The selected pesticides are extracted with ethyl acetate–sodium sulphate and an aliquot is evaporated to dryness and reconstituted in 10 ml of light petroleum. Sample clean-up is accomplished by aspirating 2 ml of the light petroleum extract through a silica gel solid-phase disposable cartridge. Following aspiration, the sample is eluted with 2 ml of diethyl ether–light petroleum (50:50) and is ready for GC with electron-capture detection. The method provides an excellent clean-up for all matrices studied. The recoveries varied from 73 to 106%, except for captan (51%), with relative standard deviations from 3.5 to 20.4% in all instances. Detection limits of less than 0.01 mg/kg were obtained. The sample throughput is ca. 51 per 24 h. These results were confirmed by GC–MS. Results are also presented for extracts of four different food product types fortified with the target pesticides. Data for real residues of these pesticides found in vegetables during 1 year routinely applying the multi-residue method are also presented.

## 1. Introduction

Monitoring of pesticide residues in agricultural products has become a priority field in pesticide research and analysis. The main objectives of such residue monitoring are to enforce tolerance levels in food, to acquire incidence/level data on designated commodity pesticides and to carry out total diet studies. This concern is reflected in the publication by the EEC jointly with the

government of each country of the maximum recommended limits (MRLs) for pesticide residues in a variety of agricultural foods [1]. Hence the development of improved multi-residue methods (MRMs) to cover the agricultural chemicals of current interest in which the repetition of time-consuming operations is minimized is of great interest in monitoring food supplies.

Several multi-residue procedures have been proposed in recent years for the determination of organochlorine compounds (OCs) and organophosphorus compounds (OPs) in crops by using

\* Corresponding author.

GC to separate the individual residues followed by detection with selective and sensitive methods such as electron-capture detection (ECD), nitrogen–phosphorus detection and flame photometric detection [2–8]. Among these, few are adequate for screening both classes of pesticides (OPs and OCs) in horticultural samples with a single sample preparation [6,7].

Chlorinated hydrocarbon pesticides are of special concern because of their persistence in the environment and in animal tissues [9] and their significance to human health [10], and so are usually an important objective in food analysis. Acetonitrile extraction (Mills method) [11] is usually preferred in the determination of these compounds in horticultural samples when no clean-up methods are applied as vegetable extracts in acetonitrile are cleaner than those obtained with other solvents of similar polarity. Owing to its high separation power and sensitivity, GC–ECD is the favoured technique for the determination of OC pesticides [12]. However, carefully control of degradation due to thermal or column reaction processes is necessary with this technique, especially with phthalimide fungicides such as captan and folpet, which are notoriously prone to adsorption and degradation processes [13,14].

Nowadays, the use of ethyl acetate for multi-

residue solvent extraction is replacing with good results other MRM procedures [15–17] owing to its simplicity, speed and the solvent, resulting in cheaper analyses. Thus, the National Food Administration of Sweden adopted in 1989 an ethyl acetate multi-residue method as a single sample preparation for OCs and OPs [18]. Unfortunately, this extraction also removes an abundance of co-extractives in most agricultural commodities. In such a situation an efficient clean-up is required before determination, especially in complex matrices such as pepper. Solid-phase extraction (SPE) provides a useful alternative [19–23] to the traditional liquid–liquid extraction-based methods [24] or gel permeation chromatographic (GPC) clean-up methods [7,25].

In a previous paper [26], we described an ethyl acetate method (MRM) for the separation of a selected group of OP pesticides, but its direct application to OC determination suffered from serious interference problems, as mentioned above.

In this study, this rapid and accurate multi-residue protocol was developed by incorporating a clean-up step for the determination of thirteen organochlorine and pyrethroid pesticides (for structures see Fig. 1) currently applied to horticultural crops grown in greenhouses in south-eastern Spain. The work described proceeded in

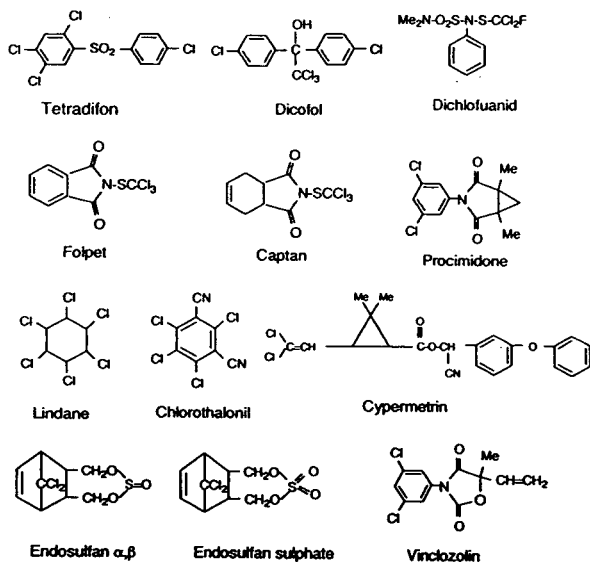


Fig. 1. Structures of the compounds studied.



Table 1  
Maximum residue limits (MRLs) in mg/kg established in two European countries and USA and EEC regulations

| No.  | Compound                | Sweden | Spain | USA  | EEC |
|------|-------------------------|--------|-------|------|-----|
| 1    | Lindane                 | 1.0    | 1.0   | 1.0  | 1.0 |
| 2    | Chlorothalonil          | 1.0    | 0.01  | –    | –   |
| 3    | Vinclozolin             | 2.0    | 2.0   | –    | –   |
| 4    | Dichlofuanid            | 5.0    | 5.0   | –    | 5.0 |
| 5    | Captan <sup>a</sup>     | 0.1    | 0.1   | 25.0 | 0.1 |
| 6    | Folpet <sup>a</sup>     | 0.1    | 0.1   | –    | –   |
| 7    | Procimidone             | 0.1    | 2.0   | –    | –   |
| 8–10 | Endosulfan <sup>b</sup> | 0.5    | 1.0   | 2.0  | 1.0 |
| 11   | Dicofol                 | 3.0    | 0.5   | –    | 0.5 |
| 12   | Tetradifon              | 2.0    | 1.0   | 1.0  | –   |
| 13   | Cypermethrin            | 2.0    | 1.0   | –    | –   |

<sup>a</sup> As sum of captan and folpet.

<sup>b</sup> As sum of endosulfan I, II and III.

the following stages: (a) optimization of the GC conditions taking into account the factors mentioned below which gave the best chromatographic resolution and the shortest time of analysis; (b) confirmation by GC-MS; (c) clean-up study on silica gel cartridges; (e) determining the linearity, reproducibility and recoveries of the method; (g) evaluating the performance of the method on different samples fortified with selected target compounds; and (f) application of the proposed method to crops possibly containing residues of OCs and pyrethroid pesticides in routine practice for nearly 1 year. A list of the compounds included in the present study together with maximum limits (MRLs) for peppers established according to different regulations are shown in Table 1.

## 2. Experimental

### 2.1. Chemicals

Pesticide-grade ethyl acetate, light petroleum and anhydrous sodium sulfate (12–60 mesh) were obtained from Merck (Darmstadt, Germany). Solid-phase extraction disposable columns (6 ml) containing 500 mg of silica gel were obtained from Varian (Harbor City, CA, USA). The pesticide standards (Pestanal quality) listed in Table 1 were obtained from Riedel-de Haën

(Seelze, Germany). Stock standard solutions were prepared by dissolving 10.0–15.0 mg of each purity-certified pesticide in 100 ml of light petroleum to give 100.0–150.0 mg/l stock standard solutions. A working standard solution was prepared by transferring 1 ml of each stock standard solution into a 100-ml volumetric flask and diluting to volume with light petroleum-diethyl ether (1:1), giving a 1.0–1.5 mg/l working standard solution.

### 2.2. Chromatographic analysis

#### GC-ECD

A Perkin-Elmer (Beaconsfield, UK) model 8600 gas chromatograph equipped with a <sup>63</sup>Ni electron-capture detector was used for GC analysis. An HP1 fused-silica capillary column (30 m × 0.53 mm I.D.) coated with methylsilicone (2.65 μm) (Hewlett-Packard, Palo Alto, CA, USA) was used. Helium was the carrier gas at a flow-rate of 8 ml/min. The temperatures of the injector and detector were maintained at 240 and 300°C, respectively. The conditions used for gas chromatography were optimized. The injection volume was 1 μl.

#### GC-MS

A Hewlett-Packard Model 5995 system with a Model 59970 data system was used for GC-MS in the electron impact (EI) mode. The same

fused-silica column as described above was used. The sample was introduced directly into the ion source. The carrier gas was helium. The other chromatographic conditions were identical with those described for GC-ECD. EI mass spectra were obtained at 70 eV.

### 2.3. GC optimization

The optimization of the temperature programming cycle was carried out by a computer-assisted method [27] taking into account the following parameters.

#### Response function

The selection of a chromatographic response function (*CRF*) based on the criteria given by Schoenmakers [28] is defined as

$$CRF = n + \sum R_{i,j} + 1/2(T_T - T_L) \quad (1)$$

where  $T_L$  is the retention time of the last peak and  $T_T$  the target retention time for the last peak; the term  $T_T - T_L$  in the function is only included if  $T_L$  exceeds  $T_T$ ;  $n$  is the number of peaks detected;  $R_{i,j}$  is the resolution between adjacent peaks  $i$  and  $j$  ( $R_{i,j}$  is limited to a maximum value of 1.5 to avoid  $\sum R_{i,j}$  being determined largely by the largest values of  $R_{i,j}$ ).

Only the four least well resolved pairs of peaks were considered in the present calculations of  $n$  and  $R_{i,j}$ . The target retention time was fixed at  $y_t = 25$  min as the maximum acceptable retention time of the last peak. Hence a maximum value of  $CRF = 14$  can be expected.

#### Selection variables

The next step is to define the variable space or search region. Relying on literature data [29] and previous experience, we selected the following temperature programming cycle:

A final temperature of 260°C was chosen to avoid column bleeding. An initial temperature of 150°C (1-min hold) and a rate 30°C/min were chosen for the initial conditions, ramp 1 and time 1. Thus a three-variable space (temperature 2, time hold 2 and ramp 2) with ranges 180–230°C, 0–6 min and 5–20°C/min, respectively, was used in the optimization procedure.

#### Experimental design

A very general second-order linear model with interaction Eq. 2 was fitted to the experimental data:

$$y = b_0 + b_1X_1 + b_2X_2 + b_3X_3 + b_4X_1^2 + b_5X_2^2 + b_6X_3^2 + b_7X_1X_2 + b_8X_1X_3 + b_9X_2X_3 \quad (2)$$

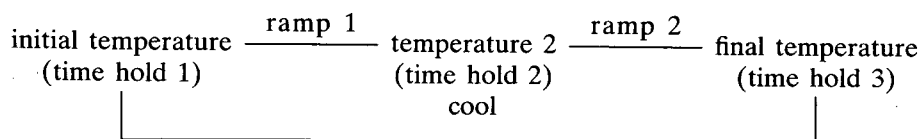
where  $X$  are the independent variables ( $X_1 =$  temperature 2,  $X_2 =$  time hold 2 and  $X_3 =$  ramp 3),  $y$  is the dependent variable (measured response *CRF*, from the experimental runs) and  $b_0$ – $b_9$  are the coefficients to be evaluated.

The experimental data were obtained by carrying out, in randomized order, twenty experimental runs according to the rotate central composite design proposed by Box and Hunter [30]. Each response value was calculated from two replicate injections for each set of parameters. The XYZ computer program used [27] computes the coefficients of the selected model.

The optimum conditions selected were an increase from 150°C (1-min hold) at 30°C/min to 215°C (6-min hold) and then at 15°C/min to 260°C.

### 2.4. SPE clean-up

Solid-phase disposable extraction cartridges with silica as packing material were used. The breakthrough volumes were established in the range 2.5–3.5 ml for the pesticides studied in



light petroleum. Therefore, 2-ml volume of light petroleum extract can be safely used for vegetable sample extracts. The elution behaviour of the OCs and pyrethroid compounds on the silica solid-phase cartridges was studied by application of 2 ml of a pepper extract containing a standard solution of pesticides to the silica minicolumn and subsequent elution with 2-ml volumes of elution solvent. Light petroleum with diethyl ether as modifier was used in the desorption process in order to avoid dilution and to limit the final volume to 2 ml. If pure light petroleum ether was used an elution volume of at least 5 ml was necessary to recover all thirteen compounds. Fractions of 2 ml of diethyl ether in light petroleum in different ratios were collected separately in each clean-up experiment and analysed off-line by GC.

### 2.5. Sample preparation

Different fruit and vegetable samples were collected at greenhouses in the vicinity of Almería, Spain (where all of the OCs compounds mentioned in Table 1 are currently used) and were extracted in our laboratory according to the following procedure.

Weigh 50 g of chopped sample into a high-speed blender and add 40 g of anhydrous sodium sulfate. Mix thoroughly, add 100 ml of ethyl acetate and blend the mixture for 5 min. Filter the supernatant liquid with suction through a filter-paper and a layer of 20 g of anhydrous sodium sulfate. Rinse the filter with 50 ml of ethyl acetate and evaporate the combined extracts on a vacuum rotary evaporator using a 40–60°C water-bath. Dissolve the residue in 10 ml of light petroleum and pass through to a silica gel (500 mg) disposable SPE cartridge previously conditioned with 5 ml of light petroleum and 2 ml of the vegetable extract in light petroleum. Elute the SPE minicolumn with of 2 ml of diethyl ether–light petroleum (50:50) at a flow-rate of 1–2 ml/min and adjust the volume to 2 ml with a diethyl ether–light petroleum (50:50). Inject 1  $\mu$ l of this eluate into the GC–ECD system.

### 2.6. Recovery studies

Fresh green pepper samples, which had not been treated with the pesticides studied, were fortified with 0.20–0.30 mg/kg of each pesticide as follows. A 10-ml volume of the working standard solution described above was added to 50 g of chopped sample in a high-speed blender jar. After evaporation of the light petroleum with an air stream, the sample was homogenized for 2 min. After 1 h, the sample was again homogenized for 1 min and immediately analysed by application of the previously described method. The recovery assays were replicated ten times. For three other food products types the recovery studies were carried out identically but in duplicate.

## 3. Results and discussion

### 3.1. GC optimization

After the twenty experiments mentioned above, the values of the different coefficients were as follows:  $b_0 = 11.56$ ,  $b_1 = -0.46$ ,  $b_2 = 0.79$ ,  $b_3 = -0.49$ ,  $b_4 = -0.24$ ,  $b_5 = -0.23$ ,  $b_6 = 0.24$ ,  $b_7 = 0.27$ ,  $b_8 = 0.31$  and  $b_9 = 0.22$ . These parameters were calculated by a least-squares method and all the coefficients were representative ( $t_{\text{student}} \geq 1.8$ ). An ANOVA test was applied to validate the model. The resulting  $F$  values calculated from the experimental data were higher than the  $F$  values tabulated for three and six degrees of freedom at a level of significance  $\alpha = 0.05$ . A correlation coefficient  $R^2 = 0.91$  between the theoretical and experimental models shows that a high degree of explanation of the variability of the experimental data is achieved by the model. To obtain a graphical representation of the response surface of the variables to be optimized it was necessary to fix one variable and to represent the response of the other two. Fig. 2 shows the representation of the isoresponse as a function of the temperature 2 and ramp 2 at a constant time hold (time hold 2) of 6 min.

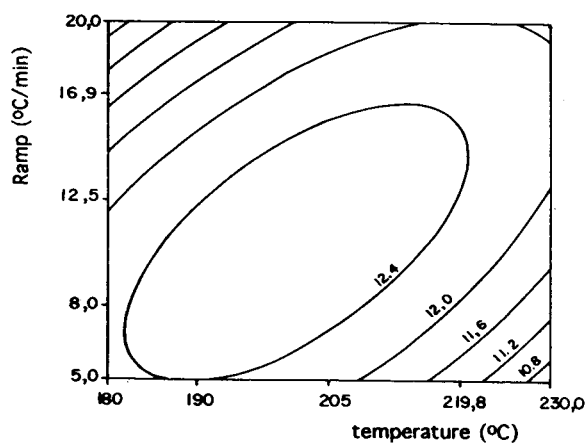


Fig. 2. Isoresponse ( $CRF = 10.8, 11.2, 11.6, 12.0, 12.4$ ) contour plot obtained from Eq. 2 at a constant time hold (time hold 2) of 6 mins. See text for more details.

The optimum conditions selected were an increase from 150°C (1-min hold) at 30°C/min to 215°C (6-min hold) and then at 15°C min to 260°C.

### 3.2. GC analysis

The optimum temperature programme resulted in the retention behaviour shown in Table

Table 2

Retention times ( $t_R$ ) and relative standard deviations (R.S.D.s) of retention times and average recoveries and R.S.D.s for test compounds in green pepper samples using GC-ECD.

| No. | Compound                  | $t_R$ (min) | R.S.D. (%) | Average recovery (%) | R.S.D. (%) |
|-----|---------------------------|-------------|------------|----------------------|------------|
| 1   | Lindane ( $\gamma$ -HCH)  | 6.351       | 0.57       | 97                   | 4.9        |
| 2   | Chlorothalonil            | 6.823       | 0.62       | 95                   | 9.5        |
| 3   | Vinclozolin               | 7.996       | 0.61       | 100                  | 4.4        |
| 4   | Dichlofuanid              | 9.242       | 0.62       | 105                  | 3.5        |
| 5   | Captan                    | 11.233      | 0.49       | 51                   | 20.4       |
| 6   | Folpet                    | 11.564      | 0.41       | 106                  | 16.0       |
| 7   | Procimidone               | 11.841      | 0.39       | 100                  | 12.5       |
| 8   | $\alpha$ -Endosulfan      | 12.748      | 0.31       | 92                   | 5.2        |
| 9   | $\beta$ -Endosulfan       | 13.845      | 0.23       | 89                   | 6.3        |
| 10  | Endosulfan sulphate       | 14.695      | 0.25       | 79                   | 10.6       |
| 11  | Dicofol                   | 10.015      | 0.61       | 73                   | 15.8       |
| 12  | Tetradifon                | 16.823      | 0.31       | 105                  | 14.5       |
| 13  | Cypermethrin <sup>a</sup> | 22.099      | 0.33       | 98                   | 16.2       |

Fortification level 0.20–0.30 mg/kg ( $n = 10$ ). Chromatographic conditions and sample preparation are described in text.

<sup>a</sup> Only the first peak is considered.

2. An example of a gas chromatogram of the mixture of OCs and pyrethroid compounds is shown in Fig. 3. Two problems were noticed: (i) a minor degradation of captan and folpet confirmed by GC-MS (see below); these degradation products of captan and folpet appeared at 7.7 min, which is a common problem in the GC determination of these phthalimide pesticides, which are prone to adsorption and degradation in the column [13,14]; (ii) the overlapping of the four N° 13) cypermethrin isomers (*cis*-A, *trans*-C, *cis* B and *trans* D) (peaks 13) typical in the determination of this pyrethroid [31,32]. Therefore, the determination of this pesticide was carried out as the sum of the four peaks. The total run time is 23 min plus an extra 5 min for equilibration at the initial temperature conditions. Hence the analysis of 51 samples within 24 h is feasible.

The linear dynamic range of the detector response was checked for all the target compounds in the working standard solution and appeared to be from 0.05 to 5 ng, except for captan, folpet and procymidone (0.2–5 ng), absolute injected amount and the correlation coefficients were higher than 0.999 in all instances except for captan (0.991) and folpet

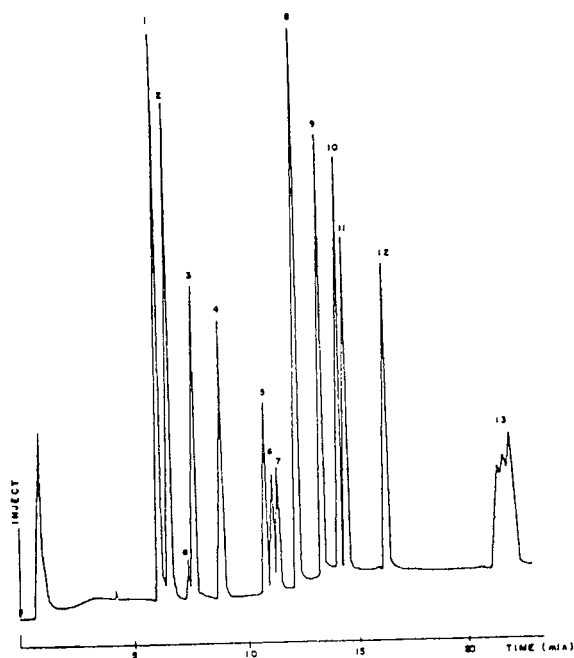


Fig. 3. GC-ECD of the pesticide mixture containing 1.0–1.5 mg/l (injection volume 1  $\mu$ l). Numbers above the peaks correspond to compounds numbers in Table 1.

(0.989), probably owing to the decomposition processes mentioned above. This is also the practical working range. These results were calculated using peak-height measurements, except for cypermethrin (peak-area measurements). Detection limits based on a signal-to-noise ratio

of 3 are on average 10 pg, except for captan, folpet and procymidone (40 pg), absolute injected amount, equivalent to 0.002 and 0.008 mg/kg, respectively.

### 3.3. GC-MS confirmation

Solutions containing all the target compounds were analysed by GC-MS in the EI mode with a scan range from  $m/z$  30 to 600 under full-scan conditions. The main fragments obtained and their relative abundances are shown in Table 3. These data are in good agreement with the different diagnostic ions reported for these organochlorine and pyrethroid pesticides [20–26].

In order to detect the possible decomposition processes than can occur in the GC analysis, a solution containing 50 mg/l of captan and folpet was analysed separately under identical conditions but varying the injector temperature (150, 200 and 250°C) with intense cleanness of the injector liner. In all instances temperature-dependent decomposition products for captan and folpet were detected at 7.7 min (Fig. 4). Based on the sensitivity requirements for captan and folpet, the injector temperature selected was 240°C.

The EI mass spectra of captan and folpet degradation products are shown in Fig. 5 as unknowns 1 and 2. The mass spectrum of the unknown 1 contained fragments ions at  $m/z$  79

Table 3  
Main ions and relative abundances in EI mass spectra of the organophosphorus pesticides studied

| No. | Compound             | $M_r$ | Main ions [ $m/z$ (relative abundance, %)]                            |
|-----|----------------------|-------|---|
| 1   | Lindane              | 288   | 77 (25), 111 (66), 147 (29), 183 (100), 219 (66), 254 (19)            |
| 2   | Chlorothalonil       | 264   | 98 (19), 109 (30), 124 (24), 133 (22), 133 (18), 266 (100)            |
| 3   | Vinclozolin          | 285   | 97 (31), 124 (95), 178 (86), 198 (80), 212 (100), 285 (61)            |
| 4   | Dichlofuanid         | 332   | 77 (18), 92 (20), 123 (100), 167 (32), 224 (26)                       |
| 5   | Captan               | 299   | 79 (100), 117 (12), 149 (28), 264 (8)                                 |
| 6   | Folpet               | 295   | 76 (68), 104 (100), 130 (80), 260 (94), 295 (20)                      |
| 7   | Procymidone          | 283   | 67 (53), 96 (100), 186 (8), 255 (9), 283 (19)                         |
| 8   | $\alpha$ -Endosulfan | 404   | 109 (69), 121 (68), 160 (79), 195 (99), 237 (100), 265 (52), 339 (21) |
| 9   | $\beta$ -Endosulfan  | 404   | 109 (32), 120 (50), 160 (91), 195 (100), 237 (96), 267 (47), 339 (30) |
| 10  | Endosulfan sulphate  | 420   | 109 (18), 121 (26), 170 (34), 237 (58), 272 (100), 387 (24)           |
| 11  | Dicofol              | 368   | 75 (41), 111 (42), 139 (100), 250 (16)                                |
| 12  | Tetradifon           | 354   | 75 (78), 111 (100), 159 (89), 229 (43), 356 (32)                      |
| 13  | Cypermethrin         | 415   | 77 (31), 91 (39), 127 (32), 163 (100), 181 (89), 209 (29), 415 (3)    |

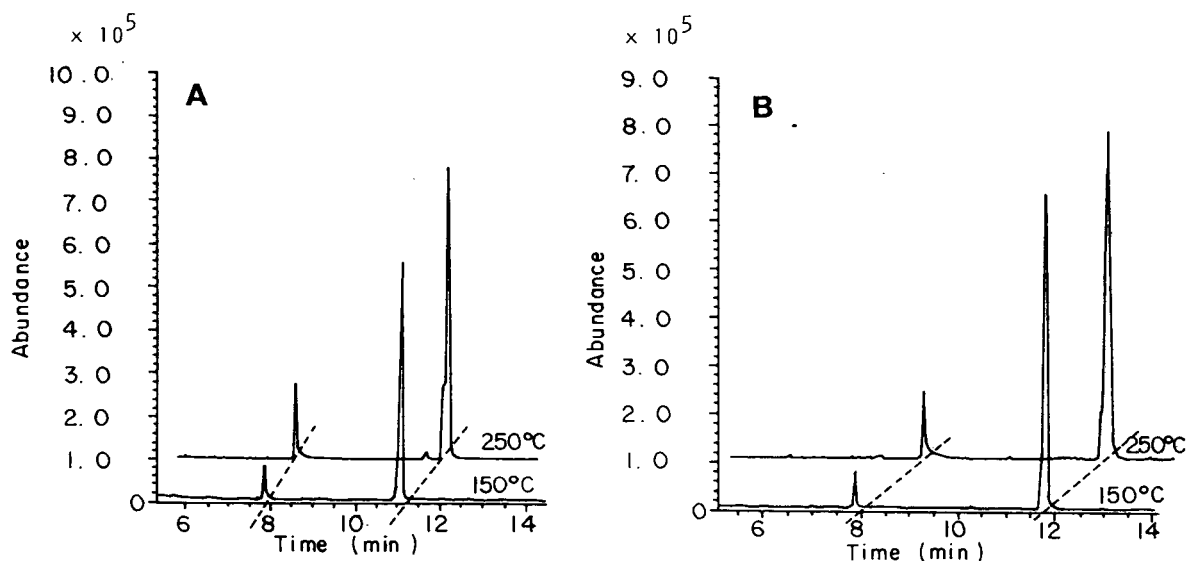


Fig. 4. GC-MS of (A) captan and (B) folpet (50 mg/l) at different injector temperatures: 150°C; 250°C.

(100%),  $m/z$  123 (9%) and  $m/z$  151 (50%), and it can be assigned to the degradation of captan in tetrahydrophthalimide according to the tentative fragmentation pattern indicated in Fig. 5. The mass spectrum of unknown 2 contained fragments ions at  $m/z$  76 (90%),  $m/z$  104 (75%) and  $m/z$  147 (100%) and it can be assigned to the degradation of folpet in phthalimide according to the tentative fragmentation pattern indicated in Fig. 5. Hence we can expect a peak at 7.7 min from co-eluting degradation products of captan and folpet under these chromatographic conditions.

### 3.4. SPE clean-up

Fractions of 2 ml of diethyl ether in light petroleum in different ratios were collected separately in each clean-up experiment and analysed off-line by GC. The elution pattern at different diethyl ether percentages (10, 20 30 and 50%) is presented in Fig. 6.

It is apparent that all the target compounds except captan and folpet elute in the first 2 ml. If complete elution of captan and folpet in the two

first 2 ml is required, the volume fraction of diethyl ether in the eluent has to be increased to 70%. Increasing the volume fraction of the diethyl ether, however, also increases the concentration of interfering compounds in the eluate, thus making the clean-up less effective. The reproducibility of the elution pattern was optimum at a flow-rate of 1–2 ml/min.

It can be seen that the silica column clean-up (Fig. 7) removes the interferents efficiently from the matrix.

### 3.5. Recoveries and repeatability

The retention times and recoveries of the different OCs and pyrethroid compounds were tested by fortifying ten fresh pepper samples, using the procedure described above (Table 2). The repeatability of retention time was satisfactory in all instances. The recoveries of the different OCs and pyrethroids appeared to be in the range 73–106%, except for captan (51%), with a R.S.D.s less than 17% in all the instances except for captan (20.4%), which is acceptable.

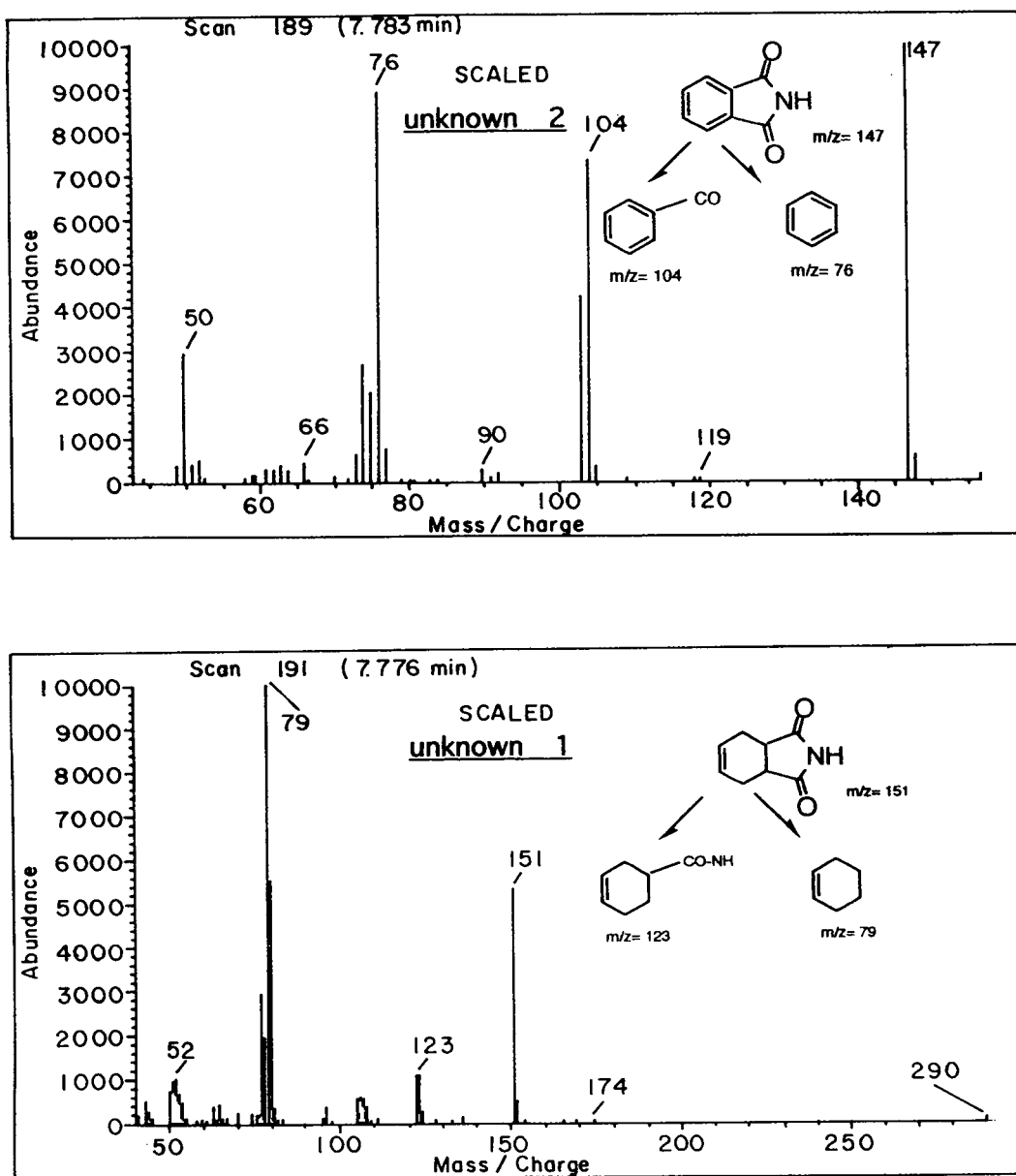


Fig. 5. Mass spectra of captan (unknown 1) and folpet (unknown 2) degradation products.

### 3.6. Method performance with cucumber, beans and melons

The proposed screening method was assessed for the analysis of cucumber, beans and melon,

collected at a greenhouse in Almería (Spain), in order to observe the effect of the matrix on the recoveries, separation and interfering peaks. The homogenized samples were fortified with the thirteen target compounds in the range 0.20–

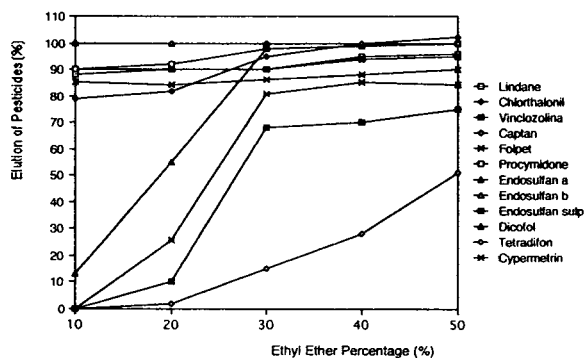


Fig. 6. Elution pattern of target compounds from silica cartridges at different diethyl ether percentages.

0.30 mg/kg. The analyses were carried out in duplicate (in this test, pepper samples were also included). All compounds were identified correctly and the average recoveries were dependent, as expected, on the matrix, but nevertheless were acceptable (Fig. 8). These values are in

the range 87–114% in all instances except for captan, endosulfan sulphate and dicofol (44–80%).

### 3.7. Routine crop analysis

In our laboratory, the proposed GC method for the determination of residues of OCs and pyrethroid pesticides in fruits and vegetables has now been in use interruptedly for 3 years. During this period, the method has evolved from the AOIAC-recommended method to the ultimate SPE clean-up–ethyl acetate method. In this latter form, the method has demonstrated, during more than 1 year of routine application, very high efficiency, sensitivity, selectivity and precision. In Table 4, the residue data for a 1-year period (January 1993–January 1994) are summarized. Positive residues could be detected in nearly 40% of all samples analysed. Endosulfan occurred most frequently and procimidone, vic-

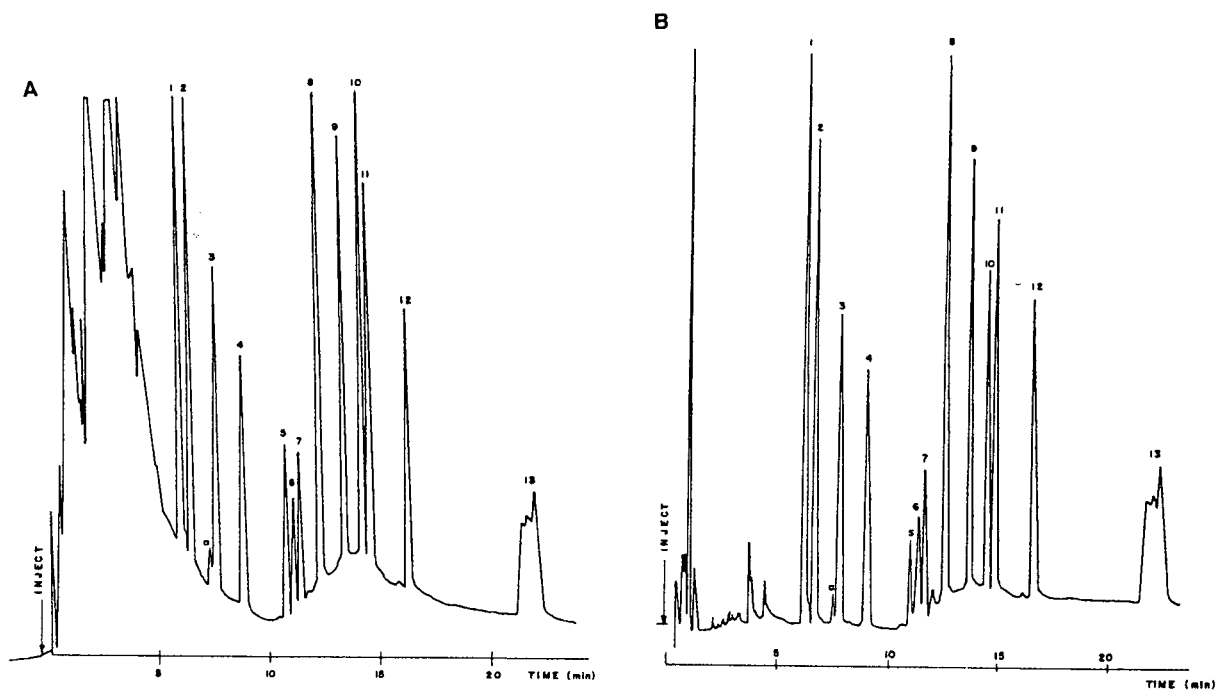


Fig. 7. GC-ECD of fortified green peppers (0.2–0.30 mg/kg) obtained by operating (A) without clean-up and (B) with clean-up using silica cartridges.



Table 4  
Residues of organochlorine and pyrethroid pesticides found in vegetables in 1993–94

| Compound       | Commodity <sup>a</sup> |    |           |   |          |   |            |   |       |   | No. of positive residues |
|----------------|------------------------|----|-----------|---|----------|---|------------|---|-------|---|--------------------------|
|                | Peppers                |    | Cucumbers |   | Tomatoes |   | Egg-Plants |   | Beans |   |                          |
|                | A                      | B  | A         | B | A        | B | A          | B | A     | B |                          |
| Lindane        | 5                      |    |           |   |          |   |            |   |       |   | 5                        |
| Chlorothalonil | 2                      | 2  | 1         | 1 |          |   |            |   |       |   | 3                        |
| Vinclozolin    | 16                     |    |           |   |          |   |            |   |       |   | 16                       |
| Dichlofuanid   | 2                      |    | 1         |   |          |   |            |   |       |   | 3                        |
| Captan         |                        |    |           |   |          |   |            |   |       |   |                          |
| Folpet         |                        |    |           |   |          |   |            |   |       |   |                          |
| Procimidone    | 32                     | 1  | 9         |   | 7        |   | 2          |   | 2     |   | 52                       |
| Endosulfan     | 193                    | 10 | 27        |   | 3        |   |            |   | 4     |   | 227                      |
| Dicofol        |                        |    |           |   |          |   |            |   |       |   |                          |
| Tetradifon     |                        |    |           |   |          |   |            |   |       |   |                          |
| Cypermethrin   | 1                      |    |           |   | 2        | 1 |            |   |       |   | 3                        |
| Total analysed | 546                    |    | 141       |   | 41       |   | 26         |   | 20    |   | 309                      |

<sup>a</sup> (A) Positive residues; (B) exceeding of residue tolerances (Swedish maximum residue limits).

lozolin, lindane, cypermethrin and chlortalonil were detected occasionally. The Swedish maximum residue limits (MRLs) for these compounds were exceeded ca. 2% of the number of all samples analysed or 5% of the number of all samples that were found to contain residues of OCs and pyrethroids.

#### Acknowledgements

This study was supported by FIAPA Project 22/3/93 and CICYT Project ALI 93-0589. The authors are grateful to Dr. J.J. Tabera for his collaboration.

#### References

- [1] Community Directive 93/58 EEC, Off. J. Eur. Commun. L 211/6, European Community, Brussels, 1993.
- [2] R.A. Baumann, G.F. Ernst, J.T.A. Jansen, A. de Kok, P.D.A. Olthof, L.G.M.T. Tuinstra, W. Wervaal, P. Van Zoonen and F. Hernandez Hernandez, *Fresenius' J. Anal. Chem.*, 339 (1991) 357.
- [3] M.V. Russo, G. Goretti and A. Liberti, *Chromatographia*, 35 (1993) 290.
- [4] *Official Methods of Analysis of the Association of Official Analytical Chemists*, AOAC, Arlington, VA, 1984, Sect. 29.
- [5] *J. Assoc. Off. Anal. Chem.*, 68 (1985) 385.
- [6] M.A. Luke, J.E. Froberg, G.M. Doose and T.H. Masumoto, *J. Assoc. Off. Anal. Chem.*, 64 (1981) 1187.
- [7] S.M. Lee, M.L. Paphatakis, H.C. Feng, G.F. Hunter and J.E. Carr, *Fresenius' J. Anal. Chem.*, 339 (1991) 376.
- [8] A. Ambrus, J. Lantos, E. Visi, I. Csatlos and L. Sarvari, *J. Assoc. Off. Anal. Chem.*, 64 (1981) 733.

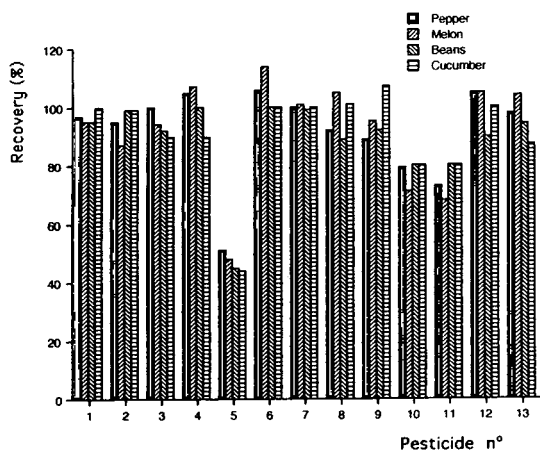


Fig. 8. Average recoveries from duplicate determinations of the target compounds as a function of the matrix. Fortification level, 0.2–0.3 mg/kg.

- [9] H.M. Lott and S.A. Barker, *J. Assoc. Off. Anal. Chem.*, 76 (1993) 67.
- [10] S.T. Hadfield, J.K. Sadler, E. Bolygo and I.R. Hill, *Pestic. Sci.*, 34 (1992) 207.
- [11] P.A. Mills, J.H. Onley and R.A. Gaither, *J. Assoc. Off. Anal. Chem.*, 48 (1983) 186.
- [12] R.R. Watts (Editor), *Manual of Analytical Methods for the Analysis of Pesticides; EPA-600/8-80-038*, Environmental Protection Agency, Environmental Toxicology Division, Health Effects Research Laboratory, Research Triangle Park, NC, 1980.
- [13] D.M. Gilvydis and S.M. Walters, *J. Assoc. Off. Anal. Chem.*, 74 (1991) 830.
- [14] T. Cairns, E.G. Siegmund and G.M. Doose, *Bull. Environ. Contam. Toxicol.*, 30 (1983) 117.
- [15] A. Andersson and B. Ohlin, *Var Föda*, 38 (1986) 79.
- [16] A. Valverde Garcia, E. Gonzalez and A. Agüera, *J. Agric. Food Chem.*, 39 (1991) 2188.
- [17] H. Steinwandter, *Fresenius' J. Anal. Chem.*, 343 (1992) 604.
- [18] A. Andersson and H. Palsheden, *Fresenius' J. Anal. Chem.*, 339 (1991) 365.
- [19] C. Bicchi, A. D'Amato and I. Tonutli, *Chromatographia*, 20 (1985) 219.
- [20] M.V. Russo, G. Goretti and A. Liberti, *Chromatographia*, 35 (1993) 290.
- [21] R.W. Martindale, *Analyst*, 113 (1988) 1229.
- [22] L. Kadenczki, A. Zoltan and I. Gardi, *J. Assoc. Off. Anal. Chem.*, 75 (1992) 53.
- [23] H.J. Scattenberg, III, and J.P. Hsu, *J. Assoc. Off. Anal. Chem.*, 75 (1992) 925.
- [24] D.P. Goodspeed and L.I. Chestnut, *J. Assoc. Off. Anal. Chem.*, 74 (1991) 388.
- [25] S.W. Tillkes, *Fresenius' J. Anal. Chem.*, 322 (1985) 443.
- [26] A. Agüera, M. Contreras and A.R. Fernandez-Alba, *J. Chromatogr. A*, 655 (1993) 293.
- [27] J. Vllen, F.J. Señoraiz, M. Herraiz, G. Reglero and J. Tabera, *J. Chromatogr. Sci.*, 30 (1992) 261.
- [28] P.J. Schoenmakers, *Optimization of Chromatographic Selectivity — A Guide to Method Development.*, Elsevier, Amsterdam, 1986.
- [29] V. Lopez-Avila, J. Bendicto, E. Baldin and W.F. Beckert, *J. High Resolut. Chromatogr.*, 15 (1992) 319.
- [30] G.E.P. Box and J.S. Hunter, *Ann. Math. Stat.*, 28 (1957) 195.
- [31] T.J. Class, *J. High Resolut. Chromatogr.*, 14 (1991) 48.
- [32] E. Bolygo and S.T. Hadfield, *J. High Resolut. Chromatogr.*, 13 (1990) 457.

# Determination of nonylphenols as pentafluorobenzyl derivatives by capillary gas chromatography with electron-capture and mass spectrometric detection in environmental matrices

Núria Chalaux, Joseph M. Bayona\*, Joan Albaigés

*Environmental Chemistry Department, CID-CSIC, Jordi Girona 18, E-08034 Barcelona, Spain*

First received 31 May 1994; revised manuscript received 11 August 1994

## Abstract

Procedures for the trace level determination of nonylphenols, the toxic and final refractory metabolites of polyethoxylated nonylphenol, in sewage sludge and river and coastal sediments were developed. Soxhlet extracts of freeze-dried samples are cleaned up through a neutral alumina column, derivatized with pentafluorobenzyl bromide and determined by capillary GC with electron-capture detection and/or electron impact and negative-ion chemical ionization MS. The detection limits achieved by the two capillary GC-MS techniques in the selected-ion monitoring were, respectively, 10 and 2.7 pg (absolute) and 1.4 and 0.3 pg/g (for a 10-g sample).

## 1. Introduction

Nonylphenol polyethoxylates (NPEO,  $n = 1-18$ ) constitute the major class of non-ionic surfactants used in industrial applications (i.e., emulsifiers, detergents, wetting and dispersing agents, radical inhibitors, etc.) and in household products [1,2].

Nonylphenols (NP) are the most toxic and refractory metabolites of NPEO [3,4] and can cause severe hazards to aquatic ecosystems. Their significant hydrophobic character ( $\log K_{ow} \approx 4.2$ ) [5] would implicate adsorption on to water column-suspended particles and sediments.

Extraction procedures for the determination of

NPEO in treatment plant effluents [6–8] and river and enclosed bay sediments [9,10] have been reported. Their occurrence at high concentrations in these environmental matrices allows their determination by LC using fluorescence detection. On the other hand, the detection of NPEO by other more sensitive procedures, such as those involving capillary GC (cGC) with flame ionization detection (FID) or cGC-MS in the electron impact (EI) mode, are only partially successful owing to their lack of selectivity [11]. The use of softer ionization techniques, e.g. cGC-MS in the chemical ionization (CI) mode [12] or with a 20-eV EI energy [13], although allowing the characterization of the NP molecular ions, do not provide sufficient sensitivity for trace level determinations in environmental samples.

\* Corresponding author.

The aim of this work was the development of a selective and sensitive procedure for the determination of the toxic and final refractory metabolites of NPEO, namely NP, in relevant environmental matrices containing low levels of these compounds. The use of NP pentafluorobenzyl derivatives (PFB) was evaluated in order to improve the sensitivity and selectivity in cGC-ECD and cGC-MS. Negative-ion CI (NCI) MS is evaluated for the first time and the results are compared with those obtained by cGC-EI-MS.

## 2. Experimental

### 2.1. Sample origin and handling

Sewage sludges were collected in the effluent of the Barcelona primary treatment plant during 1991–92 and coastal sediments offshore Barcelona, using a box corer, during 1988. Discrete horizons of 2 cm were obtained in situ and frozen at  $-20^{\circ}\text{C}$  in aluminium trays until analysis. River sediments were collected in the Nile estuary using a grab sampler during 1991. A 24-h sample composite was obtained from the Joint Water Pollution Control Plant (JWPCP) at Los Angeles (USA) during 1987.

### 2.2. Reagents and materials

Neutral alumina (70–230 mesh) and pesticide-grade solvents (*n*-hexane, dichloromethane, methanol) were obtained from Merck (Darmstadt, Germany). Analytical-reagent grade sodium sulphate was purchased from Panreac (Barcelona, Spain) and was used after activation at  $120^{\circ}\text{C}$  overnight. Neutral alumina was Soxhlet extracted with dichloromethane–methanol (2:1) for 18 h and then activated at  $120^{\circ}\text{C}$  overnight. 4-Nonylphenol isomeric mixture and *p*-(1,1',3,3'-tetramethylbutyl)phenol were obtained from Fluka (Buchs, Switzerland) and pentafluorobenzyl bromide (PFBBr) from Aldrich (Steinheim, Germany) (caution: PFBBr is a strong lachrymator and should be handled with appropriate precautions).

### 2.3. Analytical procedures

Freeze-dried samples were Soxhlet extracted with dichloromethane–methanol (2:1) for 24 h. *p*-(1,1',3,3'-Tetramethylbutyl)phenol was used as a recovery standard and it was added into the sample prior to the extraction. However, some samples already contained that compound, hence for those particular samples it could not be used as an NP surrogate. Organic extracts were rotary evaporated to low volume, then concentrated under a gentle stream of nitrogen and finally fractionated by open-column chromatography using 8 g of neutral alumina (bottom) and 1.5 g of sodium sulphate (top), as described previously [14]. The NP-containing fraction (IV) was derivatized with PFBBr to yield the pentafluorobenzyl (PFB) derivatives according to previously described procedures [15]. Briefly, 100  $\mu\text{l}$  of an acetone solution of 5% PFBBr reagent, 100  $\mu\text{l}$  of a 10% aqueous potassium carbonate and 1.5 ml of acetone were added to fraction IV and were kept at  $60^{\circ}\text{C}$  for 1 h. Then, the derivatized nonylphenols were recovered with *n*-hexane after removing the excess of derivatization reagent with a gentle stream of nitrogen.

Instrumental analyses were performed with a Model 5890 capillary gas chromatograph equipped with an electron-capture detector and a Model 7673A autosampler (Hewlett-Packard, Palo Alto, CA USA). Helium was used as the carrier gas at 30 cm/s and a 30 m  $\times$  0.25 mm I.D. fused-silica capillary column coated with 0.25  $\mu\text{m}$  of DB-5 (J&W, Folsom, CA, USA) was used. Samples were dissolved in 1 ml of iso-octane and injected at  $270^{\circ}\text{C}$  in the splitless mode using a purge time of 40 s. The detector temperature was held at  $310^{\circ}\text{C}$ . The column temperature was programmed from 70 to  $130^{\circ}\text{C}$  at  $20^{\circ}\text{C}/\text{min}$ , then to  $280^{\circ}\text{C}$  at  $6^{\circ}\text{C}/\text{min}$  and to  $310^{\circ}\text{C}$  at  $15^{\circ}\text{C}/\text{min}$ , holding the final temperature for 10 min.

cGC-MS in the EI mode was performed with a Fisons (Milan, Italy) MD 800 instrument. The ion source and transfer line temperatures were held at 200 and  $300^{\circ}\text{C}$ , respectively. cGC-MS in the NCI mode was performed with a Finnigan (San Jose, CA, USA) XL system using 22.5 bar

of methane in the analyser. The ion source and transfer line temperatures were held at 130 and 300°C, respectively. A 30 m × 0.25 mm I.D. fused-silica capillary column coated with 0.25 μm of DB-5MS (J&W) was used. The oven temperature was programmed from 70 to 130°C at 20°C/min, then to 250°C at 6°C/min and finally to 300°C at 10°C/min. Other chromatographic conditions were similar to those described above. Selected-ion monitoring (SIM) in the EI [ $m/z$  246 (internal standard, I.S.), 301, 302, 315, 316, 329, 330, 343 and 400] and NCI ( $m/z$  205 and 219) acquisition programmes were used with a dwell time of 0.08 and 0.4 s per single ion, respectively. 1-Phenyldodecane was used as the I.S. for quantification by cGC–EI–MS. Blanks for every batch were processed as real samples. The recovery of NP from spiked sediments (ca. 100 ng/g, dry mass) was  $70 \pm 10\%$  ( $n = 4$ ).

### 3. Results and discussion

#### 3.1. cGC–ECD of PFB derivatives

Technical NP constitutes a complex mixture of isomers due to the substitution pattern in the alkyl chain. The complete resolution of all isomers has not yet been achieved, but the use of trimethylsilyl (TMS) derivatives leads to an improvement in their resolution when non-polar stationary phases are used [8,11]. However, the determination of NP as TMS derivatives by cGC–FID is prone to the presence of interferences due to the lack of selectivity in FID.

In order to overcome this problem, the use of PFB derivatives and ECD was evaluated in this study. The cGC–ECD profile of a PFB-derivatized NP standard mixture is shown in Fig. 1A. The isomeric distribution pattern is very similar to that found in the original mixture, showing the quantitative derivatization of all the isomers. Conversely, the NPEO cannot be derivatized owing to the lower activity of the ethoxy group.

Derivatization with PFBBR and cGC–ECD determination have been reported previously for chlorophenolic compounds in water, with a limit

of detection (LOD) of 0.1 ng/l [15,16]. However, this is the first time that the PFB derivatization procedure has been applied to the trace level determination of NP. The absolute LOD of PFB NP derivatives is in the picogram range. However, the limit of quantification (LOQ) is several orders of magnitude higher owing to the presence of many interferences in the cGC–ECD trace (Fig. 1B and Table 1).

#### 3.2. cGC–MS of PFB derivatives

In order to circumvent the interferences in the cGC–ECD trace, cGC–MS in the EI mode was developed. Fig. 2A shows the mass spectra of a selected isomer in the EI mode. The fragmentation pattern shows a base peak at  $m/z$  181, which corresponds to the cleavage of the PFB group, and it is common for all the isomers. Other fragments corresponding to the alkyl chain cleavage are isomer specific because the cleavage occurs in the substitution position (Table 2) [17]. Despite the high abundance of the  $m/z$  181 ion, it is non-specific for NP because is common to all PFB derivatives. Instead, the ions corresponding to the alkyl cleavage were used ( $m/z$  301 +  $n \times 14$ ,  $n = 1-4$ ). The shift of these fragments to higher masses in comparison with underivatized NP ( $m/z$  107 +  $n \times 14$ ,  $n = 1-6$ ) leads to an improved selectivity. The absolute LOD [signal-to-noise ratio (S/N) = 3] of the SIM method in the EI mode for total NP was 1.4 pg.

The NCI mass spectrum shown in Fig. 2B is common to all the isomeric NP. The molecular ion was not detected under the analysis conditions used. Instead, a base peak at  $m/z$  219 was the base peak which corresponds to a dissociative electronic capture fragmentation. It is worth mentioning that the ion at  $m/z$  219 corresponds to the alkylphenolate anion, which is the complementary fragment at  $m/z$  181 found in the EI mode. The NCI mass spectrum of underivatized NP (Fig. 2C) shows a complex fragmentation pattern with the  $[M + 1]$  anion attributable to radical–molecule reactions [18]. Further, the sensitivity was significantly reduced in comparison with the PFB derivatives. Consequently, NP can only be determined by GC–MS

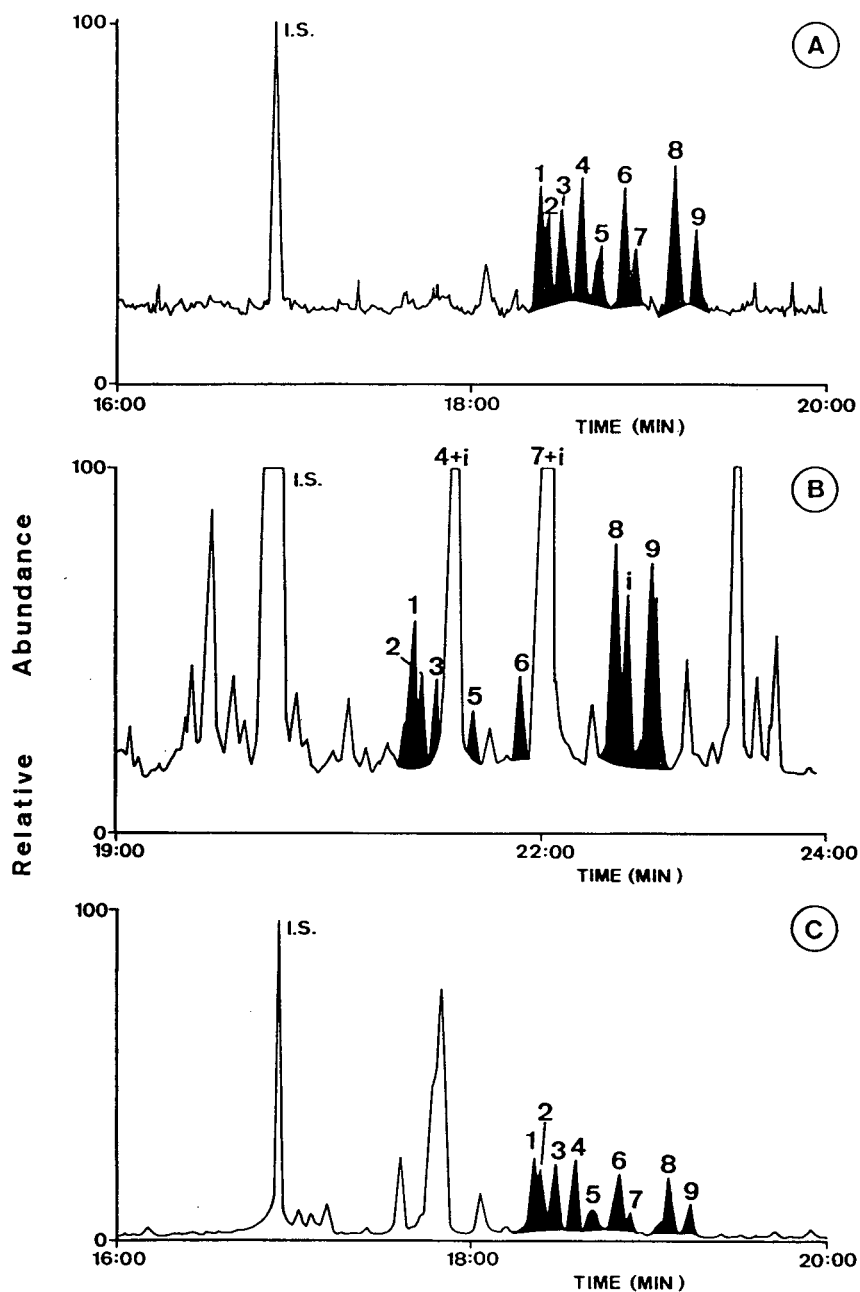


Fig. 1. (A) cGC-ECD of standard mixture of octyl-PFB (I.S., 0.5 ng) and NP-PFB derivatives (2 ng). (B) cGC-ECD of a marine sediment (50 ng/g). (C) cGC-NCI-MS with SIM of NP-PFB from the same sample. NP components are shaded and numbered on the peak apex. Interferences to NP are indicated as i.

Table 1  
Intercomparison between detection systems used for the PFB derivatives of NP with cGC

| Detection        | Linearity       | LOD              |                                 | R.S.D. <sup>b</sup> (%)<br>(n = 3) |
|------------------|-----------------|------------------|---------------------------------|------------------------------------|
|                  |                 | Absolute<br>(pg) | Relative <sup>a</sup><br>(pg/g) |                                    |
| ECD <sup>c</sup> | 10 <sup>3</sup> | 20               | 2.9                             | 2.2                                |
| EI-MS            | 10 <sup>3</sup> | 10               | 1.4                             | 2.1                                |
| NCI-MS           | 10 <sup>2</sup> | 2                | 0.3                             | 2.7                                |

<sup>a</sup> For a 10-g (dry mass) sample.

<sup>b</sup> Relative standard deviation of the determination; the R.S.D. of whole analytical procedure is 10%.

<sup>c</sup> The LOQ is several orders of magnitude higher owing to ECD interferences.

in the NCI mode when the PFB derivatives are prepared.

Accordingly, a SIM acquisition procedure was developed using the diagnostic ions of both octyl- and nonylphenols ( $m/z$  205 and 219). The relative LOD for total NP was in the range 0.3 pg/g ( $S/N=3$ ) and is one order of magnitude lower than in the SIM method in the EI mode. The higher sensitivity can be accounted for by the absence of fragmentation found under the NCI conditions, allowing the use of a smaller number of ions for the NP determination. Further, the precision of the cGC–NCI-MS profiles with SIM (R.S.D. = 2.7%,  $n=3$ ) compares favourably with those of other cGC–MS methods (Table 1). Fig. 1C illustrates the application of this procedure to the trace level determination of NP in marine sediments free of interferences, in clear contrast with the ECD trace obtained from the same sample.

### 3.3. Application to environmental samples

In Table 3 are listed the concentration ranges found in potential sources of coastal pollution such as rivers (Nile) and sewage effluents (JWPCP and Barcelona) and sediment samples collected offshore Barcelona. It is remarkable that the same procedure permits the determination of NP in a variety of environmental samples at different levels and the estimated relative LODs (for a 10-g sample they are 0.3 and 1.4 pg/g for the NCI and EI modes, respectively) are below the environmental levels found

in coastal sediments (Table 3), which could allow their determination at remote sites.

The occurrence of NP in coastal sediments is reported here for the first time. Although their concentration in this particular matrix is at the low ng/g level, their high toxicity [19] makes their determination necessary for a better assessment of their fate in the marine environment and the possible effects on ecosystems.

## 4. Conclusions

The intercomparison between different detection systems (ECD, EI-MS and NCI-MS) for the detection of NP in different environmental matrices has shown that the use of PFB derivatives confers sensitivity and selectivity for the trace level determination of these compounds in a variety of environmental samples.

The main limitation of the procedure concerns the restricted applicability of the derivatization reaction to non-ethoxylated compounds. Further, the use of aqueous bases as catalysts in the derivatization reaction makes the solvent evaporation step time consuming, which can lead to some losses by volatilization. In this respect, volatile organic bases could be more suitable for the PFB derivatization reaction.

Finally, the use of cGC–NCI-MS for the determination of PFB derivatives of NP enhances the sensitivity of the cGC–ECD and cGC–EI-MS determination procedures. The highest selectivity of NCI yielded the lowest

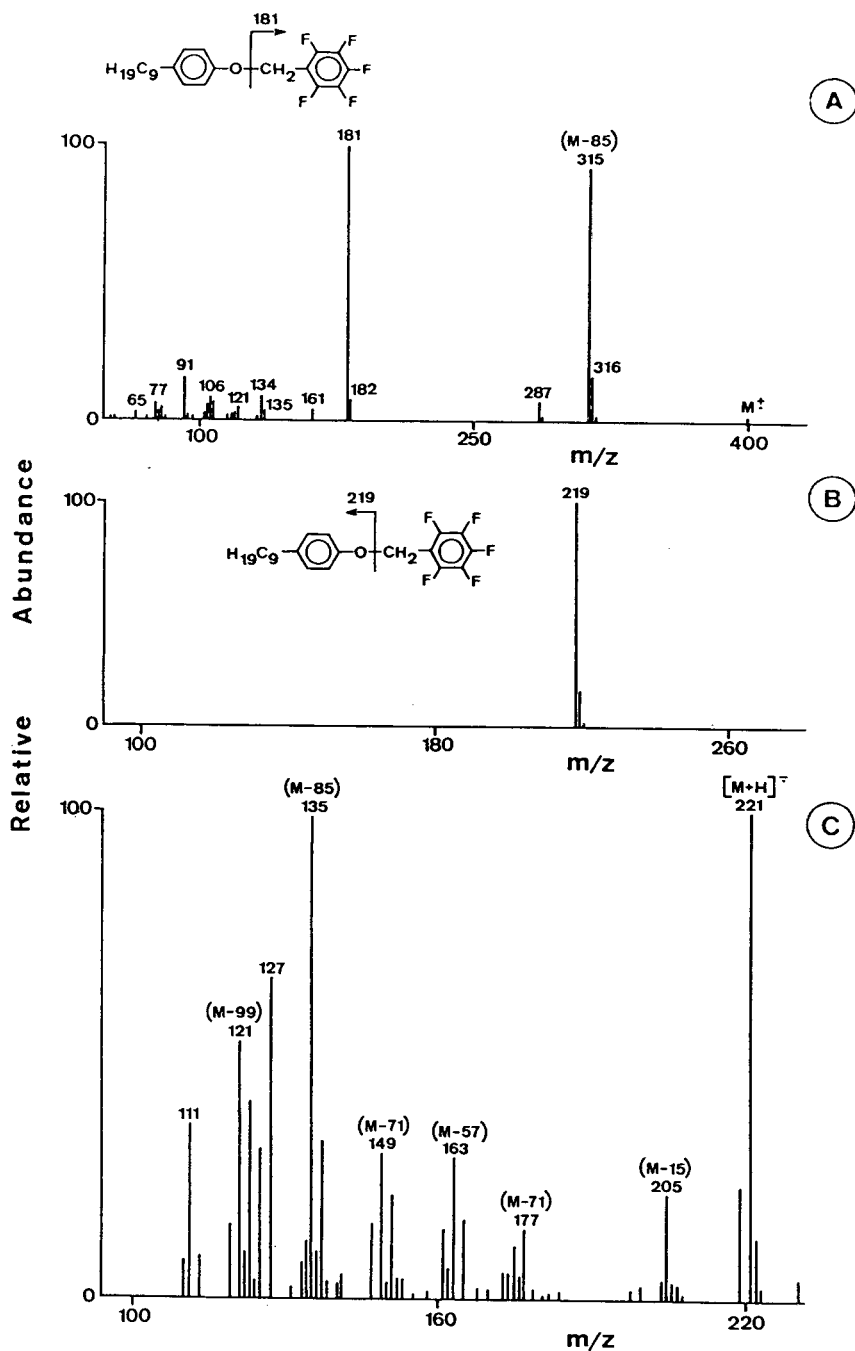


Fig. 2. Mass spectra of isomeric NP obtained: (A) cGC-EI-MS and, (B) cGC-NCI-MS of PFB derivatives and (C) cGC-NCI-MS of underivatized NP.



Table 2  
Assignment of some of the diagnostic ions ( $m/z$ ) of the PFB derivatives of NP used in the cGC–MS SIM acquisition programmes

| Mode | $M^{+}$ | $M - C_7H_2F_5$ | $M - C_4H_9$ | $M - C_5H_{11}$ | $M - C_6H_{13}$ | $M - C_7H_{15}$ |
|------|---------|-----------------|--------------|-----------------|-----------------|-----------------|
| EI   | 400     | – <sup>a</sup>  | 343          | 329             | 315             | 301             |
| NCI  | –       | 219             | –            | –               | –               | –               |

<sup>a</sup> Not detected.

Table 3  
Concentrations of NP in selected environmental matrices

| Matrix                     | Sampling site              | No. of samples | Concentration range    |
|----------------------------|----------------------------|----------------|------------------------|
| Sewage sludge <sup>a</sup> | Barcelona (Spain)          | 4              | 20–350 $\mu\text{g/g}$ |
| Sewage sludge <sup>b</sup> | Los Angeles (USA)          | 1              | 370 $\mu\text{g/g}$    |
| River sediment             | Nile estuary (Egypt)       | 2              | 19–44 ng/g             |
| Coastal sediment           | Offshore Barcelona (Spain) | 4              | 6–69 ng/g              |

<sup>a</sup> Primary treatment plant effluent.

<sup>b</sup> Primary–partially secondary effluent.

LOQ, exhibiting a similar precision between the detection systems evaluated.

### Acknowledgements

Financial assistance was provided by the Spanish Plan for Research (Grant NAT 93-0693) and NATO (CRG 920437). One of us (N.C.) acknowledges a PhD fellowship from the Education Department of the Catalan Government (Generalitat de Catalunya). Technical assistance in the MS research facilities was kindly provided by Mrs. Roser Chaler. The authors are indebted to Indira Venkatesan and Dr. Damià Barceló for making available the samples from Los Angeles and the River Nile.

### References

- [1] S.J. Ainsworth, *Chem. Eng. News*, January (1994) 34–59.
- [2] W.V. Titow (Editor), *PVC Technology*, Elsevier Applied Science, London, 4th ed., 1984.
- [3] D.W. McLeese, V. Zitko, D.B. Sergeant, L. Burrige and C.D. Metcalfe, *Chemosphere*, 10 (1981) 723–730.
- [4] M. Ahel, T. Conrad and W. Giger, *Environ. Sci. Technol.*, 21 (1987) 697–703.
- [5] M. Ahel and W. Giger, *Chemosphere*, 26 (1993) 1471–1478.
- [6] M. Ahel and W. Giger, *Anal. Chem.*, 57 (1985) 1577–1583.
- [7] P.H. Brunner, S. Capri, A. Marcomini and W. Giger, *Water Res.*, 22 (1988) 1465–1472.
- [8] N. Chalaux, J.M. Bayona, M.I. Venkatesan and J. Albaigés, *Mar. Pollut. Bull.*, 24 (1992) 403–407.
- [9] M. Ahel, W. Giger and Ch. Schaffner, *Wat. Res.*, 28 (1994) 1143–1152.
- [10] A. Marcomini, B. Pavoni, A. Sfriso and A.A. Orio, *Mar. Chem.*, 29 (1990) 307–323.
- [11] M. Valls, J.M. Bayona and J. Albaigés, *Int. J. Environ. Anal. Chem.*, 39 (1990) 329–348.
- [12] E. Stephanou, *Chemosphere*, 13 (1984) 43–51.
- [13] N. Chalaux, unpublished results.
- [14] N. Chalaux, H. Takada and J.M. Bayona, *Mar. Environ. Res.*, in press.
- [15] H.B. Lee, L.D. Weng and A.S.Y. Chau, *J. Assoc. Off. Anal. Chem.*, 67 (1984) 1086–1091.
- [16] J. Albaigés, F. Cassadó and F. Ventura, *Water Res.*, 20 (1986) 1153–1159.
- [17] B.D. Bhatt, J.V. Prasad, G. Kalpana and S. Ali, *J. Chromatogr. Sci.*, 30 (1992) 203–210.
- [18] E.A. Stemmler and R.A. Hites, *Biomed. Environ. Mass Spectrom.*, 17 (1988) 311–328.
- [19] E. Stephanou and W. Giger, *Environ. Sci. Technol.*, 16 (1982) 800–805.



# Zone sharpening of neutral solutes in micellar electrokinetic chromatography with electrokinetic injection<sup>☆</sup>

Kurt R. Nielsen, Joe P. Foley\*

Department of Chemistry, Villanova University, Villanova, PA 19085, USA

First received 2 February 1994; revised manuscript received 6 August 1994

## Abstract

Zone sharpening has been used extensively to enhance both efficiency and detectability of *charged* solutes with either electrokinetic or hydrodynamic injection. In the present study, we report the zone sharpening of *neutral* solutes by sharpening the zones of charged micelles which serve as carriers for neutral (and charged) molecules. Zone sharpening with electrokinetic injection can be accomplished only when the effective electrophoretic velocity,  $v_{\text{eff}}$ , of the solute and the electroosmotic velocity are in the same direction *during the injection process*. In order to maximize the amount of solute loaded into the capillary under zone sharpening conditions, it was necessary to use a cationic mixed micelle in the *sample buffer*. The zone sharpening of a homologous series of alkylphenones was accomplished using electrokinetic injection with cationic mixed micelles of cetyltrimethylammonium bromide and dodecyl dimethyl-(3-sulfopropyl)ammonium hydroxide inner salt. The *running buffer* contained *only* sodium dodecyl sulfate and phosphate buffer. As a result of the increased amount of solute loaded into the capillary without significant loss in efficiency, the limits of detection (LOD's) for the solutes studied were in some cases lowered by a factor of ten using zone sharpening. Efficiencies for heptanophenone exceeding 1 000 000 theoretical plates were generated in under 10 min on a 50-cm capillary. Such high efficiencies can be predicted from band broadening models developed for micellar electrokinetic chromatography (MEKC). If properly utilized, zone sharpening can eliminate most if not all of the band broadening associated with sample introduction, and can thus be an important tool in the fundamental study of band broadening in MEKC.

## 1. Introduction

The popularity of capillary electrophoresis (CE) has increased dramatically over the past 15 years. The successful application of CE, in many cases, is a result of the tremendous resolving power. The number of theoretical plates gener-

ated in a CE separation is routinely in excess of 100 000, much larger than the number of theoretical plates generated in a typical reversed-phase HPLC separation. Based on the assumption that the number of theoretical plates in CE is diffusion limited, the number of theoretical plates predicted for solutes with small diffusion coefficients (i.e., proteins) can be  $> 10^6$ . Unfortunately, there are a number of other intracolumn and extracolumn sources of band broadening that limit the maximum attainable efficiency in CE. Intracolumn sources of band

\* Corresponding author.

☆ Presented at the 6th International Symposium on High Performance Capillary Electrophoresis, San Diego, CA, 31 January–3 February 1994.

broadening that have been identified thus far are longitudinal diffusion [1,2], wall effects [3], hydrostatic flow [4], deviations from “plug flow” [5,6], Joule heating [7–10], and conductivity differences between the solute ions and the buffer ions [11,12]. Extracolumn sources arise from the injection and detection of the solute(s), and several authors have discussed the contribution(s) of these processes to the total plate height [4,13–15]. In particular, Delinger and Davis [16] discussed in significant detail how the length of the injection plug affects efficiency in CE. The authors concluded that in many cases poor injection procedures (i.e., injection plugs that were too long) were the main source of low values for efficiency. The authors recommended using zone sharpening [17] to reduce the effective injection plug length and hence increase efficiency.

Zone sharpening is not a new concept in electrophoresis [18–20], but it has experienced a rebirth in the past few years in CE [21–24]. A requirement of all the experimental approaches for zone sharpening is that the solute have a non-zero mobility. In addition to increasing efficiency, zone sharpening can also be used to reduce the limit of detection (LOD) for a solute [24,25]. The short optical path length of most CE instruments results in LOD's that are typically 1 to 2 orders of magnitude lower than for comparable detectors in HPLC [26]. Therefore, any method that will lower detection limits is a valuable tool to improve overall performance of CE. Zone sharpening is, in most cases, inexpensive and relatively simple to use with commercial instrumentation and, for these reasons, its use in CE is increasing.

Neutral solutes can be separated in a CE format using micellar electrokinetic chromatography (MEKC) [27,28]. The charged micelles provide a pseudostationary phase with which neutral molecules can interact in order to achieve a separation. The band broadening mechanisms resulting from the use of micelles in the running buffer have been the subject of a limited number of studies [29,30] and currently is a subject of considerable debate. However, the sources of extracolumn variance in MEKC are very similar to those for CE [31,32].

Zone sharpening for charged solutes in MEKC has been reported [33] but it has also been implied that zone sharpening is not practical for neutral solutes [32,33]. This is based on the premise, that because the solutes are neutral, they possess no inherent mobility and are unaffected by typical zone sharpening conditions. We have demonstrated in a previous study [34], that although neutral solutes have no inherent mobility, in MEKC their interactions with charged micelles impart them with an effective mobility and are consequently sensitive to zone sharpening conditions with *hydrodynamic injection*. In the present study, we will show that zone sharpening for neutral solutes can be accomplished with *electrokinetic injection* in order to improve efficiency and reduce LOD's. In addition, we will discuss how zone sharpening can be used to eliminate extracolumn band broadening due to sample introduction in order to more effectively study theoretical models of intracolumn band broadening.

## 2. Theory

A detailed theoretical discussion of zone sharpening of neutral solutes in MEKC has been presented previously [34] and only the essential highlights will be presented here.

If the solutes are injected into a portion of the capillary in a buffer that has a lower conductivity than the buffer in the remainder of the capillary, the electric field will be larger in the buffer region of lower conductivity. As a result of the amplified electric field the solutes will migrate rapidly toward the interface between the buffer regions. Once the solutes cross the interface, the electric field is no longer amplified and the solute velocity decreases dramatically. The change in solute velocity between the two buffer regions results in the solute zone occupying a much smaller volume after crossing the interface. The conductivity difference between the two buffer regions is most easily achieved by dissolving the sample in water or very dilute running buffer.

In MEKC, solutes can interact with a charged micelle and, consequently, will have a net velocity,  $v_{sol}$ , as described below:

$$v_{\text{sol}} = v_{\text{eff}} + v_{\text{eo}} = E\mu_{\text{eff}} + E\mu_{\text{eo}} \quad (1)$$

where  $v_{\text{eff}}$  is the effective electrophoretic velocity,  $v_{\text{eo}}$  is the electroosmotic velocity,  $E$  is the electric field strength,  $\mu_{\text{eff}}$  is the effective electrophoretic mobility and  $\mu_{\text{eo}}$  is the electroosmotic mobility. The effective electrophoretic mobility is given by:

$$\mu_{\text{eff}} = \frac{1}{1+k} \cdot \mu_{\text{ep}} + \frac{k}{1+k} \cdot \mu_{\text{mc}} \quad (2)$$

where  $\mu_{\text{ep}}$  is the absolute electrophoretic mobility of the solute,  $\mu_{\text{mc}}$  is the absolute electrophoretic mobility of the micelle and  $k$  is the retention factor. If we then substitute Eq. 2 into Eq. 1 we get the following expression for the solute velocity as a function of mobility and field strength:

$$v_{\text{sol}} = E \cdot \left( \frac{1}{1+k} \cdot \mu_{\text{ep}} + \frac{k}{1+k} \cdot \mu_{\text{mc}} \right) + E\mu_{\text{eo}} \quad (3)$$

According to Eq. 3, if the electric field strength in the sample buffer region is higher than in the running buffer region, the solute velocity will be greater in the sample buffer than in the running buffer. Consequently, as the solute crosses the interface between the two buffer regions, zone sharpening will occur. It is important to note that the electroosmotic velocity is not affected in the same way as the effective electrophoretic velocity of the solute in an amplified electric field. The electroosmotic velocity is a bulk property and consequently, is the weighted average of the electroosmotic velocities in the two buffer regions [25].

Another consideration when performing zone sharpening with electrokinetic injection is the direction (i.e., sign) of the effective electrophoretic velocity. The effective electrophoretic velocity must be in the same direction (i.e., same sign) as the electroosmotic velocity during the injection process for zone sharpening to occur. If the effective electrophoretic velocity is in the opposite direction (i.e., opposite sign) as the electroosmotic velocity during the injection process, then the solutes will not cross the concentration boundary, hence zone sharpening will not occur. This is discussed in more detail at the

end of this section and in the Results and discussion section.

For neutral solutes  $\mu_{\text{ep}}$  is zero by definition; thus Eq. 3 reduces to the following:

$$v_{\text{sol}} = E \cdot \frac{k}{1+k} \cdot \mu_{\text{mc}} + E\mu_{\text{eo}} \quad (4)$$

The larger the retention term in Eq. 4,  $k/(1+k)$ , the greater the effective electrophoretic mobility of a neutral solute. And the larger the effective mobility *in the sample plug*, the more effective the zone sharpening will generally be. Given these relationships, and the fact that  $k$  is the product of the phase ratio ( $\beta$ ) and the solute micelle water partition coefficient ( $P_{\text{wm}}$ ), it is important to consider each of the latter ( $P_{\text{wm}}$ ,  $\beta$ ) when optimizing the zone sharpening effect.

Although the  $P_{\text{wm}}$  values of different solutes in a given sample may vary by as much as three orders of magnitude, for nearly all surfactant–buffer systems they will generally be the largest when no organic modifiers are present. Thus, except when an organic solvent is necessary to solubilize the analyte(s) within a sample, no organic solvents should be used in the sample buffer. And since it is generally better to keep the composition of injection and running buffers as similar as possible (while maintaining zone sharpening conditions), it would thus appear to be desirable to omit organic solvent from the running buffer as well.

The other way to maximize the effective electrophoretic mobility of a neutral solute in the sample buffer is to maximize  $k$  via  $\beta$  *in the sample buffer*. The phase ratio,  $\beta$ , in MEKC can be calculated by :

$$\beta = \frac{\bar{V}([\text{SURF}] - \text{CMC})}{1 - \bar{V}([\text{SURF}] - \text{CMC})} \quad (5)$$

where  $[\text{SURF}]$  is the concentration of the surfactant, CMC is the critical micelle concentration and  $\bar{V}$  is the partial molar volume of the surfactant. As can be seen in Eq. 5,  $\beta$  can be increased by increasing the surfactant concentration or increasing  $\bar{V}$ . Since  $\bar{V}$  is a constant for a given set of conditions, we can only increase  $\beta$  by increasing the surfactant concentration. If the surfactant concentration is increased with an

ionic surfactant, however, the phase ratio will increase but so will the conductivity of the buffer, and no (field amplified) zone sharpening will be possible. If the surfactant concentration is increased with a *net zero charge* (non-ionic or zwitterionic) surfactant, it is possible to simultaneously increase the phase ratio of the sample buffer while keeping its conductivity low.

Besides the phase ratio and the conductivity of the sample buffer, one additional parameter to consider is the absolute mobility of the micelle,  $\mu_{mc}$ . In order for the micelle's electrophoretic mobility to be non-zero (a necessary condition for zone sharpening), its net charge must also be non-zero, and this is typically achieved by mixing a charged surfactant with the net zero charge surfactant. The mobility of these mixed micelles will depend on their composition; micelles with a high mole ratio of ionic to net zero charge surfactant will have a larger electrophoretic mobility. Obviously the maximum micelle mobility will be for solutions that contain 100% ionic surfactant and the minimum micelle mobility will be for 100% net zero charge surfactant. Mixed micelles of ionic and net zero charge surfactants will have intermediate values for the micelle mobility but will allow us to fulfill our goals with respect to the phase ratio and buffer conductivity in order to accomplish zone sharpening for neutral solutes [34].

In order to effectively utilize zone sharpening with electrokinetic injection, solutes must have an effective electrophoretic velocity ( $v_{eff} = E\mu_{eff}$ ) in the same direction as electroosmotic flow. This requirement thus precludes the use of micelles of the same charge type in the sample buffer as in the running buffer. *In other words, under typical conditions in MEKC with anionic surfactants in the running buffer [e.g., sodium dodecyl sulfate (SDS)-phosphate, electroosmotic flow from anode to cathode], a cationic mixed micelle must be employed in the sample buffer in order to achieve zone sharpening. Conversely, if a cationic surfactant is employed in the running buffer [e.g., cetyltrimethylammonium bromide (CTAB)-phosphate, electroosmotic flow from cathode to anode], an anionic mixed micelle must be employed in the sample buffer.*

An interesting potential application of zone sharpening in MEKC during electrokinetic injection as described above (with an oppositely charged micellar system in the sample buffer) is the simultaneous zone sharpening of cationic and anionic solutes. Under similar CE conditions, such simultaneous zone sharpening is only possible using polarity switching [35], a feature not universally available on laboratory-made or commercial CE equipment. Under the presently described conditions, ions that would normally oppose electroosmotic flow and migrate away from the sample–running buffer interface (and thus not be zone sharpened) will now, because of strong interactions with oppositely charged micelles, migrate toward the sample–running buffer interface with sufficient velocity to be zone sharpened along with neutral solutes and solutes of opposite charge. Zone sharpening using oppositely charged mixed micelles may thus provide a more broadly applicable solution to the problem of simultaneous zone sharpening of anionic, cationic and neutral molecules, and may also reduce the quantitative biases that are normally observed with electrokinetic injection.

### 3. Experimental

Either of two Quanta 4000 CE systems (Waters Chromatography, Milford, MA, USA) with UV detection at 254 nm (slit dimensions 75  $\mu\text{m} \times 1000 \mu\text{m}$ ) were used throughout the study. The sample was loaded into the capillary by either electrokinetic injection with an applied voltage of 2.5 kV or hydrodynamic injection (siphoning using a height difference between the buffers reservoirs of ca. 9.5 cm) for appropriate lengths of time. Data were collected at a rate of 20 Hz and processed on a Macintosh IICI (Cupertino, CA, USA) computer using a MacLab 4-channel A/D converter with appropriate vendor software (ADInstruments, Milford, MA, USA). The capillary tubing was 50  $\mu\text{m}$  I.D.  $\times$  370  $\mu\text{m}$  O.D., purchased from Polymicro Technologies, (Tucson, AZ, USA) and cut to 50 cm in length (injection to detector). The capillaries were activated [36] and electroosmotic velocities were

measured [37] using previously published methods. Applied voltages and operating currents appear in the text where appropriate. Liquid levels in the buffer reservoirs were kept as even as possible to reduce band broadening due to hydrodynamic flow [4]. The homologous series of alkylphenones was obtained as a kit from Aldrich (Milwaukee, WI, USA). In addition, dodecylmethyl-(3-sulfopropyl)ammonium hydroxide inner salt (SB-12), CTAB, HPLC-grade water and acetonitrile were also obtained from Aldrich. SDS was purchased from Sigma (St. Louis, MO, USA) and used as received. The running buffer was 50 mM SDS and 20 mM phosphate buffer (pH 7.2). The composition of the various sample buffers appears in the text where appropriate. Buffers were prepared by weighing the proper amounts of surfactant and pipetting the proper amount of 100 mM phosphate buffer stock solution. The latter was prepared by dissolving the appropriate amount of  $\text{NaH}_2\text{PO}_4$  in water and adjusting the pH to 7.2 with 1 M NaOH.

### 3.1. Calculations

Variances were calculated by the following:

$$\sigma^2 = \left( \frac{W_{0.10}}{4.2919} \right)^2 \quad (6)$$

where  $W_{0.10}$  is the width (in time units) of the peak at 10% of its height. The number of theoretical plates was calculated using:

$$N = \left( \frac{t_r}{\sigma} \right)^2 \quad (7)$$

where  $t_r$  is the migration time. We did not use the Foley–Dorsey equation [38] in this study because the asymmetry values provided by the commercial software were unreliable; the Gaussian-based equation above (Eq. 6), although less accurate than the Foley–Dorsey equation, is considerably more accurate than all other commonly used Gaussian-based equations (half-height, inflection points, etc.), and is sufficient for our purposes here. The efficiencies reported are those measured directly from the chromatogram. In some cases the relatively large detector

window in our instrument may have significantly biased the observed efficiency. Therefore, the efficiency values were corrected for the band broadening due to the detector [39], in order to give the reader an idea of the magnitude of  $N$  that could be expected with a shorter, more appropriate detector window. Finally, the values used for  $t_{mc}$  (the time required for micelles to migrate from the capillary inlet to the detector) were calculated using the iterative procedure of Bushey and Jorgenson [40].

## 4. Results and discussion

In order to achieve zone sharpening for neutral solutes with electrokinetic injection it was necessary to use mixed cationic micelles of CTAB and SB-12. The SB-12 serves as the net zero charge surfactant used to increase the phase ratio without increasing conductivity and the  $\text{CTA}^+$  surfactant ion is used to impart an overall positive charge to the micelle. Using this approach to zone sharpening, the efficiency ( $N$ ) increased by a factor of between 2 and 5 over controls for solutes with  $k > 30$  and decreased by a factor of 2 for solutes with  $k < 30$ . The increased  $N$  and the increased amount of solute injected into the capillary using this approach, lead to significantly reduced LODs for solutes with  $k > 30$ . We are currently investigating the use of zone sharpening with electrokinetic injection to simultaneously zone sharpen anionic, cationic and neutral solutes.

As in previous studies we wanted to maximize the difference in the conductivity of the sample and running buffer to achieve a large amplification of the electric field. This meant first reducing the concentration of the ionic species in the *sample buffer* by reducing the phosphate buffer to 1 mM, and the CTAB to 15 mM. The phase ratio in the sample buffer was increased by using 75 mM SB-12. Further reductions in the phosphate concentration may result in insufficient buffering capacity; further reductions in the concentration of CTAB will result in mixed micelles with a mobility too small to be useful [34]. The next step was to maximize the conduc-

tivity of the *running buffer* without creating large currents and significant Joule heating effects. The resulting running buffer was 50 mM in SDS and 20 mM in phosphate. For an applied voltage of 25 kV ( $\approx 450$  V/cm), the operating currents were less than 60  $\mu$ A. (Note that the cationic mixed micelle is only in the sample buffer and the running buffer contains only SDS and phosphate buffer.)

Shown in Fig. 1 is a comparison of the separation of alkylphenones (acetophenone through heptanophenone) with “proper” electrokinetic

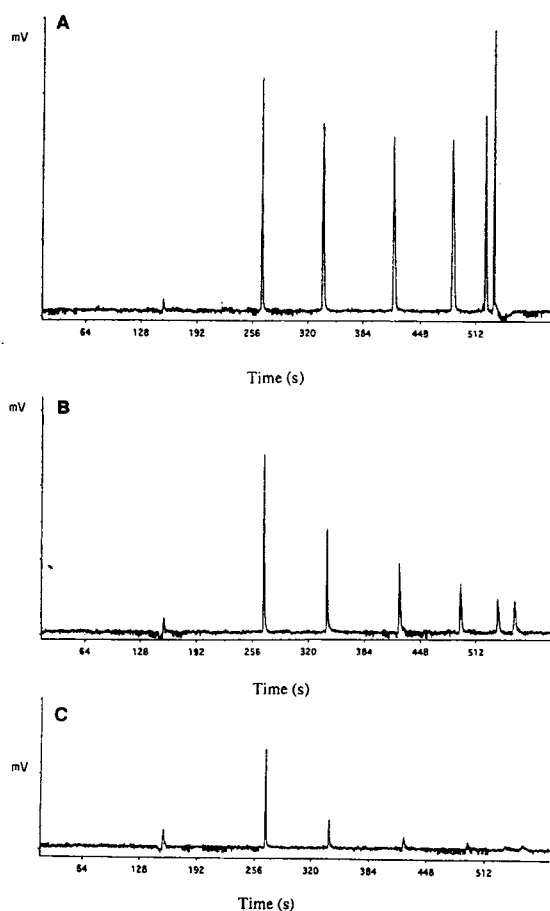


Fig. 1. Comparison of the MEKC separation of alkylphenones (acetophenone through heptanophenone) after a 10-s, 2.5-kV electrokinetic injection with (A) appropriate zone sharpening (CTAB–SB-12 mixed micelles), (B) no zone sharpening (sample buffer = running buffer) and (C) inappropriate zone sharpening (SDS–SB-12 mixed micelles). Other conditions as in the Experimental section.

zone sharpening (Fig. 1A, “appropriate” mixed micelles, i.e., micelles that swim downstream), without electrokinetic zone sharpening (Fig. 1B, control), and with “improper” electrokinetic zone sharpening (Fig. 1C, “inappropriate” mixed micelles, i.e., micelles that try to swim upstream). Peak heights for all the solutes obtained under proper conditions were larger than the corresponding ones obtained with the control or under improper conditions. The largest differences in the peak heights between the zone sharpened chromatogram (Fig. 1A) and control (Fig. 1B) are for the solutes with the largest  $k$ , and consequently the largest effective mobility (Eq. 2). Fig. 1C illustrates why electrokinetic zone sharpening should not be performed with micelles that oppose electroosmotic flow. The direction and magnitude of the solute velocity under these conditions is such that the amount of solute entering the capillary is reduced; not surprisingly this effect is most noticeable for solutes with the largest  $k$ .

As in a previous study it was observed (results not shown) that as the injection time was increased, the apparent  $k$  of the solutes increased. We have attributed this effect to the excess surfactant introduced into the running buffer from the sample buffer. During the zone sharpening process, the CTAB–SB-12 micelles cross the interface between the two buffer regions and the surfactant monomers will then be distributed among the “pure” SDS micelles, thus increasing  $\beta$  and therefore  $k$ . Consequently, this type of surfactant system may not be suitable for thermodynamic studies.

In addition to increasing the amount of solute injected into the capillary under zone sharpening conditions, there were changes in efficiency for the various solutes in compared to controls. Fig. 2 shows the trends in efficiency as a function of retention factor for a 10-s hydrodynamic injection, 10-s electrokinetic injection and 10-s electrokinetic injection with simultaneous zone sharpening. For solutes with  $k > 30$ , the efficiency was increased by factors of 2–5, consistent with the results obtained for zone sharpening after hydrodynamic injection [34]. For solutes with  $k < 30$ , the efficiency with electrokinetic injec-



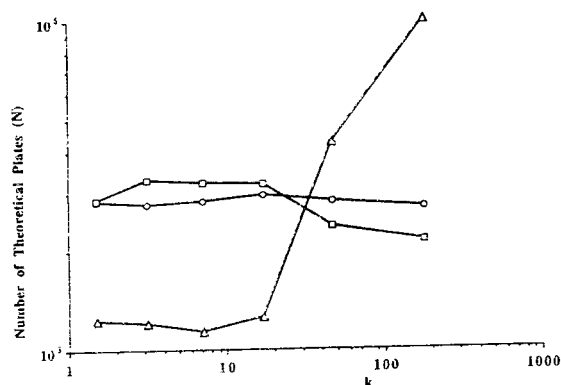


Fig. 2. Experimentally measured dependence of efficiency on retention factor for three different conditions: hydrodynamic injection (○) and electrokinetic injection (□) without zone sharpening; and electrokinetic injection with zone sharpening (Δ). In all cases, the injection time was 10 s. Other conditions as in the Experimental section.

tion zone sharpening was about half that of the controls, in contrast to the slightly higher efficiencies obtained with zone sharpening after hydrodynamic injection [34]. The lower efficiency for solutes with  $k < 30$  will result in approximately a 30% reduction in their resolution, which may be tolerable in cases where improvements in detection limits are needed for high- $k$  solutes. In an attempt to improve the overall enhancement in efficiency, a small water plug was injected into the capillary before the zone sharpening step [23], but this had an insignificant effect for all of the solutes studied. We are currently developing a computer model which may provide some insight as to the mechanism of the reduced efficiency when using zone sharpening with electrokinetic injection for solutes with  $k < 30$ .

For solutes that are effectively zone sharpened, detection limits can significantly reduced by zone sharpening during electrokinetic injection. Fig. 3 shows that for a given concentration of hexanophenone, the detector signal (peak area) obtained with zone sharpening is approximately six times that obtained under non-zone-sharpening conditions. Since the zone sharpening had no effect on the amount of noise, if we approximate the LOD as ca. 3 times  $S/N$ , the

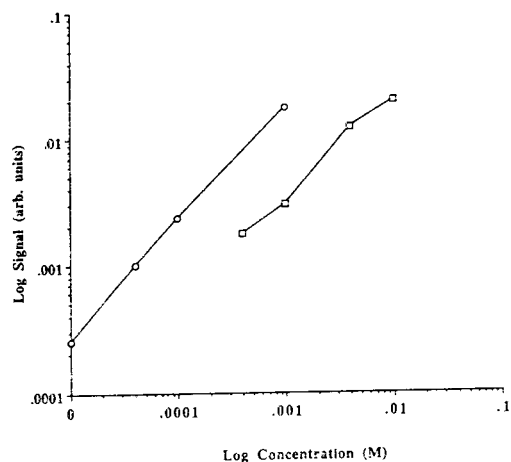


Fig. 3. Comparison of the detectability of hexanophenone with (○) and without (□) zone sharpening. Experimental conditions as in Fig. 1. There were no differences in the amount of noise in chromatograms with and without zone sharpening.

LOD for hexanophenone is  $2 \cdot 10^{-5} M$  and  $1.5 \cdot 10^{-4} M$  with and without zone sharpening, respectively. Since at present the effectiveness of zone sharpening is positively correlated with solute retention factor, reductions in detection limits via zone sharpening conditions will be largest for highly retained solutes ( $k > 30$ ) and smaller for other solutes ( $k < 30$ ).

Another potential application of zone sharpening is the validation of a proper theoretical model for intracolumn band broadening in MEKC. At present there are two band broadening models for neutral solutes in MEKC [29,30], and for  $k > 1$  and a given set of operating conditions, both predict a decrease in variance as  $k$  increases. Shown in Fig. 4 are theoretical curves calculated from each of these models (A and B) and three sets of experimental data obtained in our laboratory (C, D and E) that are representative of band broadening due to injection and/or intracolumn phenomena.

For sample injection (hydrodynamic or electrokinetic) without zone sharpening (Fig. 4, curve C), the variance is relatively constant over a wide range of retention factors. This suggests that the injection variance, the largest source of extracolumn band broadening, is obscuring the

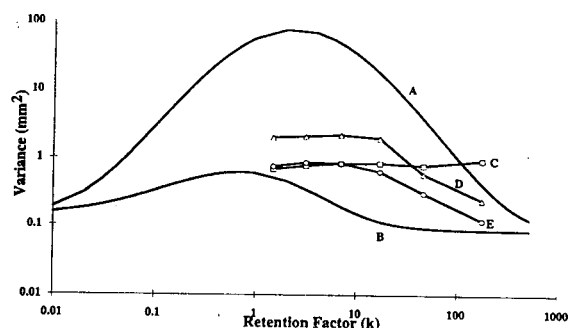


Fig. 4. Comparison of theory and experiment for the dependence of peak variance on the retention factor in MEKC. Theoretical curves were calculated using the band broadening models proposed by Davis [29] (A) and Terabe et al. [30] (B). Parameters used in the calculations:  $D_{\text{aq}} = 8.5 \cdot 10^{-4} \text{ mm}^2/\text{s}$ ,  $D_{\text{mc}} = 5.0 \cdot 10^{-5} \text{ mm}^2/\text{s}$ ,  $t_0/t_{\text{mc}} = 0.25$ , micelle residence time ( $t_{\text{mc}}^*$ ) =  $1 \cdot 10^{-5} \text{ s}$  for  $0 \leq k \leq 10$  and  $1 \cdot 10^{-4} \text{ s}$  for  $k \geq 10$ , and  $v_{\text{eo}} = 3.5 \text{ mm/s}$ . Experimentally measured peak variances are for hydrodynamic injection (SDS micelles) without zone sharpening (C), electrokinetic injection (CTAB–SB-12 micelles) with zone sharpening (D) and hydrodynamic injection (SDS–SB-12 micelles) with zone sharpening (E). Other experimental conditions as in Fig. 1.

trends in intracolumn band broadening that would otherwise be observed. Further evidence of this is provided by curves D and E of Fig. 4, which represent total measured variances after most (if not all) of the electrokinetic or hydrodynamic injection variance, respectively, has been eliminated by zone sharpening. As can be seen, the variances of curves D and E decrease as the retention factor increases, in better agreement with the theoretically predicted trends of curves A and B than the data obtained without zone sharpening (curve C). Zone sharpening may thus be a valuable tool in the development and validation of a comprehensive band broadening model in MEKC for neutral and charged solutes.

### Acknowledgements

The authors wish to thank Waters Chromatography for the Quanta 4000 CE unit employed in this study, the continuing support of Merck Research Laboratories, and the Student Travel Grant Committee of HPCE'94.

### References

- [1] C. Schwer and E. Kenndler, *Chromatographia*, 33 (1992) 331–335.
- [2] E. Kenndler and C. Schwer, *J. Chromatogr.*, 595 (1992) 313–318.
- [3] P.D. Grossman and J.C. Colburn (Editors), *Capillary Electrophoresis: Theory and Practice*, Academic Press, New York, 1992.
- [4] E. Grushka, *J. Chromatogr.*, 559 (1991) 81–93.
- [5] F. Foret, M. Deml and P. Boček, *J. Chromatogr.*, 452 (1988) 601–613.
- [6] H.K. Jones, N.T. Nguyen and R.D. Smith, *J. Chromatogr.*, 504 (1990) 1–19.
- [7] E. Grushka, R.M. McCormick and J.J. Kirkland, *Anal. Chem.*, 61 (1989) 241–246.
- [8] W.A. Gobie and C.F. Ivory, *J. Chromatogr.*, 516 (1990) 191–210.
- [9] J.M. Davis, *J. Chromatogr.*, 517 (1990) 521.
- [10] J.H. Knox and I.H. Grant, *Chromatographia*, 24 (1990) 135.
- [11] S. Hjertén, *Electrophoresis*, 11 (1990) 665–690.
- [12] P.D. Grossman, in P.D. Grossman and J.C. Colburn (Editors), *Capillary Electrophoresis: Theory and Practice*, Academic Press, New York, 1992, pp. 3–43.
- [13] K. Otsuka and S. Terabe, *J. Chromatogr.*, 480 (1989) 91–94.
- [14] X. Huang, W.F. Coleman and R.N. Zare, *J. Chromatogr.*, 480 (1989) 95–110.
- [15] E.V. Dose and G. Guiochon, *Anal. Chem.*, 64 (1992) 123–128.
- [16] S. Delinger and J. Davis, *Anal. Chem.*, 64 (1992) 1749.
- [17] R.L. Chien and D.S. Burgi, *Anal. Chem.*, 64 (1992) 489A–496A.
- [18] S. Hjertén, S. Jerstedt and A. Tiselius, *Anal. Biochem.*, 11 (1965) 219–223.
- [19] H. Haglund and A. Tiselius, *Acta Chem. Scand.*, 4 (1950) 957–962.
- [20] L. Ornstein, *Ann. N.Y. Acad. Sci.*, 121 (1964) 321.
- [21] F.E.P. Mikkers, F.M. Everaerts and T.P.E.M. Verheggen, *J. Chromatogr.*, 169 (1979) 1–10.
- [22] F.M. Everaerts, T.P.E.M. Verheggen and F.E.P. Mikkers, *J. Chromatogr.*, 169 (1979) 11–20.
- [23] R.L. Chien and D.S. Burgi, *J. Chromatogr.*, 559 (1991) 141–152.
- [24] D.S. Burgi and R.L. Chien, *J. Microcol. Sep.*, 3 (1991) 199–202.
- [25] R.L. Chien and D.S. Burgi, *Anal. Chem.*, 64 (1992) 1046–1050.
- [26] M. Albin, P.D. Grossman and S.E. Moring, *Anal. Chem.*, 65 (1993) 489A–496A.
- [27] S. Terabe, K. Otsuka, K. Ichikawa, A. Tsuchiya and T. Ando, *Anal. Chem.*, 56 (1984) 111–113.
- [28] S. Terabe, K. Otsuka and T. Ando, *Anal. Chem.*, 57 (1985) 834–841.
- [29] J.M. Davis, *Anal. Chem.*, 61 (1989) 2455–2461.

- [30] S. Terabe, K. Otsuka and T. Ando, *Anal. Chem.*, 61 (1989) 251–260.
- [31] D.E. Burton, M.J. Sepaniak and M.P. Maskarinec, *Chromatographia*, 21 (1986) 583–586.
- [32] P. Sandra and J. Vindevogel, *Introduction to Micellar Electrokinetic Chromatography*, Hüthig, Heidelberg, 1992.
- [33] R. Szucs, J. Vindevogel, P. Sandra and L.C. Verhagen, *Chromatographia*, 36 (1993) 323–329.
- [34] K.R. Nielsen, E.S. Ahuja and J.P. Foley, *Anal. Chem.*, (1994) in press.
- [35] R.L. Chien and D.S. Burgi, *J. Chromatogr.*, 559 (1991) 153–161.
- [36] E.L. Little and J.P. Foley, *J. Microcol. Sep.*, 4 (1992) 145–154.
- [37] E.S. Ahuja, E.L. Little and J.P. Foley, *J. Liq. Chromatogr.*, 15 (1992) 1099–1113.
- [38] J.P. Foley and J.G. Dorsey, *Anal. Chem.*, 55 (1983) 730–737.
- [39] K.R. Nielsen and J.P. Foley, *Anal. Chem.*, (1994) submitted for publication.
- [40] M.M. Bushey and J.W. Jorgenson, *J. Microcol. Sep.*, 1 (1989) 125–130.





ELSEVIER

Journal of Chromatography A, 686 (1994) 293–307

JOURNAL OF  
CHROMATOGRAPHY A

# Enantiomeric differentiation of a wide range of pharmacologically active substances by capillary electrophoresis using modified $\beta$ -cyclodextrins

Anthony Aumatell<sup>a,\*</sup>, Robert J. Wells<sup>a</sup>, Danny K.Y. Wong<sup>b</sup>

<sup>a</sup>Australian Government Analytical Laboratory, 1 Suakin Street, Pymble, NSW 2073, Australia

<sup>b</sup>School of Chemistry, Macquarie University, Sydney, NSW 2109, Australia

First received 5 May 1994; revised manuscript received 4 July 1994

## Abstract

This paper shows the versatility of modified charged and uncharged  $\beta$ -cyclodextrins (CDs) in the direct chiral resolution of  $\beta$ -agonists,  $\beta$ -antagonists, phenylethyamines and alcohol stimulants, and thalidomide and its metabolites. A total of 42 compounds were optically resolved using hydroxypropyl- $\beta$ -CD and 20 with sodium sulfobutyl ether- $\beta$ -CD. The degree of enantiomeric separation for most substances is dependent on the modified CD concentration. The separation efficiency reaches a maximum at a particular CD concentration. The separation efficiency reaches a maximum at a particular CD concentration, after which further increases in CD concentration causes a progressive decrease in chiral differentiation. Chiral separation of amphetamine enantiomers indicated that a three-point hydrogen bond interaction between the chiral guest molecule and host CD is not necessary for chiral separation under the conditions used.

## 1. Introduction

A large number of pharmaceutical drugs contain one or more chiral atoms and can exist in two or more isomeric forms [1]. In most instances, only one of the isomeric forms is highly active therapeutically [1]. The other form can be either much less active, inactive or sometimes even toxic. An example is the drug (*R,S*)-thalidomide, which was administered during early pregnancy to alleviate symptoms of morning sickness, with its *R*-enantiomer exhibiting

strong activity as a minor tranquillizer, and yet the *S*-enantiomer was found to be toxic [2,3]. More recently, (*R,S*)-thalidomide has also been found to suppress the HIV virus, alleviating the symptoms of mass loss, fever and skin lesions associated with HIV [2,3]. The drug regulatory agencies in many countries have expressed an interest in investigations of the stereoisomeric composition of drugs and their associated therapeutic and toxicological consequences. In general, only the highly active isomers are used in the production of drugs [1,4]. Hence there is a real need to develop rapid and sensitive chiral separation methods required in the investigation of drug enantiomer composition.

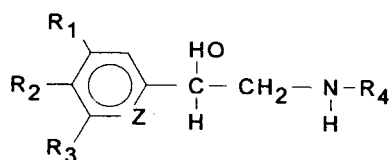
\* Corresponding author. Present address: Beckman Instruments, P.O. Box 218, Gladesville, NSW 2111, Australia.

Two common chiral separation techniques used to resolve optically active drugs are gas chromatography (GC) [5] and high-performance liquid chromatography (HPLC) [6]. In the last decade, capillary electrophoresis (CE) has developed into a powerful technique for the separation of small ions, peptides, carbohydrates, oligonucleotides, pharmaceutical drugs and more recently chiral substances [7]. The separation principle of CE is based on the different electrophoretic mobilities of solutes which, in turn, depend on charge densities [8]. Also, cyclodextrin (CD) inclusion complexes can be used for the optical resolution of stereoisomers by CE based on the difference in electrophoretic mobility of the complexes arising from different inclusion formation constants with the analyte [9].

We are interested in the separation and identification of several phenylamine optical isomers of forensic significance, including amphetamines and ephedrines. Amphetamines are illicit drug substances, while ephedrine enantiomers are widely used in a large number of proprietary cough and decongestant remedies. A variety of amphetamine enantiomers possess different

pharmacological activities [10]. For example, (*S*)-amphetamine gives greater locomotor stimulation [11] and hyperthermic activity [12] than the *R*-enantiomer [11]. Qualitative analysis of these optical isomers will aid in identifying the synthetic route and may provide additional information of the drug seizer origins as reflected by the impurity profile. We are also interested in the separation and identification of some adrenergic  $\beta$ -receptor agonists (abbreviated as  $\beta$ -agonists here) and  $\beta$ -receptor antagonists (abbreviated as  $\beta$ -antagonists), drugs which are structurally similar to phenylethylamines. In general,  $\beta$ -agonists are used for the relief of reversible bronchospasm in humans with obstructive airway diseases such as asthma, bronchitis and emphysema. On the other hand,  $\beta$ -antagonists are adrenergic  $\beta$ -receptor blocking agents used in the treatment of hypertension and angina. The *S*-enantiomers of many  $\beta$ -antagonist drugs have been demonstrated to be more biologically active than the *R*-enantiomers [13,14]. Pharmacokinetic studies have also shown differences in the adsorption, metabolism and elimination kinetics for the enantiomers of  $\beta$ -antagonists [13,14]. All of these drugs are expressively banned by the

Table 1  
Structures of the phenylethyl alcohols studied.



| Compound    | R <sub>1</sub> | R <sub>2</sub>  | R <sub>3</sub>     | R <sub>4</sub>                   | Z  |
|-------------|----------------|-----------------|--------------------|----------------------------------|----|
| Pirbuterol  | H              | HO              | CH <sub>2</sub> OH | C(CH <sub>3</sub> ) <sub>3</sub> | NH |
| Salbutamol  | H              | HO              | CH <sub>2</sub> OH | C(CH <sub>3</sub> ) <sub>3</sub> | C  |
| Cimaterol   | H              | NH <sub>2</sub> | HO                 | C(CH <sub>3</sub> ) <sub>3</sub> | C  |
| Clenbuterol | Cl             | NH <sub>2</sub> | Cl                 | C(CH <sub>3</sub> ) <sub>3</sub> | C  |
| Terbutaline | HO             | H               | HO                 | C(CH <sub>3</sub> ) <sub>3</sub> | C  |
| Labetalol   | H              | HO              | H <sub>2</sub> NCO |                                  | C  |
| Epinephrine | HO             | HO              | H                  | CH <sub>3</sub>                  | C  |

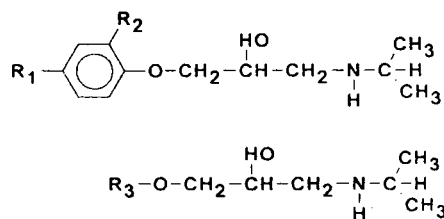
International Olympic Committee [15] because they can be used as doping agents to reduce sympathetic activity in cases when high psychological pressure may impair athletic performance [16].

There have been reports on the use of CDs to separate enantiomers of hydroxyphenylamines [13,14,16–28],  $\beta$ -agonists [27–30] and  $\beta$ -antagonists [20,21,23,29,31–37] by CE. In these chiral CE methods, low-pH buffers with various concentrations of  $\beta$ -CDs (up to 20 mM) [7,13,17,18,20,30], and modified  $\beta$ -CDs (up to 40 mM) [14,16,19,21–23,26–29,31] were used, and dimethyl- $\beta$ -CD has been demonstrated to

resolve optically the largest number of chiral compounds [14,16,19,26,29,31]. However, to date, no direct chromatographic separation method for the simultaneous separation of phenylethylamines and alcohols enantiomers has been reported.

This paper reports a CE separation method using the ether derivatives of  $\beta$ -CD to resolve a wide range of pharmacologically active drugs including  $\beta$ -agonists,  $\beta$ -antagonists (shown in Tables 1 and 2), phenylethylamines and alcohol stimulants (shown in Table 3) and thalidomide and its metabolites (shown in Fig. 1). The development of such a technique will then per-

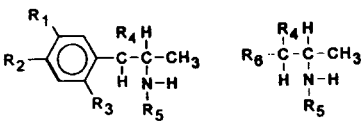
Table 2  
Structures of the modified phenylethyl alcohols studied

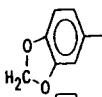
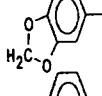
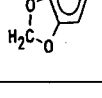


| Compound    | R <sub>1</sub>                                       | R <sub>2</sub>                      | R <sub>3</sub> |
|-------------|--|-------------------------------------|----------------|
| Nadolol     | –  | –                                   |                |
| Oxprenolol  | H  | OCH <sub>2</sub> CH=CH <sub>2</sub> | –              |
| Pindolol    | –  | –                                   |                |
| Atenolol    | H <sub>2</sub> NCOCH <sub>2</sub>                    | H                                   | –              |
| Alprenolol  | H  | CH <sub>2</sub> CH=CH <sub>2</sub>  | –              |
| Propranolol | –  | –                                   |                |
| Metoprolol  | CH <sub>3</sub> OCH <sub>2</sub> CH <sub>2</sub>     | H                                   | –              |
| Acebutolol  | CH <sub>3</sub> (CH <sub>2</sub> ) <sub>2</sub> CONH | COCH <sub>3</sub>                   | –              |
| Timolol     | –  | –                                   |                |

Table 3

Structures of the phenylethylamines studied



| Compound                          | R <sub>1</sub>    | R <sub>2</sub>  | R <sub>3</sub>    | R <sub>4</sub> | R <sub>5</sub>                  | R <sub>6</sub>   |
|-----------------------------------|-------------------|-----------------|-------------------|----------------|---------------------------------|--|
| 2,5-Dimethoxy-4-methylamphetamine | CH <sub>3</sub> O | CH <sub>3</sub> | CH <sub>3</sub> O | H              | H                               | —  |
| Ephedrine                         | H                 | H               | H                 | HO             | CH <sub>3</sub>                 | —  |
| Pseudoephedrine                   | H                 | H               | H                 | HO             | CH <sub>3</sub>                 | —  |
| Norephedrine                      | H                 | H               | H                 | HO             | H                               | —  |
| Amphetamine                       | H                 | H               | H                 | H              | H                               | —  |
| Methylamphetamine                 | H                 | H               | H                 | H              | CH <sub>3</sub>                 | —  |
| 4-Bromo-2,5-dimethoxyamphetamine  | CH <sub>3</sub> O | Br              | CH <sub>3</sub> O | H              | H                               | —  |
| Methyldimethoxyamphetamine        | —                 | —               | —                 | H              | H                               |   |
| Methyldimethoxymethylamphetamine  | —                 | —               | —                 | H              | CH <sub>3</sub>                 |   |
| Methyldimethoxyethylamphetamine   | —                 | —               | —                 | H              | CH <sub>2</sub> CH <sub>3</sub> |  |

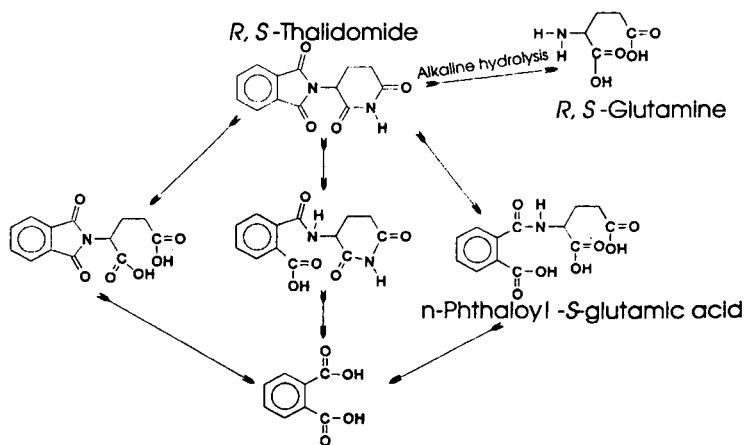


Fig. 1. Major metabolic pathway of thalidomide. Compounds named were resolved in this work.



mit a study of the pharmacokinetic effects of a wide range of optically active drugs directly using a simple chromatographic technique.

## 2. Experimental

### 2.1. Reagents

(*R,S*)-Clenbuterol, (*R,S*)-terbutaline, (*R,S*)-cimaterol, (*R,S*)-salbutamol, (*R,S*)-pirbuterol, (*R,S*)-atenolol, (*R,S*)-nadolol, (*R,S*)-propranolol, (*R,S*)-timolol, (*R,S*)-oxprenolol, (*R,S*)-pindolol, (*R,S*)-alprenolol, (*R,S*)-labetalol, (*R,S*)-acebutolol, (*R,S*)-metoprolol, (*R,S*)-amphetamine, (*R*)-amphetamine, (*S*)-amphetamine, (*R*)-methylamphetamine, (*S*)-methylamphetamine, (*R,S*)-methyldimethoxyamphetamine, (*R,S*)-methyldimethoxymethylamphetamine, (*R,S*)-methyldimethoxymethylamphetamine, (*R,S*)-2,5-dimethoxy-4-methylamphetamine, (*R,S*)-4-bromo-2,5-dimethoxyamphetamine, (*R,S*)-norephedrine, (*S*)-ephedrine, (*R*)-ephedrine, (*S*)-pseudoephedrine, (*R*)-pseudoephedrine, (*R,S*)-thalidomide, (*R*)-thalidomide and (*S*)-thalidomide, were supplied by the Curator of Standards, Australian Government Analytical Laboratories (Pymble, NSW, Australia). Hydroxypropyl- $\beta$ -cyclodextrin (average molar hydroxypropyl group substitution 0.6 and 0.8), (*R*)-propranolol, (*S*)-propranolol, (*R,S*)-epinephrine, (*S*)-epinephrine and (*R,S*)-glutamine were supplied by Sigma (St. Louis, MO, USA). (*R*)-Atenolol, (*S*)-atenolol, (*S*)-alprenolol-(*S*)-tartrate and N-phthaloyl-(*S*)-glutamic acid were supplied by Aldrich. Sodium IV sulfobutyl ether- $\beta$ -cyclodextrin was supplied by Isco (Lincoln, NE, USA). All other chemicals and solvents were of analytical-reagent or HPLC grade and were used as received.

### 2.2. Preparation of buffers

A pH 2.5 stock buffer solution of 232 mM citric acid–44.7 mM disodium hydrogenphosphate was used. The running buffer with 100 mM citric acid–19.27 mM disodium hydrogenphosphate was prepared using the appropriate vol-

ume of stock buffer and mass of modified  $\beta$ -CD. The resulting running buffer was degassed by sonication and filtered through a 0.2- $\mu$ m PTFE filter (Micro Filtration Systems, Dublin, CA, USA) before use.

### 2.3. Apparatus

Qualitative work was performed with fused-silica capillary tubes (Isco) (100 cm  $\times$  50  $\mu$ m I.D.) with an effective length of 50 cm to the detector window. An Isco Model 3140 electropherograph was used for all analyses. The instrument was operated at 30 kV and thermostated at 23°C with the detector placed on the cathode side. The sample solution was loaded into the capillary under vacuum (vacuum level 4.0 kPa/s for Isco 3140 electropherograph). The compounds were detected at 200 nm and 0.01 AUFS. Electropherograms were recorded and processed with the ICE data management and control software supplied with the Model 3140 electropherograph.

### 2.4. Procedure for capillary preparation and handling

Prior to extended use, the capillary was filled with 1 M sodium hydroxide solution and allowed to stand for 1 h. This solution was replaced with 0.1 M sodium hydroxide solution, then the capillary was allowed to stand for a further 1 h and washed with deionized water before filling with the running buffer (between runs the capillary was flushed with 10  $\mu$ l of running buffer). The capillary was used for a maximum of 40 sample injections before rinsing with 1 M sodium hydroxide solution (200  $\mu$ l), deionized water (200  $\mu$ l) and running buffer (200  $\mu$ l); it was then left filled with running buffer ready for sample injection.

The resolution was calculated via the relationship [40]

$$R_s = 2\Delta T / (W_1 + W_2) \quad (1)$$

where  $\Delta T$  is the difference in migration time between enantiomers and  $W_1$  and  $W_2$  are the widths of the peaks at the baseline.

### 3. Results and Discussion

#### 3.1. CE separation with hydroxypropyl- $\beta$ -cyclodextrin (HP- $\beta$ -CD)

The  $\beta$ -CD water solubility and enantioselectivity can be increased by chemically modifying the CD with alkyl substituents [29,38–42] which increase the flexibility of the CD cavity [39,40]. The orientation of bulky and/or charged substituents on the CD cavity can decrease the enantioselectivity by causing steric hindrance and/or columbic repulsion, preventing guest–host inclusion complex formation [39,43]. HP- $\beta$ -CD used in this work is an alkyl-modified  $\beta$ -CD and is generally available in tow grades varying in the molar proportion of hydroxypropyl group substitution on the  $\beta$ -CD (Ave. MS) of 0.6 and 0.8. The physical characteristics of HP- $\beta$ -CD appear to make it an attractive chiral additive in CE in three respects: (1) it exhibits potentially similar steric restrictions to the CD cavity as alkylated- $\beta$ -CDs [39,43], resulting in a similar guest–host complex formation; (2) it is highly water soluble [44], in fact well in excess of the parent  $\beta$ -CD; and (3) each grade is a complex cocktail of related substances varying in both the position and the number of hydroxy propyl groups attached [39,43].

HP- $\beta$ -CD is a complex mixture, where one of these CDs might form guest–host complexes with a certain racemate that approaches the optimum for separation by CE whereas another might be more suitable in the CE separation of another racemate. Further, the high water solubility of the mixed HP- $\beta$ -CDs enables those CD derivatives which give optimum separation of certain racemates to achieve a sufficiently high concentration in solution to effect that separation. This same argument can be applied to dimethyl- $\beta$ -CD, explaining the wider range of structural types optically resolved by CE, when compared with  $\beta$ -CD. We therefore investigated the use of HP- $\beta$ -CD Ave. MS 0.6 and 0.8 in the CE separation of a variety of drug racemates.

The drugs studied here are categorized into three main classes (1)  $\beta$ -agonists, amphetamines, ephedrine; (2)  $\beta$ -antagonists; and (3)

thalidomide and metabolites. The general structures of classes 1 and 2 are shown in Tables 1–3 and class 3 in Fig. 1. Note that all the drugs studied in this work have a common feature of mono- or bicyclic aromatic rings in their structures.

In order to select the CD and concentration that optically resolve the greatest number of enantiomers,  $\beta$ -agonists,  $\beta$ -antagonists, amphetamines and ephedrine were analysed with various amounts of HP- $\beta$ -CD Ave. MS 0.6 and 0.8. HP- $\beta$ -CD Ave. MS 0.6 and 0.8 were added separately to the background electrolyte (100 mM citric acid–19.27 mM Na<sub>2</sub>HPO<sub>4</sub>, pH 2.5), by increasing the amount of the chiral additive. The effect of HP- $\beta$ -CD Ave. MS 0.8 and 0.6 concentration on the migration time of clenbuterol, terbutaline, cimaterol and salbutamol is illustrated in Fig. 2a and b, respectively. An increase in HP- $\beta$ -CD Ave. MS 0.8 and 0.6 concentration increases not only the buffer viscosity but also the solute migration time. This is more evident when HP- $\beta$ -CD Ave. MS 0.8 is used as a chiral additive. The optical isomers of clenbuterol and terbutaline co-elute when HP- $\beta$ -CD Ave. MS 0.6 is used as a chiral additive, but are all well resolved with HP- $\beta$ -CD Ave. MS 0.8. The distribution and size of the substituent are important to the CD complexation, as the most chemically reactive primary hydroxyls (C<sub>6</sub>) are located around the smaller opening of the CD, and the less reactive and optically active secondary hydroxyl (C<sub>2</sub>, C<sub>3</sub>) are located around the larger opening [43], as illustrated in Fig. 3. Optical selectivity can only be promoted by the juxtaposition with the optically active group or through the stereogenic centre (involving the optically active group indirectly) [45]. The CD complex formed was reported to increase monotonically as a function of the CD concentration [46]. Plots of resolution between each pair of optical isomers ( $R_s$ ) as a function of CD concentration are shown for a number of  $\beta$ -agonists,  $\beta$ -antagonists, amphetamines and ephedrine in Fig. 4a,b and c.  $R_s$  for propranolol, labetalol, clenbuterol, terbutaline, salbutamol, alprenolol, pirbuterol, amphetamine, cimaterol, atenolol, oxprenolol, pindolol, epinephrine and methyl-

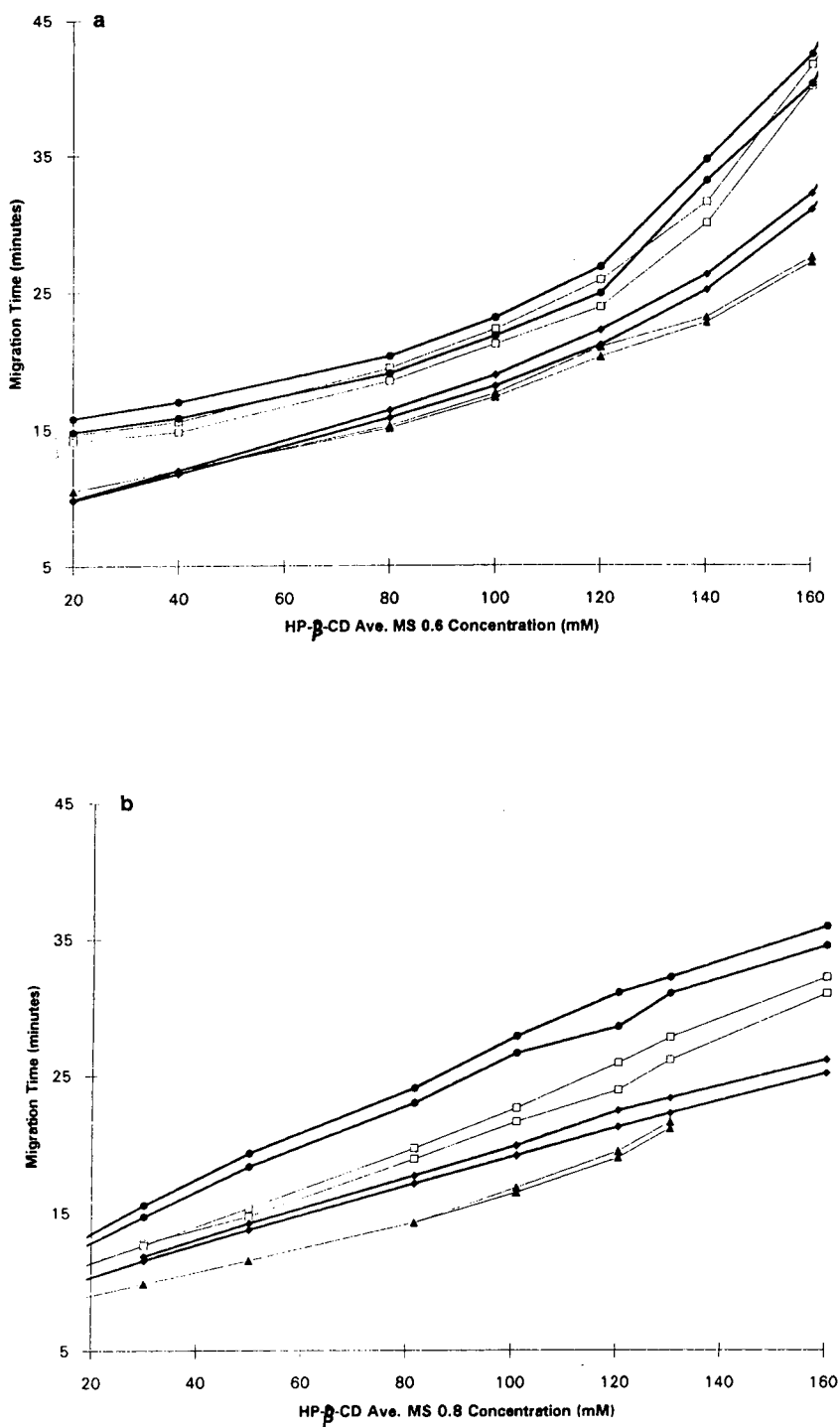


Fig. 2. Plots of  $\beta$ -agonist and  $\beta$ -antagonist migration times versus (a) concentration of HP- $\beta$ -CD Ave. MS 0.6 and (b) concentration of HP- $\beta$ -CD Ave. MS 0.8.  $\square$  = Clenbuterol;  $\bullet$  = terbutaline;  $\blacklozenge$  = cimaterol;  $\blacktriangle$  = salbutamol.

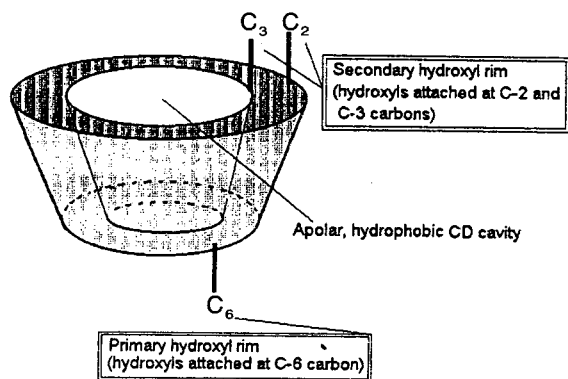


Fig. 3. Representation of “natural” cyclodextrin showing primary and secondary hydroxyl rims forming cyclodextrin complex.

amphetamine increased with HP- $\beta$ -CD Ave. MS 0.6 and 0.8 concentration, showing an  $R_s$  maximum at 120 mM, after which  $R_s$  decreased with increasing CD concentration (Fig. 4)  $R_s$  for

methylendioxyamphetamine increased proportionally with HP- $\beta$ -CD Ave. MS 0.6 concentration, showing no  $R_s$  maximum. The HP- $\beta$ -CD concentration that gave the largest  $R_s$  for the  $\beta$ -agonists,  $\beta$ -antagonists, amphetamines and ephedrines studied was 120 mM for both HP- $\beta$ -CD Ave. MS 0.8 and 0.6 (Fig. 4). HP- $\beta$ -CD Ave. MS 0.8 and 0.6 produced separations with ca.  $3 \cdot 10^5$  theoretical plates. Both 120 mM HP- $\beta$ -CD Ave. MS 0.8 and 0.6 resolved equal numbers of compounds, but HP- $\beta$ -CD Ave. MS 0.8 gave less co-migrations, as shown in Fig. 2a and b.

### 3.2. Multi-component chiral separation of $\beta$ -Agonists and $\beta$ -Antagonists

Fig. 5 shows an electropherogram of twelve racemates of  $\beta$ -agonists and  $\beta$ -antagonists optically resolved in less than 45 min with the order of migration indicated. Note that the optical

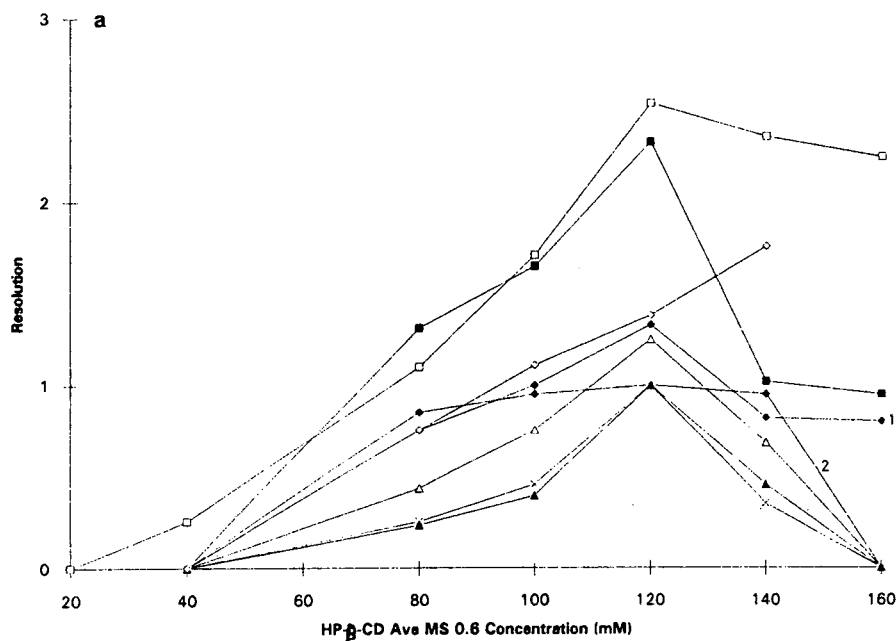


Fig. 4. Resolution of  $\beta$ -agonists,  $\beta$ -antagonists, phenylethylamines and alcohols ( $\Delta T$ ) versus (a) and (b) concentration of HP- $\beta$ -CD Ave. MS 0.6 and (c) concentration of HP- $\beta$ -CD Ave. Ms 0.8. (a)  $\Delta$  = Atenolol;  $\blacklozenge$  (1) = oxprenolol;  $\blacklozenge$  (2) = propranolol;  $\blacksquare$  = pindolol;  $\times$  = alprenolol;  $\blacktriangle$  = labetalol;  $\diamond$  = methylidimethoxyamphetamine;  $\square$  = epinephrine. (b)  $\square$  = Clenbuterol;  $\blacksquare$  = terbutaline;  $\diamond$  = cimaterol;  $\blacklozenge$  = salbutamol;  $\times$  = pirbuterol;  $\triangle$  = amphetamine;  $\blacktriangle$  = methylamphetamine; (c)  $\blacksquare$  = Clenbuterol;  $\diamond$  = terbutaline;  $\square$  = cimaterol;  $\triangle$  = salbutamol;  $\blacktriangle$  = pirbuterol;  $\blacklozenge$  = methylamphetamine;  $\times$  = amphetamine.

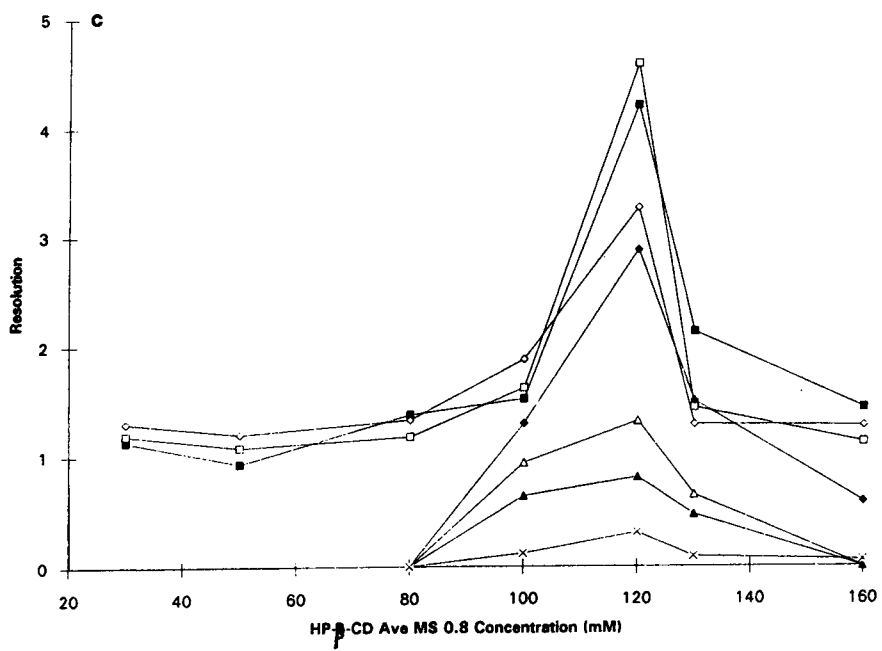
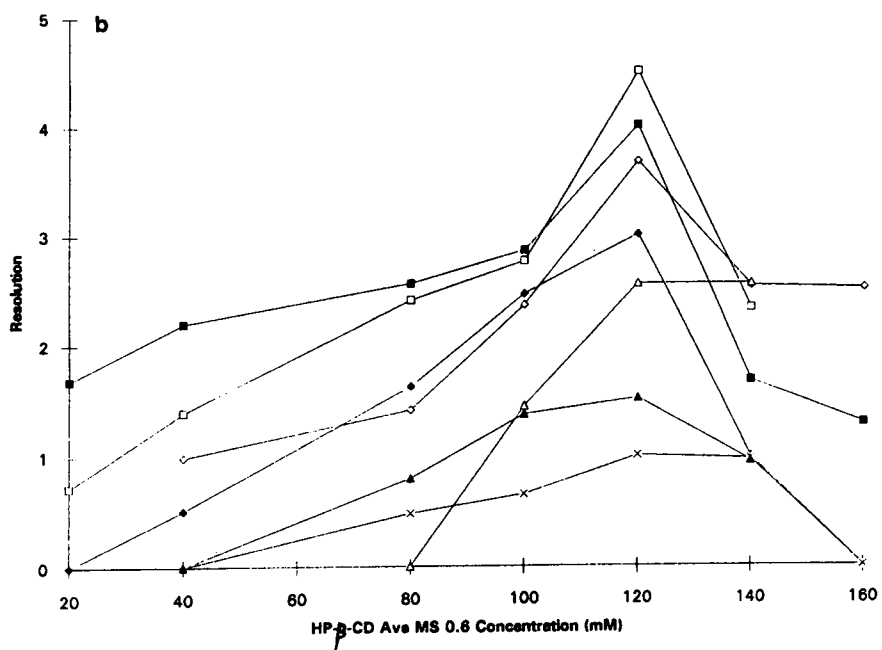


Fig. 4 (continued).

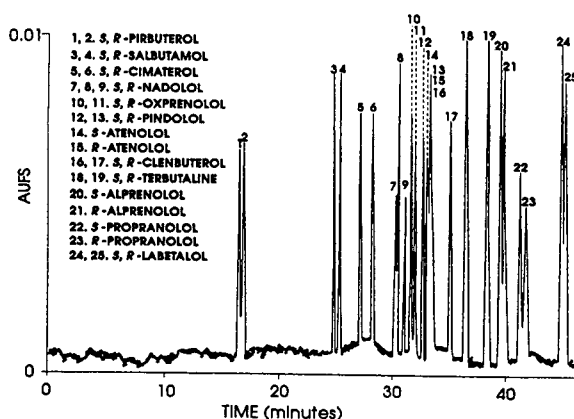


Fig. 5. Electropherogram of phenylamine alcohols optically resolved using 120 mM HP- $\beta$ -CD Ave. Ms 0.8 (each compound at 600  $\mu$ g/ml).

migration order is only given for optically pure isomers obtained. (*R*)-Atenolol was observed to co-elute with one of the optical isomers of pindolol and clenbuterol. This is attributed to the large number of structurally related compounds simultaneously resolved into closely migrating bands, depleting the available CD concentration which decreases the resolution [47]. Also, high local solute conductivity can be produced by closely migrating bands causing electrodispersion, which can decrease resolution. This is reflected by larger  $R_s$  values for each injected compound compared with a mixture. Peaks for acebutolol and timolol are not shown in Fig. 5 as they were not optically resolved and also metoprolol was only poorly resolved optically. (*R,S*)-Nadolol standard appears to contain a mixture of (*R,S*)-*cis*- and -*trans*-nadol, as shown in Table 2. With a racemic mixture of (*R,S*)-*cis*- and -*trans*-nadolol, an equal concentration of the four isomers exists. A more stable inclusion complex with HP- $\beta$ -CD will form with the "*cis*" configuration, because of the planar symmetry of the two hydroxy groups in comparison with the "*trans*" conformation [48]. This would be reflected by a large migration time difference between *cis*- and *trans*-nadolol isomers. The existence of three peaks having a peak-height ratio of 1:2:1 shown in Fig. 5 may account for two of the optical isomers being

resolved and the other two co-eluting under one peak. Unfortunately, a pure standard of *cis*-nadolol and *trans*-nadolol could not be found.

### 3.3. Chiral resolution of amphetamines

Fig. 6 shows an electropherogram of eight racemates of phenylethylamines and alcohols optically resolved in less than 45 min with the order of migration indicated. Note that the optical migration order is only given for optically pure isomers obtained. 2,5-Dimethoxy-4-methylamphetamine and 4-bromo-2,5-dimethoxyamphetamine were not optically resolved. 4-Bromo-2,5-dimethoxyamphetamine co-elutes with (*S*)-methylamphetamine and (*R*)-epinephrine with (*S*)-ephedrine (Fig. 6). Peaks for norephedrine are not shown in Fig. 6 as it was not optically resolved.

The optically resolved phenylethylamines migrated in the order of increasing molecular mass within homologous series.

### 3.4. Chiral resolution limits for HP- $\beta$ -CD

There are a few compounds that failed to be optically resolved with HP- $\beta$ -CD, including acebutolol, 2,5-dimethoxy-4-methylamphetamine, 4-bromo-2,5-dimethoxyamphetamine,

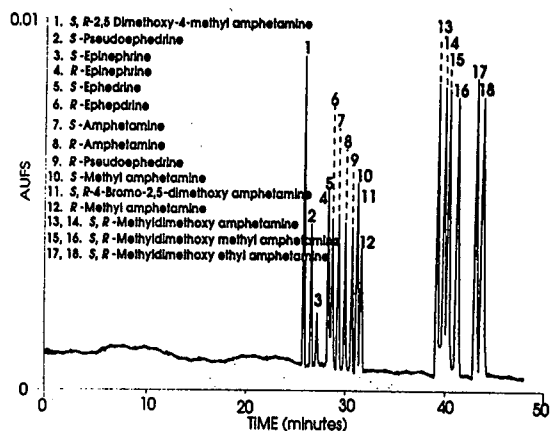


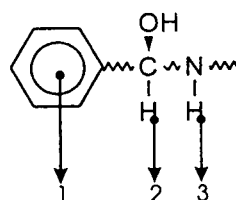
Fig. 6. Electropherogram of phenylamines optically resolved using 120 mM HP- $\beta$ -CD Ave. Ms 0.8 (each compound at 600  $\mu$ g/ml).

timolol and norephedrine. Chiral resolution for acebutolol and 2,5-dimethoxy-4-methylamphetamine, 4-bromo-2,5-dimethoxyamphetamine appears to be impaired by the protruding aromatic substituent (see Tables 2 and 3). This prevents the aromatic ring from penetrating sufficiently into the CD for hydrogen bonding to occur with the stereogenic centre. Conversely, optical resolution is impaired with timolol by the large distance between the stereogenic centre and hydrogen bonding groups on the CD. A broad peak was obtained with norephedrine. This was attributed to the small difference in hydrogen bond strength between the hydroxyl and primary amine groups in norephedrine and the CD. The difference in hydrogen bond strength between the hydroxyl and primary amine groups in norephedrine and the CD is decreased by substituting a methyl group on the primary amine group, producing a secondary amine (ephedrine). Ephedrine with a hydroxy group and secondary amine group was optically resolved with HP- $\beta$ -CD, as shown by Fig. 6. Norephedrine is optically resolved with only methyl-substituted  $\beta$ -CD [13,14,16–18, 20,24,26,27]. These results show that the position and type of CD alkyl derivative affect the formation of the guest–host complex.

### 3.5. Solute cyclodextrin interactions

The optical isomers of  $\beta$ -agonists,  $\beta$ -antagonists, ephedrines and amphetamines resolved with HP- $\beta$ -CD were observed to elute with the *S*-form first, followed by the *R*-form, suggesting a common mechanism operative with the sixteen optically pure isomers studied. In order to obtain a direct separation with CD, it is necessary for three different interactions to take place between the enantiomer and the CD, as proposed in the three-point interaction model of Dalglish [48]. The three points of contact proposed as being necessary for enantioselectivity to occur for  $\beta$ -agonists,  $\beta$ -antagonists and hydroxyphenylamines are illustrated in Fig. 7A. The aromatic portion (hydrophobic end) of the molecule is likely to fit into the CD cavity (Fig. 7a, point 1) [45]. The molecule requires a hydrogen bonding site near the chiral centre for hydrogen bonding

#### A) $\beta$ -Agonists, $\beta$ -antagonists and ephedrines



#### B) Amphetamines

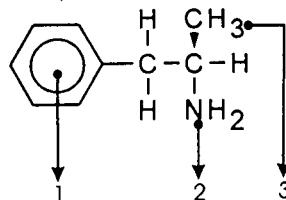


Fig. 7. The three points of CD interaction with (A)  $\beta$ -agonists,  $\beta$ -antagonist and ephedrines, and (B) amphetamines.

with the CD, and the chiral centre is close enough to the CD activity for such bonding to be possible. The three points of contact necessary for enantioselectivity to occur with amphetamines is illustrated in Fig. 7B. The aromatic portion (hydrophobic end) of the molecule is likely to fit into the CD cavity (Fig. 7B, point 1). CD hydrogen bonding occurs with the amphetamine primary amine group near the chiral centre. The optically active methyl substituent in amphetamine is the third point of contact with HP- $\beta$ -CD. Optical differentiation of (*R*)- and (*S*)-amphetamines is made possible by steric hindrance between the hydroxypropyl groups in HP- $\beta$ -CD and the optically active methyl substituent in amphetamine.

### 3.6. Sodium sulfobutyl ether- $\beta$ -CD Ave. MS 0.4 (SBE- $\beta$ -CD)

We postulated that increasing the alkyl substituent from hydroxypropyl to hydroxybutyl on the CD would further increase the flexibility and hydrophobicity of the CD cavity. Also, migration of a charged CD in the opposite direction to the analyte would increase the partition per unit volume between the molecule and charged CD, resulting in smaller amounts of CD being re-

quired to achieve a separation. This in part was obtained using SBE- $\beta$ -CD as a chiral additive. The versatility of such a system was shown with SBE- $\beta$ -CD optically resolving  $\beta$ -agonist,  $\beta$ -antagonist and amphetamines using a citrate buffer at pH 2.5. In an attempt to study the range of compounds that could be resolved with SBE- $\beta$ -CD, thalidomide and some metabolites were employed in the experiment.

Fig. 8 shows an electropherogram of six racemates of  $\beta$ -agonists,  $\beta$ -antagonist and thalidomide optically resolved in less than 25 min with 2 mM SBE- $\beta$ -CD, with retention times and  $R_s$  values given in Table 4. Note that the optical migration order is only given for optically pure isomers obtained. Increasing the SBE- $\beta$ -CD

concentration from 2 to 4.6 mM causes the racemates to elute within 15 min in the order of N-phthaloyl-(*S*)-glutamic acid, terbutaline, clenbuterol, (*R*)-thalidomide, (*R,S*)-glutamine and (*S*)-thalidomide, as shown in Figs. 9 and 10, with the corresponding retention times and  $R_s$  values given in Table 4. Increasing the SBE- $\beta$ -CD concentration in the CE running buffer would have increased the ionic strength and conductivity of the medium, hence reducing the migration time of the solutes. This is most pronounced with thalidomide, where the migration time is halved and  $R_s$  decreased with increases in SBE- $\beta$ -CD concentration from 2.0 to 4.6 mM, as shown in Table 4.

In order to improve the chiral separation of

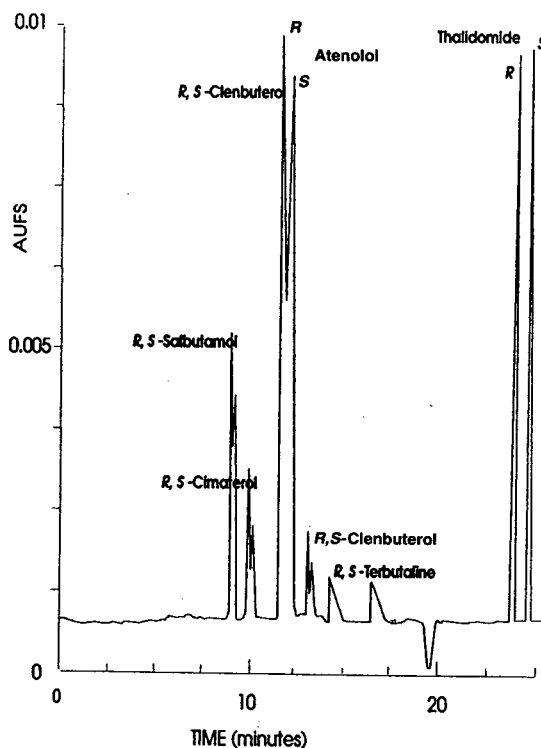


Fig. 8. Electropherogram of (*R,S*)-salbutamol, (*R,S*)-cimaterol, (*R,S*)-clenbuterol, (*R,S*)-atenolol, (*R,S*)-terbutaline and (*R,S*)-thalidomide optically resolved. Conditions: 2 mM SBE- $\beta$ -CD, 20 mM citric acid-phosphate buffer (pH 2.5), anode at injection side, 20 kV, 220 nm, 4 kPa injection of 300  $\mu$ g/ml solution.

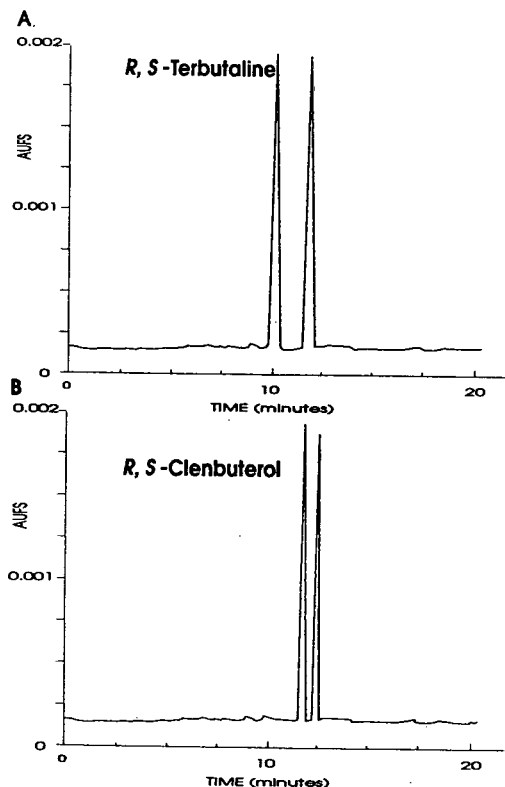


Fig. 9. Electropherograms of (A) (*R,S*)-terbutaline and (B) (*R,S*)-clenbuterol optically resolved. Conditions: 4.6 mM SBE- $\beta$ -CD, 20 mM citric acid-phosphate buffer (pH 2.5), cathode at injection side, 20 kV, 220 nm, 4 kPa injection of 300  $\mu$ g/ml solution.



Table 4  
Compounds optically resolved with various SBE- $\beta$ -CD concentrations in 20 mM citric acid–phosphate buffer (pH 2.5) using 1-propanol as organic modifier

| SBE- $\beta$ -CD concentration (mM) | Compound optically resolved               | Retention time (min) |       | Resolution |
|-------------------------------------|---|----------------------|-------|------------|
|                                     |   |                      |       |            |
| 2.0                                 | ( <i>R,S</i> )-Salbutamol                 | 8.81                 | 8.93  | 1.00       |
| 2.0                                 | ( <i>R,S</i> )-Cimaterol                  | 10.04                | 10.22 | 0.75       |
| 2.0                                 | ( <i>R,S</i> )-Atenolol                   | 13.03                | 13.25 | 0.67       |
| 2.0                                 | ( <i>R,S</i> )-Clenbuterol                | 14.53                | 14.88 | 1.31       |
| 2.0                                 | ( <i>R,S</i> )-Terbutaline                | 14.68                | 16.88 | 2.80       |
| 2.0                                 | ( <i>R,S</i> )-Thalidomide                | 23.55                | 24.87 | 2.25       |
| 4.6                                 | N-Phthaloyl-( <i>S</i> )-glutamic acid    |                      | 9.89  |            |
| 4.6                                 | ( <i>R,S</i> )-Terbutaline                | 10.31                | 12.09 | 2.88       |
| 4.6                                 | ( <i>R,S</i> )-Methylamphetamine          | 12.21                | 13.01 | 1.78       |
| 4.6                                 | ( <i>R,S</i> )-Clenbuterol                | 12.23                | 12.57 | 1.67       |
| 4.6                                 | ( <i>R,S</i> )-Amphetamine                | 13.98                | 15.13 | 1.33       |
| 4.6                                 | ( <i>R,S</i> )-Glutamine                  |                      | 14.57 |            |
| 4.6                                 | ( <i>R,S</i> )-Thalidomide                | 14.14                | 14.69 | 2.00       |
| 4.6                                 | ( <i>R,S</i> )-Atenolol                   | 15.77                | 16.44 | 3.13       |
| Addition of 5% (V/V) 1-propanol     |   |                      |       |            |
| 2.0                                 | ( <i>R,S</i> )-Clenbuterol                | 12.33                | 12.44 | 0.40       |
| 2.0                                 | ( <i>R,S</i> )-Methyldimethoxyamphetamine | 14.37                | 14.71 | 0.71       |

the compounds studied at 2.0 mM SBE- $\beta$ -CD, an organic modifier was used to modify the host-guest complex. Based on previous work [38], the buffer system was modified with 5% (v/v) of 1-propanol. Compounds which normally resolved without organic modifier failed to do so; only methyldioxyamphetamine was resolved and clenbuterol poorly, as shown in Table 4.

At pH 2.5, SBE- $\beta$ -CD can optically resolve only positively charged compounds. This is probably because they migrate under the influence of an applied voltage. However, under these conditions, carboxylic acids are protonated and hence do not migrate electrophoretically.

#### 4. Conclusions

The highly water-soluble HP- $\beta$ -CD was used at elevated concentrations enabling those CD derivatives to give the optimum separation of certain racemates to achieve a high enough

concentration in solution to effect that separation. This provided the means to resolve optically many  $\beta$ -agonists,  $\beta$ -antagonists, amphetamines and ephedrines with a single buffer system. The native CD is made more size dependent by introducing a bulky hydroxypropyl substituent. Steric factors are also relevant for chiral recognition; at least one polar group with the proper hydrogen bonding ability must be in proximity to the stereogenic centre, such as hydroxyl groups and/or secondary amines. This work has shown the versatility of CE in the simultaneous multi-component chiral separation of illicit and pharmaceutical drug substances for direct pharmacokinetic studies of a wide range of optically active drugs.

#### Acknowledgement

Thanks are due to the Australian Government Analyst, Dr. C.J. Dahl, for support of this work.

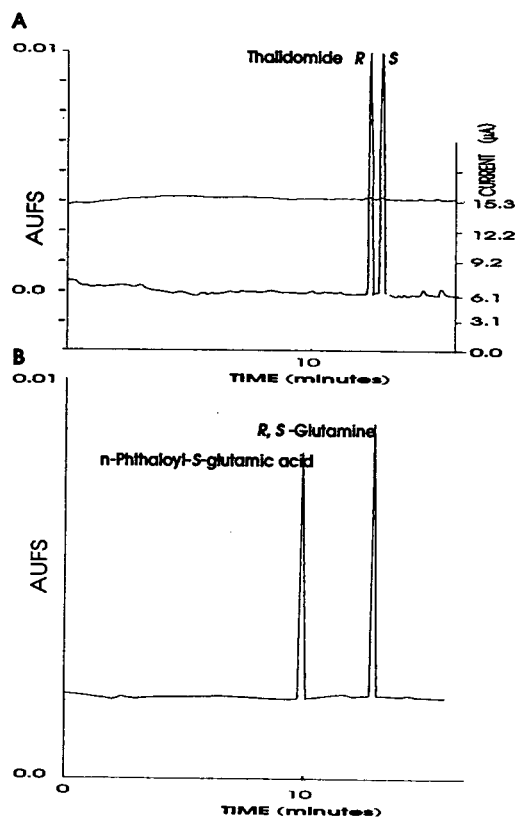


Fig. 10. Electropherograms of (A) (R)- and (S)-thalidomide and (B) (R,S)-glutamine and phthaloyl-(S)-glutamic acid. Conditions: 4.6 mM SBE- $\beta$ -CD, 20 mM citric acid-phosphate buffer (pH 2.5), 20 kV, anode at injection side, 220 nm, 4 kPa injection of 300  $\mu$ g/ml solution.

## References

- [1] M.J. Cope, *Anal. Proc.*, 30 (1993) 498.
- [2] E.J. Ariens, *Eur. J. Clin. Pharmacol.*, 26 (1984) 663.
- [3] H. Koch, *Sci. Pharm.*, 49 (1981) 67.
- [4] M.J. Cope, *Anal. Proc.*, 29 (1992) 180.
- [5] V. Schurig and H.P. Nowotny, *Angew. Chem.*, 9 (1990) 969.
- [6] D. Sybliska and J. Zukowski, in A.M. Krstulovic (Editor), *Chiral Separations by H.P.L.C: Applications to Pharmaceutical Compounds*, Ellis Horwood, Chichester, 1989, Ch. 7, p. 147.
- [7] S.F. Li, *Capillary Electrophoresis: Principles, Practice and Applications (Journal of Chromatography Library, Vol. 52)*, Elsevier, Amsterdam, 1992, pp. 259–270.
- [8] J.W. Jorgenson and K.D. Lukas, *Anal. Chem.*, 53 (1981) 1298.
- [9] R. Kuhn and S. Hoffstetter-Kuhn, *Chromatographia*, 34 (1992) 505.
- [10] N. Weiner, in A.G. Goodman, L.S. Goodman and A. Gilman (Editors), *The Pharmacological Basis of Therapeutics*, Macmillan, New York, 6th ed., 1980, p. 159.
- [11] S.H. Snyder and K.M. Taylor, *Science*, 168 (1970) 1487.
- [12] G.T. Hajos and S. Garattini, *J. Pharm. Pharmacol.*, 25 (1973) 418.
- [13] J. Snopeck, I. Jelinek and E. Smolková-Keulemansová, *J. Chromatogr.*, 472 (1989) 308.
- [14] S. Fanali, *J. Chromatogr.*, 474 (1989) 441.
- [15] *List of Doping Classes and Methods*, International Olympic Committee, Lausanne, 1991.
- [16] M.E. Swartz, *J. Liq. Chromatogr.*, 14 (1991) 923.
- [17] J. Snopek, I. Jelinek and E. Smolková-Keulemansová, *J. Chromatogr.*, 609 (1992) 1.
- [18] J. Snopek, I. Jelinek and E. Smolková-Keulemansová, *J. Chromatogr.*, 438 (1988) 211.
- [19] S. Fanali and P. Boček, *Electrophoresis*, 11 (1990) 757.
- [20] C. Quang and M.G. Khaledi, *Anal. Chem.*, 65 (1993) 3354.
- [21] T.E. Peterson, *J. Chromatogr.*, 630 (1993) 353.
- [22] T.E. Peterson and D. Trowbridge, *J. Chromatogr.*, 603 (1992) 298.
- [23] S.A.C. Wren and R.C. Rowe, *J. Chromatogr.*, 636 (1993) 57.
- [24] M. Chicharro, A. Zapparodiol, E. Bermejo, J.A. Perez and L. Hernández, *J. Chromatogr.*, 622 (1993) 103.
- [25] R. Kuhn, F. Erni, T. Bereuter and J. Häusler, *Anal. Chem.*, 64 (1992) 2815.
- [26] M.W.F. Nielen, *Anal. Chem.*, 65 (1993) 885.
- [27] M. Heuermann and G. Blaschke, *J. Chromatogr.*, 648 (1993) 267.
- [28] R.J. Tait, P. Tan, D.O. Thompson, V.J. Stella and J.F. Stobaugh, presented at the *5th International Symposium on High Performance Capillary Electrophoresis, Orlando, FL, January 1993*, paper W214.
- [29] S. Fanali, *J. Chromatogr.*, 545 (1991) 437.
- [30] K.D. Altria, D.M. Goodall and M.M. Rogan, *Chromatographia*, 34 (1992) 19.
- [31] H. Soini, M.L. Rickkola and M.V. Novotny, *J. Chromatogr.*, 608 (1992) 265.
- [32] V.L. Herring and J.A. Johnson, *J. Chromatogr.*, 612 (1993) 215.
- [33] S.A.C. Wren and R.C. Rowe, *J. Chromatogr.*, 635 (1993) 113.
- [34] S. Li and D.K. Lloyd, *Anal. Chem.*, 65 (1993) 3684.
- [35] S.A.C. Wren and R.C. Rowe, *J. Chromatogr.*, 609 (1992) 363.
- [36] L. Valtcheva, J. Mohammad, G. Pettersson and S. Hjertén, *J. Chromatogr.*, 638 (1993) 263.
- [37] S. Fanali, L. Ossicini, F. Foret and P. Boček, *J. Microcol. Sep.*, 1 (1989) 190.
- [38] A. Aumatell and R.J. Wells, *J. Chromatogr. Sci.* 31 (1993) 502.
- [39] R.J. Tait, D.J. Skanchy, D.P. Thompson, N.C. Chetwyn, D.A. Dunshee, R.A. Rajewski, V.J.S.

- Higuchi and J.F. Stobaugh, *J. Pharm. Biomed. Anal.*, 10 (1992) 615.
- [40] M.J. Sepaniak, R.O. Cole and B.K. Clark, *J. Liq. Chromatogr.*, 15 (1992) 1023.
- [41] R. Kuhn and S. Hoffstetter-Kuhn, *Chromatographia*, 34 (1992) 505.
- [42] A. Guttman, A. Paulus, S. Cohen, N. Grinberg and B.L. Karger, *J. Chromatogr.*, 448 (1988) 41.
- [43] I. Cruzado, Y.Y. Rawjee, A. Shitangkoon, G. Vigh, presented at the *5th International Symposium on High Performance Capillary Electrophoresis, Orlando, FL, January 1993*, paper W203.
- [44] D.Y. Pharr, Z.S. Fu, T.K. Smith and W.L. Hinze, *Anal. Chem.*, 61 (1989) 275.
- [45] L. Coventry, in W.J. Lough (Editor), *Chiral Liquid Chromatography*, Chapman and Hall, New York, 1989, p. 148.
- [46] T. Higuchi and K.A. Connors, *Adv. Anal. Chem. Instrum.*, 4 (1965) 117.
- [47] C.E. Dalglish, *J. Chem. Soc.*, 132 (1952) 3940.
- [48] S. Pálmarsdóttir and L.E. Edholm, *J. Chromatogr. A*, 666 (1994) 337.





ELSEVIER

Journal of Chromatography A, 686 (1994) 309–317

JOURNAL OF  
CHROMATOGRAPHY A

# Preparative capillary zone electrophoresis of synthetic peptides Conversion of an autosampler into a fraction collector

Huey G. Lee<sup>a</sup>, Dominic M. Desiderio<sup>a,b,c,\*</sup>

<sup>a</sup>*The Charles B. Stout Neuroscience Mass Spectrometry Laboratory, University of Tennessee, Memphis, TN 38163, USA*

<sup>b</sup>*Department of Neurology, College of Medicine, University of Tennessee, 956 Court Avenue, Room A218, Memphis, TN 38163, USA*

<sup>c</sup>*Department of Biochemistry, University of Tennessee, Memphis, TN 38163, USA*

First received 13 June 1994; revised manuscript received 29 August 1994

## Abstract

Preparative capillary zone electrophoresis of three synthetic peptides was performed either manually or automatically by simple manipulations of a commercial electropherograph that is equipped only with an autosampler without any built-in fraction collection capability. Manual fraction collection was achieved by replacing the outlet (cathode) beaker with a microcentrifuge tube, and automatic fraction collection was accomplished by converting the electropherograph's autosampler into a fraction collector. The latter was easily achieved mainly by the use of an extension wire, which completed the electrical circuit and facilitated fraction collection either at a specified time or within fixed time intervals.

## 1. Introduction

The publications of Jorgenson and Lukacs [1,2] in the early 1980s have popularized capillary zone electrophoresis (CZE) as an experimental technique for peptide separation and analysis [3–14]. High electrophoretic resolution can be achieved using high voltage (10–30 kV) because of the efficient heat dissipation that is achievable by using small internal diameter (I.D. 50–100  $\mu\text{m}$ ) thin-walled fused-silica or glass capillaries that have a large surface-to-volume ratio. Other advantages of modern CZE include

a high level of detection sensitivity and selectivity, rapid analyses, on-line detection, interfacing to mass spectrometry (MS), long column life, low sample/reagent consumption and automation.

Fraction collection is also possible using this micro-column electrophoretic separation technique [15–30]. In most cases, electrical contact is maintained during the electrophoretic separation and collection, and voltage is turned off during the transfer of the capillary and electrode to a collection vial [15–24] that contains the electrolyte or to a moving membrane [25] that is submerged in the electrolyte. Alternatively, Huang and Zare [26,27] constructed an on-column frit to maintain the electrical contact and to collect the eluent on a moving surface. Furthermore, hydrodynamic elution using a syringe

\* Corresponding author. Address for correspondence: Department of Neurology, College of Medicine, University of Tennessee, 956 Court Avenue, Room A218, Memphis, TN 38163, USA.

pump [28] after the voltage is turned off or using the available pressure [29] have also been reported. In all cases, automated fraction collection would facilitate repetitive and multiple collections.

Our laboratory has an electropherograph, which has an autosampler but not a fraction collector. Accordingly, in this present study, we report that such an autosampler can be easily converted to an automated fraction collector. That fraction collector was used to collect electrophoretically three synthetic peptides [Dynorphin A<sub>1-24</sub> or A<sub>1-17</sub> (DynA<sub>1-24</sub> or DynA<sub>1-17</sub>), substance P (SP), and leucine enkephalin-lysine (LE-K)] separated in a single electrophoretic experiment. This conversion is significant, because automatic fraction collection is possible either at a specified time, or within a fixed time interval.

The applications of CZE in biomedical research have been reviewed recently [31–33]. For many years, this laboratory has been involved in analyzing neuropeptides from biological sources, including human tissues and fluids, by using multi-dimensional reversed-phase high-performance liquid chromatography (RP-HPLC) for sample preparation [34], and by using radioimmunoassay (RIA) [35], MS [36], and tandem MS (MS–MS) [37] for qualitative and quantitative analyses [38]. CZE may be used to substitute for, or to complement, RP-HPLC for sample preparation prior to RIA, MS, and/or MS–MS detection.

## 2. Experimental

### 2.1. Reagents and materials

DynA<sub>1-17</sub>, SP, and LE-K were purchased from Sigma (St. Louis, MO, USA) and DynA<sub>1-24</sub> was obtained from Peninsula Labs. (Belmont, CA, USA). These synthetic peptides were used without any further purification. Ammonium formate (J.T. Baker, Phillipsburg, NJ, USA) and trifluoroacetic acid (TFA; Pierce, Rockford, IL, USA) were used to prepare the volatile CZE buffer. Fused-silica capillary with 50 or 100  $\mu\text{m}$

I.D. and 360  $\mu\text{m}$  O.D. was purchased from Polymicro Technologies, Phoenix, AZ, USA.

### 2.2. Instrumentation

An ISCO (Lincoln, NE, USA) Model 3140 electropherograph outfitted with an IBM (Armonk, NY, USA) Personal System/2 Model 30 286 computer was used. Operation of the instrument and data collection/analysis were controlled by the manufacturer's ICE 3.1.0 level software. According to a recent survey of capillary electrophoresis instrumentation [39], ISCO is listed as one of the major suppliers of the electropherographs that have been purchased. However, ISCO's electropherographs, including the Model 3140, are not equipped with any built-in fraction collection capability.

### 2.3. Methods

#### CZE

The fused-silica capillary used in the manual fraction collection experiment was a 98 cm  $\times$  50  $\mu\text{m}$  I.D. capillary, with a 68 cm length from the inlet of the column to the detector; whereas a 100 cm  $\times$  100  $\mu\text{m}$  I.D. capillary, with a 60 cm length from the inlet of the column to the detector, was used in the automatic fraction collection experiment. The 50  $\mu\text{m}$  I.D. capillary column volume was 2  $\mu\text{l}$ , and the 100  $\mu\text{m}$  I.D. was 8  $\mu\text{l}$ . Prior to daily use, the capillary was preconditioned with the following sequence of solvents by applying the electropherograph's "high vacuum" ( $\Delta p = 28$  kPa) [40] from the outlet beaker for at least two column volumes for each solvent: water, 1 M NaOH, 0.1 M HCl, water and finally buffer (20 mM ammonium formate, titrated to pH 2.5 with TFA) for the experiment. This volatile buffer is similar to that used by Johansson et al. [41], and was chosen so that the fractions collected may be analyzed subsequently by MS. A 1 mM buffer was also used in some experiments.

The mixture of peptides contained 0.3  $\mu\text{g}$  (75 to 439 pmol each) of each peptide (ca. 1  $\mu\text{g}$  total for the three peptides) per  $\mu\text{l}$  of buffer (1 mM). Injection was performed by applying the instru-

ment's injection vacuum from the outlet beaker [40,42]. An injection volume of ca. 30 nl (corresponding to applied amounts of 2.4, 7.1, and 14.0 pmol for DynA<sub>1–24</sub>, SP, and LE-K, respectively) was injected into the 50  $\mu$ m I.D. capillary for the manual fraction collection. The injection volume for the 100  $\mu$ m I.D. capillary in the automatic fraction collection was ca. 100 nl, corresponding to injected amounts of 15.1, 24.0, and 47.4 pmol of DynA<sub>1–17</sub>, SP, and LE-K, respectively. Reinjections of those collected fractions were used to identify electrophoretically the collected peptide. The applied voltage was 27 or 13.5 ( $\pm 1\%$ ) kV [43], and the temperature was regulated to  $30 \pm 0.5^\circ\text{C}$  by the electropherograph's built-in air-circulating system.

#### Manual fraction collection

This fraction collection mode (cf. [16]) was performed by replacing the outlet buffer reservoir (beaker) with a microcentrifuge tube containing 10  $\mu$ l of either 1 or 20 mM buffer. Because the electropherogram of the three synthetic peptides (e.g. Fig. 1A) provides only the electrophoretic migration time that it takes an analyte to reach the detector, the corresponding longer migration time that it takes an analyte to reach the capillary outlet must be calculated [18] (see below, *Calculation of migration time for fraction collection*). The analyte collected in the microcentrifuge tube was reinjected for electrophoretic confirmation. For example, the middle peak (SP) in Fig. 1A was collected and analyzed in this manner (See Fig. 1B and C).

#### Automatic fraction collection

The instrumental configuration for automating the fraction collection is shown in Fig. 2, where the autosampler is now labeled as a fraction collector. This scheme illustrates four basic different features between the original instrumental configuration and the modification required for automatic fraction collection. First, and most importantly, an extension wire is used to electrically connect the ground (–) outlet, positioned near the outlet beaker, with the platinum wire attached to the sampler arm. That platinum wire on the sampler arm was originally intended for

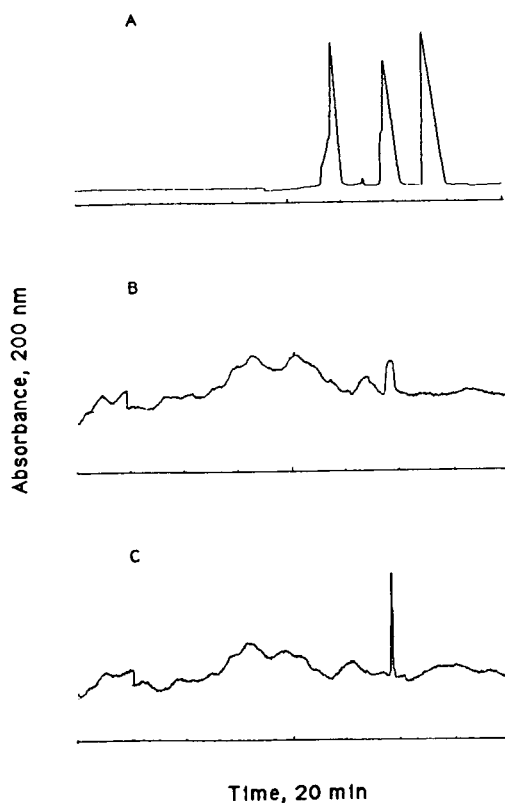


Fig. 1. Capillary zone electropherograms of synthetic peptides. (A) Electropherogram of three synthetic peptides; peaks from left to right are DynA<sub>1–24</sub>, SP, and LE-K, respectively. (B and C) Electropherograms of the reinjected SP peak, collected in 20 mM CZE (B) or in 1 mM CZE buffer (C). AUFS values are 0.1, 0.002, and 0.002 for A–C, respectively.

electrokinetic injection using the autosampler. It now serves to complete the electrical circuit required for the electrophoretic migration of an analyte during fraction collection.

Second, the capillary inlet (segment A) and capillary outlet (segment B) are positioned opposite to the original configuration (i.e., on the opposing side of the detector), so that the capillary outlet end can now reach the fraction collector instead of only the outlet beaker.

Third, the sample vials (e.g., 300- $\mu$ l microcentrifuge tube) originally used in the built-in sample carousel are now the vials used for the outlet buffer reservoir for the fraction collector.

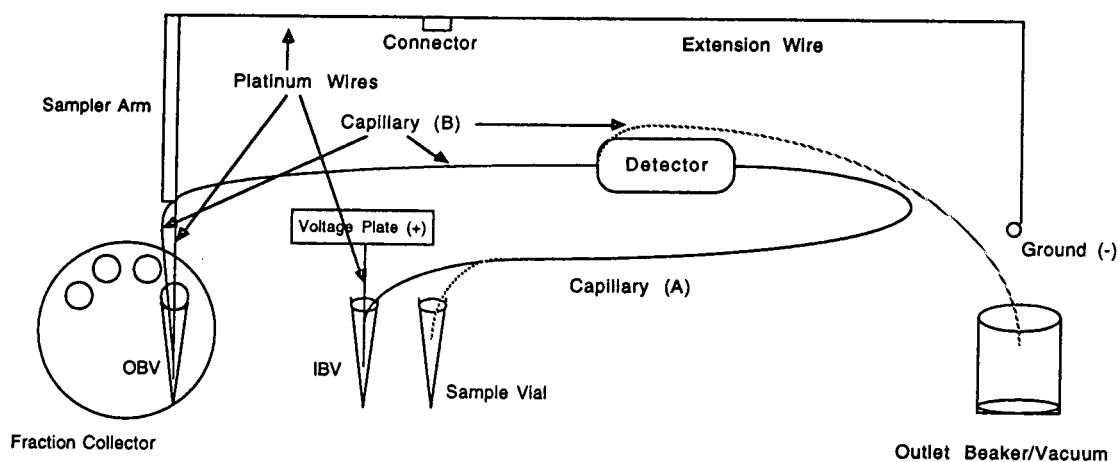


Fig. 2. Instrumental configuration for automatic fraction collection. IBV = Inlet buffer vial; OBV = outlet buffer vial. See text for details.

That same type of vial (or an inlet beaker) is used as the inlet buffer reservoir positioned beside the high voltage plate. Prior to the modification, the anode and cathode reservoirs both used the 10-ml inlet (not shown in Fig. 2) and outlet beakers, respectively, supplied by the company.

Finally, for vacuum injection, the capillary segment B (dashed line) is redirected back to the outlet beaker, and capillary segment A (dashed line) is inserted into a sample vial (positioned wherever convenient). Vacuum is applied as described [40]. After the sample injection, the capillary inlet is repositioned manually back to the inlet buffer vial (IBV), and the capillary outlet is also returned manually to the outlet buffer vial (OBV) via the sampler arm. Voltage can now be applied.

In the automatic fraction collection experiment, each peptide migrated into an OBV that contained 5  $\mu$ l of the 20 mM CZE buffer. The applied voltage during the fraction collection was halved to achieve higher recovery [18]. To avoid peptide contamination from one collected fraction to the next, the ground electrode and the capillary outlet tip were rinsed by inserting them into a vial that contained a larger volume (e.g., 300  $\mu$ l) of 20 mM buffer for a brief period (e.g., 15 s) without voltage prior to moving to the next OBV for the next fraction collection. At the end

of each electrophoretic collection in an OBV, a programmed delay of 1 min maximized the diffusion of the eluted peptide from the column and electrode into the OBV solution. The collected samples were lyophilized and reconstituted in 2  $\mu$ l water for reinjection analysis under "stacking" conditions [44].

#### Computer

The electropherograph is controlled via the computer, which has two operating modes: normal or extended. The normal mode gives the manufacturer's defined sequence of operations [43] for injection of sample from the autosampler and for electrophoresis in a continuous fashion. The extended mode allows one to instruct the electropherograph via the computer to perform every single step of the instrument operation, and to perform a group of distinct functions with a program specially written for that mode. The program is easily written by inputting the step-by-step commands selected from the available command selection [43]. Furthermore, several programs may be executed continuously in a "batch" mode.

For manual collection, one uses the normal mode or the programmable extended mode to perform an initial electrophoretic separation. However, after replacing the outlet beaker with a microcentrifuge tube, an extended mode pro-



gram must be used to restart the electrophoresis for fraction collection. In principle, the extended mode electrophoretic programs may be used to collect manually more than one fraction per separation.

For the automatic fraction collection, all operations are performed with the extended mode programs. First, an injection program is written to perform vacuum injection under the instrumental configuration shown in Fig. 2. Second, an extended mode program is written to instruct the electropherograph via the computer to perform electrophoresis. At the appropriate time within the program, voltage is turned off. Third, programs are written to move the sampler arm (and thus the platinum ground wire and the capillary outlet) to the next OBV in the carousel for fraction collection or to a rinsing vial between collections. Execution of the second and third programs in the “batch” mode is the basis of the automatic fraction collection. The electrophoretic migration times of the eluents and the time intervals required for fraction collection are input to the computer.

#### Calculation of migration time for fraction collection

It is necessary to calculate the window of migration time within which an analyte is collected. That window encompasses the leading and tailing edges of the UV absorbance. The following equation is used to calculate those migration times corresponding to those leading and tailing edges. The migration time of an analyte to the detector is converted to the corresponding migration time to the capillary outlet by the equation:

$$t_e = (L/l)t \quad (1)$$

where  $t_e$  = the electrophoretic migration time of the peak to the capillary outlet (min or s),  $L$  = total capillary length,  $l$  = capillary length from the inlet to the detector and  $t$  = migration time (min or s) to the UV detector.

For manual fraction collection, only the peptide (SP) that migrates in the middle of the three synthetic peptides was collected (see Fig. 1A).

The detected leading and tailing portions of the SP peak are at 14.3 and 15.4 min, respectively. Thus,  $t_e = 20.6$  and  $22.2$  min, respectively, because  $L = 98$  cm and  $l = 68$  cm. Therefore, a fraction collection beginning at 20 min, and lasting ca. 2 min was programmed for the collection of that SP peak. The safety margin of 0.6 min earlier than the expected time of collection was empirically determined.

For automatic fraction collection, three peptides were collected into three different fractions in a single electrophoretic separation. The electrophoretic time points ( $t_{1-4}$ ) needed for the migration time calculations for the automatic fraction collection of the three migrating peaks are shown in the electropherogram in Fig. 3. Each of these time points gives the  $t$  (migration time as determined by UV detector) values (Table 1). Each  $t$  value is decreased by 15 s (due to the 30 s of the initial linear voltage ramping) to give  $t_c$  (migration time corrected for voltage ramping) value. These  $t_c$  values are converted to the respective  $t_e$  (migration time of analyte at the capillary outlet) values by multiplying by the factor (100/60) because  $L = 100$  cm and  $l = 60$  cm. Finally, wherever possible, a safety margin for time to compensate for any errors or irreproducibility was incorporated. In this case, 0.5 min was subtracted from  $t_{e1}$ , giving  $t_{fc1}$  (actual migration time used at time point 1 for fraction collection). Similarly, a safety margin of 0.5 min was added to  $t_{e4}$ , giving  $t_{fc4}$ . Therefore, the electrophoretic separation (at the UV window) ends at  $t_{fc1}$ . The duration of the electrophoretic collection of the first peak ( $\Delta 1$ ) was calculated as follows,

$$\Delta 1 = [(t_{fc2} - t_{fc1} - 0.1 \text{ min}) \times 2] - 0.25 \text{ min} \quad (2)$$

where 0.1 min accounts for the voltage deramping time [18], the factor of 2 accounts for the fact the voltage was halved during the collection process, and 0.25 min accounts for the linear ramping time of 0.5 min used to ramp up the voltage up to a constant level (13.5 kV) during the electrophoretic fraction collection. The values of  $\Delta 2$  and  $\Delta 3$  are calculated similarly, except that for  $\Delta 2$ ,  $t_{fc2}$  was subtracted from  $t_{fc3}$  and that for  $\Delta 3$ ,  $t_{fc3}$  was subtracted from  $t_{fc4}$ . Accordingly,

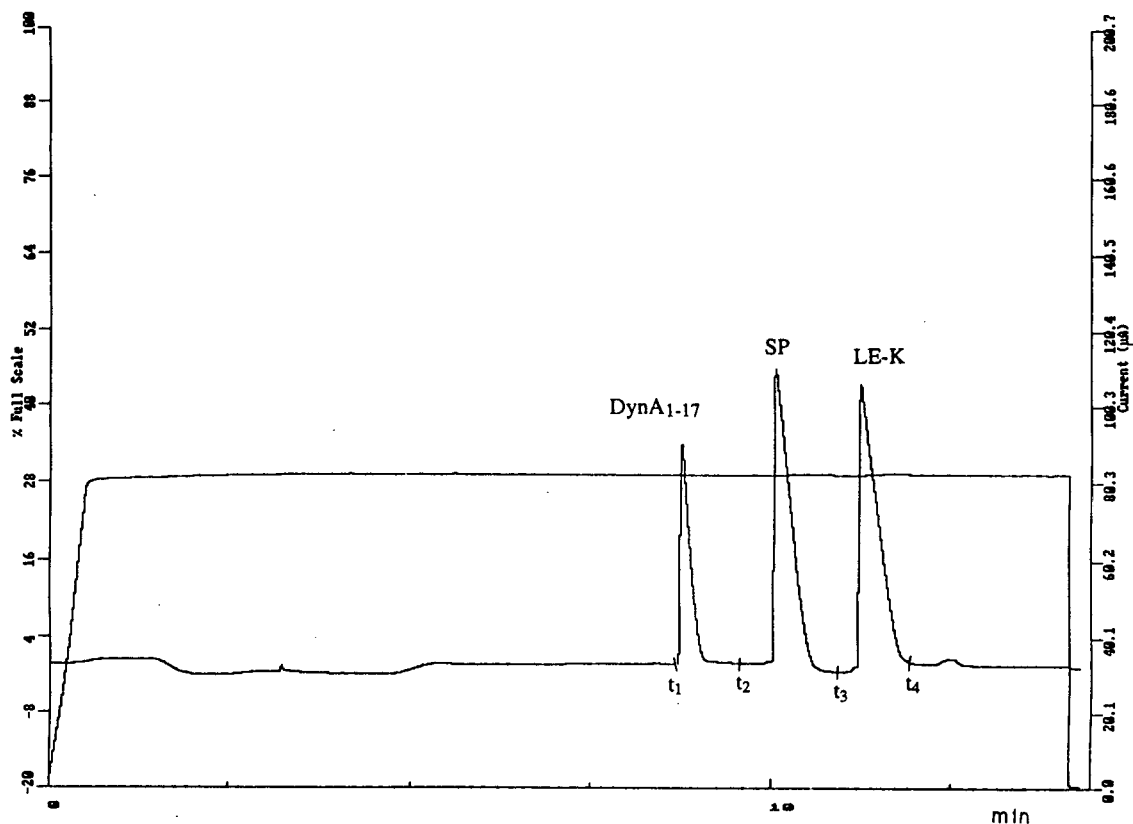


Fig. 3. Electropherogram for automatic fraction collection of three synthetic peptides. A 1 m  $\times$  100  $\mu$ m I.D. capillary, with 60 cm to the detector, was used. The electrophoretic time points  $t_{1-4}$  were used for calculating collection windows and for programming the automatic fraction collection times. The horizontal line is the monitored current (ca. 83  $\mu$ A). The ramping of current observed initially is due to the voltage ramping that occurs linearly in 30 s (see text). AUFS = 0.2.

Table 1  
Conversion of the migration time at the detection window to its corresponding collection time

| Time point | Migration time (s) |       |       |          |
|------------|--------------------|-------|-------|----------|
|            | $t$                | $t_c$ | $t_e$ | $t_{fc}$ |
| 1          | 521                | 506   | 843   | 813      |
| 2          | 574                | 559   | 932   | 932      |
| 3          | 655                | 640   | 1067  | 1067     |
| 4          | 713                | 698   | 1163  | 1193     |

$t$  = Migration time as recorded on the electropherogram;  $t_c$  = migration time corrected for voltage ramping;  $t_e$  = migration time of electroelution at the capillary outlet;  $t_{fc}$  = the actual time used for programming the fraction collection.

$\Delta 1-3$  values equal to 211, 243, and 225 s, respectively, were put into the computer programs. These times were manually selected to allow for the collection of all three fractions into three different OBVs in a single electrophoretic separation.

### 3. Results and discussion

Fig. 1A shows the electropherogram from which the migration time of the middle peak (SP) is calculated, and used for the fraction collection. Fig. 1B shows the electropherogram of the reinjected SP that had been collected into

10  $\mu\text{l}$  of the same CZE buffer (20 mM, pH 2.5) and demonstrates that a sufficient amount of SP was collected in a single electrophoresis for the reinjection to be detected by high sensitivity (0.002 AUFS) UV detection. Although the collected SP fraction was confirmed electrophoretically in Fig. 1B, reinjection of the sample collected in 1 mM of the CZE buffer gives a much narrower peak width (Fig. 1C) due to the improved electrophoretic “focusing” effect [44].

This fraction collection demonstrated by the data in Fig. 1 proves that manual fraction collection on this instrument is possible. However, manual fraction collection is tedious and involves a manual change of outlet beaker to collection vial, and a change of vials for multiple collections and for the capillary/electrode rinse between collections. The collection of more than one fraction becomes too time-consuming and impractical, especially when an experiment involves the fraction collection of a completely unknown sample and requires the collection of many different fractions for further analysis such as with MS to identify each analyte of interest. Furthermore, repetitive fraction collection is often necessary to accumulate a sufficient amount of material for further analysis. Therefore, the collection of more than one fraction in a single electrophoretic separation and repetitive collections would be facilitated by an automatic fraction collector.

Accordingly, the autosampler of our electropherograph was converted for use as an automatic fraction collector, although the instrument was not designed for such a function. Fig. 2 demonstrates this conversion. Basically, after sample injection (shown by the dotted lines), the capillary outlet was manually and easily positioned to the sampler arm that inserts both the capillary outlet and the ground electrode into the appropriate OBV in the 40-sample carousel. Through the extended mode computer program(s) that enables one to instruct the electropherograph to perform step-by-step operations, multiple fraction collection becomes possible using this modified configuration. Furthermore, repeated collection of the fractions is made more conveniently. The key to this successful conver-

sion is the extension wire that electrically connects the ground (–) electrode to the auto-sampler (fraction collector), thus completing the electrical circuit required for electrophoresis.

Fig. 3 shows the four manually selected times used in Table 1. Table 1 summarizes the step-by-step transformation of those migration times into empirical times for fraction collection. Based on these calculations, DynA<sub>1–17</sub>, SP, and LE-K were collected in a single electrophoretic separation. Fig. 4A is the electropherogram of the mixture used in Fig. 3, but now with a 50  $\mu\text{m}$  I.D. capillary. In Fig. 4B–D the electropherograms of the three individual peptides that were reinjected from the three collected fractions are shown; they all agree well (>98%) with the migration times of the electropherogram of the mixture of the three peptides (Fig. 4A). Also, note the absence of any memory effect in the electropherograms in Fig. 4B–D. The recovery of peptide in the electropherograms shown in Fig. 4B–D, compared to Fig. 4A, is high (75%). That high recovery demonstrates that the calculation of each collection window is accurate.

We have observed that a combination of (a) a programmed delay of ca. 1 min after the termination of the applied voltage before moving on to the next fraction collection vial and (b) voltage ramping and a two-fold reduction of the voltage during the fraction collection increases the analyte recovery. The programmed delay allows the analyte that might have bound to the electrode and the capillary to diffuse into the solution in the collection vial. Voltage ramping at the onset of the electrophoretic collection process minimizes any rapid heating and thermal expansion of the buffer. Voltage reduction enhances peptide recovery, presumably because the interaction between the electrode and analyte decreases. Based on peak areas, we estimate that the recovery of each peptide was typically >65% under these experimental conditions. Biehler and Schwartz [18] also reported that, by reducing the voltage during fraction collection, recovery could be increased, and obtained a recovery of ca. 60%, also based on peak areas. Finally, to avoid any memory effect during the fraction collection, it is recommended that the

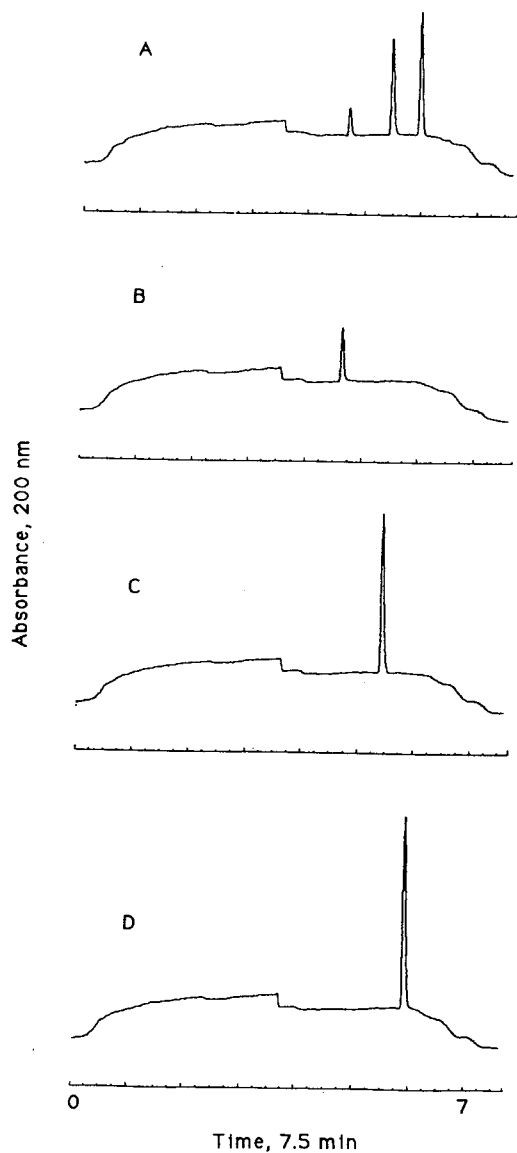


Fig. 4. Electropherograms of the mixture of three peptides, and of the three collected fractions reinjected under analytical conditions. A 63 cm  $\times$  50  $\mu$ m I.D. capillary, with 41 cm length to the UV detector, was used. The injection volume was ca. 20 nl. (A) Electropherogram of the mixture of the three synthetic peptides used in Fig. 3 (in Fig. 3, an ca. 200-fold greater amount was injected); peaks from left to right represent DynA<sub>1-17</sub> ( $t = 4.7$  min), SP ( $t = 5.5$  min), and LE-K ( $t = 6.0$  min), respectively. (B–D) Electropherograms of the individually collected DynA<sub>1-17</sub> ( $t = 4.7$  min), SP (5.4 min), and LE-K (5.9 min) fractions, respectively. AUFS = 0.005 for A–D.

ground electrode and the capillary be rinsed in a buffer vial between collections.

#### 4. Conclusions

Manual and automatic fraction collection are demonstrated for a commercial electropherograph using 50 and 100  $\mu$ m I.D. capillaries. When important factors such as voltage ramping/deramping, electrode/capillary rinsing, and empirical safety margin are experimentally determined and regulated, precise single or multiple collection without any memory effect is possible under these experimental conditions. A combination of reduced voltage and a delay period after the voltage is turned off maximizes the peptide recovery. Subsequent manipulation and analysis of the analyte obtained from the preparative CZE are important steps in identifying a peptide such as with amino acid sequence determination, especially when studying samples from biological sources.

#### Acknowledgement

This work was supported by NIH GM 26666 (D.M.D.).

#### References

- [1] J.W. Jorgenson and K.D. Lukacs, *Anal. Chem.*, 53 (1981) 1298–1302.
- [2] J.W. Jorgenson and K.D. Lukacs, *Science*, 222 (1983) 266–272.
- [3] F. Nyberg, M.D. Zhu, J.L. Liao and S. Hjertén, in C. Shaefer-Nielsen (Editor), *Electrophoresis '88*, VCH, New York, 1988, p. 141.
- [4] Z. Deyl, V. Rohlicek and R. Struzinsky, *J. Liq. Chromatogr.*, 12 (1989) 2515–2526.
- [5] Z. Deyl, V. Rohlicek and M. Adam, *J. Chromatogr.*, 480 (1989) 371–378.
- [6] J. Frenz, S.-L. Wu and W.S. Hancock, *J. Chromatogr.*, 480 (1989) 379–391.
- [7] P.D. Grossman, J.C. Colburn and H.H. Lauer, *Anal. Biochem.*, 179 (1989) 28–33.

- [8] T.A.A.M. Van de Goor, P.S.L. Janssen, J.W. Van Nispen, M.J.M. Van Zeeland and F.M. Everaerts, *J. Chromatogr.*, 545 (1991) 379–389.
- [9] E.C. Rickard, M.M. Strohl and R.G. Nielsen, *Anal. Biochem.*, 197 (1991) 197–207.
- [10] J.R. Florance, Z.D. Konteatis, M.J. Macielag, R.A. Lessor and A. Galdes, *J. Chromatogr.*, 559 (1991) 391–399.
- [11] H.-J. Gaus, A.G. Beck-Sickinger and E. Bayer, *Anal. Chem.*, 65 (1993) 1399–1405.
- [12] V.J. Hilser, Jr., F.D. Worosila and S.E. Rudnick, *J. Chromatogr.*, 630 (1993) 329–336.
- [13] H.J. Issaq, G.M. Janini, I.Z. Atamna, G.M. Muschik and J. Lukszo, *J. Liq. Chromatogr.*, 15 (1992) 1129–1142.
- [14] H.G. Lee and D.M. Desiderio, *J. Chromatogr. A*, 667 (1994) 271–283.
- [15] D.J. Rose and J.W. Jorgenson, *J. Chromatogr.*, 438 (1988), 23–34.
- [16] A.S. Cohen, D.R. Najarian, A. Paulus, A. Guttman, J.A. Smith and B.L. Karger, *Proc. Natl. Acad. Sci. U.S.A.*, 85 (1988) 9660–9663.
- [17] A. Guttman, A.S. Cohen, D.N. Heiger and B.L. Karger, *Anal. Chem.*, 62 (1990) 137–141.
- [18] R. Biehler and H.E. Schwartz, *Technical Bulletin TIBC-105*, Beckman Instruments, Palo Alto, CA, 1991.
- [19] M. Albin, S.-M. Chen, A. Louie, C. Pairaud, J. Colburn and J. Wiktorowicz, *Anal. Biochem.*, 206 (1992) 382–388.
- [20] P. Camilleri, G.N. Okafo, C. Southan and R. Brown, *Anal. Biochem.*, 198 (1991) 36–42.
- [21] N. Banke, K. Hansen and I. Diers, *J. Chromatogr.*, 559 (1991) 325–335.
- [22] C. Schwer and F. Lottspeich, *J. Chromatogr.*, 623 (1992) 345–355.
- [23] K.D. Altria and Y.K. Dave, *J. Chromatogr.*, 633 (1993) 221–225.
- [24] A.-F. Lecoq, S.D. Biase and L. Montanarella, *J. Chromatogr.*, 638 (1993) 363–373.
- [25] Y.-F. Cheng, M. Fuchs, D. Andrews and W. Carson, *J. Chromatogr.*, 608 (1992) 109–116.
- [26] X. Huang and R.N. Zare, *Anal. Chem.*, 62 (1990), 443–446.
- [27] X. Huang and R.N. Zare, *J. Chromatogr.*, 516 (1990) 185–189.
- [28] P. Camilleri, G.N. Okafo and C. Southan, *Anal. Biochem.*, 196 (1991) 178–182.
- [29] J. Gagnon and P. Goeltz, *Application Note DS-801*, Beckman Instruments, Palo Alto, CA, 1991.
- [30] S. Hjertén and M.-D. Zhu, *J. Chromatogr.*, 327 (1985) 157–164.
- [31] B.L. Karger, A.S. Cohen and A. Guttman, *J. Chromatogr.*, 492 (1989) 585–614.
- [32] Z. Deyl and R. Struzinsky, *J. Chromatogr.*, 569 (1991) 63–122.
- [33] J.P. Landers, R.P. Oda, T.C. Spelsberg, J.A. Nolan and K.J. Ulfelder, *BioTech.*, 14 (1993) 98–111.
- [34] J.L. Lovelace, J.J. Kusmierz and D.M. Desiderio, *J. Chromatogr.*, 562 (1991) 573–584.
- [35] X. Zhu and D.M. Desiderio, *J. Chromatogr.*, 616 (1993) 175–187.
- [36] J.J. Kusmierz, C. Dass, J.T. Robertson and D.M. Desiderio, *Int. J. Mass Spectrom. Ion Proc.*, 111 (1991) 247–262.
- [37] D.M. Desiderio, J.J. Kusmierz, X. Zhu, C. Dass, D. Hilton, J.T. Robertson and H.S. Sacks, *Biol. Mass Spectrom.*, 22 (1993) 89–97.
- [38] D.M. Desiderio, in D.M. Desiderio (Editor), *Mass Spectrometry of Peptides*, CRC Press, Boca Raton, FL, 1990, pp. 367–400.
- [39] *Analytical Consumer*, Vol. 3, No. 12, Analytical Consumer, Carlisle, MA, 1993.
- [40] H.G. Lee and D.M. Desiderio, *J. Chromatogr.*, 655 (1994) 9–19.
- [41] I.M. Johansson, E.C. Huang, J.D. Henion and J. Zweigenbaum, *J. Chromatogr.*, 554 (1991) 311–327.
- [42] J. Harbaugh, M. Collette and H.E. Schwartz, *Technical Bulletin TIBC-103*, Beckman Instruments, Spinco Division, Palo Alto, CA, 1990.
- [43] *Model 3140 Capillary Electropherograph Instruction Manual*, Isco, Lincoln, NE, 1991.
- [44] D.S. Burgi and R.-L. Chien, *Anal. Chem.*, 63 (1991) 2042–2041.



## Separation of imidazole and its derivatives by capillary electrophoresis<sup>☆</sup>

C.P. Ong<sup>a</sup>, C.L. Ng<sup>b</sup>, H.K. Lee<sup>b</sup>, S.F.Y. Li<sup>b,\*</sup>

<sup>a</sup>Analytical Services, Quality Department, Glaxo Development, 1 Pioneer Road, Sector 1, Jurong, Singapore 2262, Singapore

<sup>b</sup>Department of Chemistry, National University of Singapore, Kent Ridge Crescent, Singapore 0511, Singapore

First received 31 January 1994; revised manuscript received 1 August 1994

### Abstract

The use of capillary electrophoresis (CE) for the separation of imidazole and its derivatives is reported. In the first part of the investigation, efforts were focused on method development, where the effects of buffer pH, types of buffer modifiers and modifier concentration on the separation of these compounds were examined. The second part was focused on method validation, where the ruggedness, selectivity, limits of detection and linearity were investigated. In the final part, the CE method was applied to commercial-grade imidazole. A comparison of the results obtained using the CE system was made with those obtained by HPLC. Good correlation between the two sets of results was obtained and superior efficiencies and better peak shapes for most of the imidazoles were also achieved using the CE system.

### 1. Introduction

The use of capillary electrophoresis (CE) in separation science has increased tremendously in recent years. Major attributes of CE are the high efficiencies and separation selectivities possible [1,2]. As a result, separations of mixtures which in the past have been classified as inseparable or very difficult to chromatograph may nowadays be possible using CE. Consequently, there is growing interest in its use as a supplement to or as a replacement for existing methods such as high-performance liquid chromatography (HPLC) and gas chromatography (GC) [1].

In this work, the use of CE for the separation of imidazole and its derivatives is demonstrated. The imidazole ring is a component of several important groups of compounds such as purine, histamine and histidine. As a result, imidazoles are widely used as starting materials in the pharmaceutical industry [3] and as important intermediates in herbicides [4]. Therefore, the purity of imidazole and its derivatives used as starting materials is an important aspect to consider in industrial processes.

Currently, most imidazoles are analysed using techniques such as HPLC or GC. HPLC, even though routinely used, suffers from the usual peak tailing commonly observed in the analysis of basic compounds. GC analysis is limited to only a few volatile imidazoles. Therefore, in this work, attempts were made to study the feasibility of using CE for the separation of imidazoles.

\* Corresponding author.

<sup>☆</sup> Presented at the 6th International Symposium on High Performance Capillary Electrophoresis, San Diego, CA, 31 January–3 February 1994.

As part of method development, the effects of buffer pH, modifiers and modifier concentrations on the separation of these compounds were examined. The migration behaviour of these compounds under the various experimental conditions was investigated. A key focus of this work was an attempt to perform method validation on the CE system. In this regard, the ruggedness, selectivity, limits of detection and linearity range of the CE system were examined. The methodology developed was demonstrated using laboratory-built and commercial instruments. Further, the results obtained were compared with those obtained by HPLC.

### 3. Experimental

#### 3.1. Instrumental

Experiments were conducted on a laboratory-built CE system and two commercial instruments. In the laboratory-built instrument, a Spellman (Plainview, NY, USA) RM15P10KD power supply capable of delivering up to 15 kV was used. A Carlo Erba (Milan, Italy) MicroUVis20 UV detector with the wavelength set at 214 nm was used for the detection of peaks. A P/ACE 2000 (Beckman, Palo Alto, CA, USA) and a Waters Quanta 4000 (Milford, MA, USA) were on loan from the respective instrument companies. UV filters of 214 nm were used for both commercial instruments. Untreated fused-silica capillaries were obtained from Polymicro Technologies (Phoenix, AZ, USA). Chromatographic data were collected and analysed using a Hewlett-Packard (Avondale, Palo Alto, CA, USA) HP3394A integrator and a Shimadzu (Kyoto, Japan) R-6A integrator.

#### 3.2. Chemicals and materials

Sodium dodecyl sulphate (SDS), sodium tetraborate and sodium dihydrogenphosphate were purchased from Fluka (Buchs, Switzerland), tetrabutylammonium hydrogensulphate (TBA) from Sigma (St. Louis, MO, USA) and 1-methylimidazole and 4-methylimidazole from

Aldrich (Milwaukee, WI, USA). Standards of imidazole and 2-methylimidazole of analytical-reagent grade were gifts from Glaxo Development (Singapore). Samples of 2-methylimidazole used for the assay and impurity studies were also supplied by Glaxo Development.

#### 3.3. Procedures

Standards at a concentration of 1 mg/ml were dissolved in HPLC-grade methanol. SDS and TBA of various concentrations were dissolved in 25 mM sodium tetraborate–sodium dihydrogenphosphate buffers.

### 4. Results and discussion

#### 4.1. Method development

##### *Effect of pH*

Initial experiments performed using capillary zone electrophoresis (CZE) conditions at various pHs showed some interesting trends. At  $\text{pH} < 8$ , two peaks corresponding to the four imidazoles which eluted before methanol were noted. On the other hand, a single peak was observed at  $\text{pH} > 8$ .

This observation is consistent with the fact that the imidazoles are moderately strong bases. As a result, positive charges may reside on the imidazole ring under suitable pH conditions (in this case,  $\text{pH} < 8$ ). As in typical CZE separations, these positively charged species would tend to migrate out earlier than the neutral solvent molecules. However, at higher pH ( $> 8$ ), these compounds are neutral. As selectivity in CZE tends to be poor for the separation of neutral compounds, it was therefore expected that at  $\text{pH} > 8$  the neutral imidazoles would co-elute with methanol.

As the imidazole derivatives are very similar in structure, optimization of separation by varying the pH alone would not be sufficient. In CE separations of neutral species, modifiers such as surfactants [5] and tetrabutylammonium salts are usually added to enhance selectivity. In this



work, SDS and TBA as modifiers were investigated.

#### Effect of sodium dodecyl sulphate (SDS)

Fig. 1 shows the migration behaviour of the imidazole derivatives at various SDS concentrations. A general trend observed is that with the addition of SDS to the buffer system, e.g. at 60 mM, almost complete separation of the imidazoles was obtained. This marked improvement in the selectivity is possible as the addition of SDS is expected to provide a micellar environment which acts as a pseudo-stationary phase for the system [5]. The neutral imidazole molecules, in response to the micellar environment, are expected to undergo interaction with SDS micelles

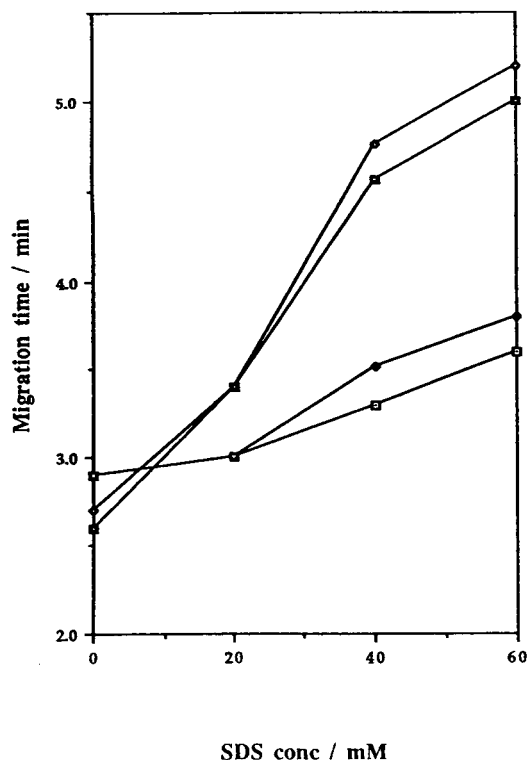


Fig. 1. Plot of migration times versus SDS concentration. Electrophoretic conditions: 25 mM phosphate–borate buffer (pH 8) with various SDS concentrations; voltage, 15 kV; column, 40 cm effective length  $\times$  50  $\mu$ m I.D. fused silica; detection wavelength, 214 nm. □ = Imidazole; ◆ = 1-methylimidazole; ■ = 2-methylimidazole; ◇ = 4(5)-methylimidazole.

via solubilization into the cavity of the SDS micelles. The extent of interaction is expected to be dependent on the hydrophobicity of the imidazoles. The more hydrophobic, i.e., the more alkylated, the imidazole is, the more it would favour solubilization and therefore, it would migrate out later. In this way, different imidazoles would be separated as a result of the enhancement in selectivity due to the addition of SDS.

Another trend observed is that with increasing amount of SDS in the system, a corresponding increase in migration times for the imidazole was noted. It should be recognized that the increase in concentration of SDS in the buffer would promote and increase the probability of the interaction of the neutral imidazole with the micellar environment. As the negatively charged micelles are electrophoretically attracted to the anode, this would subsequently lead to a corresponding increase in migration times of the imidazoles.

#### Effect of tetrabutylammonium hydrogensulphate (TBA)

Fig. 2 shows the optimum chromatogram obtained with the addition of 10 mM TBA to the electrolyte solution. It can be seen that a signifi-

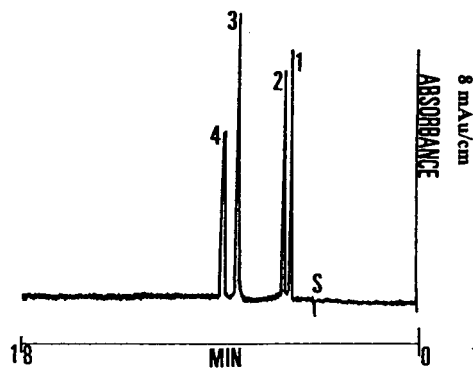


Fig. 2. Typical electropherogram for the separation of the imidazole derivatives. Electrophoretic conditions: 25 mM phosphate–borate buffer (pH 8.7)–100 mM SDS–10 mM TBA; voltage, 15 kV; column, 40 cm effective length  $\times$  50  $\mu$ m I.D. fused silica; detection wavelength, 214 nm. Peaks: S = methanol; 1 = imidazole; 2 = 1-methylimidazole; 3 = 2-methylimidazole; 4 = 4(5)-methylimidazole.

cant improvement in the peak shape was achieved using this system. This observation is consistent with those observed by Ong et al. [6] and Nishi et al. [7], i.e., the addition of TBA not only provided an additional pseudo-stationary phase to enhance selectivity, but also improved the overall peak shape of the positively charged imidazole derivatives by decreasing the interaction of these compounds with the negative charges on the capillary wall.

#### 4.2. Method validation

##### Selectivity

From Fig. 2, it can be seen that all the peaks were completely separated from each other with a resolution of at least 1.5. It should be emphasized that even though most of the imidazole derivatives differ from each other merely by the difference in the attachment of the methyl group to the main imidazole structure, the CE system developed in this work was able to provide the selectivity required for separation. In addition, the reduction in peak tailing and improvement in selectivity synergistically improved the overall separation and quantification capability. As a result, the method would provide an accurate identification and quantification method for imidazole and its derivatives. Further, it is worth noting that the total analysis time required was less than 10 min. This is a very attractive feature for implementation as a routine analytical method.

##### Ruggedness

The results obtained so far were obtained using the laboratory-built system. To demonstrate the ruggedness of the method, the same separation was performed on two commercial CE systems. Figs. 3 and 4 show the results obtained using the Beckman and Waters CE systems. Similar separation profiles with all three systems are observed (Figs. 2–4). The slight differences in migration times and detection responses observed were attributed to the differences in column lengths and detection windows. Nevertheless, from these results, it can be clearly seen that the CE method developed is a very

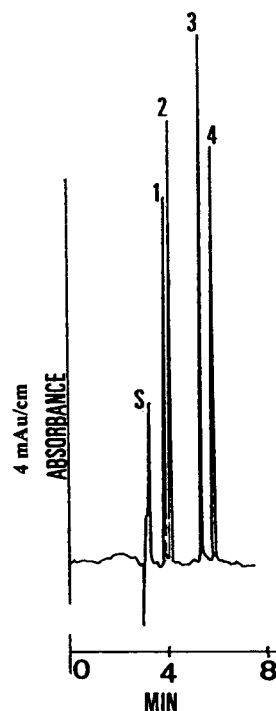


Fig. 3. Typical electropherogram for the separation of the imidazole derivatives using the Beckman commercial CE system. Electrophoretic conditions and peak identification as in Fig. 2.

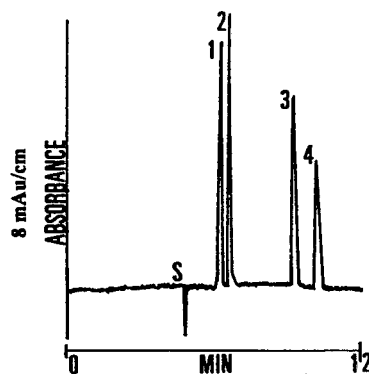


Fig. 4. Typical electropherogram of the separation of the imidazole derivatives using the Waters commercial CE system. Electrophoretic conditions and peak identification as in Fig. 2.

Table 1  
Comparison of the assay of 2-methylimidazole using HPLC and CE with commercial instruments

| HPLC       |                       | Beckman    |                       | Waters     |                       |
|------------|-----------------------|------------|-----------------------|------------|-----------------------|
| Purity (%) | R.S.D. (%)<br>(n = 3) | Purity (%) | R.S.D. (%)<br>(n = 3) | Purity (%) | R.S.D. (%)<br>(n = 4) |
| 100.2      | 0.2                   | 100.0      | 0.25                  | 99.5       | 3.0                   |

robust technique that is independent of instrumentation as long as similar parameters are used.

#### Linearity and detection limits

A linear calibration graph was obtained for the 2-methylimidazole at concentrations up to 1 mg/ml. Excellent linearity was observed with correlation coefficients greater than 0.999. A detection limit at ca. 30 pg using UV detection at 214 nm was obtained. These results are within the regular working range suitable for the analysis of these compounds.

#### 4.3. Application

The method was successfully employed to analyse samples obtained commercially. The results are given in Table 1. A typical HPLC trace and an electropherogram obtained using the Beckman instrument are shown in Figs. 5 and 6, respectively. A very important observa-

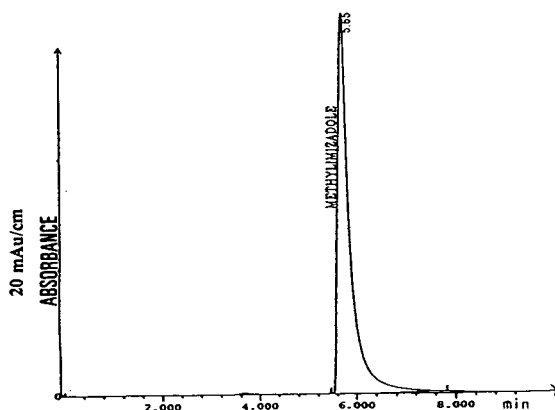


Fig. 5. Typical chromatogram for a commercial sample obtained using HPLC.

tion is that the extent of peak tailing in the CE analysis is much less than that in HPLC (Fig. 5). From Table 1, it can be seen that a good correlation was obtained for the three sets of results. The use of an internal standard, 4-methylimidazole, and more efficient temperature control resulted in better reproducibility in the CE analysis using the Beckman instrument compared with the Waters system. Although the R.S.D. for the analysis using the Waters instrument was slightly higher than those obtained by HPLC and the Beckman instrument, the results correlate very well with each other.

#### 5. Conclusions

CE is a viable alternative method for the separation of imidazole and its derivatives. Method validation was successfully performed to

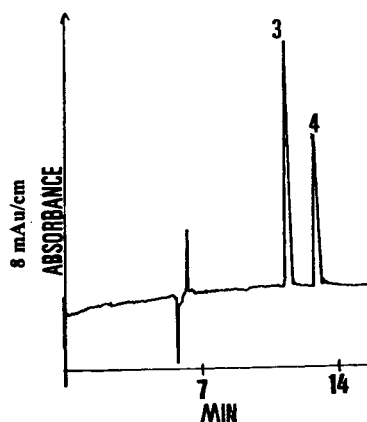


Fig. 6. Typical electropherogram for a commercial sample obtained using the Beckman commercial CE system. Electrophoretic conditions and peak identification as in Fig. 2.

confirm the ruggedness, selectivity and detection limits of the method. When comparing the results with those of HPLC, a good correlation was obtained between the two techniques. Further, CE exhibits less peak tailing and hence is preferable in terms of quantification and selectivity. The relatively short analysis time required for the analysis is another feature of the technique that is especially attractive for implementation in routine analysis.

#### Acknowledgements

The authors thank the National University of Singapore for financial support and Beckman (S) Pte. and Millipore (S) Pte. for the loan of commercial instruments.

#### References

- [1] S.F.Y. Li, *Capillary Electrophoresis—Principles, Practice and Applications* (Journal of Chromatography Library, Vol. 52), Elsevier, Amsterdam, 1992, Ch. 1.4, pp. 22–28.
- [2] J.W. Jorgenson and K.D. Lukacs, *Anal. Chem.*, 53 (1981) 1298–1302.
- [3] M.D. Nair and K. Nagarajan, *Prog. Drug Res.*, 27 (1983) 163–252.
- [4] K. Ebel, H. Koehler, A.O. Gamer and R. Jackh, in F.D. Snell and L.S. Ettre (Editors), *Encyclopedia of Industrial Analysts*, Vol. A13, Wiley, New York, 1971, pp. 661–668.
- [5] S. Terabe, K. Otsuka, K. Ichikawa, A. Tsuchiya and T. Ando, *Anal. Chem.*, 56 (1984) 111.
- [6] C.P. Ong, C.L. Ng, H.K. Lee and S.F.Y. Li, *J. Chromatogr.*, 588 (1991) 335–339.
- [7] H. Nishi, N. Tsumagari and S. Terabe, *Anal. Chem.*, 61 (1989) 2434.



ELSEVIER

Journal of Chromatography A, 686 (1994) 325–332

JOURNAL OF  
CHROMATOGRAPHY A

# Speciation of heavy metals by capillary electrophoresis<sup>☆</sup>

Carla Vogt\*, Gerhard Werner

*University of Leipzig, Faculty of Chemistry and Mineralogy, Institute of Analytical Chemistry, Linnéstrasse 3, 04103 Leipzig, Germany*

First received 30 January 1994; revised manuscript received 1 August 1994

## Abstract

The general abilities of capillary electrophoretic methods [capillary zone electrophoresis (CZE), isotachopheresis and isoelectric focusing] to perform species analysis are described. Several examples of the speciation of heavy metal complexes (e.g., complexes of gadolinium, platinum and iron) and metal oxoanions (arsenic and selenium) using CZE are demonstrated and the applicability to separation problems in the fields of medicine, pharmacology and ecology is discussed.

## 1. Introduction

In recent years, the level of knowledge about the different chemical forms of the elements has continually increased. The term "speciation" was used in the past only for metals. Today speciation, the determination of the different bonding forms and oxidation states of an element in a sample, which together add up to the total concentration, is applied to the whole Periodic System (excluding C, H and O). The reasons for stepping up species analysis are attributed to the different chemical and biological behaviours of each species. For the general assessment of ecosystems it is essential to know which species of the elements exist in the systems, as they have a major influence on the processes of distribution, accumulation and decomposition. In medi-

cine bioavailability, toxicity, essentiality or enzymatic principles of action are determined by the interaction of different species in the biological material. All species possess their own characteristic behaviour and can react in different matrices to different reaction products. Therefore, high demands are placed on analytical methods and sample preparation to determine all bonding forms of a particular element in a sample simultaneously, as the species can possess very similar in addition to very different chemical and physical properties. Most analytical methods are not applicable to a direct species analysis, because the resolving power of the technique sets limits for the differentiation between very similar species or the species are transformed irreproducibly during the analysis. In Table 1 an overview is given of the few analytical methods that can be used for direct speciation. If an additional separation step is integrated into the analysis, speciation is also possible using a number of common analytical methods (Table 2). Among them, capillary elec-

\* Corresponding author.

<sup>☆</sup> Presented at the 6th International Symposium on High Performance Capillary Electrophoresis, San Diego, CA, 31 January–3 February 1994.

Table 1  
Analytical methods for direct speciation measurements

| Analytical method      |   | Detection parameter              |
|------------------------|---|----------------------------------|
| AES                    | Auger electron spectroscopy   | <i>E</i> of Auger electrons      |
| XPS                    | X-ray photoelectron spectroscopy  | <i>E</i> of photoelectrons       |
| EXAFS                  | Energy-dispersive X-ray absorption fine structure   | $K\alpha$                        |
| ESR                    | Electron spin resonance spectroscopy  | <i>E</i> of resonance absorption |
| NMR                    | Nuclear magnetic resonance spectroscopy of the nuclei $^{19}\text{F}$ , $^{25}\text{Mg}$ , $^{27}\text{Al}$ , $^{29}\text{Si}$ , $^{31}\text{P}$ , $^{43}\text{Ca}$ , $^{113}\text{Cd}$ , $^{195}\text{Pt}$ , $^{199}\text{Hg}$ and $^{207}\text{Pb}$ | $\nu$ frequency of resonance     |
| Mössbauer spectroscopy | Mass spectrometry   | <i>m/z</i>                       |
| Electrochemistry       | Amperometry, polarography   | $U^0$                            |

trophoresis is characterized by the highest resolving power and extensive possibilities of varying the analytical conditions. The separation process is performed on the basis of the different electrophoretic mobilities, which depend on the structures and the radii of the ions, therefore possessing ion-specific characteristics. Even very similar species with nearly the same electrophoretic mobilities (e.g., differences of 0.05% between two electrophoretic mobilities) can be separated by this method and the preservation of the original bonding forms is often possible by choosing suitable buffer systems. An overview of the few papers dealing with direct speciation through electrophoretic separations in capillaries is given in Table 3.

In this work, we tested the potential of capillary zone electrophoresis (CZE) for speciation measurements using different kinds of samples, especially pharmaceutical formulations. We dem-

Table 3  
Speciation measurements with capillary electrophoresis methods (CZE, ITP, IEF)

| Species   | Method used | Ref.  |
|---|-------------|-------|
| $[\text{Fe}(\text{CN})_6]^{3-}$ , $[\text{Fe}(\text{CN})_6]^{4-}$             | ITP         | 1     |
| $[\text{Fe}(\text{CN})_6]^{3-}$ , $[\text{Fe}(\text{CN})_6]^{4-}$             | CZE         | 2     |
| $\text{SeO}_3^{2-}/\text{SeO}_4^{2-}$ , $\text{TeO}_3^{2-}/\text{TeO}_4^{2-}$ | ITP         | 3     |
| Aluminium fluoride and oxalate  | CZE         | 4     |
| Organic selenium and lead compounds   | CZE         | 5     |
| Cobaltocboranes   | ITP         | 6     |
| Cobalamines   | CZE, HPLC   | 7, 8  |
| Haemoglobins  | IEF, CZE    | 9, 10 |
| $\text{AsO}_3^{3-}/\text{AsO}_4^{3-}$   | CZE         | 11    |

onstrate the ability of the method to separate metal oxoanions (species of arsenic and selenium) with very different and metal complexes (species of platinum, gadolinium and iron) with very similar electrophoretic mobilities.

Table 2  
Analytical methods for direct speciation after a separation step

| Analytical method               | Specific property used for separation                    | Detection parameter                                    |
|---------------------------------|--|--|
| HPLC (HPLC–AAS or HPLC–ICP–AES) | Distribution, adsorption, ion exchange, steric exclusion | $\lambda$ of atomic absorption and emission lines      |
| GC (GC–AES or GC–MS)            | Distribution, adsorption                                 | $\lambda$ of atomic emission lines, <i>m/z</i>         |
| Ion chromatography              | Distribution, ion exchange                               | $pK_a$ , conductivity                                  |
| Electrophoresis (IEF, ITP, CZE) | Electrophoretic mobility, <i>pI</i>                      | UV–vis absorption, fluorescence emission, conductivity |

## 2. Experimental

### 2.1. Materials

All phosphate and chromate buffers were prepared with sodium salts of research grade (Merck, Darmstadt, Germany). Methanol (LiChrosolv for chromatography) (Merck) and acetonitrile (R Chromasolv for HPLC) (Riedel-de Haën, Seelze, Germany) were used for the addition to the separation buffers. To adjust the pH of the buffer, tris(hydroxymethyl)amino-methane(Tris) and sodium hydroxide (both from Merck) were used. Hexadecyltrimethylammonium bromide (HTAB) (Merck) was used as an osmotic flow modifier and sodium dodecyl sulfate (SDS) (Riedel-de Haën) as a micelle-forming agent.

For the preparation of standard solutions of different metal-containing species, the following substances (all of research grade) were employed: NaAsO<sub>2</sub> (solution), H<sub>3</sub>AsO<sub>4</sub>, NaCl, Na<sub>2</sub>SO<sub>4</sub> (all from Merck), Na<sub>2</sub>SeO<sub>3</sub>·5H<sub>2</sub>O, Na<sub>2</sub>SeO<sub>4</sub> (Fluka, Buchs, Switzerland) and ferrocene, ferrocenecarboxaldehyde, butylferrocene, Gd(Cl)<sub>3</sub>·6H<sub>2</sub>O and diethylenetriaminepentaacetic acid (all from Aldrich, Steinheim, Germany). The ligand for the Gd complex Roman 1 was synthesized according to a new procedure [12]. Rat serum and lobaplatin [1, 2 - di(aminomethyl)cyclobutaneplatinum(II) lactate] were supplied by Arzneimittelwerk Dresden (Dresden, Germany).

### 2.2. Apparatus

A P/ACE 2000 capillary electrophoresis system from Beckman (Palo Alto, CA, USA) was used for CZE measurements. In all measurements the UV-Vis absorption of the double or triple bonds in the organic part of the analyte compounds or the UV signals of the buffer systems were utilized for the detection of the species at 200, 214 and 254 nm using a detector system with fixed wavelengths. Polyimide-clad fused-silica capillary tubing of 50 and 75 μm I.D. was obtained from CS-Chromatographie Service (Langerwehe, Germany).

## 3. Results and discussion

### 3.1. Species of arsenic and selenium

The inorganic species arsenite, arsenate, selenite and selenate were the first to be subjected to species analysis. Several papers have dealt with the simultaneous determination of both oxidation states of these elements [3,11,13] and of their organometallic compounds [14,15].

In aqueous solution the species exist as small oxoanions, which possess one to three negative charges depending on the pH of the electrophoresis buffer. Therefore, they rapidly migrate to the anode and can be separated in the same buffers such as chloride, sulfate or carbonate. Because of the low absorptivity in the UV region, a UV-absorbing buffer such as chromate, which must migrate fairly fast, is to be preferred. As can be seen from Table 4, the anions in the higher oxidation states, arsenate and selenate, possess very low pK<sub>a,1</sub> values and even at medium pH have two negative charges. Arsenate and selenate will migrate very fast over a wide pH range of 6.5–10. Arsenite and selenite show a higher charge density on the surface because of smaller ionic radii and therefore the dissociation of protons makes higher demands on energy consumption. Hence the pK<sub>a,1</sub> values are high and both oxoanions possess only a negative charge of <-1. Large differences in charge at medium pH are not useful for fast speciation, because the slowly migrating species arsenite and selenite give broad peak shapes and the analysis time is very long. If only selenite and selenate have to be separated, a pH of 9 is sufficiently high for a fast separation. Fig. 1 shows the separation of all four species operating at pH 10.

Table 4  
pK<sub>a</sub> values of arsenic and selenium acids

| Acid                            | pK <sub>a,1</sub> | pK <sub>a,2</sub> | pK <sub>a,3</sub> |
|---------------------------------|-------------------|-------------------|-------------------|
| H <sub>3</sub> AsO <sub>4</sub> | 2.18              | 6.77              | 11.23             |
| H <sub>3</sub> AsO <sub>3</sub> | 9.40              | 13.52             |                   |
| H <sub>2</sub> SeO <sub>4</sub> | <0                | 1.92              |                   |
| H <sub>2</sub> SeO <sub>3</sub> | 2.54              | 8.02              |                   |

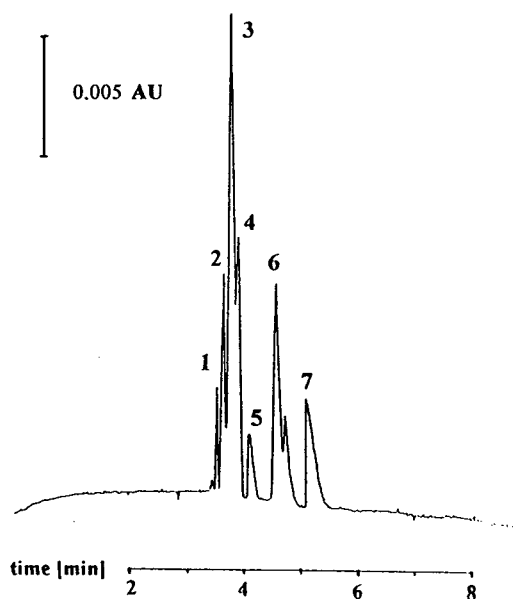


Fig. 1. Separation of arsenic and selenium species. Buffer, 5 mM chromate (pH 10.0, adjusted with Tris)–0.25 mM HTAB; capillary, 50/57 cm  $\times$  75  $\mu$ m I.D.;  $U = -15$  kV; indirect detection at 254 nm. Pressure injection of a  $10^{-4}$  M solution of each component. Peaks: 1 =  $\text{Cl}^-$ ; 2 =  $\text{SO}_4^{2-}$ ; 3 =  $\text{HAsO}_4^{2-}$ ; 4 =  $\text{SeO}_4^{2-}$ ; 5 =  $\text{F}^-$ ; 6 =  $\text{SeO}_3^{2-}$ ; 7 =  $\text{H}_2\text{AsO}_3^-$ .

Only at this pH is speciation of arsenite and arsenate possible in the chromate buffer system. For a good separation of all compounds in this sample, measurements at reversed polarity and with the addition of an osmotic flow modifier (OFM), such as HTAB, is necessary. Depending on the concentration of this modifier the negative charge of the capillary wall, generated by the dissociation of silanol groups, is decreased, removed or reversed. In this way the separation time can be shortened by elimination or reversal of the electroosmotic flow.

### 3.2. Complexes of gadolinium

There is a continuing search for suitable paramagnetic compounds usable as contrasting agents in magnetic resonance imaging. Gadolinium–diethylenetriaminepentaacetic acid complex (Gd–DTPA) possesses the most suitable characteristics of high magnetic moment,

high stability ( $\log K = 23$ ) and low toxicity. Because of the high toxicity of free  $\text{Gd}^{3+}$  ion, the determination of the dissociation behaviour of the complex in vivo and the separation of the Gd–DTPA complex from other gadolinium complexes is required.

A complete separation of all three components, Gd–DTPA, free DTPA ligand and free  $\text{Gd}^{3+}$  ion, has not previously been successful because of the very different chemical properties of the three components and their poor absorption characteristics in the UV–Vis region. Separation of the complex and the ligand was achieved by Vora et al. [16] using HPLC. In our work we tried to separate Gd–DTPA from another gadolinium complex, which was formed with a new polyaminopolyacetic acid ligand, synthesized after a recently developed procedure [12] and currently the subject of suitability tests

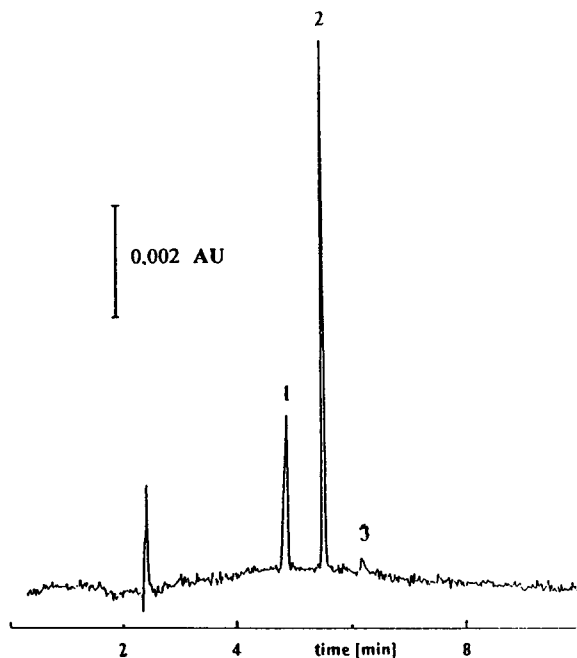


Fig. 2. Separation of Gd complexes. Buffer, 25 mM phosphate (pH 6.8)–10% acetonitrile; capillary, 50/57 cm  $\times$  50  $\mu$ m I.D.;  $U = 25$  kV;  $I = 60$   $\mu$ A; detection at 200 nm. Pressure injection of a mixture of Gd–DTPA complex and Roman 1 (Gd complex), each complex  $10^{-3}$  M. Peaks: 1 = Roman 1 (Gd complex); 2 = Gd–DTPA complex; 3 = impurity from 2.



for magnetic resonance imaging. Both complexes possess high stability constants, and therefore a separation in an electrophoretic buffer is possible. The chosen separation conditions, demonstrated in Fig. 2, allow a very fast separation of both complexes, although the free ligands could not be detected. The free ligands are highly dissociated and because of the absence of ion-pairing compounds in the buffer the negative charges could not be compensated. The hydrated free  $Gd^{3+}$  moves very fast. Nevertheless, the detection of the ion was impossible because of its very low molar absorptivity in the detectable UV region.

The demonstrated separation is suitable for the determination of complex stabilities and will be used for the characterization of newly synthesized polyaminopolyacetic acids as ligands for

gadolinium complexes in comparison with the DTPA ligand.

### 3.3. Separation of diastereomeric platinum complexes

Platinum complexes have been successfully applied in cancer therapy for many years [17]. Well known is cisplatin [*cis*-diamminedichloroplatinum(II)] as the first compound to be administered. Second-generation substances are iproplatin [*cis*-dichloro-*trans*-dihydroxydi(isopropylamine)platinum(IV)] and lobaplatin [1,2-di(aminomethyl)cyclobutaneplatinum(II) lactate], which are now undergoing clinical tests.

Lobaplatin is a racemic mixture of diastereomers. To control the efficiency of dosages given to patients, separation of the diastereomers in

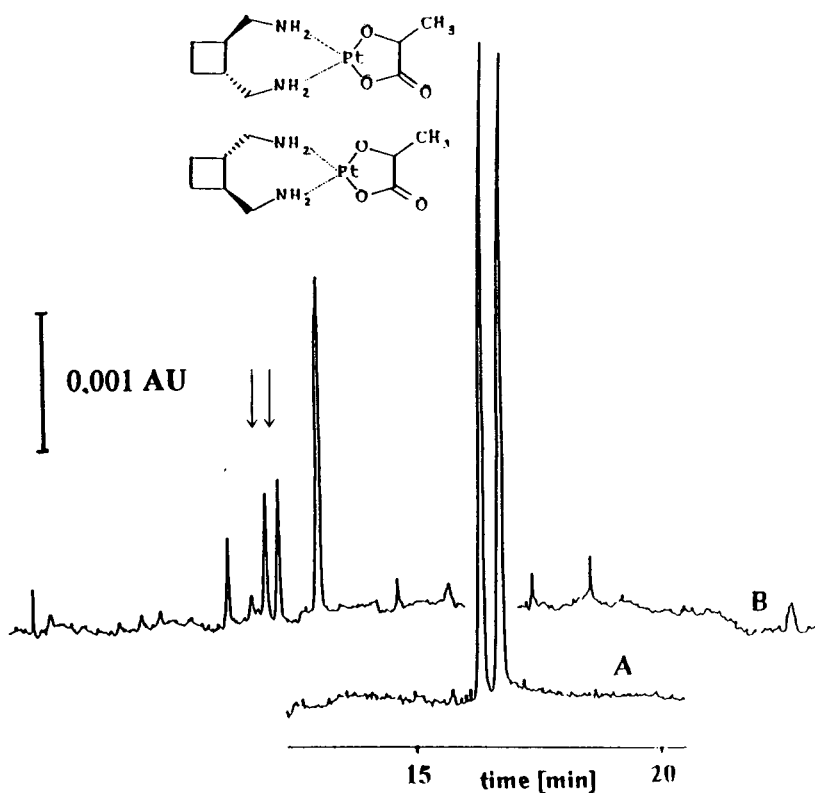


Fig. 3. Separation of diastereomeric platinum complexes (lobaplatin). Buffer, 20 mM phosphate (pH 6.7)–(90 mM SDS; capillary, 70/77 cm  $\times$  75  $\mu$ m I.D.;  $U = 20$  kV;  $I = 190$   $\mu$ A; detection at 214 nm. (A) Standard solution ( $5 \cdot 10^{-4}$  M) of platinum complexes; (B) rat serum (diluted 1:4 with water), spiked with platinum complexes.

plasma is necessary. In Fig. 3A a lobaplatin standard containing  $2.82 \cdot 10^{-4}$  M of each diastereomer was separated. The buffer was chosen considering the pH range of real samples. Various concentrations of the micelle-forming agent SDS were applied to optimize the separation. The addition of micelle-forming compounds to the buffer leads to the introduction of supplementary separation effects, comparable to the interaction of an analyte with the stationary phase in liquid chromatography and therefore called a "quasi-stationary phase" [18]. Hydrophobic components are able to interact inside the micelles, which also possess a hydrophobic character. Differences in the partition coefficients between the buffer and the micelles, existing for two compounds with nearly the same electrophoretic mobilities, result in different migration times owing to the electrophoretic migration of the micelles. Advantage can be taken of this effect for the separation of diastereomers. With increasing amount of added SDS an increase in resolution of the diastereomers was achieved, explainable by the different partition coefficients for the two diastereomers inside the micelles. Fig. 3A represents an optimum separation concerning resolution and analysis time. In Fig. 3B, prior to the analysis lobaplatin was adjusted to a concentration of  $1.41 \cdot 10^{-4}$  M for each diastereomer in the rat plasma. In addition to lobaplatin diastereomers some proteins of the plasma could also be separated. Reproducible repetitions of this analysis are difficult to achieve, however, because of protein adsorption on uncoated capillary walls. Unfortunately, under the chosen analytical conditions without a preconcentration step the detection limit for platinum compounds is not low enough for a real plasma analysis because of the relatively low absorptivity of the compounds and the comparatively fixed detection volumes.

### 3.4. Ferrocene and ferrocene derivatives

Ferrocenes are characterized by wide applicability in the modern industry [19], especially as catalysts and photosensitizers in the or-

ganometallic and semiconductor industry, and in medicine as anticancer drugs. We developed a separation method for ferrocenes to control the purity of commercially available and newly synthesized compounds and to investigate degradation processes of these substances.

In Fig. 4, the separation of three purchased ferrocenes is demonstrated. To avoid recrystallization of the dissolved ferrocenes inside the capillary, the application of a buffer containing large amounts of acetonitrile was essential. At the applied buffer pH all three compounds possess a net charge of zero, and therefore the differences in their migration should be reduced to the interaction inside the micelles of the SDS molecules. For butylferrocene we were able to confirm the specification of a content of 97% certified by the manufacturer.

Fig. 5 shows the separation of the synthesized ferrocene derivatives [20]. These compounds are candidates for application as mediators in scan-

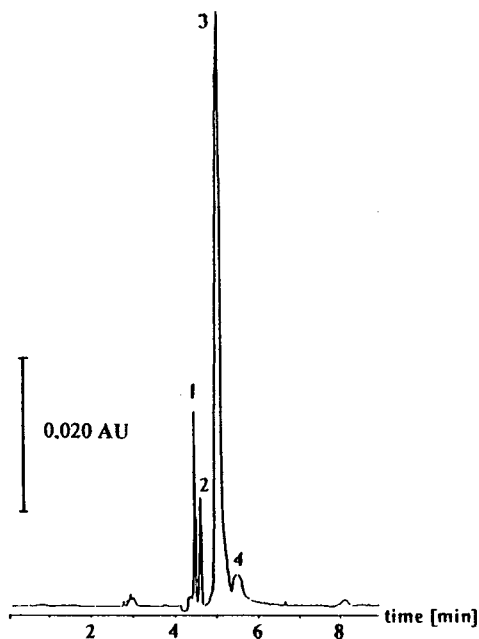


Fig. 4. Separation of ferrocene derivatives. Buffer, 10 mM phosphate (pH 6.7)–30 mM SDS–35% acetonitrile; capillary, 70/77 cm  $\times$  75  $\mu$ m I.D.;  $U = 25$  kV;  $I = 86$   $\mu$ A; detection at 214 nm. Peaks: 1 = ferrocenecarboxaldehyde; 2 = ferrocene; 3 = butylferrocene; 4 = impurity from 3.

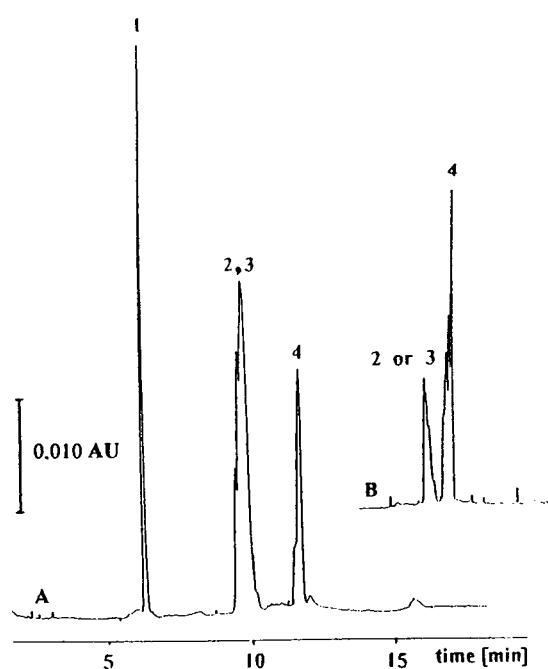


Fig. 5. Separation of ferrocene derivatives. Buffer, 10 mM phosphate (pH 6.6)–30 mM SDS–35% acetonitrile; capillary, 70/77 cm  $\times$  75  $\mu$ m I.D.;  $U = 30$  kV;  $I = 72$   $\mu$ A; detection at 214 nm; pressure injection. Peaks: 1 = (trimethylaminomethyl)ferrocene; 2 = (dimethyl-*n*-dodecylaminomethyl)ferrocene ( $n = 5$ ); 3 = (dimethyl-*n*-hexadecylaminomethyl)ferrocene ( $n = 7$ ); 4 = (dimethyl-*n*-octylaminomethyl)ferrocene ( $n = 3$ ). (A) Mixture of all four ferrocene derivatives; (B) (dimethyl-*n*-octylaminomethyl)ferrocene.

ning electrochemical microscopy and for the surface modification of electrodes for electrochemical measurements, where the expected signals should depend on the chain length of the fixed ferrocenes. The separation of all four synthesized derivatives (Fig. 5A) was not completely achieved, only the two compounds with the shortest chain length are well separated. The observed migration order is not typical of CZE or even HPLC, where in most instances a proportionality between chain length and migration/retention time is found. It appears that the synthesis of the compounds giving peaks 2 and 3 did not produce the expected compounds. This assumption was also confirmed by NMR measurements which were performed later. In Fig.

5B the separation of (dimethyl-*n*-octylaminomethyl)ferrocene shows that even during this synthesis byproducts were formed. We found that the alkyl bromides purchased for the synthesis were mixtures of bromides with different lengths of the alkyl chains. Further investigations are now directed to synthesizing pure derivatives usable for analytical purposes.

Because of its resolving power, CZE is well suited to separate different species of one element simultaneously with both nearly the same and very different electrophoretic mobilities. In the future efforts need to be made to achieve lower detection limits for species with low molar absorptivities in the UV–Vis region utilizing preconcentration steps or suitable detection systems.

## References

- [1] M. Tazaki, M. Takagi and K. Ueno, *Chem. Lett.*, 5 (1982) 639.
- [2] M. Aguilar, T. Huang and R.N. Zare, *J. Chromatogr.*, 480 (1989) 427.
- [3] H. Yoshida and M. Hida, *J. Chromatogr.*, 351 (1986) 388.
- [4] N. Wu, W.J. Horvath, P. Sun and C.W. Huie, *J. Chromatogr.*, 635 (1993) 307.
- [5] C.L. Ng, H.K. Lee and S.F.Y. Li, *J. Chromatogr. A*, 652 (1993) 547.
- [6] M. Koval, D. Kaniansky, L. Matel and F. Macasek, *J. Chromatogr.*, 243 (1982) 144.
- [7] D. Lambert, C. Adjalla, F. Felden, S. Benhanyoun, J.P. Nicolas and J.L. Guéant, *J. Chromatogr.*, 608 (1992) 311.
- [8] S. Fanali, L. Ossicini and M. Sinibaldi, *Chromatographia*, 23 (1987) 811.
- [9] M. Zhu, T. Wehr, V. Levi, R. Rodrigues, K. Shiffer and Z.A. Cao, *J. Chromatogr. A*, 652 (1993) 119.
- [10] M. Zhu, R. Rodriguez, T. Wehr and Ch. Siebert, *J. Chromatogr.*, 608 (1992) 225.
- [11] B.L. Wildman, P.E. Jackson, W.R. Jones and P.G. Alden, *J. Chromatogr.*, 546 (1991) 459.
- [12] *German Pat. Appl.*, No. 4406 465.9.
- [13] I.T. Urasa and F. Ferede, *Anal. Chem.*, 59 (1987) 1563.
- [14] G. Rauret, R. Rubio and A. Padro, *Fresenius' Z. Anal. Chem.*, 340 (1991) 157.
- [15] D.O. Duebelbeis, S. Kapila, D.E. Yates and S.E. Manahan, *J. Chromatogr.*, 351 (1986) 465.

- [16] M.M. Vora, S. Wukovnic, R.D. Finn, A.M. Emran, T.E. Boothe and P.J. Kothari, *J. Chromatogr.*, 369 (1986) 187.
- [17] B.K. Keppler (Editor), *Metal Complexes in Cancer Chemotherapy*, VCH, Weinheim, 1993.
- [18] S. Terabe, K. Otsuka, K. Ichikawa, A. Tsuchiya, T. Ando, *Anal. Chem.*, 56 (1984) 111.
- [19] B.W. Rockett and G. Marr, *J. Organomet. Chem.*, 416 (1991) 327.
- [20] M. Gomez and A.E. Kaifer, *J. Chem. Educ.*, 69 (1992) 502.

Short communication

## Synthesis and characterization of biospecific adsorbents containing glucose, usable to retain concanavalin A

C. Alvarez<sup>a</sup>, H. Bertorello<sup>a,\*</sup>, M. Strumia<sup>a</sup>, E.I. Sanchez<sup>b</sup>

<sup>a</sup>*Departamento de Química Orgánica, Facultad de Ciencias Químicas, Universidad Nacional de Córdoba, 5016 Córdoba, Argentina*

<sup>b</sup>*Facultad de Ciencias Naturales, Universidad Nacional de la Patagonia y San Juan Bosco, 9000 Chubut, Argentina*

First received 19 April 1994; revised manuscript received 2 August 1994

### Abstract

The synthesis and characterization of poly(butadiene–hydroxyethylmethacrylate–epichlorhydrin–D-glucose) (PB–HEMA–ECH–D–Glu) and poly(butadiene–hydroxyethylmethacrylate–epichlorhydrin–L-glucose) (PB–HEMA–ECH–L–Glu) hydrogels are presented. The applicability of these products was studied in order to establish their stereospecific capacity in the retention of concanavalin A.

### 1. Introduction

The synthesis of biospecific adsorbents used in affinity chromatography to purify biological macromolecules such as proteins, antibodies and enzymes is an important area of research [1–3]. Lectins, proteins capable of specific interaction with carbohydrate-containing substances, possess the ability to agglutinate erythrocytes of specific blood groups and different types of cells [4,5]. Concanavalin A (Con A), a lectin isolated from jack bean (*Canavalia ensiformis*), has become the most widely investigated lectin because it exhibits a series of remarkable properties. It has been used as haemagglutinin [6,7], for studies of cell surface and cell division, to examine the nature of the carbohydrate residues responsible for blood-group specificity and to distinguish between malignant or abnormal and normal cells. This glucose-binding lectin has been iso-

lated and purified to homogeneity by affinity chromatography on biospecific adsorbents: cross-linked dextran gel (Sephadex) [8–12], Sepharose as adsorbent followed by elution with methyl- $\alpha$ -D-glucosamino pyranoside [5] or using D-glucosamine immobilized on diol-bonded silica [13].

In this paper, we describe the synthesis and characterization of affinity materials and report on their utility in the biospecific retention of Con A. Epichlorhydrin was used for the introduction of reactive oxirane groups into a poly(butadiene–hydroxyethylmethacrylate) (PB–HEMA) synthetic matrix, followed by coupling of glucose (D- or L-).

### 2. Experimental

#### 2.1. Materials and analysis

Epichlorhydrin was obtained from Riedel-de

\* Corresponding author.

Haën, D-glucose from Anedra and L-glucose and concanavalin A from Sigma.

Determinations of hydroxyl and oxirane equivalents were carried out using the acetyl and pyridinium chloride methods, respectively [14].

Microdetermination of glucose (D- or L-) was carried out by spectrophotometry using the phenol-sulfuric acid method [15].

IR spectra were recorded on a Nicolet 5-SXC spectrometer. Scanning electron microscopy (SEM) was performed on a Phillips SEM 501 B instrument at the laboratories in the Centro de Investigaciones de Materiales y Metrología (CIMM).

Swelling indices ( $S_w$ ) were determined in water, after 48 h, as the ratio of the swollen ( $V_s$ ) and dried ( $V_d$ ) volumes of samples, respectively ( $S_w = V_s/V_d$ ).

Glass transition temperatures ( $T_g$ ) were determined on a Mettler TA 3000 DSC system at the laboratories in the Instituto de Desarrollo Tecnológico para la Industria Química (INTEC).

Lectins were measured using a modified version of the Lowry method [16] and UV-Vis spectra were measured with a Shimadzu UV 260 recording spectrophotometer.

## 2.2. Preparation of biospecific affinity adsorbents

### Activation of PB-HEMA matrix

The synthesis of the PB-HEMA matrix was carried out by graft copolymerization, using polybutadiene resin (PB), hydroxyethylmethacrylate (HEMA) and benzoyl peroxide. The activation of the synthesized matrix was performed using epichlorhydrin under alkaline conditions [17]. The matrix (PB-HEMA) and the corresponding epoxy-activated product poly-(butadiene-hydroxyethylmethacrylate-epichlorhydrin) (PB-HEMA-ECH) have been purified and characterized previously [17].

### Coupling of glucose (D- or L-) to the activated matrix

The biospecific adsorbents for concanavalin A lectin were prepared as follows: the epoxy-acti-

vated PB-HEMA-ECH matrix (1 g) was swollen in dimethylformamide (DMF) (10% w/v) for 17 h. This wet gel was mixed with a solution of D-glucose (or L-glucose) (2 g) in 0.1 M NaOH (48.84 ml) and  $\text{NaBH}_4$  ( $4 \cdot 10^{-3}$  g) was added. The mixture was incubated at 45°C for 8.5 h on a shaker in a water-bath.

The PB-HEMA-ECH-D-Glu and PB-HEMA-ECH-L-Glu hydrogels were washed extensively with water, 0.2 M sodium acetate buffer (0.5 M NaCl) at pH 4.0 and 0.2 M borate buffer (0.5 M NaCl) at pH 8.0. They were then studied by IR spectrometry, SEM and differential scanning calorimetry (DSC).

A portion of each product (0.1 g) was hydrolysed with 2 M HCl in dioxane-water (8:2) at 100°C for 23 h and the amount of carbohydrate covalently bound to the activated matrix was subsequently determined.

## 2.3. Biospecific affinity chromatography

A portion of each biospecific adsorbent obtained (0.1 g) was incubated with solutions of Con A (10 ml) at different concentrations (0.2, 0.4 and 0.8 mg/ml) in 1 M NaCl,  $1 \cdot 10^{-3}$  M  $\text{CaCl}_2$  and  $1 \cdot 10^{-3}$  M  $\text{MnSO}_4$  for 16 h at room temperature with stirring. All determinations were carried out in triplicate.

The amount of remaining and bound Con A per gram or millilitre of hydrogel was determined. The possible retention of Con A by epoxy-activated PB-HEMA-ECH matrix was also measured.

## 3. Results and discussion

### 3.1. Preparation of biospecific affinity adsorbents

#### Activation of PB-HEMA matrix

The PB-HEMA matrix, a yellowish powder, able to swell in water, contained 3.93 mequiv. of hydroxyl groups per gram of dry gel, which confers a hydrophilic character on the matrix and

provides non-ionic reactive functional groups capable of undergoing chemical modifications.

The reaction carried out between epichlorhydrin and the matrix involved its activation and attainment of a product with a high content of terminal oxirane functional groups, 0.74 mequiv. per gram of dry gel.

#### *Coupling of glucose (D- or L-) to the activated matrix*

The synthesis of PB-HEMA-ECH-D-Glu and PB-HEMA-ECH-L-Glu hydrogels involved the coupling of glucose (D- or L-) to the activated matrix under alkaline conditions, for which sodium borohydride was added in catalytic amounts to minimize side-reactions (decoloration, oxidative attack and decomposition) of the carbohydrates. The reactions were carried out using DMF as solvent in which the epoxidized matrix was highly swellable.

Both biospecific adsorbents, PB-HEMA-ECH-D-Glu and PB-HEMA-ECH-L-Glu, presented the same swelling index in water,  $S_w = 4.0$ . Samples were hydrolysed and the sugar contents were determined. The PB-HEMA-ECH-D-Glu gel was found to contain 40.08  $\mu\text{mol}$  of D-glucose per gram of dry gel or 10.02  $\mu\text{mol}$  of D-glucose per ml of swollen gel and therefore it was established that 65.11  $\mu\text{mol}$  of L-glucose had been attached per gram of dry gel or 16.25  $\mu\text{mol}$  of L-glucose had been attached per ml of swollen gel. It is known [18] that in the structure of the hydrogels, the carbohydrate binds preferentially by the primary hydroxyl of C-6, the most reactive hydroxyl group.

Bands at 3040, 1150–1160, 1050–1150 and 1030  $\text{cm}^{-1}$  were observed by IR spectrometry in the spectra, attributable to the stretching vibrations of primary and secondary hydroxyl groups, secondary hydroxyl groups of the glucose, ether and primary alcohol groups, respectively.

The microphotographs obtained from products by SEM showed a porous surface needed for the inclusion of biological macromolecules. This can be seen in Fig. 1.

The  $T_g$  of the products PB-HEMA, PB-HEMA-ECH and PB-HEMA-ECH-D-Glu, obtained from DSC curves, with values of 49.96,

41.10 and 35.20, respectively, suggested that, at room temperature, the products are rigid and hard. The fact that the  $T_g$  values do not rise with chemical modification by incorporation of epichlorhydrin and the ligand on the cross-linked PB-HEMA matrix could indicate that they occur on the surfaces in absence of cross-linkages. In general, the incorporation of aliphatic side-chains decreases the  $T_g$  value [19]. This is in accordance with the results obtained, leading to less rigid structures.

#### *3.2. Biospecific affinity chromatography*

In the binding to glucosidic residues, Con A requires  $\text{Mn}^{2+}$  and  $\text{Ca}^{2+}$  ions to form a quaternary structure and create the binding points to the carbohydrates. A transition metal such as  $\text{Mn}^{2+}$  is needed to bind  $\text{Ca}^{2+}$  and both are necessary for glucose or mannose binding [20].

Tables 1 and 2 summarize the results for the retention of Con A using the PB-HEMA-ECH-D-Glu and the PB-HEMA-ECH-L-Glu adsorbents, respectively, which differ in the relative capacity to retain the lectin. The absence of non-specific interactions (hydrophobics) was corroborated by using the epoxidized matrix, whose capacity to retain Con A was zero.

As can be observed in Table 1, the PB-HEMA-ECH-D-Glu adsorbent retained  $49.0 \pm 0.4$  mg of Con A lectin per gram of dry gel or 12.3 mg of Con A lectin per ml of swollen gel. The retention of Con A using PB-HEMA-ECH-L-Glu indicated a saturation of 4.1 mg of Con A lectin per ml of swollen gel (see Table 2).

In general, in affinity chromatography, the level of saturation of a ligand bound to the matrix is hyperbolically related to the concentration of proteins or biological macromolecules [21]. Consequently, to reach a high degree of gel saturation, the solution that contains the protein must be as concentrated as possible. This hypothesis was corroborated from the results for the retention of Con A lectin using the PB-HEMA-ECH-D-Glu hydrogel obtained.

Fig. 2 shows the structures of D-glucose and L-glucose. D-Glucose is a monosaccharide that contains binding points with Con A lectin

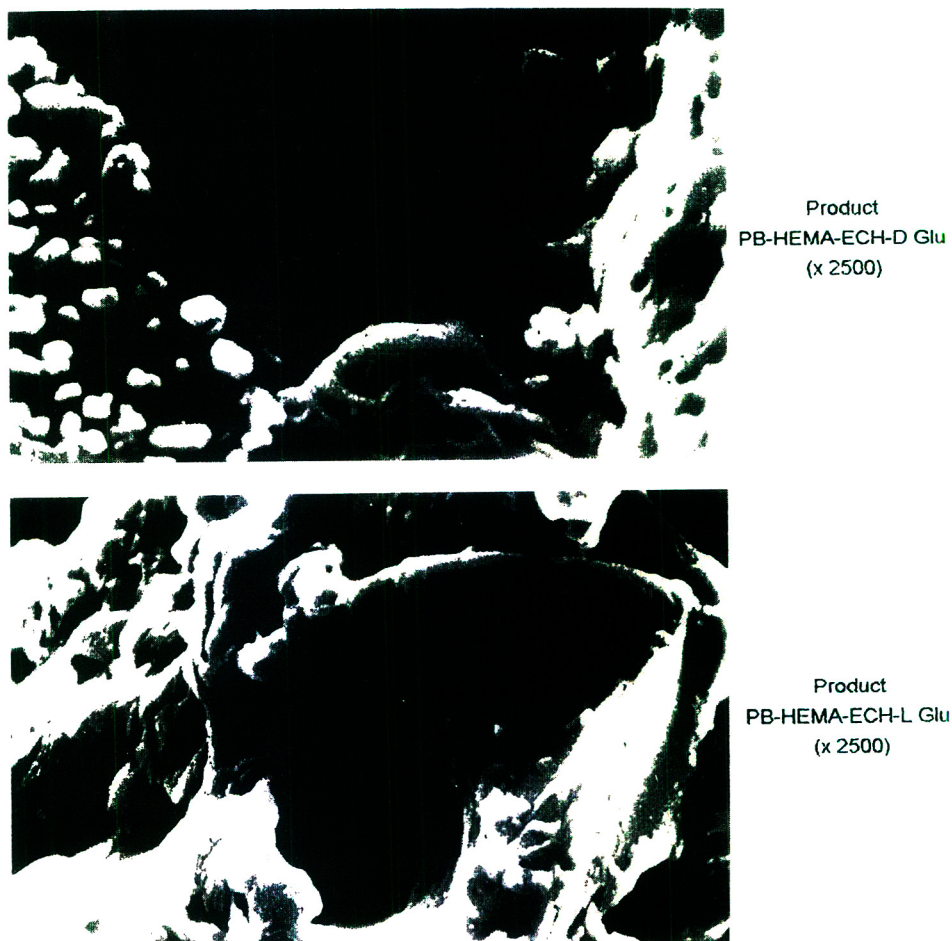


Fig. 1. Microphotographs of the hydrogels obtained by SEM.

through the hydroxyl groups of C-3, C-4 and C-6 of the pyranosic ring. The specificity of the interaction indicates the preference for the “ $\alpha$ ” anomer of C-1 and the equatorial form for the

hydroxyl groups of C-3 and C-4. Any modification of these hydroxyl groups, such as a change in configuration, drastically decreases or abolishes the interaction with the protein [22].

Table 1  
Retention of Con A using PB-HEMA-ECH-D-Glu adsorbent

| Concentration of Con A (mg/ml) | Con A per gram of dry gel (mg) | Con A per ml of swollen gel (mg) |
|--------------------------------|--------------------------------|----------------------------------|
| 0.2                            | 16.7 $\pm$ 0.8                 | 4.2                              |
| 0.4                            | 25.6 $\pm$ 0.9                 | 6.4                              |
| 0.8                            | 49.0 $\pm$ 0.4                 | 12.3                             |

Table 2  
Retention of Con A using PB-HEMA-ECH-L-Glu adsorbent

| Concentration of Con A (mg/ml) | Con A per gram dry gel (mg) | Con A per ml of swollen gel (mg) |
|--------------------------------|-----------------------------|----------------------------------|
| 0.2                            | 13.3 $\pm$ 0.8              | 3.4                              |
| 0.4                            | 13.6 $\pm$ 0.8              | 3.4                              |
| 0.8                            | 16.5 $\pm$ 1.4              | 4.1                              |



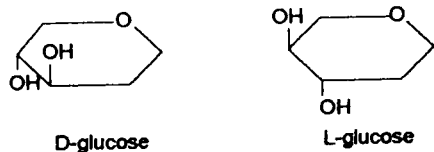


Fig. 2. Structures of D-glucose and L-glucose based on configuration of hydroxyl groups at C-3 and C-4 [23].

As seen in Fig. 2, the hydroxyl groups of C-3 and C-4 of L-glucose show changes in configuration with respect to D-glucose [23].

The binding points with the Con A lectin in D-glucose could be displayed in a specific binding form, as indicated by the results obtained using PB-HEMA-ECH-D-Glu adsorbent, with high retention of lectin. A change in the configuration for L-glucose clearly decreases the retention of lectin using PB-HEMA-ECH-L-Glu adsorbent, corroborating the importance of the arrangement of the hydroxyl groups of C-3 and C-4 in an equatorial form in PB-HEMA-ECH-D-Glu hydrogel.

#### 4. Conclusions

The synthesis of PB-HEMA-ECH-D-Glu and PB-HEMA-ECH-L-Glu hydrogels has been achieved. The activation of the PB-HEMA matrix yielded an epoxidized product with a high content of terminal oxirane functional groups (0.74 mequiv. per gram of dry gel). This value is comparable to those for activated matrices obtained by other workers [24] from natural polysaccharides and epichlorhydrin.

On the other hand, the amount of carbohydrates bound to the activated matrix (40.08  $\mu\text{mol}$  of D-glucose per gram of PB-HEMA-ECH-D-Glu dry gel and 65.11  $\mu\text{mol}$  of L-glucose per gram of PB-HEMA-ECH-L-Glu dry gel) may be assumed to represent typical incorporation values for monosaccharides under the coupling reaction described, as 3.3–66  $\mu\text{mol}$  of ligand per gram of dry gel or 1–20  $\mu\text{mol}$  of ligand per ml of rehydrated gel is suitable for most adsorbents [25].

The retention of Con A using PB-HEMA-

ECH-D-Glu ( $49.0 \pm 0.4$  mg of Con A lectin per gram of dry gel) was comparable to those attained using commercial gels such as agarose- $\beta$ -D-glucose obtained from macromolecules from natural sources, that retained 10–20 mg of Con A lectin per ml of rehydrated gel [26].

#### Acknowledgements

The authors thank CONICOR and CONICET for financial assistance and C.A. acknowledges the receipt of a fellowship from CONICOR.

#### References

- [1] J.H. Pazur, *Adv. Carbohydr. Chem. Biochem.*, 39 (1980) 405.
- [2] P. Vretblad, *Biochim. Biophys. Acta*, 434 (1976) 169.
- [3] I.J. Goldstein and C.E. Hayes, *Adv. Carbohydr. Chem. Biochem.*, 35 (1978) 136.
- [4] N. Sharon and H. Lis, *Science*, 177 (1972) 949.
- [5] I. Liener, *Annu. Rev. Plant Physiol.*, 27 (1976) 291.
- [6] I.J. Goldstein and R.N. Iyer, *Biochim. Biophys. Acta*, 121 (1966) 197.
- [7] M. Inbar and L. Sachs, *Nature*, 223 (1969) 710.
- [8] I.J. Goldstein and L.L. So, *Arch. Biochem. Biophys.*, 111 (1965) 407.
- [9] B.B.L. Agrawal and I.J. Goldstein, *Biochem. J.*, 96 (1965) 23 C.
- [10] B.B.L. Agrawal and I.J. Goldstein, *Biochim. Biophys. Acta*, 147 (1967) 262.
- [11] M.O.J. Olson and I.E. Liener, *Biochemistry*, 6 (1967) 105.
- [12] T. Uchida and T. Matsumoto, *Biochim. Biophys. Acta*, 257 (1972) 230.
- [13] R.R. Walters, *Anal. Chem.*, 55 (1983) 1395.
- [14] H. Lee and K. Neville, *Handbook of Epoxy Resins*, McGraw-Hill, New York, 1967. Ch. 4, pp. 17 and 22.
- [15] M. Dubois, *Anal. Chem.*, 28 (1956) 350.
- [16] O.H. Lowry, N.J. Rosebrough, L. Farr and R.J. Randall, *J. Biol. Chem.*, 193 (1951) 265.
- [17] C. Alvarez, H. Bertorello and M. Strumia, *J. Appl. Polym. Sci.*, in press.
- [18] R. Uy and F. Wold, *Anal. Biochem.*, 81 (1977) 98.
- [19] A.H. Frazer, in H.F. Marck and E.H. Immergut (Editors), *High Temperature Resistant Polymers (Polymer Reviews)*, Wiley, New York, 1968, Ch. 1, p. 5.
- [20] J. Yariv, A.J. Kalb and A. Levitzki, *Biochim. Biophys. Acta*, 165 (1968) 303.
- [21] A.J. Graves and Y. Wu, *Methods Enzymol.*, 34 (1974) 141.

- [22] I.E. Liener, N. Sharon and I.J. Goldstein, *The Lectins: Properties, Functions and Applications in Biology and Medicine*, Academic Press, New York, 1986, Ch. 2, p. 58.
- [23] I.J. Goldstein and C. Hayes, *Adv. Carbohydr. Chem. Biochem.*, 35 (1978) 141.
- [24] L. Sundberg and J. Porath, *J. Chromatogr.*, 90 (1974) 87.
- [25] *Affinity Chromatography. Principles and Methods*, Pharmacia, Uppsala, 1979, Ch. 6, p. 84.
- [26] *Sigma Catalog*, Sigma, St. Louis, MO, 1992, p. 1597.



ELSEVIER

Journal of Chromatography A, 686 (1994) 339–343

JOURNAL OF  
CHROMATOGRAPHY A

Short communication

# Combined pH gradient and anion-exchange high-performance liquid chromatographic separation of oligodeoxyribonucleotides

Tao Lu<sup>1</sup>, Horace B. Gray, Jr.\*

*Department of Biochemical and Biophysical Sciences, University of Houston, Houston, TX 77204-5934, USA*

Received 14 July 1994

## Abstract

A novel method of elution using a pH gradient to separate small thymidine- and guanosine-containing oligonucleotides on a Pharmacia Mono Q HR anion-exchange column is described. The method is based on the alkaline titration of ring protons of the thymine and guanine base moieties and results in excellent separations of di-, tri- and tetranucleotides that either are not resolved in salt gradients near neutral pH or require long elution times when salt gradient elution is used with strongly alkaline eluents.

## 1. Introduction

High-performance liquid chromatography (HPLC) has been applied to oligonucleotides, DNA restriction fragments and plasmid and phage DNAs using several techniques, including reversed-phase chromatography [1], ion-pair/reversed-phase methods [1–5], separations on ion-exchange resins eluted with organic solvent or salt gradients [1,4,6–10] and size-exclusion chromatography [11,12]. Both the ion-exchange and ion-pair methods can separate DNA polymers over a very wide range of sizes ranging from small single-stranded oligonucleotides [1–4,8,10] to large double-stranded restriction fragments and the intact form [5,6,8,9]. However, the separation of oligonucleotides by either of these

techniques depends not only on the chain length but on base composition and sequence in a manner that is difficult to predict [1].

The Pharmacia–LKB Mono Q HR 5/5 anion-exchange column has been used to separate nucleotides and oligonucleotides using neutral [9], mildly alkaline (pH 9.7) [4] and strongly alkaline (10 mM NaOH) ([10], originally suggested by column supplier) salt gradients. Elution of this resin at pH 9.7 resulted in the co-elution of oligomers of a given chain length (isopliths) differing minimally in sequence while these species produced more than one peak when eluted at neutral pH, indicating that separation is based more on the chain length alone at mildly alkaline pH. Strongly alkaline salt gradients used with anion-exchange resins, however, are expected to result in the base composition-dependent separation of oligomers of a given chain length (isopliths) owing primarily to the titration at such pH values of the ring protons of the dT and dG residues, which

\* Corresponding author.

<sup>1</sup> Present address: Department of Molecular Genetics, The University of Texas System Cancer Center, M.D. Anderson Hospital and Tumor Institute, Houston, TX 77030, USA.

increases the negative charge on the oligomer. This presumably played a major role in the separation of complementary DNA strands in work with an earlier resin using alkaline elution [7].

Elution of a Mono Q column with an alkaline salt gradient (pH 12) was attempted to separate isopliaths of small DNA oligonucleotides (up to the tetramer) containing dT residues which failed to resolve on elution near neutral pH. However, the time required to elute species as small as a tetramer containing titratable residues was prohibitively long. This paper reports the use of a pH gradient for elution, which results in reproducible baseline-to-baseline separations, in a predictable order, of dT- and dG-containing oligomers from isopliaths not containing these residues and elution of all species in a reasonable time.

## 2. Experimental

### 2.1. Chemicals

Analytical-reagent grade inorganic chemicals were used. Mono- and dinucleotides were obtained from Sigma (St. Louis, MO, USA). The tri- and tetranucleotides were synthesized on a Biosearch (San Rafael, CA, USA) Model 8600 DNA synthesizer and were further purified by HPLC on a Mono Q HR 5/5 (Pharmacia Biotech, Piscataway, NJ, USA)  $5 \times 0.5$  cm I.D. column (quaternary amine resin, particle size 10  $\mu$ m) using an alkaline salt gradient elution as described [13] after the blocking groups had been removed. All species except mononucleotides lacked a 5'-phosphate group.

### 2.2. Chromatography

A Model 421 controller (Beckman Instruments, Palo Alto, CA, USA) with Model 110A pumps in conjunction with a Hitachi UV-visible monitor set at 260 nm and a Model 3390 integrator (Hewlett-Packard, Avondale, PA, USA) were used. The flow-rate through the Mono Q column (above) was 0.5 ml/min in all instances

and all gradients were nominally linear. All experiments were carried out at room temperature.

Stock solutions of mono- and oligonucleotides were prepared by dissolving solid compounds in or diluting chromatographed compounds with 20 mM Tris-HCl-1 mM EDTA (pH 8). These were appropriately diluted, by a factor of at least ten, with the starting buffer for each elution prior to injection of 20- $\mu$ l samples.

For elutions near neutral pH, the solvents were 20 mM Tris-HCl (pH 8.0)-0.1 M NaCl (buffer A) and 20 mM Tris-HCl (pH 8.0)-1.0 M NaCl (buffer B); for alkaline elution, 10 mM NaOH-0.1 M NaCl (solvent A) and 10 mM NaOH-1.0 M NaCl (solvent B); for pH gradient elution, 0.1 M NaCl-20 mM sodium phosphate (pH 11.0) (adjusted by titration with NaOH before dilution to the final volume) (buffer C) and 0.1 M NaCl-20 mM sodium phosphate (pH 8.0) (buffer D). Elution in a pH gradient was also carried out in 0.1 M NaCl containing 20 mM Tris base or Tris-HCl with the alkaline and neutral solutions at pH 12 (adjusted as above) (solvent C) and 8 (solvent D), respectively. For the near-neutral pH chromatography, the elution profiles were 100% buffer A for 5 min then buffer B to 8% in 15 min. Alkaline pH elution was carried out with 100% solvent A for 10 min followed by an increase to 50% solvent B in an additional 50 min. For the pH gradient elutions in phosphate buffer, pumping of buffer C for 2 min was followed by an increase to 100% buffer D in 5 min and elution with this solvent for 15.5 min, then a return to 100% buffer C over 3 min. Pumping of this solvent for ca. 20 min restored the pH to the initial value (ca. 10.8) and prepared the column for the next injection. Elution profiles for Tris-buffered pH gradients went from 100% solvent C to 30% solvent D in 20 min and then to 100% solvent D in 8 min. All buffers were filtered and degassed before use. The identities of peaks in all instances were confirmed by chromatographing the individual compounds.

The pH profile was determined for the phosphate-buffered solvent pair using a small combination electrode on 0.5-ml fractions from a

gradient programmed identically with those used in the elutions of the mixture and the individual compounds. Times presented are those corresponding to the collection of the mid-point of each fraction.

### 3. Results and discussion

Elution in a salt gradient near neutral pH shows increasing elution times with increasing oligomer length, as expected, but would not adequately resolve isopliths (see times for monomers, dimers and trimers in Table 1) as baseline-to-baseline separation requires at least 2 min of peak separation at the peak widths obtained here (those in Fig. 1 are representative for all four elution methods). Excellent resolution of isopliths based on the mole fraction of dT residues was observed in the alkaline salt gradient (Table 1) but d(TTA) required over 36 min to elute and d(AATT) eluted in a broad peak beginning at over 45 min. With pH gradient elutions, the order of elution is unchanged from that for the alkaline salt gradient (Table 1) but all species are eluted within 31 min. As the third ionization of orthophosphate lends phosphate solutions a very weak buffering capacity at pH 11, the studies of pH gradient elution, including determination of the pH of effluents, were initially done using the

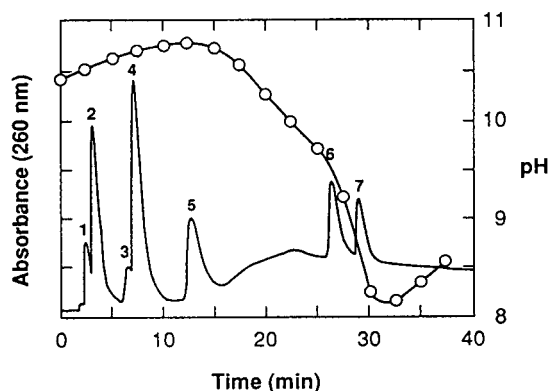


Fig. 1. Separation of a mixture of dA- and dT-containing mono- and oligonucleotides by pH gradient elution in phosphate buffer as described under Experimental. Peaks: 1 = d(A)<sub>2</sub>; 2 = pdA; 3 = d(AAT); 4 = pdT; 5 = d(T)<sub>2</sub>; 6 = d(TTA); 7 = d(AATT).

phosphate-buffered solvents. It was subsequently found that a Tris-buffered solvent pair, the alkaline member of which has no significant buffering capacity in that pH range, also gave reproducible separations (Table 1). Indeed, while there is some loss of resolution with the phosphate pH gradient compared with the alkaline gradient [the pairs pdA–d(A)<sub>2</sub> and pdT–d(ATT) are poorly resolved], the Tris pH gradient provided excellent resolution of all species in the mixture. The reproducibility does not

Table 1  
Retention times and nominal electric charges of mono- and oligonucleotides under different chromatographic conditions

| Compound          | Charge |       | Uncorrected retention times (min) |                    |                          |                          |
|-------------------|--------|-------|-----------------------------------|--------------------|--------------------------|--------------------------|
|                   | pH 8   | pH 12 | pH 8 <sup>a</sup>                 | pH 12 <sup>b</sup> | pH gradient <sup>c</sup> | pH gradient <sup>d</sup> |
| d(A) <sub>2</sub> | -1     | -1    | 2.85                              | 2.5                | 2.54 ± 0.00              | 2.91 ± 0.03              |
| pdA               | -2     | -2    | 4.72                              | 4.5                | 3.40 ± 0.02              | 5.20 ± 0.05              |
| d(AAT)            | -2     | -3    | 3.74                              | 13.3               | 6.53 <sup>e</sup>        | 17.0 ± 0.2               |
| pdT               | -2     | -3    | 3.97                              | 15.4               | 7.38 ± 0.04              | 20.6 ± 0.2               |
| d(T) <sub>2</sub> | -1     | -3    | 2.73                              | 27.2               | 12.75 ± 0.04             | 24.3 ± 0.6               |
| d(TTA)            | -2     | -4    | 4.24                              | 36.5               | 26.8 ± 0.1               | 30.9 ± 0.5               |
| d(AATT)           | -3     | -5    | 8.39                              | >45                | 29.4 ± 0.2               | 37.2 ± 0.2               |

<sup>a</sup> Salt gradient elution near neutral pH. Times are for the individually chromatographed species.

<sup>b</sup> Salt gradient elution of a mixture at pH 12.

<sup>c</sup> pH gradient elution of mixtures using phosphate buffer. Errors are ± half the range for two experiments.

<sup>d</sup> pH gradient elution of mixtures using Tris buffer. Errors are standard deviations for five experiments.

<sup>e</sup> Peak resolved well enough to be assigned a time by the integrator in only one experiment.

appear to be as good as for the phosphate-buffered gradient.

Fig. 1 shows the elution profile of a mixture of the oligodeoxynucleotides in Table 1 with the pH values (phosphate buffers) superimposed. The uncorrected (observed) retention times are used and the pH values represent those of the column effluent. The effluent pH gradient lags well behind the solvent gradient (compare the programme in the Experimental section with the profile in Fig. 1). It is expected, as noted by the manufacturer, that anionic buffers will bind to the quaternary amine resin, so that part of the fully doubly charged phosphate groups at pH 11 must be displaced/titrated by the pH 8 phosphates, which contain a fraction of singly ionized groups. The volume of buffer required to cause an appreciable pH change (ca. 8 ml after 100% buffer D is reached) is reasonable in the light of the ionic capacity of the column given by the supplier. This feature spreads out the pH gradient, which would nominally go through most of its range by the time 25% B is reached (1.2 min of pumping), to cover ca. 13 min of elution (Fig. 1).

As the solvent near the top of the column, where the oligonucleotides are adsorbed, changes pH well before pH changes are seen in the effluent, some of the compounds represented in peaks 3–7 of Fig. 1 (corresponding to species with titratable residues) should begin to migrate before the effluent pH changes significantly if such a change is required to desorb them. However, it appears that large changes in pH are needed only to elute the last two species. Apparently the species of peaks 1–5 are not tightly bound to the resin at pH near 11 and migrate according to different equilibrium constants for the ratio of species in the mobile and stationary phases. The progressive elution of the last two dT-containing compounds clearly depends on the protonation of titrated thymine moieties to reduce the net charge on the molecule. The good reproducibility of the elution times (Table 1) implies that the solvent changes involved are well defined.

The order of elution for the alkaline salt gradient and both types of pH gradient elutions

follow the net charges on the various species at alkaline pH if it is assumed that internucleotide phosphates and thymine residues carry a charge of  $-1$  and that a 5'-phosphate has a charge of  $-2$  (Table 1). The elution times of isopliths should therefore increase with increasing mole fraction of dT and/or dG residues. There is no obvious rationale for the order of elution of the three species with nominal  $-3$  charge (Table 1) where  $d(T)_2$  is well separated from the other two (unresolved)  $-3$  compounds in phosphate-buffered gradients and all three are well resolved in pH gradients containing Tris. At neutral pH, where only the phosphates are charged, species of a given charge are poorly separated, if at all. This leads to poor separation of the isoplith pairs  $d(A)_2-d(T)_2$  and  $d(AAT)-d(TTA)$ , which are well resolved in the alkaline salt and both types of pH gradients.

The role of titratable residues was confirmed in a single set of experiments with dG-containing compounds using the Tris-containing pH gradient.  $d(TG)$  eluted at 26.2 min, close to the time for  $d(T)_2$ , while  $d(GC)$  appeared at 9.6 min, well behind  $d(A)_2$  as expected.  $pdG$  appeared, surprisingly, near 30.3 min, roughly 10 min after the other titratable mononucleotide  $pdT$ .  $pdC$  eluted at 4.3 min and would not have been resolved from  $pdA$ .

Elution at alkaline pH depends very strongly on the titratable residue content. The resulting long elution time for a species of nominal charge  $-5$  suggests that alkaline salt gradient chromatography of DNA oligomers with this resin may fail to elute peaks corresponding to oligomers containing several titratable residues in reasonable times and caution with respect to this effect should be exercised even with higher final salt concentrations.

The pH gradient elution method known as chromatofocusing [14,15] is widely used for protein purification but has not, to our knowledge, been used to separate nucleic acids. The methods are analogous in that elution is facilitated by a pH-mediated reduction in net charge opposite to that of the resin. However, the elution buffers in chromatofocusing contain components that buffer over the entire pH range and titration of

the column resin itself is involved, neither of which is true of the simple procedure described here.

The present method extends the methods available for separating small oligonucleotides because it can resolve isopliths which fail to separate at neutral pH and also separate initially titrated species of the same nominal charge, but does not suffer from the long retention times/broad bands for oligomers containing titratable bases that can occur in elutions using alkaline gradients.

### Acknowledgement

This work was supported in part by Biomedical Research Support Grant SO7RR-07147 (University of Houston).

### References

- [1] W. Haupt and A. Pingoud, *J. Chromatogr.*, 260 (1983) 419.
- [2] W. Jost, K. Unger and G. Schill, *Anal. Biochem.*, 119 (1982) 214.
- [3] B. Alliquant, C. Musenger and E. Schuller, *J. Chromatogr.*, 326 (1985) 281.
- [4] M.V. Cubellis, G. Marino, L. Mayol, G. Piccialli and G. Sanna, *J. Chromatogr.*, 329 (1985) 406.
- [5] S. Eriksson, G. Glad, P. Pernemalm and E. Westman, *J. Chromatogr.*, 359 (1986) 265.
- [6] A. Landy, C. Foeller, R. Rezelbach and B. Dudock, *Nucleic Acids Res.*, 3 (1976) 2575.
- [7] H. Eshaghpour and D.M. Crothers, *Nucleic Acids Res.*, 5 (1978) 13.
- [8] M. Colpan and D. Riesner, *J. Chromatogr.*, 296 (1984) 339.
- [9] W. Muller, *Eur. J. Biochem.*, 155 (1986) 203.
- [10] X.-G. Zhou and H.B. Gray, Jr., *Biochim. Biophys. Acta*, 1049 (1990) 83.
- [11] Y. Kato, M. Sasaki, T. Hashimoto, T. Murotsu, S. Fukushige and K. Matsubara, *J. Biochem.*, 95 (1984) 83.
- [12] Y. Kato, Y. Yamasaki, T. Hashimoto, T. Murotsu, S. Fukushige and K. Matsubara, *J. Chromatogr.*, 329 (1985) 440.
- [13] C.A. Hauser, *Ph.D. Dissertation*, University of Houston, Houston, TX, 1989.
- [14] L.A.Æ. Sluyterman and O. Elgersma, *J. Chromatogr.*, 150 (1978) 17.
- [15] L.A.Æ. Sluyterman and J. Wijdenes, *J. Chromatogr.*, 150 (1978) 31.



ELSEVIER

Journal of Chromatography A, 686 (1994) 344-349

JOURNAL OF  
CHROMATOGRAPHY A

Short communication

## Ion-pair reversed-phase liquid chromatographic determination of dihydralazine

C. Laugel\*, P. Chaminade, A. Baillet, D. Ferrier

*Laboratoire de Chimie Analytique III, Faculté de Pharmacie, 1 Avenue Jean-Baptiste Clément,  
F-92296 Châtenay-Malabry Cedex, France*

First received 14 December 1993; revised manuscript received 30 August 1994

### Abstract

Dihydralazine, a vasodilator drug chemically related to the structural class of the hydrazinophthalazines, was used as a tracer to monitor (water-oil-water) multiple emulsion stability. The hydrophilic character of the ionized form of dihydralazine hinders its chromatographic behaviour by inducing a low retention with alkyl-grafted supports. In addition, the two hydrazine functions induce some important interactions with the polar sites of the stationary phase. This yields highly tailing and poorly retained peaks, hence there is a need to develop an ion-pair technique on a stationary phase recommended for the analysis of basic drugs. After optimization, the optimum chromatogram was obtained with a C<sub>8</sub> RP-Select B column using a mobile phase consisting of a mixture of methanol (50%) and an aqueous solution of phosphate ( $2.5 \cdot 10^{-2} M$ ) and sodium heptanesulfonate ( $2.5 \cdot 10^{-2} M$ ) at pH 4.4. This method was found to be accurate and precise for a range of dihydralazine concentrations from 1 to 120  $\mu\text{g/ml}$ .

### 1. Introduction

Dihydralazine is a vasodilator drug with anti-hypertensive properties. Several methods have been reported for its determination in biological fluids by UV or visible spectrophotometry [1-3], gas chromatography [4], potentiometry [5] and also electrochemical methods [6]. However, direct spectrophotometric and potentiometric determinations can show a lack of specificity when performing the analysis in complex matrices, and a derivatization step is essential for gas chro-

matographic assay. In liquid chromatography, the determination of dihydralazine is complicated by the amine functions of this drug. Serious peak tailing, due to the interaction with free silanol groups of the stationary phase, is encountered with various chromatographic columns. To overcome this problem, precolumn derivatization can be used. An HPLC procedure has been reported that is suitable for determining dihydralazine in human plasma [7].

In this paper, we describe an ion-pair RP-HPLC technique without derivatization that allows the rapid and precise determination of dihydralazine. The influence of two ion-pair reagents and buffers on solute retention using various stationary phases is discussed.

\* Corresponding author.



## 2. Experimental

### 2.1. Instrumentation

Chromatographic measurements were made with a Jasco PU 980 pump (Prolabo, Paris, France) equipped with a Rheodyne model 7125 injection valve with a 20  $\mu$ l loop. UV detection at 310 nm (maximum absorbance of dihydralazine in the mobile phase) was effected with a Shimadzu SPD-2A UV spectrophotometer (Touzart et Matignon, Vitry-sur-Seine, France). The flow-rate was set at 1 ml/min. The chromatograms were recorded using a Hewlett-Packard Model 3395 integrator.

Two RP columns filled with chromatographic supports from different manufacturers were tested: 5-mm C<sub>18</sub> SGE 250 GL 4 P815, 250  $\times$  4 mm I.D. (SGE, Villeneuve-St.-George, France), and 5-mm C<sub>8</sub> LiChrospher RP-Select B, 125  $\times$  4 mm. I.D. (Merck, Nogent-sur-Marne, France).

The mobile phase was filtered through a 0.22- $\mu$ m Millipore filter under vacuum.

### 2.2. Chemicals

Method validation was carried out using the Merck C<sub>8</sub> column and a LiChrospher 100 RP-18 end-capped C<sub>18</sub> guard column (10  $\times$  4 mm I.D.) (Merck).

Methanol, obtained from Prolabo, was of HPLC grade. Ultra-high quality water was obtained from a Milli-Q plus 185 system (Millipore, St.-Quentin, France).

Potassium dihydrogenphosphate was obtained from Merck. The pH of the mobile phase was adjusted to 4.4 using orthophosphoric acid. Sodium 1-heptane sulfonate and sodium dodecyl hydrogensulfate LiChropur quality were obtained from Merck. Dihydralazine was obtained from Ciba-Geigy.

## 3. Results and discussion

The optimization of the chromatographic conditions was achieved by considering two param-

eters: the capacity factor  $k'$  and asymmetry factor ( $B/A$ ). The latter was calculated at 10% of the peak height using the ratio of the widths of the rear and front sides of the peak.

In a recent study devoted to the analysis of basic drugs using various chromatographic supports, Vervoort et al. [8] reviewed some of the factors affecting the peak symmetry and solute retention. First, the peak symmetry can be related to the interaction between the ionized functions of a drug and the free silanols of the packing. Interactions between silanols and solutes can be lowered by the use of tetrabutylammonium phosphate or phosphate buffer at pH <3.5. This pH could not be met in our case as lowering the pH could compromise the emulsion stability, and hence could lead to overestimation of the emulsion breakdown.

Second, the peak asymmetry increases with increasing  $k'$  values. In our case, the capacity factor was not retained as critical, as only one compound was to be determined. The target  $k'$  value for dihydralazine was set at  $k' \approx 1$ .

Third, the peak asymmetry increases with increasing  $pK_a$  of the solute and also with the flexibility of the protonated amine function. Owing to its two hydrazine functions, dihydralazine appears as a strongly interacting substance. The determination of the  $pK_a$  of dihydralazine was achieved by potentiometric titration: in aqueous solution, this compound exhibits two  $pK_a$  values, 6.4 and 10.5, corresponding to the two amine functions. The pH of the mobile phase was set at 4.4, which corresponds to the pH of the inner aqueous phase of the water–oil–water (W/O/W) multiple emulsion. At this pH, dihydralazine is in its fully ionized form.

These three factors explain the poor results encountered with two conventional (C<sub>18</sub> and phenyl) bonded supports in earlier stages of the method development. Those preliminary experiments showed a poor retention of this analyte and serious peak tailing. When observing the chromatographic behaviour of dihydralazine at different operating conditions, two cases were generally noticed: either the compound eluted very close to the solvent front as a symmetrical

peak, or its retention time was longer but the peak tailing was excessive.

The experiments were continued with two chromatographic supports recommended for the analysis of basic drugs: RP-Select B ( $C_8$ ) and SGE 250 ( $C_{18}$ ). The SGE 250 column is based on a  $C_{18}$  chain grafted on a polymeric support. The advantage over silica-based columns is that there is no hydroxyl group present within the support [9]. The RP-Select B column is offered as a stationary phase specially deactivated for the chromatographic analysis of basic compounds [10]. Three factors were investigated. First, the influence of the phosphate buffer concentration on the capacity factor and asymmetry factor was studied; second, we inspected the effect of the type and concentration of two counter ions with increasing phosphate buffer concentration; finally, mobile phase refinement was undertaken.

### 3.1. Influence of the buffer concentration

The influence of the phosphate buffer concentration on the capacity and asymmetry factors was studied by plotting those two values against five concentrations of buffer from 0.01 to 0.1 *M*. As expected, the solute  $k'$  decreases with increasing ionic strength of the mobile phase [11–13]. The asymmetry factor increases with increasing  $k'$  values. However, on both the  $C_8$  and  $C_{18}$  columns, even if the ionic strength is critical, a proper chromatogram cannot be obtained by only varying the buffer concentration. To overcome the dependence between asymmetry factor and capacity factor [14], ion pairing was investigated.

### 3.2. Nature and concentration of counter ion

The performances of sodium 1-heptanesulfonate (HS) and sodium dodecyl hydrogen-sulfate (DS) were compared. These two counter ions differ by the lipophilicity of the hydrocarbon chain and the strength of the functional group [11]. Two levels of concentration of each counter ion (0.025 and 0.05 *M* for DS and 0.05 and 0.1 *M* for HS) and four levels of buffer molarity, from 0.01 to 0.1 *M*, were investigated. The

upper limit of the counter ion concentration was due to its solubility [15].

The effectiveness of complexation was demonstrated by the increase in  $k'$  with increasing concentration of the counter ion (Fig. 1a). Owing to its higher lipophilic character, the minimum concentration required to obtain ion-pair formation is lower with DS than HS and the retention times are significantly longer.

The  $B/A$  factors encountered with DS using the two chromatographic supports were too high (1.5–3.5). They can be lowered by increasing the

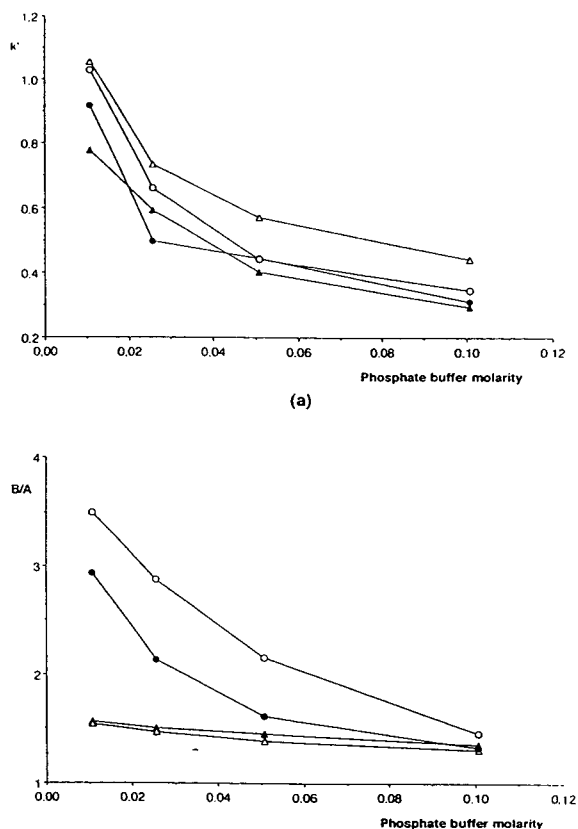


Fig. 1. Comparison of (a)  $k'$  and (b)  $B/A$  values vs. phosphate buffer concentrations with heptanesulfonate at two levels, from two stationary phases: RP-Select B and SGE 250 GL. Chromatographic conditions: mobile phase, methanol-buffer (50:50); flow-rate, 1 ml/min; detection, UV at 310 nm.  $\blacktriangle$  = RP-Select B, 0.005 *M* HS;  $\triangle$  = RP-Select B, HS = 0.01 *M*;  $\bullet$  = SGE 250 GL, HS = 0.005 *M*;  $\circ$  = SGE 250 GL, HS = 0.01 *M*.

buffer molarity but high buffer concentrations may deteriorate the chromatographic system, so DS was rejected.

An ion pair is not formed on  $C_{18}$  grafted polymeric support: when the HS concentration increased, the retention times were not altered. In contrast, ion-pair formation is observed from the large effect on solute retention when using the RP-Select B.

The asymmetry factor remains nearly unchanged (1.3–1.5) whatever the HS concentration when using RP-Select B (Fig. 1b). Therefore, the method development was carried out with the use of HS and the RP-Select B column.

### 3.3. Final mobile phase refinement

In the preceding experiments using HS on RP-Select B, the capacity factor remained inadequate. As the peak symmetry appears to be roughly independent of the capacity factor (Fig. 2), when the ion pair is effective, three parameters were then taken into account: the buffer concentration, the HS concentration and the organic modifier content of the mobile phase.

From Fig. 1a, a low buffer concentration was

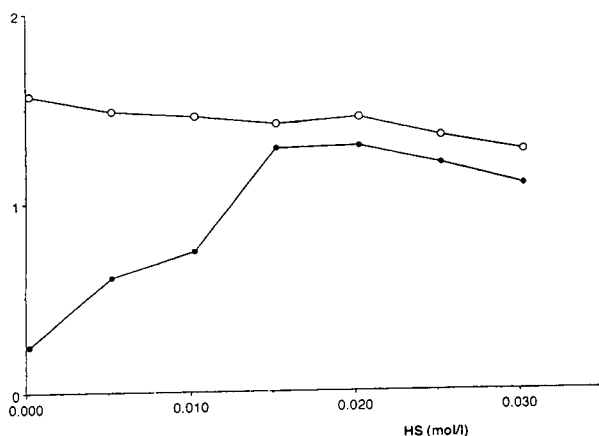


Fig. 2. Plots of (●)  $k'$  and (○)  $B/A$  vs. heptanesulfonate concentration of the mobile phase. Chromatographic conditions: column, LiChrospher RP-Select B; mobile phase, methanol–buffer (50:50), with  $2.5 \cdot 10^{-2}$  M phosphate buffer at pH 4.4.

preferred as it induces a higher  $k'$ . The buffer molarity was set at 0.025 M.

From Fig. 2, the  $k'$  of dihydralazine increases from 0.2 to reach a maximum of 1.4 at HS concentrations between 0.015 and 0.020 M. For higher concentrations of HS,  $k'$  decreases with increasing ionic strength of the mobile phase. From this plot, the best compromise between retention and peak asymmetry is at  $2.5 \cdot 10^{-2}$  M HS.

As proposed by Goldberg et al. [15], the organic modifier content of the mobile phase was kept constant during the preceding steps of the optimization. A final refinement of the elution strength was studied by varying the methanol content of the mobile phase from 35 to 50%, as this could affect the hydrophobic interactions and the surface concentration of the counter ion [16]. As expected, the  $k'$  of dihydralazine decreases with increasing percentage of organic modifier. As no improvement could be expected, we decided to keep the methanol content of the mobile phase at 50%.

The resulting mobile phase used for method validation with the  $C_8$  column was phosphate buffer  $2.5 \cdot 10^{-2}$  M, heptanesulfonate  $2.5 \cdot 10^{-2}$  M and MeOH–H<sub>2</sub>O (50:50).

## 4. Application

### 4.1. Validation of the analytical method

The method was applied to determine the yield in the preparation of W/O/W multiple emulsions. Dihydralazine was used as a UV-tracer incorporated in the internal aqueous phase. The efficiency of entrapment of this marker molecule was determined through the concentration of residual dihydralazine in the external aqueous phase. Consequently, the calibration must take into account a broad range of concentrations in order to detect 0–100% entrapment.

The area and height of the dihydralazine peaks were recorded for nine injections at seven levels ranging from 0.001 to 0.12 g/l. The corresponding calibration graphs exhibit good lineari-

ty ( $r^2 = 1.000$ ) in both instances. The plot of residuals ( $e_i$ ) vs.  $C$  shows a uniform variance and a within-group error proportional to  $C$ . For both area and height this error is about 1% from 0.001 to 0.025 g/l and 4% at 0.12 g/l.

#### 4.2. Method specificity

The components included in the emulsion formula (emulsifier, oil and inorganic salts) do not lead to significant UV absorbance at 310 nm. Further, the injection of the emulsion without dihydralazine shows that the small peaks generated by those compounds do not interfere with the dihydralazine peak (Fig. 3).

To verify if one of the components included in the W/O/W emulsion generates an analytical bias (matrix effect) by inhibiting or enhancing

the solute response, a simplified calibration graph was constructed with five injections at three levels. In this solution, all the components of the W/O/W emulsion were added. For both area and height, the slope of the relationship does not differ significantly for the dihydralazine diluted in mobile phase and the spiked solution (with  $\alpha = 0.05$  and 76 df).

The method specificity is also confirmed by the values of the intercept of the calibration graphs for the spiked solutions, which are close to zero (with  $\alpha = 0.05$  and 13 df).

The limit of detection [17], defined as the lowest concentration of dihydralazine that the method can detect with a signal-to-noise ratio of 3, is about  $1.6 \cdot 10^{-6}$  g/l (area) and  $3 \cdot 10^{-5}$  g/l (height).

The accuracy was calculated as the difference

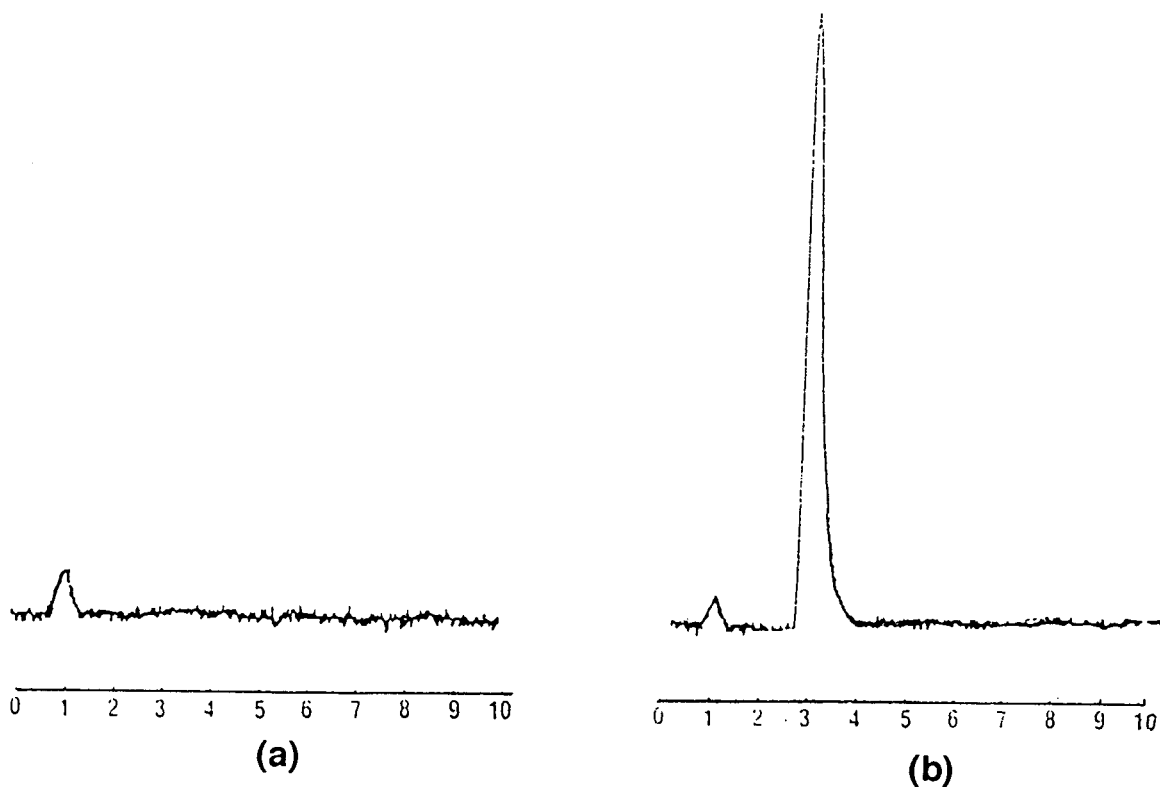


Fig. 3. Chromatogram of the components of the W/O/W multiple emulsion (a) without and (b) with dihydralazine. Chromatographic conditions: column, LiChrospher RP-Select B; mobile phase, methanol-buffer (50:50), with  $2.5 \cdot 10^{-2}$  M phosphate buffer at pH 4.4 and heptanesulfonate  $2.5 \cdot 10^{-2}$  M.

between the mean value and the true value of known concentrations. Student's *t*-test for height and area showed that the method is accurate with  $\alpha = 0.05$  and  $df = 4$ .

The repeatability was established by performing five consecutive calibrations within the same day and the reproducibility was calculated from a unique calibration repeated on each of five days. The R.S.D. was below 1% for the area-based calculation and about 2% for height, hence the method is both repeatable and reproducible.

The yield in the preparation of a W/O/W multiple emulsion was determined on three batches of 100-g size. During the preparation, 0.03 g of dihydralazine was incorporated in each batch. After dilution and centrifugation of the emulsion, the concentration of residual dihydralazine in the supernatant was measured by HPLC. The efficiency of entrapment was calculated as  $91 \pm 1\%$ .

## 5. Conclusions

This work has demonstrated that the ion-pair technique improves the liquid chromatographic behaviour of dihydralazine. Ion-pair formation with heptanesulfonate allows the peak retention to be increased without affecting the peak symmetry when using the RP-Select B stationary phase. The described method allows the rapid, simple and reliable determination of this basic compound. The application of the technique will be extended to stability studies of multiple emulsions.

## References

- [1] P. Issopoulos, *Int. J. Pharm.*, 61 (1990) 261–264.
- [2] H. Perry, *J. Lab. Clin. Med.*, 41 (1953) 566–573.
- [3] A.F. Youssef, S.A. Ibrahim and S.R. Elshabouri, *J. Pharm. Sci.*, 66 (1977) 116–118.
- [4] P.H. Degen, S. Brechbuhler, W. Schneider and P. Zbinden, *J. Chromatogr.*, 233 (1982) 375–380.
- [5] S. Pinzaui, V. Dal Piaz and E. La Poita, *J. Pharm. Sci.*, 63 (1974) 1446–1448.
- [6] F. Janvik, B. Budesinsky and J. Korbl, *Cesk. Farm.*, 9 (1960) 304–307.
- [7] A.R. Waller, L.F. Chasseaud and T. Taylor, *J. Chromatogr.*, 173 (1979) 202–207.
- [8] R.J.M. Vervoort, F.A. Maris and H. Hindriks, *J. Chromatogr.*, 23 (1992) 207–220.
- [9] E. Kwong, A.M.Y. Chiu, S.A. McClintock and M.L. Cotton, *J. Chromatogr. Sci.*, 28 (1990) 563–566.
- [10] M. Bogusz, M. Erkens, R.D. Maier and I. Schroder, *J. Liq. Chromatogr.*, 15 (1992) 127–150.
- [11] P.J. Schoenmakers, *Optimization of Chromatographic Selectivity (Journal of Chromatography Library, Vol. 35)*, Elsevier, Amsterdam, 1986.
- [12] A. Bartha and G. Vigh, *J. Chromatogr.*, 395 (1987) 503–509.
- [13] A.R. Zoest, C.T. Hung, F.C. Lam, R.B. Taylor and S. Wanwimolruk, *J. Liq. Chromatogr.*, 15 (1992) 395–410.
- [14] C.T. Hung, R.B. Taylor and N. Paterson, *J. Chromatogr.*, 240 (1982) 61–73.
- [15] A.P. Goldberg, E. Nowakowska, P.E. Antle and L.R. Snyder, *J. Chromatogr.*, 316 (1984) 241–260.
- [16] H.F. Zou, Y.K. Zhang, M.F. Hong and P.C. Lu, *Chromatographia*, 32 (1991) 329–333.
- [17] D.L. Massart, B.G. Vandeginste, S.N. Deming, Y. Michotte and Y. Kaufman, *Chemometrics: A Textbook*, Elsevier, Amsterdam, 1988.

Short communication

# Determination of atropine and obidoxime in automatic injection devices used as antidotes against nerve agent intoxication

Juhani Pohjola\*, Marco Harpf

*Military Pharmacy, Mannerheimintie 164, 00300 Helsinki, Finland*

First received 13 June 1994; revised manuscript received 17 August 1994

---

## Abstract

A capillary gas-liquid chromatographic (GLC) and an ion-pair high performance liquid chromatographic (HPLC) method were developed for the assay of atropine sulphate and obidoxime chloride from a parenteral solution in commercial automatic injection devices. The injectors are aimed for the emergency treatment of poisoning by nerve agents. The two-step GLC method consists of extraction of atropine as a free base prior to GLC analysis using scopolamine as an internal standard. Obidoxime is determined directly in a diluted sample solution by reversed-phase HPLC using sodium 1-heptanesulphonate as a counter ion in the mobile phase. The relative standard deviation (R.S.D.) was 1.81% for the GLC procedure with injectors containing only atropine and 2.37% for the GLC of atropine in atropine-obidoxime injectors. The R.S.D. for the HPLC procedure of obidoxime in atropine-obidoxime injectors was 0.82%. The corresponding R.S.D.s for the sampling of atropine-obidoxime injectors were 0.36% and 0.27%. The coefficient of determination ( $r^2$ ) was 1.000 for both methods. The recoveries at the target concentration averaged 101.0% and 98.7% with a standard error of the mean of 0.30 for both methods. The retention times for atropine and obidoxime were 6.27 and 4.29 min, respectively.

---

## 1. Introduction

The organophosphate nerve gas agents are a serious threat in the battlefield. These agents affect the nervous system by blocking the enzyme acetylcholinesterase, which plays an essential role in the process of transmitting information between nerves and from nerves to muscles and glands.

Atropine (AT) in combination with certain oximes, obidoxime (OB) or pralidoxime, in a

parenteral solution is used for the emergency treatment of poisoning by toxic organophosphates. To be effective the therapy must begin within minutes after intoxication. With this in view, automatic injectors have been developed, which permit a rapid and convenient means for the intramuscular self-administration of the antidote [1–4].

In the battlefield the storage of pharmaceuticals is often complicated. Varying storage conditions may change, e.g., the given shelf-lives and stability prediction may become impossible. If preparations stored in such field conditions, are to be used, however, it is important to have a

---

\* Corresponding author.

means to control and ensure their identity, strength, purity and quality [5–7].

Determinations of AT in pharmaceuticals have been performed by means of UV spectrophotometry [8], thin-layer chromatography (TLC) [9,10], high-performance liquid chromatography (HPLC) [11–23] and gas-liquid chromatography (GLC) [24–29]. GLC and HPLC are generally used today in the determination of AT. Few assays for the determination of OB have been reported. However, UV spectrophotometric [30], polarographic [31] and TLC [32] methods have been described. An HPLC [33] method was presented for blood samples. UV, TLC and polarographic methods for the determination of AT or OB are known to be associated with complicated and tedious sample preparations. Moreover, these methods are mostly aimed at one-component formulations [24,26]. Similarly, HPLC methods are suitable for the analysis of samples containing AT only [13–18]. Accordingly, investigations in our laboratory indicated that samples containing both AT and OB could not be analysed quantitatively by these methods. GLC procedures instead have been shown to distinguish well between AT and oximes, although interference by decomposition products from the latter compounds [26] and lack of sensitivity [17] have been experienced. In addition, because of unsatisfactory reproducibility [26], detection [26] or sample matrix [24,26,28] different to ours, the previous GLC methods described could not be applied as such in this study.

## 2. Experimental

### 2.1. GLC analysis of atropine sulphate

#### Equipment and supplies

The analyses were carried out on a Hewlett-Packard (Waldbronn, Germany) (HP) model 5890 gas chromatograph equipped with a flame ionization detector. ChemStation software was installed in a HP Vectra QS/20 personal computer (Hewlett-Packard, Roseville, CA, USA) for data handling. An HP-5 capillary cross-linked 5% phenylsilicone column (Hewlett-Packard,

Avondale, PA, USA), 25 m × 0.32 mm I.D. with a film thickness of 0.52 μm was used. The column was operated in the split mode with a splitting ratio of 10:1. The column temperature was programmed as follows: initial temperature 160°C, increased at 20°C min<sup>-1</sup> to 200°C, then at 50°C min<sup>-1</sup> to 270°C, the final temperature being held for 4.20 min; the total time was 7.60 min. The injection port was maintained at 255°C and the detector at 285°C. The carrier gas (helium) flow-rate was 1.0 ml min<sup>-1</sup>; the hydrogen and air flow-rates were 30 and 400 ml min<sup>-1</sup>, respectively. Under these conditions the retention times of AT and the internal standard (I.S.) scopolamine (SC) were 6.27 and 7.23 min, respectively (see Fig. 1). The least-squares linear regression equation for AT was  $y = 2.0397x - 0.0058$ , where  $y$  is the AT/SC peak-area ratio and  $x$  is the AT concentration in mg ml<sup>-1</sup>. The calibration graph for AT was calculated using Harward Graphics software (Software Publishing, Mountain View, CA, USA).

#### Reagents

Atropine (*dl*-hyoscyamine) sulphate monohydrate (Sigma, St. Louis, MO, USA) and scopolamine hydrobromide trihydrate pure substances (Boehringer Ingelheim International, Ingelheim am Rhein, Germany) were used as references. Chloroform (99.4%) (Merck, Darmstadt, Germany) was of analytical-reagent grade.

The composition of AtroPen (Solvay Duphar, Weesp, Netherlands) was atropine sulphate (2.86 mg), glycerin (17.81 mg), citric acid (4.67 mg), sodium citrate (4.35 mg) and phenol (4.00 mg) in water (1 ml). The composition of ComboPen (Solvay Duphar) was atropine sulphate (1.00 mg), obidoxime chloride (87.50 mg) and phenol (4.20 mg) in water (1 ml).

Borax buffer (pH 9.80) was prepared by dissolving borax (4.77 g) and sodium hydroxide (0.40 g) in deionized water (100 ml) and adjusting the pH to 9.80 by adding sodium hydroxide.

#### Sample preparation procedure

*Assay for AtroPen samples.* A 500-μl volume of I.S. solution (SC, 1.00 mg ml<sup>-1</sup>) was added to

250  $\mu\text{l}$  of sample solution. The solution was made alkaline with 140  $\mu\text{l}$  of ammonia solution (1.2%) and 4.0 ml of buffer solution (pH 9.80) were added. The mixture was extracted with 4 ml of chloroform and the organic layer was transferred into a vial. The chloroform phase was evaporated to dryness on a water-bath (70°C). The dried residue was dissolved in 1.00 ml of chloroform and 1  $\mu\text{l}$  was injected into the GC column.

*Assay for ComboPen samples.* A 500- $\mu\text{l}$  volume of I.S. solution (SC, 1.00 mg ml<sup>-1</sup>) was added to 500  $\mu\text{l}$  of sample solution. The solution was made alkaline with 330  $\mu\text{l}$  of ammonia solution (6.3%) and 4.0 ml of buffer solution (pH 9.80) were added. The procedure was continued as described for AtroPen samples.

## 2.2. HPLC analysis of obidoxime chloride

### Equipment and supplies

The assay was developed using an HP 1050 series liquid chromatograph (Hewlett-Packard) equipped with a high-pressure quaternary pump, variable-wavelength detector and a 20- $\mu\text{l}$  loop injector. An HP 3396A series integrator was obtained from Hewlett-Packard. The stationary phase in the RP-18 column (Merck), 125 mm  $\times$  4 mm I.D., was LiChrospher 100 with an average particle diameter of 5  $\mu\text{m}$ . The mobile phase consisted of 16% acetonitrile and 15% methanol in water containing sodium 1-heptanesulphonate (10 mM) as a counter ion. The pH of the eluent was 6.30. The flow-rate of the mobile phase was 1.5 ml min<sup>-1</sup> and the absorbance was measured at 220 nm. All separations were performed at ambient temperature. A 500- $\mu\text{l}$  volume of comboPen sample was diluted to 25.00 ml and 100  $\mu\text{l}$  were injected into the 20- $\mu\text{l}$  loop injector. The retention times were 2.40 and 4.29 min for phenol and OB chloride, respectively (see Fig. 2). OB was determined by the external standard method. The calibration graph for OB was calculated as for AT. The linear regression equation was  $y = 92.6972x + 1.9171$ , where  $y$  is the peak area at 220 nm expressed in integration units and  $x$  is the concentration of OB chloride in mg ml<sup>-1</sup>.

### Reagents

Acetonitrile (99.8%) and methanol (99.9%) (Mallinckrodt Specialty Chemicals, Paris, KY, USA) were of HPLC-grade. Sodium 1-heptanesulphonate (98%) (Sigma, St. Louis, MO, USA) was of analytical-reagent grade. Obidoxime chloride pure substance used as a reference was obtained from Duphar (Amsterdam, Netherlands).

## 3. Results and discussion

In the present study the simultaneous determination of AT and OB by HPLC was unsuccessful under both isocratic and gradient conditions. Either retention of OB was irreversible under the conditions defined for AT or AT was not quantitatively eluted under the conditions defined for OB. The determination of AT and OB simultaneously by GLC would have required a tedious and time-consuming sample preparation procedure owing to their different extraction properties. In addition, OB has proved to be a relatively unstable compound at the elevated temperatures needed for GLC analyses [26]. Hence it seemed reasonable to develop separate methods for the determination of AT and OB in the auto-injectors: a GLC method for atropine sulphate and an HPLC method for obidoxime chloride.

In the GLC method proposed here, the sample was made alkaline before treatment with chloroform in order to extract AT quantitatively as a free base. Preliminary studies indicated that the recovery of extracted AT was optimum at pH 9.80, to which the pH of the sample solutions was adjusted with borax buffer. SC was selected to be the I.S. on the basis of its extraction properties and GLC retention time. Compound decomposition caused by initial temperatures higher than 160°C and programming rates faster than 20°C min<sup>-1</sup> was avoided by using a two-step temperature programme. This also provided good separation and a short analysis time.

The calibration graph was constructed from analyses of standard solutions containing known concentrations of AT sulphate. The graph was found to be linear over the concentration range



0–1.50 mg ml<sup>-1</sup> ( $r^2 = 1.000$ ). The analytical reproducibility for the entire two-step GLC procedure was evaluated by analysing six successive samples of a single auto-injector. The relative standard deviations (R.S.D.s) were 1.81% for AtroPen and 2.37% for ComboPen samples. The reproducibility of sampling determined for ComboPen samples was 0.36%. The recoveries of AT were determined by assaying standard samples using a standard addition method. The average recovery of AT at the target concentration (0.50 mg ml<sup>-1</sup>;  $n = 6$ ) was found to be 101.0% with a standard error of the mean (SEM) of 0.27%.

A GLC trace of an AtroPen sample is presented in Fig. 1. The peaks are symmetrical and the retention times are sufficient for the distinct separation of AT and SC. OB together with the pharmaceutical additives in auto-injector samples did not interfere with the determination of

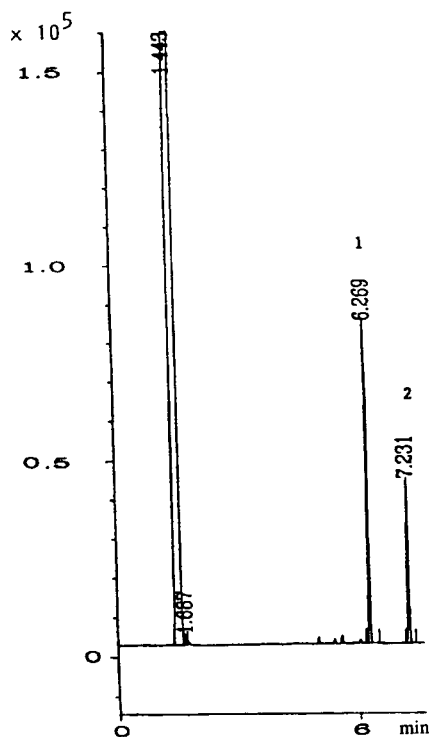


Fig. 1. GLC of an AtroPen auto-injector sample. Peaks: 1 = atropine; 2 = scopolamine (internal standard).

AT because they were not extracted with AT. The AT/SC peak-area ratio was calculated and the amount of AT sulphate present in the sample was determined with reference to the calibration graph.

Because of the quaternary structure of pyridinium aldoximes ion-pair reversed-phase LC was expected to be a suitable method for determination of OB in ComboPen samples. In this study sodium 1-heptanesulphonate proved to be the most appropriate ion-pairing agent to form a lipophilic complex with OB.

The calibration graph obtained with spiked standard solutions of OB was found to be linear over the concentration range 0–2.50 mg ml<sup>-1</sup> ( $r^2 = 1.000$ ). The analytical reproducibility for OB was determined by analysing six successive sample solutions diluted from a single ComboPen injector. The R.S.D. was 0.82%. The reproducibility of sampling was 0.27%. As the reproducibility was satisfactorily controlled by the loop injector, an internal standard was not required. The recovery of the HPLC method determined by assaying six spiked standard solutions of OB chloride at the target concentration (1.75 mg ml<sup>-1</sup>) averaged 98.7% with an SEM of 0.30%.

A chromatogram of a ComboPen sample is presented in Fig. 2. It is seen that phenol produced a separate peak, which did not interfere with the determination of OB. Tailing of the OB chloride peak might have been caused by injecting a relatively large amount of drug (35 µg).

## Conclusions

The described GLC and HPLC methods are accurate and precise for the determination of atropine sulphate and obidoxime chloride in parenteral auto-injector solutions. The linearity and reproducibility are very good for both methods. The recoveries were 101% and 99%, respectively. The methods are also rapid and fairly simple. The GLC method consists of two steps: extraction of atropine as a free base with chloroform and subsequent GLC analysis. Obidoxime

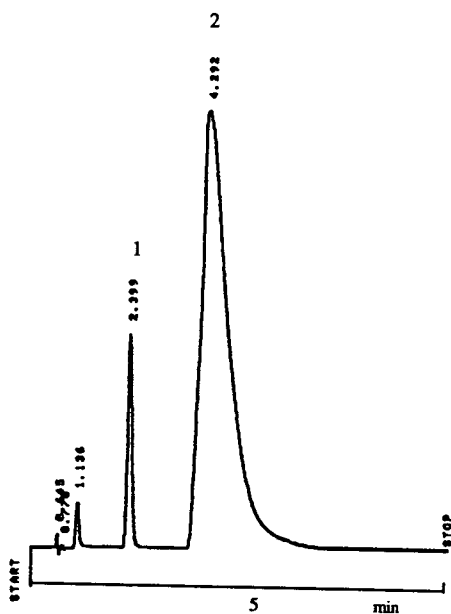


Fig. 2. HPLC of a ComboPen auto-injector sample. Peaks: 1 = phenol; 2 = obidoxime chloride.

is determined directly in diluted sample solution by ion-pair HPLC. The methods can be readily adapted to, e.g., stability studies of AtroPen and ComboPen auto-injectors.

### Acknowledgements

This work received financial support from the Scientific Committee of National Defence and the Health Care Section of the Defence Staff. Duphar (Amsterdam, Netherlands) is thanked for supplying obidoxime chloride.

### References

- [1] V. Riihimäki, E. Kantolahti and R. Visakorpi, in K. Koskenvuo (Editor), *Kenttälääkintä. Ensihoidon Perusteet*, Finnish Defence Forces, Hämeenlinna, 1993, p. 494.
- [2] R.E. Gosselin, H.C. Hodge, R.P. Smith and M.N. Gleason, *Clinical Toxicology of Commercial Products*, Williams and Wilkins, Baltimore, 4th ed., 1976.
- [3] F. Hobbiger, in G.B. Koelle (Editor), *Handbuch der Experimentellen Pharmakologie (Cholinesterases and Anticholinesterases)*, Vol. XV, Springer, Heidelberg, 1963, p. 921.
- [4] G. Puu, E. Artursson and G. Bucht, *Biochem. Pharmacol.*, 35 (1986) 1505.
- [5] J. Pohjola, T. Wikberg, A. Laitinen and A. Ytti, *Acta Pharm. Fenn.*, 94 (1985) 137.
- [6] J. Pohjola, I. Kari and O. Sillantaka, *Ann. Med. Milit. Fenn.*, 58 (1983) 160.
- [7] J. Pohjola, A. Laitinen and P. Karttunen, *Ann. Med. Milit. Fenn.*, 58 (1983) 164.
- [8] S.M. Hassan and A.G. Davidson, *J. Pharm. Pharmacol.*, 36 (1984) 7.
- [9] Th. Jira and R. Pohloudek-Fabini, *Pharmazie*, 38 (1983) 520.
- [10] R. Pohloudek-Fabini and Th. Jira, *Pharmazie*, 38 (1983) 390.
- [11] *US Pharmacopeia, 22nd Revision*, US Pharmacopeial Convention, Rockville, MD, 1990.
- [12] H.-G. Eigendorf, *Pharmazie*, 43 (1988) 287.
- [13] Th. Jira, Th. Beyrich and E. Lemke, *Pharmazie*, 39 (1984) 351.
- [14] Th. Jira and Th. Beyrich, *Pharmazie*, 43 (1988) 768.
- [15] A. Richard and G. Andermann, *Pharmazie*, 39 (1984) 866.
- [16] R.I. Ellin, A. Kaminskis, P. Zvirblis, W.E. Sultan, M.B. Schutz and R. Matthews, *J. Pharm. Sci.*, 74 (1985) 788.
- [17] U. Cieri, *J. Assoc. Off. Anal. Chem.*, 68 (1985) 1042.
- [18] T. Oshima, K. Sagara, Y.-Y. Tong, G. Zhang and Y.-H. Chen, *Chem. Pharm. Bull.*, 37 (1989) 2456.
- [19] J. Pennington and W.F. Schmidt, *J. Pharm. Sci.*, 70 (1982) 951.
- [20] P. Duez, S. Chamart, M. Hanocq and L. Molle, *J. Chromatogr.*, 392 (1985) 415.
- [21] S. Paphassarang and J. Raynard, *J. Chromatogr.*, 319 (1985) 412.
- [22] B. Pekic, B. Slavica, Z. Lepojevic and M. Gorunovic, *Pharmazie*, 40 (1985) 422.
- [23] K.-H. Plank and K.G. Wagner, *Z. Naturforsch., Teil C*, 41 (1986) 391.
- [24] B. Nieminen, *Zentralbl. Pharm.*, 110 (1971) 1137.
- [25] R. Rhodes, P. Rhodes and H. Horton McCurdy, *Am. J. Hosp. Pharm.*, 42 (1985) 112.
- [26] C.J. Briggs and K.J. Simons, *J. Chromatogr.*, 257 (1983) 132.
- [27] P. Majlat, *Pharmazie*, 39 (1984) 325.
- [28] M. Ylinen, T. Naaranlahti, S. Lapinjoki, A. Huhtikangas, M.-L. Salonen, L.K. Simola and M. Lounasmaa, *Planta Med.*, 52 (1986) 85.
- [29] *US Pharmacopeia, 19th Revision*, US Pharmacopeial Convention, Rockville, MD, 1975.
- [30] C.J. Briggs and K.J. Simons, in *Proceedings of the 27th Canadian Conference on Pharmaceutical Research, 1980, Saskatoon*, Association of the Faculties of Pharmacy of Canada, Saskatoon, 1980, p. 12.
- [31] Z. Koricnac, B. Stankovic, M. Maksimovic and Z. Binenfeld, *Acta Pharm. Jugosl.*, 32 (1982) 291.
- [32] I. Christenson, *Acta Pharm. Suec.*, 5 (1968) 23.
- [33] H.P. Benschop, K.A.G. Konings, P. Kossen and D.A. Ligtenstein, *J. Chromatogr.*, 225 (1981) 107.

## Author Index

- Agüera, A., see Fernandez-Alba, A.R. 686(1994)263  
Albaigés, J., see Chalaux, N. 686(1994)275  
Alvarez, C., Bertorello, H., Strumia, M. and Sanchez, E.I.  
Synthesis and characterization of biospecific adsorbents containing glucose, usable to retain concanavalin A 686(1994)333  
Aumatell, A., Wells, R.J. and Wong, D.K.Y.  
Enantiomeric differentiation of a wide range of pharmacologically active substances by capillary electrophoresis using modified  $\beta$ -cyclodextrins 686(1994)293  
Baillet, A., see Laugel, C. 686(1994)344  
Ball, H.L., Bertolini, G., Levi, S. and Mascagni, P.  
Purification of synthetic peptides with the aid of reversible chromatographic probes 686(1994)73  
Bayona, J.M., see Chalaux, N. 686(1994)275  
Bertolini, G., see Ball, H.L. 686(1994)73  
Bertorello, H., see Alvarez, C. 686(1994)333  
Born, J., see Grize, Y.-L. 686(1994)1  
Bossi, A., Gelfi, C., Orsi, A. and Righetti, P.G.  
Isoelectric focusing of histones in extremely alkaline immobilized pH gradients: comparison with capillary electrophoresis 686(1994)121  
Boyes, B.E., see Chloupek, R.C. 686(1994)45  
Bruno, T.J. and Caciari, M.  
Retention of halocarbons on a hexafluoropropylene epoxide-modified graphitized carbon black. III. Ethene-based compounds 686(1994)245  
Byrd, D.W. and Freeman, D.C.  
Automated static headspace sampler for gas chromatography 686(1994)235  
Byrd, D.W., see Freeman, D.C. 686(1994)225  
Caciari, M., see Bruno, T.J. 686(1994)245  
Chalaux, N., Bayona, J.M. and Albaigés, J.  
Determination of nonylphenols as pentafluorobenzyl derivatives by capillary gas chromatography with electron-capture and mass spectrometric detection in environmental matrices 686(1994)275  
Chaminade, P., see Laugel, C. 686(1994)344  
Chloupek, R.C., Hancock, W.S., Marchylo, B.A., Kirkland, J.J., Boyes, B.E. and Snyder, L.R.  
Temperature as a variable in reversed-phase high-performance liquid chromatographic separations of peptide and protein samples. II. Selectivity effects observed in the separation of several peptide and protein mixtures 686(1994)45  
Chloupek, R.C., see Hancock, W.S. 686(1994)31  
Contreras, M., see Fernandez-Alba, A.R. 686(1994)263  
Cramer, S.M., see Kim, Y.J. 686(1994)193  
De Biasi, V., see Eckers, C. 686(1994)213  
De Leer, E.W.B., see Peters, R.J.B. 686(1994)253  
Desiderio, D.M., see Lee, H.G. 686(1994)309  
East, P.B., see Eckers, C. 686(1994)213  
Eckers, C., Hutton, K.A., De Biasi, V., East, P.B., Haskins, N.J. and Jacewicz, V.W.  
Determination of clavam-2-carboxylate in clavulanate potassium and tablet material by liquid chromatography-tandem mass spectrometry 686(1994)213  
Etzel, M.R., see Suen, S.-Y. 686(1994)179  
Fernandez-Alba, A.R., Valverde, A., Agüera, A. and Contreras, M.  
Gas chromatographic determination of organochlorine and pyrethroid pesticides of horticultural concern 686(1994)263  
Ferrier, D., see Laugel, C. 686(1994)344  
Foley, J.P., see Nielsen, K.R. 686(1994)283  
Freeman, D.C. and Byrd, D.W.  
Statistical treatment of large digital chromatographic data sets 686(1994)225  
Freeman, D.C., see Byrd, D.W. 686(1994)235  
Freitag, R., Frey, D. and Horváth, C.  
Effect of bed compression on high-performance liquid chromatography columns with gigaporous polymeric packings 686(1994)165  
Frey, D., see Freitag, R. 686(1994)165  
Gelfi, C., see Bossi, A. 686(1994)121  
Goffe, R.A., see Shi, J.Y. 686(1994)61  
Gołkiewicz, W., Kuczyński, J., Markowski, W. and Jusiak, L.  
High-performance liquid chromatography of some alkaloids on unmodified silica gel with aqueous-organic solvent mixtures 686(1994)85  
Gray, H.B., see Lu, T. 686(1994)339  
Greibrokk, T., see Pedersen-Bjerggaard, S. 686(1994)109  
Grize, Y.-L., Schmidli, H. and Born, J.  
Effect of integration parameters on high-performance liquid chromatographic method development and validation 686(1994)1  
Hancock, W.S., Chloupek, R.C., Kirkland, J.J. and Snyder, L.R.  
Temperature as a variable in reversed-phase high-performance liquid chromatographic separations of peptide and protein samples. I. Optimizing the separation of a growth hormone tryptic digest 686(1994)31  
Hancock, W.S., see Chloupek, R.C. 686(1994)45  
Harpf, M., see Pohjola, J. 686(1994)350  
Haskins, N.J., see Eckers, C. 686(1994)213  
Hirokawa, T.  
Bidirectional isotachopheresis. II. Fifteen electrolyte systems covering the pH range 3.5-10 686(1994)158  
Horváth, C., see Freitag, R. 686(1994)165  
Hutton, K.A., see Eckers, C. 686(1994)213  
Ip, D.P., see Qin, X.-Z. 686(1994)205  
Ishii, K., Minato, K., Nishimura, N., Miyamoto, T. and Sato, T.  
Direct chromatographic resolution of four optical isomers of diltiazem hydrochloride on a Chiralcel OF column 686(1994)93  
Jacewicz, V.W., see Eckers, C. 686(1994)213  
Jusiak, L., see Gołkiewicz, W. 686(1994)85  
Kim, Y.J. and Cramer, S.M.  
Experimental studies in metal affinity displacement chromatography of proteins 686(1994)193  
Kirkland, J.J., see Chloupek, R.C. 686(1994)45  
Kirkland, J.J., see Hancock, W.S. 686(1994)31  
Kremer, D.M., see Nores, G.A. 686(1994)155

- Kuczyński, J., see Gołkiewicz, W. 686(1994)85
- Laugel, C., Chaminade, P., Baillet, A. and Ferrier, D.  
Ion-pair reversed-phase liquid chromatographic  
determination of dihyralazine 686(1994)344
- Lee, H.G. and Desiderio, D.M.  
Preparative capillary zone electrophoresis of synthetic  
peptides. Conversion of an autosampler into a fraction  
collector 686(1994)309
- Lee, H.K., see Ong, C.P. 686(1994)319
- Lemr, K., Zanette, M. and Marcomini, A.  
Reversed-phase high-performance liquid  
chromatographic separation of 1-naphthyl isocyanate  
derivatives of linear alcohol polyethoxylates  
686(1994)219
- Levi, S., see Ball, H.L. 686(1994)73
- Li, S.F.Y., see Ong, C.P. 686(1994)319
- Liapis, A.I., see Tongta, A. 686(1994)21
- Lu, T. and Gray, H.B.  
Combined pH gradient and anion-exchange high-  
performance liquid chromatographic separation of  
oligodeoxyribonucleotides 686(1994)339
- Marchylo, B.A., see Chloupek, R.C. 686(1994)45
- Marcomini, A., see Lemr, K. 686(1994)219
- Markowski, W., see Gołkiewicz, W. 686(1994)85
- Mascagni, P., see Ball, H.L. 686(1994)73
- McGuffin, V.L., see Tavares, M.F.M. 686(1994)129
- Minato, K., see Ishii, K. 686(1994)93
- Miyamoto, T., see Ishii, K. 686(1994)93
- Mizutamari, R.K., see Nores, G.A. 686(1994)155
- Moriguchi, S., Naito, K. and Takei, S.  
Adsorption effects on retention behaviour of  
hydrocarbons in gas-liquid and gas-solid  
chromatography with the use of modified alumina  
coated with diphenyl phthalate as column packings  
686(1994)101
- Naito, K., see Moriguchi, S. 686(1994)101
- Ng, C.L., see Ong, C.P. 686(1994)319
- Nielsen, K.R. and Foley, J.P.  
Zone sharpening of neutral solutes in micellar  
electrokinetic chromatography with electrokinetic  
injection 686(1994)283
- Nishimura, N., see Ishii, K. 686(1994)93
- Nores, G.A., Mizutamari, R.K. and Kremer, D.M.  
Chromatographic tank designed to obtain highly  
reproducible high-performance thin-layer  
chromatograms of gangliosides and neutral  
glycosphingolipids 686(1994)155
- Ong, C.P., Ng, C.L., Lee, H.K. and Li, S.F.Y.  
Separation of imidazole and its derivatives by capillary  
electrophoresis 686(1994)319
- Orsi, A., see Bossi, A. 686(1994)121
- Pedersen-Bjergaard, S. and Greibrokk, T.  
N-, O- and P-selective on-column atomic emission  
detection in capillary gas chromatography  
686(1994)109
- Peters, R.J.B., De Leer, E.W.B. and Versteegh, J.F.M.  
Identification of halogenated compounds produced by  
chlorination of humic acid in the presence of bromide  
686(1994)253
- Pohjola, J. and Harpf, M.  
Determination of atropine and obidoxime in automatic  
injection devices used as antidotes against nerve agent  
intoxication 686(1994)350
- Qin, X.-Z., Tsai, E.W., Sakuma, T. and Ip, D.P.  
Pharmaceutical application of liquid chromatography-  
mass spectrometry. II. Ion chromatography-ion spray  
mass spectrometric characterization of alendronate  
686(1994)205
- Righetti, P.G., see Bossi, A. 686(1994)121
- Sakuma, T., see Qin, X.-Z. 686(1994)205
- Sanchez, E.I., see Alvarez, C. 686(1994)333
- Sato, T., see Ishii, K. 686(1994)93
- Schmidli, H., see Grize, Y.-L. 686(1994)1
- Shi, J.Y. and Goffe, R.A.  
Comprehensive study on binding capacity of human  
immunoglobulin G to Avid AL affinity gel  
686(1994)61
- Shortt, D.W.  
Measurement of narrow-distribution polydispersity  
using multi-angle light scattering 686(1994)11
- Siehr, D.J., see Tongta, A. 686(1994)21
- Snyder, L.R., see Chloupek, R.C. 686(1994)45
- Snyder, L.R., see Hancock, W.S. 686(1994)31
- Stahl, R.  
Routine determination of anions by capillary  
electrophoresis and ion chromatography 686(1994)143
- Strumia, M., see Alvarez, C. 686(1994)333
- Suen, S.-Y. and Etzel, M.R.  
Sorption kinetics and breakthrough curves for pepsin  
and chymosin using pepstatin A affinity membranes  
686(1994)179
- Takei, S., see Moriguchi, S. 686(1994)101
- Tavares, M.F.M. and McGuffin, V.L.  
Separation and characterization of tetracycline  
antibiotics by capillary electrophoresis 686(1994)129
- Tongta, A., Liapis, A.I. and Siehr, D.J.  
Equilibrium and kinetic parameters of the adsorption  
of  $\alpha$ -chymotrypsinogen A onto hydrophobic porous  
adsorbent particles 686(1994)21
- Tsai, E.W., see Qin, X.-Z. 686(1994)205
- Valverde, A., see Fernandez-Alba, A.R. 686(1994)263
- Versteegh, J.F.M., see Peters, R.J.B. 686(1994)253
- Vetter, W. and Walther, W.  
Pyrrolidides as derivatives for the determination of the  
fatty acids of triacylglycerols by gas chromatography  
686(1994)149
- Vogt, C. and Werner, G.  
Speciation of heavy metals by capillary electrophoresis  
686(1994)325
- Walther, W., see Vetter, W. 686(1994)149
- Wells, R.J., see Aumatell, A. 686(1994)293
- Werner, G., see Vogt, C. 686(1994)325
- Wong, D.K.Y., see Aumatell, A. 686(1994)293
- Zanette, M., see Lemr, K. 686(1994)219



# Journal of Chromatography A



## NEWS SECTION

### ANNOUNCEMENTS

4th INTERNATIONAL CONFERENCE ON AUTOMATION, ROBOTICS AND ARTIFICIAL INTELLIGENCE APPLIED TO ANALYTICAL CHEMISTRY AND LABORATORY MEDICINE, MONTREUX, SWITZERLAND, 7-10 FEBRUARY, 1995

Topics for the scientific program are:

- strategies in robotic method development and applications,
- nanoscale technology,
- bioanalytical methods and instrumentation,
- environmental research,
- automation of drug discovery,
- intelligent systems technology, and
- quality control and validation of applications.

Subjects of general interest will be introduced by plenary lectures followed by brief presentations. The following topics will be covered by one-day short courses (7 February):

- LIMS: Strategy and Tactics,
- Multivariate Analysis,
- Neutral Networks,
- Fuzzy Logic, an Introduction to Laboratory Robotics, and
- An Introduction to Clinical Laboratory Robotics. Short courses will be delivered by internationally renowned instructors.

An exhibition and poster presentations will be held in a room adjacent to the conference room. Instruments and applications will be displayed by manufacturers and system integrators.

For further details contact: J. van der Greef, TNO and University of Leiden, P.O. Box 360, 3700 AJ Zeist, The Netherlands. Tel: (+31 3404) 441-44; Fax: (+31 3404) 572-24; or R.A. Felder, University of Virginia, Dept. of Pathology, Box 168, Charlottesville, VA, USA. Tel: (804) 924-5151; Fax: (804) 924-5718.

PREPTECH '95, EAST RUTHERFORD, NJ, USA, 13-15 FEBRUARY, 1995

The technical program will cover a range of topics on industrial separation science, including preparative liquid chromatography, membrane separations, electro-separation techniques, extraction, and centrifugation. Scientists with a professional interest in these and related areas are invited to submit abstracts for both oral and poster presentations. Abstracts should include the title, the names of the authors and their affiliations (omitting degrees, but indicating the name of the presenting author), company name, complete mailing address, telephone and fax number; a clear statement of the objective of the work, methodology, and results and conclusions. Abstracts not exceeding 350 words should be submitted as both hard copy and as PC or Mac files (WordPer-

fect, Word, or ASCII; 3.5" disk preferred) to Robert Stevenson, Chairman Technical Committee, Prep-Tech'95, 3338 Carlyle Terrace, Lafayette, CA 94549, USA. Tel.: (+1-510) 283-7619; Fax: (+1-510) 283-5621.

Information about attendance and exhibiting should be directed to: Joan Lantowski, Conference Coordinator, ISC Technical Conferences, Inc., 30 Controls Drive, P.O. Box 559, Shelton, CT 06484, USA. Tel.: (+1-203) 926-9300; Fax: (+1-203) 926-9310.

8th INTERNATIONAL SYMPOSIUM ON INSTRUMENTAL PLANAR CHROMATOGRAPHY, INTERLAKEN, SWITZERLAND, 5-7 APRIL, 1995

Topics to be covered at the symposium are:

- large sample number (LSN) analysis,
- environmental screening,
- electroplanar chromatography/electrophoresis,
- forensic analysis and drug screening,
- certified compendial methods,
- alternative detection methods/application of enzymes,
- quality assurance of quality control,
- integrated sample preparation,
- alternative separation phases/incorporation of enzymes,
- enantiomer separation/purity control,
- coupled/hyphenated techniques,
- automation: potential and limitations.

Authors interested in giving a lecture of presenting a paper are invited to submit an abstracts, including full details of title(s) and author(s), of at least two A4 pages to Dr H. Traitler, Nestlé Research Center, Nestec Ltd., CH-1000 Lausanne 26, Switzerland.

11th INTERNATIONAL SYMPOSIUM ON AFFINITY CHROMATOGRAPHY AND BIOLOGICAL RECOGNITION, SAN ANTONIO, TX, USA, 25-31 MAY, 1995

The main topics that will be covered at the symposium are:

- proteins purification methods,
- matrices and materials in affinity systems,
- younger scientists session,

- biorecognition in therapeutics,
- emerging technologies in biorecognition,
- biosensors and diagnostics,
- molecular aspects of biorecognition,
- DNA-protein/DNA-RNA interaction,
- molecular imprinting/polymeric artificial biorecognition sites.

The 6th Pierce Award for Affinity Chromatography, sponsored by Pierce Chemical Company, Rockford, IL, USA, will be awarded at the meeting for recent accomplishments in the field.

For further details contact: Dr William H. Scouten, Chairman Organizing Committee, Biotechnology Center, Utah State University, Logan, UT 84322-4700, USA. Tel.: (+1-801) 797 2753; Fax (+1-801) 707 2766; E-mail: BSCOUTEN@CSCFS1-USU.EDU

9th INTERNATIONAL CONFERENCE ON PARTITIONING IN AQUEOUS TWO-PHASE SYSTEMS: ADVANCES IN THE USES OF POLYMERS IN CELL BIOLOGY, BIOTECHNOLOGY AND ENVIRONMENTAL SCIENCES, ZARAGOZA, SPAIN, 4-9 JUNE, 1995

The programme will focus on the large-scale biotechnical use and new phase systems and polymer derivatives. The scientific programme will be final after receipt of the abstracts, but will include sessions on:

- characterization of biological surfaces (cells, organelles and macromolecules),
- isolation of plasma membranes,
- extraction of macromolecules from biological media (recombinant and transgenic proteins),
- large-scale biotechnical use,
- metal ion separations,
- processing of radioactive waste,
- theory of partitioning and characterization of phase behaviour,
- polymer-bound macromolecules and particles,
- biomedical applications of synthetic polymers,
- polymer protein and polymer biosurface interactions and
- emerging technologies (new phase systems and polymer derivatives).

For further details contact: Professor M.J. Lopez-

Pérez, Dep. Bioquímica y Biología Molecular, Facultad de Veterinaria, Avenida Miguel Servet, 177, 50013 Zaragoza. Spain. Tel: (+ 34 76) 492 794; Fax: (+ 34 76) 591 994; or Dr. Cristina Delgado, Molecular Cell Pathology, Royal Free Hospital Medical School, Rowland Hill Street, London NW3 2PF, UK. Tel: (+ 44-71) 794 05 00 (ext. 5387); Fax: (+ 44-71) 431 75 94.

#### 5th SYMPOSIUM ON OUR ENVIRONMENT AND FIRST ASIA-PACIFIC WORKSHOP ON PESTICIDES, SINGAPORE, 5-8 JUNE, 1995.

The scientific programme will consist of plenary lectures, invited lectures and contributed papers in the following areas:

- analytical methods and pollution monitoring,
- ecology and environmental management,
- urban environment, aquatic environment, atmospheric environment,
- exposure and risk assessment,
- pesticides, environmental values and education, and
- global environmental issues.

Arrangements are being made to publish presented papers in an international journal. All fully registered participants will receive a copy of the proceedings.

Contact: The Secretariat 5th Symposium on Our Environment, c/o Department of Chemistry, National University of Singapore, Kent Ridge, Republic of Singapore 0511. Fax: (+ 65) 779-1691.

#### 3rd INTERNATIONAL SYMPOSIUM ON APPLIED MASS SPECTROMETRY IN THE HEALTH SCIENCES AND 3rd EUROPEAN TANDEM MASS SPECTROMETRY CONFERENCE, BARCELONA, SPAIN, 9-13 JULY, 1995

The combined third meetings in these two successful symposium series will provide a unique forum for the discussion of the latest developments in mass spectrometric techniques and their application. Topics for invited and poster presentations include:

- new developments in mass spectrometric instrumentation and novel techniques,

- development in tandem mass spectrometry techniques,
- excitation and fragmentation of ions,
- high mass methods for biomolecules,
- recent trends and horizons in combined chromatographic and mass spectrometric techniques,
- applications in:
  - clinical, metabolic and biochemical studies,
  - molecular biology and biotechnology,
  - environmental and food chemistry,
  - toxicology and doping control,
  - drug assay methods and pharmacology,
  - drug assay methods and pharmacology,
  - fundamental studies and fragmentation mechanisms of biomolecules.

Contributed papers may be accepted for poster presentation. The deadline for abstracts will be 15 April 1995 and these will be refereed by the Scientific Committee.

For further details contact: Professor Emilio Gelpí, 3rd International Symposium on Applied Mass Spectrometry in the Health Sciences and 3rd European Tandem Mass Spectrometry Conference, Palau de Congressos, Dept. Convencions, Avda. Reina M. Cristina, s/n., 08004 Barcelona, Spain. Tel.: (+ 34-3) 423 3101, Ext. 8208-8213; Fax: (+ 34-3) 426 2845.

#### 5th INTERNATIONAL SYMPOSIUM ON FIELD-FLOW FRACTIONATION, PARK CITY, UT, USA, 10-12 JULY, 1995

The symposium will cover all aspects of FFF, ranging from recent theoretical and instrumental developments to applications in the chemical industry (including polymers, latexes, emulsions, etc.) biochemistry, pharmaceutical products, and environmental studies. Recent advances in the separation and analysis of diverse types of biopolymers, synthetic polymers, colloids, and cell-sized particles by FFF will be surveyed.

Authors working in these areas are invited to submit titles of proposed oral and poster presentation. Posters are particularly encouraged. Final titles will be selected by a scientific committee. For submitted papers, titles and a one-page (maximum) abstract will be due 16 January 1995. Poster titles and abstracts are due 1 February 1995. Some additional posters will be

accepted up until 27 June 1995.

The symposium will be preceded by an FFF workshop on Friday, 7 July, with an optional extension on Saturday, 8 July, which will greatly expand the opportunity for hands-on laboratory experience. Lecture topics will include basic theory, principles of operation and optimization, and instrumental systems and characteristics. Enrollment will be limited to maintain an informal learning environment.

For further details contact: Ms Julie Westwood, FFF Research Center, Department of Chemistry, University of Utah, Salt Lake City, UT 84112, USA. Tel.: (+1-801) 581 5419; Fax: (+1-801) 581 4353.

**10th INTERNATIONAL CONFERENCE ON FOURIER TRANSFORM SPECTROSCOPY, BUDAPEST, HUNGARY, 27 AUGUST-1 SEPTEMBER, 1995**

The scope of the conference comprises all aspects of Fourier transform spectroscopy in the infrared, far-infrared, visible and ultraviolet regions including Fourier transform Raman spectroscopy. Topics will range from fundamental aspects of theory, via experimental techniques, new methodology and development to analytical methods and data treatment. Areas of interest include:

- analytical applications
- atmospheric and environmental chemistry and physics
- biology, pharmacy, medical problems, chirality
- catalysis, surfaces, thin films and interfaces
- electrochemistry
- emission, absorption and all types of reflection experiments
- FT-Raman (development, applications, resonance phenomena)
- geology, mineralogy
- hyphenated techniques
- high resolution spectroscopy
- infrared sensors, fiber optics, process control
- matrix isolation, photoacoustics
- material science
- microscopy, ellipsometry
- polymers, aggregates, complexes and ordered systems
- signal processing, chemometrics, data bases
- super-, semi- and non-conductors

- solid state effects of phase, order, temperature and pressure
- time resolution, relaxation, transients
- UV-VIS and NIR applications

For further details contact: Mrs Klára Láng or Mr Attila Varga, Conference Office, Roland Eötvös Physical Society, P.O. Box 433, H-1371 Budapest, Hungary. Tel./Fax: (+36-1) 201 8682.

**5th WORKSHOP ON CHEMISTRY AND FATE OF MODERN PESTICIDES, PARIS, FRANCE, 6-8 SEPTEMBER, 1995**

Environmental chemists, food chemists, analytical chemists, toxicologists and biologists will discuss in an interdisciplinary way relevant scientific problems. Special emphasis is put on topics such as occurrence of residues of modern pesticides in the aquatic environment, foodstuffs and the indoor environment. Relevant topics will be environmental and analytical chemistry (sample preparation, solid and supercritical fluid extraction, clean-up techniques, GC, LC, SFC, CZE, hyphenated techniques, MS techniques, column switching, on-line and off-line automation, immunological and biological techniques), ecotoxicology (transport, bioaccumulation, toxic effect, biochemical and photochemical transformation), residue monitoring programs (pollution indicators) and environmental modelling.

The proceedings will be published in the *International Journal of Environmental Analytical Chemistry*.

The workshop will be preceded by a two-day short course (September 4-5) on: **SAMPLE HANDLING OF PESTICIDES IN THE AQUATIC ENVIRONMENT**, which is designed to give participants up-to-date knowledge and practical experience on the various sample handling aspects (extraction, concentration, clean-up, on-line and off-line methods, validation of results, immunoassay methods). Strategies for the various groups of pesticides and methods allowing multiresidue determinations will be developed for water, sediments and biota samples.

The symposium and short course language will be English, no simultaneous translation.

For further details contact: Professor M.-C. Henion, ESPCI, Labo. Chimie Analytique, 10 rue Vauquelin, 75005 Paris, France. Tel.: (+33-1) 4079 4651; Fax: (+33-1) 4079 4425.



**4th INTERNATIONAL CONFERENCE AND INDUSTRIAL EXHIBITION ON ION EXCHANGE PROCESSES (ION-EX '95), WREXHAM, WALES, UK, 10-14 SEPTEMBER, 1995**

Ion-Ex '95 is devoted to the industrial, analytical and preparative applications of ion exchange processes. The following areas will be covered:

- environmental aspects (water recycling and purification; the nuclear industry; environmental clean up and waste land recovery),
- techniques (ion chromatography; capillary electrophoresis),
- ion exchange materials (membranes; polymeric resins; polyelectrolytes; inorganic ion exchangers; novel materials),
- use of ion-exchange in the pharmaceutical industry,
- theoretical aspects.

Oral papers and poster presentations on the proposed scientific programme are invited. Please provide a provisional title and a one-page abstract of the presentation by 31 January, 1995.

An Industrial Exhibition will be held in conjunction with the conference and interested parties are invited to attend.

For further details contact: Ion-Ex '95, Conference Secretariat, Faculty of Science, The North East Wales Institute, Connah's Quay, Deeside, Clwyd CH5 4BR, UK. Fax: (+ 44-244) 814-305.

**5th INTERNATIONAL SYMPOSIUM ON DRUG ANALYSIS, LEUVEN, BELGIUM, 12-15 SEPTEMBER, 1995**

The purpose of Drug Analysis '95 is to bring together people from industry, universities, control laboratories and hospitals to discuss the current status of analytical techniques including instrumental applications and theoretical developments.

The main scientific themes will include:

- separation of enantiomeric drugs,
- sample pretreatment and automated analysis,
- recent developments in separation methods,
- techniques for high sensitivity analysis of drugs,
- computer-aided methods,
- methods validation and quality assurance,
- analysis of biotechnology products,

- quality control of bulk drugs and dosage forms,
- bioanalysis of drugs and metabolites.

Plenary and keynote lectures will be given by invited speakers. A limited number of papers will be presented as oral communications. Preference will be given to poster presentations; discussion sessions will also be organized. All registered participants will receive a copy of the book of abstracts. All invited and submitted papers will be considered for publication in a special issue of the *Journal of Pharmaceutical and Biomedical Analysis*.

For further information please contact: Professor J. Hoogmartens, Drug Analysis '95 - Leuven, Institute of Pharmaceutical Sciences, Van Evenstraat 4, B-3000 Leuven, Belgium. Tel.: (+ 32-16) 283-440; Fax: (+ 31-16) 283-448.

**IICS '95, INTERNATIONAL ION CHROMATOGRAPHY SYMPOSIUM, DALLAS, TX, USA, 1-4 OCTOBER, 1995**

The session topics will include:

- separations selectivity,
- developments in separation methodology,
- advances in detection,
- special sample treatment procedures,
- novel applications,
- process monitoring and control,
- separation of metal ions,
- pharmaceutical applications,
- environmental applications,
- ion analysis in the electrical generating industry,
- standard methods and data processing,
- modelling.

For further details contact: Century International, Inc., P.O. Box 493, 25 Lee Road, Medfield, MA 02052, USA. Tel. (+ 1-508) 359 8777; Fax: (+ 1-508) 359 8778.

**4th INTERNATIONAL SYMPOSIUM ON HY-PHENATED TECHNIQUES IN CHROMATOGRAPHY (HTC 4), BRUGES, BELGIUM, 6-9 FEBRUARY, 1996**

HTC 4 will cover all fundamental aspects, instrumental developments and applications of the various hyphenated chromatographic techniques

(e.g., GC-GC, GC-MS, PTV-GC-MS, GC-MS-MS, GC-FTIR, GC-AED, on-line air trap-GC, purge-and-trap-GC, extractors-GC (or LC), LC-MS, LC-NMR, LC-LC, LC-GC-MS, LC-LC-GC, LC-FIA-DAD, LC-SFC, SFC-LC, SFC-MS, SFC-FTIR, SFE-GC, SFE-LC, CZE-MS, ITP-MS, . . .). Emphasis will also be placed on the design of hyphenated, on-line and at-line, chromatographic analyzers.

Oral presentations in plenary and parallel sessions as well as poster presentations will be included in the scientific programme. A major portion of the symposium will be devoted to discussion sessions. Workshop type seminars will be organized in which scientists of the instrument manufacturers will present and discuss latest developments in instrumentation. Also a technical exhibition will be organized during the meeting. Companies interested in this exhibition should contact the Symposium Secretariat.

Participants who wish to present a paper are hereby invited to submit an abstract. Submission forms for contributed papers may be obtained from the Congress Secretariat. Abstracts for papers/posters will be accepted up to June 30, 1995. Abstracts for last minute poster presentations will be accepted up to December 15, 1995.

Abstracts of all papers will be available to registered participants. The book of abstracts will have an ISBN number and can thus be cited as an official publication.

A special volume of the *Journal of Chromatography* will be dedicated to the accepted and reviewed papers, which will be channelled through the usual refereeing system.

For further information contact: Dr R. Smits, p/a BASF Antwerp N.V., Centraal Laboratorium, Haven 725, Scheldelaan 600, B-2040 Antwerp, Belgium. Tel.: (+32-3) 561-2831; Fax: (+32-3) 561-3250. Or: Dr R. Senten, p/a Municipal Laboratory, Slachthuislaan 68, B-2060 Antwerp, Belgium. Tel.: (+32-3) 217-2905; Fax: (+32-3) 235-3323.

EUROANALYSIS IX, BOLOGNA, ITALY, 1-7 SEPTEMBER, 1996

Following Euroanalysis traditions, the 9th conference will aim to cover all branches of analytical

chemistry with emphasis on the "problem solving" role of the discipline.

The scientific program will consist of invited lectures and contributed papers (oral presentations and posters).

Special topics planned are:

- education (where the complete scheme of the "Eurocurriculum" in analytical chemistry will be discussed)
- validation in analytical chemistry
- reference materials
- calibration and traceability

The official language of the Conference is English. No simultaneous translation will be provided.

For further details contact: Professor L. Sabbatini, EUROANALYSIS IX, Dipartimento di Chimica, Università di Bari, Via Orabona 4, I-70126 Bari, Italy. Tel.: (+39-80) 242-020/16/14; Fax: (+39-80) 242-026.

## SHORT COURSE

SHORT COURSE ON CHIRAL RESOLUTION MONTEROTONDO SCALO, ROME, ITALY, 4-7 APRIL, 1995

A Short Course on Chiral Resolution will be organized by CNR, Institute of Chromatography. The Course will focus on the main aspects of chiral separations by capillary electrophoresis, however, pointing out, the efficacy of some high-performance liquid chromatographic techniques and columns for special applications (atropic isomers, preparative scale separations etc.)

Chiral separations, principles, resolution mechanisms and applications will be also discussed.

The Course is directed to the post-doctorates and is organized with lectures in the morning and experiments in the afternoon.

For further information contact: Dr. S. Fanali and Dr. M. Sinibaldi, CNR, Istituto di Cromatografia, C.P. 10-00016 Monterotondo Scalo (Rome), Italy. Tel: (+39 6) 906 25 328/ 906 258 36; Fax: (+39 6) 906 258 49.

## CALENDAR OF FORTHCOMING EVENTS

**22-25 January, 1995****Yokohama, Japan**

International Symposium on Chromatography. *Contact:* Dr Toshihiko Hanai, Int. Institute Techn. Anal., 3-492 Matsumi, Eclairer 2-913, Kanagawaku, Yokohama 221, Japan. Fax: (+81-45) 402-6361.

**29 January-2 February, 1995****Würzburg, Germany**

HPCE '95: 7th International Symposium on High Performance Capillary Electrophoresis. *Contact:* Shirley E. Schlessinger, HPCE '95 Manager, Suite 1015, 400 East Randolph Drive, Chicago, IL 60601, USA. Tel.: (+1-312) 527-2011.

**7-10 February, 1995****Montreux, Switzerland**

4th International Conference on Automation, Robotics and Artificial Intelligence Applied to Analytical Chemistry and Laboratory Medicine. *Contact:* J. van der Greef, TNO and University of Leiden, P.O. Box 360, 3700 AJ Zeist, The Netherlands. Tel: (+31 3404) 441 44; Fax: (+31 3404) 572 24; or R.A. Felder, University of Virginia, Dept. of Pathology, Box 168, Charlottesville, VA, USA. Tel: (804) 924 51 51; Fax: (804) 924 57 18.

**13-15 February, 1995****East Rutherford, NJ, USA**

PrepTech'95. *Contact:* Robert Stevenson, Chairman Technical Committee, PrepTech'95, 3338 Carlyle Terrace, Lafayette, CA 94549, USA. Tel.: (+1-510) 283 7619; Fax: (+1-510) 283 5621.

**6-10 March, 1995****New Orleans, LA, USA**

PITTCON '95. Pittsburgh Conference on Analytical Chemistry and Applied Spectroscopy. *Contact:* Pittsburgh Conference, Suite 332, 200 Penn Center Blvd., Pittsburgh, PA 15235-9962, USA

**19-23 February, 1995****Nice, France**

7th European Congress on Biotechnology. *Contact:* ECB Secrétariat Général Société de Chimie Industrielle, 28, rue St. Dominique, 75015 Paris, France. Tel: (+33-1) 45 55 69 46; Fax: (+33-1) 45 55 40 33.

**12-16 March, 1995****Sacramento, CA, USA**

7th Annual California Pesticide Residue Workshop. *Contact:* for USA: Dr Mark Lee or Dr Dianne Bennett, CDFA-Chemistry, 3292 Meadow View Road, Sacramento, CA 95832, USA. Tel.: (+1-916) 262-1434; Fax: (+1-916) 262-1572; for Europe: Dr André de Kok, Food Inspection Service, Burgpoelwaard 6, 1824 DW Alkmaar, The Netherlands. Tel.: (+31-72) 618 444; Fax: (+31-72) 625 324; for Asia: Dr Jong Sei Park, KIST, Doping Control, P.O. Box 131 Cheongryang, Seoul, Korea. Tel.: (+82-2) 969 2871; Fax: (+82-2) 968 2109.

**13-15 March, 1995****Durham, USA**

2nd Biennial International Conference Low- and No-VOC Coating Technologies. *Contact:* Ms. C. M. Northeim, Research Triangle Institute, P.O. Box 12194, Re-

search Triangle Park, NC 27709-2194. Tel: (+1-919) 541 5816; Fax: (+1-919) 541 7155.

**4-7 April, 1995****Monterotondo Scalo, Roma, Italy**

Short Course on Chiral Resolution. *Contact:* Dr. S. Fanali and Dr. M. Sinibaldi, CNR, Istituto di Cromatografia, C.P. 10-00016 Monterotondo Scalo (Roma). Tel: (+39-6) 906 25 328/ 906 258 36; Fax: (+39-6) 906 258 49.

**5-7 April, 1995****Interlaken, Switzerland**

8th International Symposium on Instrumental Planar Chromatography. *Contact:* Dr H. Traitler, Nestlé Research Center, Nestec Ltd., CH-1000 Lausanne 26, Switzerland. Fax (+41-21) 921 4267.

**23-26 April, 1995****St. Louis, MO, USA**

PBA '95: 6th International Symposium on Pharmaceutical and Biomedical Analysis. *Contact:* Shirley E. Schlessinger, Conference Manager, PBA '95, Suite 1015, 400 East Randolph Drive, Chicago, IL 60601, USA. Tel.: (+1-312) 527-2011.

**23-27 April, 1995****Ghent, Belgium**

2nd International Pharmaceutical Biotechnology Conference. *Contact:* Conference Planning Secretariat, Professor Dr E. Van den Eeckhout, University of Ghent FFW, Harelbekestraat 72, B-9000 Ghent, Belgium. Tel.: (+32-9) 221-9943; Fax: (+32-9) 220-6688.

**25–28 April, 1995**

**Leipzig, Germany**

Biochemical Analysis '95. *Contact:* Ulrike Arnold or Anneli Höhnke, Nymphenburger Straße 70, D-80335 Munich, Germany. Tel.: (+49-89) 123-4500; Fax: (+49-89) 183-248.

**7–11 May, 1995**

**Wintergreen, VA, USA**

17th International Symposium on Capillary Chromatography and Electrophoresis. *Contact:* Dr Milton L. Lee, Department of Chemistry, Brigham Young University, Provo, UT 84602-4672, USA. Tel.: (+1-801) 378-2135; Fax: (+1-801) 378-5474. Or: Joy Wise, Symposium Coordinator, P.O. Box 4153, Frederick, MD 21705-4153, USA. Tel.: (+1-301) 473-8311; Fax: (+1-301) 473-8312.

□ **7–11 May, 1995**

**San Antonio, TX, USA**

86th AOCS Annual Meeting & Expo. *Contact:* AOCS Education/Meetings Department, P.O. Box 3489, Champaign, IL 61826-3489, USA. Tel. (+1-217) 359 2344; Fax (+1-217) 351 8091.

**7–10 May, 1995**

**Lund, Sweden**

7th Symposium on Handling of Environmental and Biological Samples in Chromatography. *Contact:* Mrs. M. Frei-Häusler, IAEAC Secretariat, Postfach 46, CH-4123 Allschwil 2, Switzerland. Tel.: (+41-61) 4812789; Fax: (+41-61) 4820805.

**8–10 May, 1995**

**Lund, Sweden**

7th Symposium on Handling of Environmental and Biological Samples in Chromatography.

*Contact:* Mrs. M. Frei-Häusler, IAEAC Secretariat, Postfach 46, CH-4123 Allschwil 2, Switzerland. Tel.: (+41-61) 4812789; Fax: (+41-61) 4820805.

**9–12 May, 1995**

**Jülich, Germany**

6th International Hans Wolfgang Nürnberg Memorial Symposium on Metal Compounds in Environment and Life-Analysis, Speciation and Specimen Banking. *Contact:* Dr H.W. Dürbeck, Institute of Applied Physical Chemistry, Research Center Jülich (KFA), P.O. Box 1913, D-W 5170 Jülich, Germany.

□ **14–18 May, 1995**

**St. Malo, France**

EMAS '95: 4th European Workshop on Modern Developments and Applications in Microbeam Analysis. *Contact:* EMAS Secretariat, University of Antwerp (UIA), Department of Chemistry, Universiteitsplein 1, B-2610 Antwerp-Wilrijk, Belgium. Fax: (+32-3) 820 2376; E-mail: vantdack@schs.uia.ac.be.

□ **23 May, 1995**

**Ghent, Belgium**

Miniaturisation in Liquid Chromatography versus Capillary Electrophoresis. *Contact:* Professor Dr Willy R.G. Baeyens, Symposium Chairman, University of Ghent, Pharmaceutical Institute, Dept. Pharmaceutical Analysis, Laboratory of Drug Control, Harelbekestraat 72, B-9000 Ghent, Belgium. Tel. (+32-9) 221 8951; Fax (+32-9) 221 4175.

□ **25–31 May, 1995**

**San Antonio, TX, USA**

11th International Symposium on

Affinity Chromatography and Biological Recognition. *Contact:* Dr W.H. Scouten, Biotechnology Center, Utah State University, Logan, UT 84322-4700, USA. Tel. (+1-801) 797 2753; Fax (+1-801) 797 2766.

**28 May–2 June, 1995**

**Innsbruck, Austria**

HPLC '95, 19th International Symposium on Column Liquid Chromatography. *Contact:* HPLC'95 Secretariat, Tyrol Congress, Marktgraben 2, A-6020 Innsbruck, Austria. Tel.: (+43-52) 575-600; Fax: (+43-512) 575-607.

□ **4–9 June, 1995**

**Zaragoza, Spain**

9th International Conference on Partitioning in Aqueous Two-Phase Systems: Advances in the Uses of Polymers in Cell Biology, Biotechnology and Environmental Sciences. *Contact:* Prof. M.J. Lopez-Pérez, Dep. Bioquímica y Biología Molecular, Facultad de Veterinaria, Avenida Miguel Servet, 177, 50013 Zaragoza, Spain. Tel: (34-76) 492 794; Fax: (34-76) 591 994; or Dr. Cristina Delgado, Molecular Cell Pathology, Royal Free Hospital Medical School, Rowland Hill Street, London NW3 2PF, England, UK. Tel: (44-71) 794 05 00 (Ext. 5387); Fax: (44-71) 431 75 94.

□ **5–8 June, 1995**

**Singapore, Singapore**

5th Symposium on our Environment and 1st Asia-Pacific Workshop on Pesticides. *Contact:* The Secretariat, 5th Symposium on Our Environment, c/o Department of Chemistry, National University of Singapore, Kent

Ridge, Republic of Singapore  
0511. Fax: (+65) 779 1691.

**11-14 June, 1995**

**Washington, DC, USA**

1995 International Symposium, Exhibit & Workshops on Preparative Chromatography. *Contact:* Janet Cunningham, c/o Barr Enterprises, 10120 Kelly Road, P.O. Box 279, Walkersville, MD 21793, USA. Tel.: (+1-301) 898 3772; Fax: (+1-301) 898 5596.

□ **16-20 June, 1995**

**Montpellier, France**

Capillary Electrophoresis, Routine Method for the Quality Control of Drugs. *Contact:* Dr M. Blanchin, Lab. de Chimie Analytique, Faculté de Pharmacie, 15 Avenue Charles Flahault, F-34060 Montpellier Cedex 1, France. Tel.: (+33-67) 544 520; Fax: (+33-67) 528 915.

**7-8 July, 1995**

**Salt Lake City, UT, USA**

FFF Workshop VII. *Contact:* Ms Julie Westwood, FFF Research Center, Department of Chemistry, University of Utah, Salt Lake City, UT 84112, USA. Tel.: (+1-801) 581-5419; Fax: (+1-801) 581-4353.

**9-13 July, 1995**

**Barcelona, Spain**

3rd International Symposium on Applied Mass Spectrometry in the Health Sciences and 3rd European Tandem Mass Spectrometry Conference. *Contact:* Professor Emilio Gelpí, Palau de Congressos, Dept. Convencions, Avda. Reina M. Cristina, s/n, 08004 Barcelona, Spain. Tel.: (+34-3) 423 3101 - Ext. 8208-8213; Fax: (+34-3) 426 2845

**9-15 July, 1995**

**Hull, UK**

SAC 95, International Symposium on Analytical Chemistry. *Contact:* The Secretary, Analytical Division of the Royal Society of Chemistry, Burlington House, Piccadilly, London, W1V 0BN, UK.

**10-12 July, 1995**

**Park City, UT, USA**

5th International Symposium on Field-Flow Fractionation. *Contact:* Ms Julie Westwood, FFF Research Center, Department of Chemistry, University of Utah, Salt Lake City, UT 84112, USA. Tel.: (+1-801) 581-5419; Fax: (+1-801) 581-4353.

□ **10-13 July, 1995**

**Vancouver, BC, Canada**

5th COMTOX Symposium on Toxicology and Clinical Chemistry of Metals. *Contact:* F. William Sunderman, Jr., M.D., Departments of Laboratory Medicine and Pharmacology, University of Connecticut Medical School, P.O. Box 1292, Farmington, CT 06034-1292, USA. Tel.: (+1-203) 679-2328; Fax: (+1-203) 679-2154

**27 August-1 September, 1995**

**Budapest, Hungary**

10th International Conference on Fourier Transform Spectroscopy. *Contact:* Mrs. K. Láng or Mr. A. Varga, Conference Office, Roland Eötvös Physical Society, P.O. Box 433, H-1371 Budapest, Hungary.

□ **27 August-1 September, 1995**

**Leipzig, Germany**

Colloquium Spectroscopicum Internationale XXIX. *Contact:* Ge-

sellschaft Deutscher Chemiker, Abteilung Tagungen, P.O. Box 900440, D-60444 Frankfurt am Main, Germany. Tel.: (+49-69) 7917 358 or -360; Fax: (+49-69) 7917 475.

**6-8 September, 1995**

**Paris, France**

5th Workshop on Chemistry and Fate of Modern Pesticides. *Contact:* Professor M.-C. Hennion, ESPCI, Labo. Chimie Analytique, 10 rue Vauquelin, 75005 Paris, France. Tel.: (+33-1) 4079-4651; Fax: (+33-1) 4079-4425.

**10-14 September, 1995**

**Wrexham, Wales, UK**

ION-EX '95: 4th International Conference and Industrial Exhibition on Ion Exchange Processes. *Contact:* ION-EX '95, Conference Secretariat, Faculty of Science, The North East Wales Institute, Connah's Quay, Deeside, Clwyd CH5 4BR, UK. Fax: (+44-244) 814-305.

**12-15 September, 1995**

**Leuven, Belgium**

5th International Symposium on Drug Analysis. *Contact:* Professor J. Hoogmartens, Drug Analysis '95 - Leuven, Institute of Pharmaceutical Sciences, Van Evenstraat 4, B-3000 Leuven, Belgium. Tel.: (+32-16) 283 440; Fax: (+32-16) 283 448.

**1-4 October, 1995**

**Dallas, TX, USA**

IICS '95: International Ion Chromatography Symposium. *Contact:* Century International Inc., P.O. Box 493, 25 Lee Road, Medfield, MA 02052, USA. Tel.:

(+1-508) 359-8777; Fax: (+1-508) 359 8778.

**6-9 February, 1996**

**Bruges, Belgium**

HTC 4: 4th International Symposium on Hyphenated Techniques in Chromatography. *Contact:* Dr R. Smits, BASF Antwerp N.V., Centraal Laboratorium, Haven 725, Scheldelaan 600, B-2040 Antwerp, Belgium. Tel.: (+32-3) 561-2831; Fax: (+32-3) 561-3250; or Dr R. Senten, Municipal Laboratory, Slachthuislaan 68, B-2060 Antwerp, Belgium. Tel.: (+32-3) 217-2905; Fax: (+32-3) 235-3323.

□ **31 March- 4 April, 1996**

**Indianapolis, IN, USA**

7th International Symposium on Supercritical Fluid Chromatography and Extraction. *Contact:* Janet Cunningham, c/o Barr Enterprises, 10120 Kelly Road, P.O.

Box 279, Walkersville, MD 21793, USA. Tel. (+1-301) 898-3772; Fax: (+1-301) 898-5596.

□ **7-9 May, 1996**

**Monte Carlo, Monaco**

7th International Symposium on Luminescence Spectrometry in Biomedical Analysis - Detection Techniques and Applications in Chromatography and Capillary Electrophoresis. *Contact:* Professor Dr. Willy R.G. Baeyens, Symposium Chairman, University of Ghent, Pharmaceutical Institute, Dept. Pharmaceutical Analysis, Laboratory of Drug Control, Harelbekestraat 72, B-9000 Ghent, Belgium. Tel. (+32-9) 221 8951; Fax (+32-9) 221 4175.

□ **16-21 June, 1996**

**San Francisco, CA, USA**

HPLC '96: 20th International Symposium on High Performance

Liquid Phase Separations. *Contact:* Mrs. Janet E. Cunningham, Barr Enterprises, P.O. Box 279, Walkersville, MD 21793, USA. Tel.: (+1-301) 898-3772; Fax: (+1-301) 898-5596.

□ **1-7 September, 1996**

**Bologna, Italy**

Euroanalysis IX. *Contact:* Professor L. Sabbatini, Euroanalysis IX, Dipartimento di Chimica, Università di Bari, Via Orabona 4, I-70126 Bari, Italy. Tel.: (+39-80) 242-020/16/14; Fax: (+39-80) 242-026.

□ **15-20 September, 1996**

**Stuttgart, Germany**

21st International Symposium on Chromatography. *Contact:* Gesellschaft Deutscher Chemiker, Abteilung Tagungen, P.O. Box 900440, D-60444 Frankfurt am Main, Germany. Fax: (+49-69) 7917 475.

## PUBLICATION SCHEDULE FOR THE 1995 SUBSCRIPTION

*Journal of Chromatography A and Journal of Chromatography B: Biomedical Applications*

| MONTH  | O 1994                  | N 1994                           | D 1994                               |  |
|--|-------------------------|----------------------------------|--------------------------------------|--|
| Journal of Chromatography A                          | 683/1<br>683/2<br>684/1 | 684/2<br>685/1<br>685/2<br>686/1 | 686/2<br>687/1<br>687/2<br>688/1 + 2 | The publication schedule for further issues will be published later. |
| Bibliography Section                                 |                         |                                  |                                      |  |
| Journal of Chromatography B: Biomedical Applications |                         |                                  |                                      |  |

### INFORMATION FOR AUTHORS

(Detailed *Instructions to Authors* were published in *J. Chromatogr. A*, Vol. 657, pp. 463–469. A free reprint can be obtained by application to the publisher, Elsevier Science B.V., P.O. Box 330, 1000 AH Amsterdam, Netherlands.)

**Types of Contributions.** The following types of papers are published: Regular research papers (full-length papers), Review articles, Short Communications and Discussions. Short Communications are usually descriptions of short investigations, or they can report minor technical improvements of previously published procedures; they reflect the same quality of research as full-length papers, but should preferably not exceed five printed pages. Discussions (one or two pages) should explain, amplify, correct or otherwise comment substantively upon an article recently published in the journal. For Review articles, see inside front cover under Submission of Papers.

**Submission.** Every paper must be accompanied by a letter from the senior author, stating that he/she is submitting the paper for publication in the *Journal of Chromatography A or B*.

**Manuscripts.** Manuscripts should be typed in **double spacing** on consecutively numbered pages of uniform size. The manuscript should be preceded by a sheet of manuscript paper carrying the title of the paper and the name and full postal address of the person to whom the proofs are to be sent. As a rule, papers should be divided into sections, headed by a caption (e.g., Abstract, Introduction, Experimental, Results, Discussion, etc.). All illustrations, photographs, tables, etc., should be on separate sheets.

**Abstract.** All articles should have an abstract of 50–100 words which clearly and briefly indicates what is new, different and significant. No references should be given.

**Introduction.** Every paper must have a concise introduction mentioning what has been done before on the topic described, and stating clearly what is new in the paper now submitted.

**Experimental conditions** should preferably be given on a *separate* sheet, headed "Conditions". These conditions will, if appropriate, be printed in a block, directly following the heading "Experimental".

**Illustrations.** The figures should be submitted in a form suitable for reproduction, drawn in Indian ink on drawing or tracing paper. Each illustration should have a caption, all the *captions* being typed (with double spacing) together on a *separate sheet*. If structures are given in the text, the original drawings should be provided. Coloured illustrations are reproduced at the author's expense, the cost being determined by the number of pages and by the number of colours needed. The written permission of the author and publisher must be obtained for the use of any figure already published. Its source must be indicated in the legend.

**References.** References should be numbered in the order in which they are cited in the text, and listed in numerical sequence on a separate sheet at the end of the article. Please check a recent issue for the layout of the reference list. Abbreviations for the titles of journals should follow the system used by *Chemical Abstracts*. Articles not yet published should be given as "in press" (journal should be specified), "submitted for publication" (journal should be specified), "in preparation" or "personal communication".

Vols. 1–651 of the *Journal of Chromatography*; *Journal of Chromatography, Biomedical Applications* and *Journal of Chromatography, Symposium Volumes* should be cited as *J. Chromatogr.* From Vol. 652 on, *Journal of Chromatography A* (incl. Symposium Volumes) should be cited as *J. Chromatogr. A* and *Journal of Chromatography B: Biomedical Applications* as *J. Chromatogr. B*.

**Dispatch.** Before sending the manuscript to the Editor please check that the envelope contains four copies of the paper complete with references, captions and figures. One of the sets of figures must be the originals suitable for direct reproduction. Please also ensure that permission to publish has been obtained from your institute.

**Proofs.** One set of proofs will be sent to the author to be carefully checked for printer's errors. Corrections must be restricted to instances in which the proof is at variance with the manuscript.

**Reprints.** Fifty reprints will be supplied free of charge. Additional reprints can be ordered by the authors. An order form containing price quotations will be sent to the authors together with the proofs of their article.

**Advertisements.** The Editors of the journal accept no responsibility for the contents of the advertisements. Advertisement rates are available on request. Advertising orders and enquiries can be sent to the Advertising Manager, Elsevier Science B.V., Advertising Department, P.O. Box 211, 1000 AE Amsterdam, Netherlands; courier shipments to: Van de Sande Bakhuyzenstraat 4, 1061 AG Amsterdam, Netherlands; Tel. (+31-20) 515 3220/515 3222, Telefax (+31-20) 6833 041, Telex 16479 els vi nl. UK: T.G. Scott & Son Ltd., Tim Blake, Portland House, 21 Narborough Road, Cosby, Leics. LE9 5TA, UK; Tel. (+44-533) 753 333, Telefax (+44-533) 750 522. USA and Canada: Weston Media Associates, Daniel S. Lipner, P.O. Box 1110, Greens Farms, CT 06436-1110, USA; Tel. (+1-203) 261 2500, Telefax (+1-203) 261 0101.

# TrAC - Trends in Analytical Chemistry: Reference Edition Volume 12: 1993

TrAC Compendium Series Volume 12

The Reference Edition of *Trends in Analytical Chemistry (TrAC)* is a compilation of the archival material reprinted from the regular issues of the journal. *TrAC* provides a topical digest of current developments and new ideas in the analytical sciences. It does so in the form of broadly-based, easy-to-read scientific reviews, backed up by news and other features of interest to the international analytical chemistry community. For subscribers to the library edition of *TrAC*, the reference edition forms an integral part of the annual subscription, but for others it can be purchased individually. It provides informative and stimulating reading for all those who use analytical methods.

This latest volume contains all the archival material published in 1993. It covers a wide range of analytical techniques and applications of interest to academic and research workers in chemistry, biochemistry, clinical chemistry, pharmaceutical chemistry and toxicology.

**Contents:** *A selection of the Contents.* Single-cell analysis at the level of a single human erythrocyte (B.L. Hogan, E.S. Yeung). Charge-remote fragmentations for structural determination of lipids (J. Adams, M.J. Songer). Recent advances in speciation analysis by capillary gas chromatography-microwave induced plasma atomic emission spectrometry (R. Lobinski, F.C. Adams). Pyrolysis-mass spectrometry under soft ionization conditions (A.C. Tas, J. van der

Greef). New developments in glow discharge mass spectrometry (Y. Mei, R.K. Marcus). Enantiomeric separation by micellar electrokinetic chromatography (K. Otsuka, S. Terabe). Liquid chromatographic methods for the chiral separation of  $\beta$ -adrenergic blocking agents (C. Vandebosch *et al.*). Capillary gel electrophoresis of biopolymers (A.S. Cohen, D.L. Smisek, P. Keohavong). Vibrational spectroscopy - where are we and where are we going? (J.L. Koenig). Capillary electrophoresis of inorganic ions and low-molecular-mass ionic solutes (P.E. Jackson, P.R. Haddad). Mass spectrometric analysis of a GPI-anchored protein: the scrapie prion protein (M.A. Baldwin, A.L. Burlingame, S.B. Prusiner). *In vivo* blood-gas and electrolyte sensors: progress and challenges (M.E. Meyerhoff). Trace analysis in capillary supercritical fluid chromatography: sample introduction (T. Greibrokk, B.E. Berg). Analytical applications of electrified interfaces between two immiscible solutions (P. Vanysek). The use of gas chromatographic detectors in

column liquid chromatography (Ch.E. Kientz, U.A.Th. Brinkman). Imaging applications for chemical analysis utilizing charge coupled device array detectors (C.W. Earle *et al.*). Mass spectrometry of proteins (P. Roepstorff).

© 1993 592 pages Hardbound  
Price: Dfl. 675.00 (US\$ 385.75)  
ISBN 0-444-81805-7

*An extra supplement is included in this edition - Directory of Capillary Electrophoresis:*

- Over 450 V.I.P.s Worldwide
- Complete Addresses, Fax and Phone Numbers, and E-Mail Addresses (where available)
- Many Techniques, Applications and Research Topics
- Extensive Subject Index.

*This directory forms an integral part of the 1993 subscription to the Library Edition and is also available as a separate publication.*

## ORDER INFORMATION ELSEVIER SCIENCE B.V.

P.O. Box 330  
1000 AH Amsterdam  
The Netherlands  
Fax: (+31-20) 5862 845

### For USA and Canada

P.O. Box 945  
Madison Square Station  
New York, NY 10159-0945  
Fax: (212) 633 3680

*US\$ prices are valid only for the USA & Canada and are subject to exchange rate fluctuations; in all other countries the Dutch guilder price (Dfl.) is definitive. Customers in the European Union should add the appropriate VAT rate applicable in their country to the price(s). Books are sent post-free if prepaid.*



ELSEVIER  
SCIENCE



0021-9673(19941202)686:2;1-P